VIBRIO ALGINOLYTICUS: A PHYSIOLOGICAL, CHEMICAL, AND ECOLOGICAL CHARACTERIZATION OF AN EMERGING MARINE PATHOGEN

by

WILLIAM ANDERSON NORFOLK

(Under the Direction of Erin Lipp)

ABSTRACT

Emerging pathogens, or infectious agents that have increased in incidence substantially in recent years, are a major concern for environmental health. Management of these pathogens requires a strong understanding of their baseline biology to assess the factors that contribute to population abundance, survivability, and transmission mechanisms. *Vibrio alginolyticus* is an autochthonous marine bacterium commonly found in coastal and estuarine waters worldwide. Long known as an opportunistic pathogen, this bacterium is an established agent of human and animal disease. Animal infections are widely associated with the aquaculture industry causing disease outbreaks in marine fishes and shellfishes that range from mild epidermal lesions to mass population mortality. Human infections are predominately concentrated to tropical/subtropical regions typically manifesting as mild opportunistic infections of wounds and ears following exposure to seawater. In recent years, the incidence of *V. alginolyticus* infections have increased substantially due to the combined effects of anthropogenically-induced climate change and coastal watershed modification facilitating increased in *Vibrio* spp. abundance and human interaction. Despite this increase fueling renewed interest in *V. alginolyticus* research, much of the foundational characterization of this bacterium was completed around its discovery in the

1960s-1980s and there is a substantial need to reevaluate these characterizations through a modern lens. The research presented here examines the physiological, chemical, and ecological characteristics of *V. alginolyticus* to better understand factors that mediate population abundance and transmission in the natural environment. Combined, these assessments improve our understanding of the baseline biology and disease ecology of this bacterium through the application of a one health approach. The results of these findings can be used to improve methods of risk assessment and the development of transmission barriers to reduce the incidence and severity of future *V. alginolyticus* outbreaks.

INDEX WORDS: *Vibrio alginolyticus*, Public Health, Physiology, Metabolomics, Transmission, Microbial Ecology

A PHYSIOLOGICAL, CHEMICAL, AND ECOLOGICAL CHARACTERIZATION OF THE EMERGING MARINE PATHOGEN, *VIBRIO ALGINOLYTICUS*

by

WILLIAM ANDERSON NORFOLK

B.S., University of Mary Washington, 2012

M.S., George Mason University, 2015

A Dissertation Submitted to the Graduate Faculty of The University of Georgia in Partial Fulfillment of the Requirements for the Degree

DOCTOR OF PHILOSOPHY

ATHENS, GEORGIA

2023

© 2023

William Anderson Norfolk

All Rights Reserved

A PHYSIOLOGICAL, CHEMICAL, AND ECOLOGICAL CHARACTERIZATION OF THE EMERGING MARINE PATHOGEN, *VIBRIO ALGINOLYTICUS*

by

WILLIAM ANDERSON NORFOLK

Major Professor:	Erin K. Lipp
Committee:	James W. Porter
	William K. Fitt
	Franklin E. Leach

Electronic Version Approved:

Ron Walcott
Vice Provost for Graduate Education and Dean of the Graduate School
The University of Georgia
May 2023

DEDICATION

Dedicated in loving memory to my grandfather and first mentor in science, Leonard Gardner, who introduced me to the world of research and always encouraged me to search for answers. Without this guidance none of this would have been possible.

ACKNOWLEDGEMENTS

First and foremost, I would like to thank my wonderful adviser Dr. Erin Lipp for her continuous encouragement and support throughout the duration of this project. The example Dr. Lipp sets through her mentorship and research excellence are valuable lessons I am grateful to have experienced and will carry with me through my scientific career. I also would like to thank my committee members Dr. James Porter, Dr. William Fitt, and Dr. Franklin Leach for their encouragement and guidance throughout this research. I am very thankful for the support of our collaborators at the US Environmental Protection Agency, Dr. W. Matthew Henderson and Dr. Donna Glinski for their willingness to teach me and their assistance with metabolomics processing. I also would like to thank the amazing friends and colleagues from the Lipp Lab and/or the UGA Department of Environmental Health Science that have supported me over the years specifically, Dr. Megan Lott, Dr. Jason Westrich, Dr. Maite Bucher, Dr. Megan Beaudry, Carter Coleman, Mandy Sullivan, Marissa Howard, Elizabeth Reigelman, Nathan Greenslit, Kimberly Perez, Leah Lariscy, Lily Metsker, and our department chair Dr. Jia-Sheng Wang. I would also like to thank all of the fantastic undergraduate research assistants that have contributed throughout this research namely, Carolina Melendez-Declet, Charlyn Shue, Rachel Phan, Samantha Weatherly, and Olivia Marenda.

Most importantly, I would like to thank my family and friends for the continuous support and encouragement throughout my program. I specifically would like to thank my amazing partner Darien Bush who has been at my side from my initial application to my dissertation defense. Without her love and encouragement, this work would have been a substantially more

difficult journey. Lastly, I would like to thank my mother Susan Gardner and my grandmother Doris Gardner who have encouraged and supported me in my scientific career since the beginning.

TABLE OF CONTENTS

Page

LIST OF TABLES

Page

LIST OF FIGURES

Page

CHAPTER 1

INTRODUCTION

Foreword.

What comes to mind when you think about the management of infectious disease? Like many others, you likely imagine management from a medical perspective where disease is controlled using a combination of individual-level treatments such as rest, medication, and perhaps hospitalization in the case of serious illness. While these practices are very important to patient care and the field of medicine, public health recognizes that the control of infectious diseases must be managed at a higher level. A core pillar of public health is the principle of population-level management of disease, meaning that in the eyes of public health practitioners the patient is not an individual but rather the entire population of susceptible individuals. This level of management shifts the focus of pathogen control from the traditional medical perspective of "how can we eliminate/neutralize this pathogen from the patient?" to a public health perspective of "how can we prevent the spread/proliferation of this pathogen within the population?" Using this approach, public health practitioners have had success in the mitigation of numerous infectious diseases with control methods such as educational campaigns, improved sanitation, masking, and vaccination.

Critical to the development of these interventions is a strong understanding of pathogen biology and ecology to accurately predict how an agent will respond to stress and move through different environments or hosts. In the case of nonindigenous microorganisms, or microbes that are not a part of the natural microbial community, population-level controls are easier to manage

focusing on the prevention of person to person spread as these microbes are typically unstable in the ambient environment. However, indigenous microorganisms, or microbes that are natural members of the microbial community, are much more difficult to control. Spread of indigenous pathogens does not need to be initiated by contact with an infected individual but rather can occur opportunistically following exposure via the ambient environment. This complicates the management of transmission as exposure to the pathogen may not be preventable. Thus, prediction of risk, or the assessment of environmental conditions and behaviors that increase the potential for exposure to the pathogen, are critical for the mitigation of these outbreaks. This dissertation represents a synthesis of several studies aimed to investigate the baseline biology and ecology of the indigenous marine pathogen *Vibrio alginolyticus* to better understand that factors that contribute to its proliferation and transmission in the natural environment.

Introduction.

Bacteria in the family Vibrionaceae, or vibrios for short, are a diverse group of heterotrophic aquatic bacteria (Thompson et al., 2003; Baker-Austin et al., 2018). Best known as pathogens, several vibrios are recognized as important etiological agents of both human and animal disease. *Vibrio* infections are broadly defined by two groups, cholera and non-cholera infections (Chakraborty et al., 1997; Baker-Austin et al., 2017; Baker-Austin et al., 2018). Cholera is a well-defined disease caused by the bacterium *V. cholerae*, presenting as characteristic severe diarrheal illness upon ingestion of contaminated food and/or water (Hendrix, 1971; Colwell, 1996; Vezzulli et al., 2010). While uncommon in developed nations, cholera has played a substantial role over the course of history as a major human pathogen and remains a significant contributor of *Vibrio*-morbidity and mortality in regions were access to clean water and sanitation is limited (Pollitzer, 1954; Colwell, 1996; Kavic et al., 1999; Baker-

Austin et al., 2018). Comparatively, non-cholera infections (called vibriosis) present dynamically, with disease signs and symptoms ranging from mild epidermal lesions to hemorrhagic septicemia depending on the specific *Vibrio*-host combination (Schroeder et al., 1985; Selvin & Lipton, 2003; Zorrilla et al., 2003; Baker-Austin et al., 2018). These infections include multiple *Vibrio* spp. such as the major water/foodborne human pathogens *V. parahaemolyticus* (Daniels et al, 2000) and *V. vulnificus* (Klontz et al., 1988) as well as highly damaging aquaculture pathogens such as *V. anguillarum* (Frans et al., 2011) and *V. harveyi* (Zhang et al., 2020). In recent years, the incidence of vibriosis infections have increased globally due to the effects of anthropogenically induced climate change fueling expansion of *Vibrio* range and abundance (Baker-Austin et al., 2017; Froelich & Daines, 2020). Despite this increase, the epidemiology of many non-cholera vibrios remains poorly understood and there is a strong need for research to that fills species-level knowledge gaps required for the estimation of vibriosis risk.

V. alginolyticus is a profuse non-cholera *Vibrio* indigenous to coastal and estuarine waters (Chakraborty et al., 1997; Farmer & Janda, 2005; Thompson & Swings, 2006). A widespread species, *V. alginolyticus* is frequently identified as one of the most common species from *Vibrio* community surveys with reports of the bacterium occurring in coastal waters from every continent, excluding Antarctica (Thompson & Swings, 2006; Takemura et al., 2014; Baker-Austin et al., 2018). Infections from this bacterium are opportunistic, affecting a broad range of host species including marine fishes (Colorni et al., 1981; Balebona et al., 1998), shellfishes (Lightner & Lewis, 1975; Selvin & Lipton, 2003), and humans (Weis et al., 2011; Slifka et al., 2017). In aquaculture, these infections are linked to proliferation/persistence of the bacterium within rearing infrastructure and typically present with organ damage, lesions, and/or

hemorrhage often leading to mass mortality of target species (Balebona et al., 1998; Selvin & Lipton, 2003). By contrast, human infections are largely associated with recreational and occupational exposure to seawater presenting as secondary wound infection, ear infection, and uncommonly as gastrointestinal illness (Slifka et al., 2017). Collectively, the burden of *V. alginolyticus* infections imposes a substantial economic encumbrance with an estimated annual cost of 1 million dollars (USD) for the treatment of human infections in the United States (Ralston et al., 2011) and a global cost of 3 billion dollars (USD) for the treatment/culling of vibriosis outbreaks in aquaculture (of which *V. alginolyticus* is a major contributor) (Sanches-Fernandes, et al., 2022).

As an indigenous opportunistic pathogen, risk of *V. alginolyticus* infection is directly linked to its population abundance and microbial ecology. Thus, risk assessment for this pathogen requires a functional understanding of the limitations, response, and adaptations this bacterium exhibits as an ambient microbe. Critical to this assessment is a foundational understanding of *V. alginolyticus* physiology and ecology. Physiological assessment provides context to properly predict the response of this bacterium following shifts in the abiotic conditions of the natural environment. While early characterizations of *V. alginolyticus* (Miyamoto et al., 1961; Horie et al., 1966; Farid & Larson, 1981) detail its tolerance range for critical determinants such as temperature and salinity, many of these studies were conducted between the 1960s and 1980s and there is need to reevaluate these characterizations through a modern lens. Furthermore, there is a need to incorporate analysis of tertiary determinants such as iron availability, pH, plankton abundance, and dissolved organic carbon which can serve as major limiting factors in the absence of thermal or osmotic stress (Eiler et al., 2006; Turner et al., 2009; Asplund et al., 2011). Ecological characterization provides context for the adaptations that

V. alginolyticus employs to improve its persistence, distribution, and transmission in the natural environment. To date, few studies have directly investigated the role of inter- and intraspecies interactions on the spread of *V. alginolyticus* and there is substantial need to characterize these processes to better understand adaptations that contribute to virulence such as biofilm formation, vector interactions, and nutritional competition mechanisms.

This dissertation represents a compilation of several works designed to investigate the baseline biology of *V. alginolyticus* through the application of physiological, chemical, and ecological methods. Chapters consist of a combination of hypothesis-driven research and methodological works where methods chapters detail the development of specialized equipment or protocols required to accomplish the experimental goals of subsequent research chapters. Chapter two outlines a thorough literature review of *V. alginolyticus* research with an emphasis on the bacterial ecology of this species and a summarization of the current status of human infections in the United States as reported to the Centers for Disease Control and Prevention (CDC) Cholera and Other Vibrio Illness Surveillance (COVIS) system (CDC, 2020). Chapter 3 describes development of a low-cost prototype optical density (OD) meter designed for the spectrophotometric characterization of bacterial growth kinetics in a live culture. Chapter 4 outlines a standardized protocol for *in situ* tagging of *Vibrio* spp. with green fluorescent protein (GFP) for the localization and tracking of target vibrios in a mixed culture. Chapter 5 describes an ecological experiment designed to evaluate the validity of foodborne transmission of *V. alginolyticus* via zooplankton vector using sea anemones as a model organism of coral heterotrophy. Chapter 6 details a physiological characterization of the optimal and tolerable range of *V. alginolyticus* in response to changing temperature, salinity, and iron content using OD-based growth kinetics evaluation. Iron impacts are further characterized using gas

chromatography mass spectrometry (GC-MS) to measure the metabolic changes observed in *V. alginolyticus* following iron supplementation and deprivation. Collectively, the work presented here provides critical foundational research characterizing the baseline biology of *V. alginolyticus* which can be used to improve the management of this pathogen from a public health perspective. Furthermore, this dissertation highlights the importance of this bacterium as a prominent emerging marine pathogen and stresses the need for continued research and surveillance in the future.

Literature Cited.

Asplund ME, Rehnstam-Holm AS, Atnur V, Raghunath P, Saravanan V, Härnström K, Collin B, Karunasagar I, and Godhe. 2011. Water column dynamics of *Vibrio* in relation to phytoplankton community composition and environmental conditions in a tropical coastal area. *Environmental Microbiology.* 13(10): 2738-2751.

Baker-Austin C, Trinanes J, Gonzalez-Escalona N, and Martinez-Urtaza J. 2017. Non-cholera vibrios: the microbial barometer of climate change. *Trends in Microbiology.* 25(1): 76-84.

Baker-Austin, C, Oliver JD, Alam M, Ali A, Waldor MK, Qadri F, and Martinez-Urtaza J. 2018. *Vibrio* spp. infections. *Nature Reviews Disease Primers.* 4(8): doi.org/10.1038/s41572-018-0005-8.

Balebona MC, Andreu MJ, Bordas MA, Zorrilla I, Moriñigo MA, and Borrego JJ. 1998. Pathogenicity of *Vibrio alginolyticus* for Cultured Gilt-Head Sea Bream (*Sparus aurata*L.). *Applied and Environmental Microbiology.* 64(11): 4269-4275.

Centers for Disease Control and Prevention (CDC). 2022. Cholera and Other Vibrio Illness

Surveillance (COVIS), summary data, 1988–2019. Atlanta, GA: US Department of Health and Human Services. Accessed 14 June 2022.

Chakraborty S, Nair BG, and Shinoda S. 1997. Pathogenic Vibrios in the natural aquatic environment. *Reviews on Environmental Health*. 12(2): 63-80.

Colorni A, Paperna I, and Gordin H. 1981. Bacterial infections in gilt-head sea bream *Sparus aurata* cultured at Elat. *Aquaculture.* 23(1-4): 257-267.

Colwell RR. 1996. Global climate and infectious disease: the cholera paradigm. *Science.* 274(5295): 2025-2031.

Daniels NA, MacKinnon L, Bishop R, Altekruse S, Ray B, Hammond RM, Thompson S, Wilson S, Bean NH, Griffin PM, and Slutsker L. 2000. *Vibrio parahaemolyticus* infections in the United States, 1973-1998. *Journal of Infectious Diseases.* 181(5): 1661-1666.

Eiler A, Johansson M, and Bertilsson S. 2006. Environmental influences on *Vibrio* populations in northern temperate and boreal coastal waters (Baltic and Skagerrak Seas). *Applied and Environmental Microbiology.* 72(9): 6004-6011.

Farid AF and Larsen JL. 1981. Growth of *Vibrio alginolyticus*: Interacting effects on pH, temperature, salt concentration, and incubation time. *Zentralblatt für Bakteriologie Mikrobiologie und Hygiene: I. Abt. Originale C: Allgemeine, angewandte und ökologische Mikrobiologie.* 3(4): 68-75.

Farmer JJ and Janda JM. 2005. Order XI. “Vibrionales” In: Brenner DJ, Kreig NR, and Staley JT (eds). *Bergey's manual of systematic bacteriology. Vol. 2. The Proteobacteria. Part B, the Gammaproteobacteria*. Springer, New York, NY. 491-556.

Frans I, Michiels CW, Bossier P, Willems KA, Lievens B, and Rediers H. 2011. *Vibrio*

anguillarum as a fish pathogen: virulence factors, diagnosis and prevention. *Journal of Fish Diseases*. 34(9): 643-661.

Froelich BA and Daines DA. 2020. In hot water: effects of climate change on *Vibrio*–human interactions. *Environmental Microbiology.* 22(10): 4101-4111.

Hendrix TR. 1971. The pathophysiology of cholera. *Bulletin of the New York Academy of Medicine.* 47(10): 1169-1180.

Horie S, Okuzumi M, Kato N, and Saito K. 1966. Comparative observation on the range of growth temperature among three biotypes of *Vibrio parahaemolyticus*. *Bulletin of the Japanese Society of Scientific Fisheries.* 32(5): 424-426.

Kavic SM, Frehm EJ, and Segal AS. 1999. Case studies in cholera: lessons in medical history and science. *Yale Journal of Biology and Medicine.* 72(6): 393-408.

Klontz KC, Lieb S, Schreiber M, Janowski HT, Baldy LM, and Gunn RA. 1988. Syndromes of *Vibrio vulnificus* infections clinical and epidemiologic features of Florida cases, 1981-1987. *Annals of Internal Medicine.* 109(4): 318-323.

Lightner DV and Lewis DH. 1975. A septicemic bacterial disease syndrome of Penaeid shrimp. *Marine Fisheries Review.* 37(5-6): 25-28.

Miyamoto Y, Nakamuma K, and Takizawa K. 1961. Pathogenic halophiles. Proposals of a new genus "*Oceanomonas*" and the amended species names. *Japanese Journal of Microbiology.* 5(4): 477-486.

Pollitzer R. 1954. Cholera studies. *Bulletin of the World Health Organization.* 10(3): 421-461.

Ralston EP, Kite-Powell H, and Beet A. 2011. An estimate of the cost of acute food and water borne health effects from marine pathogens and toxins in the United States. *Journal of Water & Health.* 9(4): 680-694.

Sanches-Fernandes GMM, Sá-Correia I, and Costa R. 2022. Vibriosis outbreaks in aquaculture: addressing environmental and public health concerns and preventive therapies using gilthead seabream farming as a model system. *Frontiers in Microbiology.* 13: 904815.

Schroeder JP, Wallace JG, Cates MB, Greco SB, and Moore WB. 1985. An infection by *Vibrio alginolyticus* in an Atlantic Bottlenose Dolphin housed in an open ocean pen. *Journal of Wildlife Diseases.*21(4): 437-438.

Selvin J and Lipton AP. 2003. *Vibrio alginolyticus* associated with white spot disease of *Penaeus monodon. Diseases of Aquatic Organism.* 57: 147-150.

Slifka KM, Newton AE, and Mahon BE. 2017. *Vibrio alginolyticus* infections in the USA, 1988-2012. *Epidemiology & Infection.* 145:1491-1499.

Takemura AF, Chien DM, and Polz MF. 2014. Associations and dynamics of Vibrionaceae in the environment, from the genus to the population level. *Frontiers in Microbiology*. 5(38). https://doi.org/10.3389/fmicb.2014.00038.

Thompson FL, Iida T, and Swings J. 2003. Biodiversity of Vibrios. *Microbiology and Molecular Biology Reviews*. 68(3): 403-431.

Thompson FL and Swings J. 2006. Taxonomy of Vibrios. In: Thompson FL, Austin B, and Swings J (eds). *The Biology of Vibrios*. ASM Press, Washington DC. 29-43.

Turner JW, Good B, Cole D, and Lipp EK. 2009. Plankton composition and environmental factors contribute to *Vibrio* seasonality. *The ISME Journal*. 3: 1082-1092.

Vezzulli L, Pruzzo C, Huq Am and Colwell RR. 2010. Environmental reservoirs of *Vibrio cholerae* and their role in cholera. *Environmental Microbiology Reports.* 2(1): 27-33.

Weis KE, Hammond RM, Hutchinson R, and Blackmore CGM. 2011. Vibrio illness in Florida, 1998-2007. *Epidemiology and Infection.* 139: 591-598.

Zhang XH, He X, and Austin B. 2020. *Vibrio harveyi*: a serious pathogen of fish and invertebrates in mariculture. *Marine Life Science & Technology*. 2: 231-245.

Zorrilla I, Moriñigo MA, Castro D, Balebona MC, and Borrego JJ. 2003. Intraspecific characterization of *Vibrio alginolyticus* isolates recovered from cultured fish in Spain. *Journal of Applied Microbiology*. 95(5): 1106-1116.

CHAPTER 2

VIBRIO ALGINOLYTICUS: A REVIEW OF AN EMERGING MARINE PATHOGEN AND THE IMPLICATIONS FOR HUMAN AND ENVRIONMENTAL HEALTH

Norfolk WA and Lipp EK. To be submitted to *Molecular and Microbiology Reviews*.

Summary

Vibrio alginolyticus is an autochthonous marine bacterium known to cause opportunistic infection in both human and animal populations. This bacterium is a significant source of human extraintestinal infections and poses a serious economic risk to aquaculture facilities where outbreaks can lead to mass mortality of target species. To date, research has largely dismissed *V. alginolyticus* as a major *Vibrio* pathogen with the majority of published studies favoring *V. cholerae*, *V. parahaemolyticus*, and *V. vulnificus*. Recent increases in vibriosis infections worldwide due to anthropogenically-induced climate change has sparked renewed interest in lesser characterized vibrios. Here were review *V. alginolyticus* with respect to its ecology and pathogenicity. Focus is given to the baseline ecology of this bacterium and how ecological adaptations may play a role in disease transmission or exposure. Furthermore, we conclude with a summarization analysis of *V. alginolyticus* clinical cases in the Unites States to stress the importance of this bacterium as a public health concern. Through this work we aim to highlight the importance of *V. alginolyticus* as an emerging pathogen and encourage continued research to improve management of disease.

Discovery and Nomenclature. First described formally in Miyamoto et al. (1961), the origins of *V. alginolyticus* stem from earlier investigations of human illness outbreaks in Japan by Fujino et al. (1953) and Takikawa, (1958). Fujino et al. (1953) examines the causative agent of a food poisoning outbreak linked to sardine ingestion in 1950. During this study, the authors isolated a putative pathogen from the viscera of patients and fishes which they named "*Pasteurella parahemolytica*" (Fujino et al., 1953). Five years later, Dr. Takikawa of the National Yokohama Hospital managed a group outbreak of acute gastroenteritis where he isolated a halophilic bacterium from the feces of infected patients and suspected source foods. He identified the

bacterium to be similar to other species belonging to the genus *Pseudomonas* giving it the name "*Pseudomonas enteritis*" (Takikawa, 1958). Upon further investigation, Dr. Takikawa reclassified the strain identified by Fujino et al. (1953) to be the same species demarcating the two strains as serotype I (Fujino) and II (Takikama) (Takikawa, 1958). Following these initial studies, intermittent outbreaks of food poisoning were observed along the Pacific coast of Japan in association with mackerel ingestion. In a series of reports (Miyamoto et al., 1960; Miyamoto et al., 1961a; Miyamoto et al., 1961b), Miyamoto et al. identified *P. enteritis* as the putative agent of disease isolating the bacterium from patient feces, mackerel samples, and sea water collected from the Tokyo and Sagami Bays. These papers combined with the work of Fujino et al. (1953) and Takikawa, (1958) laid the groundwork for the recognized describing literature by Miyamoto et al. (1961).

Miyamoto et al. (1961) delves into detailed characterizations of the strains discovered by the aforementioned early works and proposes the adoption of a new genus "*Oceanomonas.*" Biochemically, the authors describe the bacteria(um) in question as similar to *Vibrio* and *Aeromonas* but differentiate them from these taxa on the grounds that the strains hold "low grade halophilic characters." From this characterization, the authors describe three species *O. enteritidis, O. parahaemolytica, O. alginolytica*: the latter of which possessed the ability to utilize sodium alginate (and would later be reclassified as *V. alginolyticus*) (Miyamoto et al., 1961).

Continued research by Sakazaki et al. (1963) rejected the proposal of "*Oceanomonas*" on the grounds that the observed halophilism of the bacterium should not take precedence taxonomically over the results of morphological and biochemical characterization. Instead, the authors of this work proposed that *O. enteritidis, O. parahaemolytica*, and *O. alginolytica* were

all members of the same species belonging to the previously described genus *Vibrio* (Sakazaki et al., 1963). Under the new species termed "*Vibrio parahaemolyticus*," the authors designated the Miyamoto et al. (1961) strains *O. enteritidis* and *O. parahaemolytica* to be *V. parahaemolyticus* biotype I (termed "subgroup" in the paper) and *O. alginolytica* to be *V. parahaemolyticus* biotype II (Miyamoto et al., 1961; Sakazaki et al., 1963). Shortly after, a detailed characterization of these two biotypes was performed by Zen-Yoji et al. (1965) which concluded that strains of biotype I were the causative agents of seafood-linked foodborne illness and that strains of biotype II were nonpathogenic. This characterization led to a revision of the original *V. parahaemolyticus* proposal by Sakazaki, (1968) suggesting that biotype II strains be reclassified as a separate species which the author coined as "*Vibrio alginolyticus*" (named after the "alginolytica" epithet derived from Miyamoto et al., 1961). In this revision, the author suggests that the pathogenicity differences described by Zen-Yoji et al. (1965) combined with the consistent observation that biotype II strains exhibited bacterial swarming capability warranted the reclassification of a new species. Interestingly, the author also notes that while the "alginolytica" moniker of Miyamoto et al. (1961) should be preserved in this reclassification, alginate utilization was not characteristic of all members of this designation and thus is a misnomer (Miyamoto et al., 1961; Sakazaki et al., 1963; Zen-Yoji et al., 1965; Sakazaki, 1968).

The final deviation in *V. alginolyticus* nomenclature came two years later with the research of Baumann et al. (1971). In this work, the authors reclassified *V. alginolyticus* (as well as several other similar species) to be members of the previously described genus "*Beneckea.*" At the time of publication, the authors justified this reclassification on the grounds of GC-content analysis and the observed development of peritrichous flagella when grown on solid media. These characteristics differed from the known traits of *V. cholerae* (the type strain for the genus

Vibrio) thus leading the authors to designate the species *B. alginolyticus* (Baumann et al., 1971). Following this study, the nomenclature *B. alginolyticus* persisted as a synonym for *V. alginolyticus* in the published literature with differing preferential usage depending on the author. Facing scrutiny from this reclassification and evidenced by data collected using new phylogenetic identification methods (rRNA homology, glutamine synthase divergence, and superoxide dismutase divergence), the genus *Beneckea* was abolished in a subsequent publication in 1980 (Baumann et al., 1971; Baumann et al., 1980). This abolition returned *V. alginolyticus* to the genus *Vibrio* where the bacterium remains to this day.

In a concomitant study with Myiamoto et al. (1961), O'Neill et al. (1961) describes the bacterium *Pseudomonas creostonesis* while investigating the degradation of creosote-treated wood pilings by marine bacteria in Hueneme Harbor, CA (O'Neill et al., 1961). While occurring independently of the works described above, this bacterium was later reclassified using DNA:rRNA hybridization to Vibrionaceae where it became a synonym of *V. alginolyticus* (De Vos et al., 1989).

Baseline Characteristics. *V. alginolyticus* is a ubiquitous Gram-negative bacterium classified taxonomically in the phylum *Proteobacteria*, class *Gammaproteobacteria*, order *Vibrionales*, family *Vibrionaceae*, and genus *Vibrio* (Farmer & Janda, 2005; Thompson & Swings, 2006). Structurally, cells are ~0.5µm wide and ~1µm long exhibiting a characteristic vibrio or "comma" shape with shorter length involution forms occurring under stressful growth conditions (Miyamoto et al., 1961; Sakazaki et al., 1963; Farmer & Janda, 2005). Metabolically, *V. alginolyticus* is a chemoorganotrophic, facultative anaerobe. Capable of respiratory and fermentative metabolism, *V. alginolyticus* can utilize D-glucose as a sole carbon source but does not produce gaseous byproducts under anaerobic conditions (Farmer & Janda, 2005). In addition

to glucose, *V. alginolyticus* is also capable of fermentation of cellobiose, maltose, D-mannitol, D-mannose, sucrose, glycerol, and trehalose (Pezzlo et al., 1979; Farmer & Janda, 2005). All strains are oxidase and nitrate reduction positive with strain-specific disagreement on the results of Voges–Proskauer and indole tests (Jo Rubin & Tilton, 1975; Pezzlo et al., 1979; Farmer & Janda, 2005; Nishibuchi, 2006). Similar to most *Vibrio* spp., salt is required to stimulate the growth of *V. alginolyticus*. Growth has been observed in salt content ranging from 0.4% to +12% (w/v) with an optimal salt concentration of ~3% (w/v) and a tolerable range (none to minimal growth inhibition) of 1% to 6% (w/v) (Jo Rubin & Tilton, 1975; Pezzlo et al., 1979; Farmer & Janda, 2005; Nishibuchi, 2006). A motile species, *V. alginolyticus* can express polar or lateral flagella. Growth in liquid media stimulates the production of a single sheathed polar flagellum allowing the bacterium to swim rapidly. Transfer to solid media promotes the formation of multiple lateral flagella and elongation of the cells allowing them to spread over the surface (Ulitzer 1975a; Atsumi et al., 1996; Farmer & Janda, 2005; Böttcher et al., 2016). This differentiation is also known to promote the formation of swarming behavior on some types of media however, further research is needed to identify the specific environmental and/or nutritional mechanisms needed to induce this behavior (Ulitzer, 1975a; Farmer & Janda, 2005; Böttcher et al., 2016).

Culture and Detection. In culture, *V. alginolyticus* grows sufficiently well on most standard media so long as the components contain a suitable substrate and adequate salt concentration. Optimal growth occurs at 35 ± 2 ^{o}C however, growth is possible at incubation temperatures ranging from 20 to 42 ^{o}C (Ulitzer, 1975b; Farid & Larsen, 1981; Farmer & Janda, 2005). Due to the robust growth rate and mucoid appearance of *V. alginolyticus* CFU, a reduced incubation temperature of 30 ± 2 ^{o}C is often used to decrease overcrowding on the culture plates for

quantification and isolation experiments. For general growth, *V. alginolyticus* is typically cultured on thiosulfate citrate bile salts sucrose agar (TCBS), Luria-Bertani broth/agar amended with additional NaCl to 2%-4% w/v (LBS), tryptic soy agar/broth (TSA/TSB) agar/broth amended with additional NaCl to 2%-4% w/v, marine agar/broth, and half marine agar/broth amended with additional NaCl to 2%-4% w/v (Farmer & Janda, 2005; Gil-Gomez & Roque, 2006). For growth in minimal media, *V. alginolyticus* is amendable to M9 minimal salts (and most derivations of this) as well as specialized artificial sea water media derivations (H-Aquil, VibFeL, artificial sea water, yeast, peptone, extract [ASW-YPE]) (Martocello et al., 2019, Zhang et al., 2019, Westrich et al., *unpublished data*). Growth on standard media produces circular, mucoid colony forming units (CFU) that are white to tan in color with a shiny or matte sheen (depending on the media type) and a regular shape. On highly nutritious solid media such as LBS 3% NaCl, *V. alginolyticus* will often swarm coating the media with a translucent layer of growth. Growth on TCBS produces regular circular CFU that are yellow in color with a mucoid appearance and reduces the change of swarming development. To date, there is no commercially available chromogenic media that can readily distinguish *V. alginolyticus* from other vibrios, however; prior research has demonstrated that the use of a modified version of brain heart infusion (BHI), termed *Vibrio alginolyticus* agar (VAL), may produce discriminable results (Chang et al., 2011). It should be noted that while non-differential, *V. alginolyticus* will readily grow on ChromAgar™ *Vibrio* appearing white in color with highly mucoid CFU.

Early efforts to detect *V. alginolyticus* often applied the use of a series of biochemical tests supplemented with antibiotic resistance characterization using Kirby Brower disk diffusion (Pien et al., 1977; Schmidt et al., 1979; Spark et al., 1979). These biochemical tests later developed into panel assays such as the Analytical Profile Index (API) 20E which was widely

used before the advent of molecular methods (Overman et al., 1985). Modern variations of these panel assays such as the VITEK® system still persist today and in some clinical settings (O'Hara et al., 2003). However, these assays have been widely replaced by molecular-based detection methods (discussed below).

Molecular Detection. Due to the lack of a defined culture-based method for *V. alginolyticus* identification, culture-independent techniques remain the accepted methods for detection and reporting of this species. At current, there is no standardized protocol for the identification of *V. alginolyticus* in clinical, food, water, or other environmental sources designated by an official governing body. However, prior studies have developed a range of different polymerase chain reaction- (PCR) and sequencing-based detection methodologies for identification. Common PCR targets (for direct detection or amplicon sequencing) for *V. alginolyticus* include the housekeeping genes 16Sr RNA (Thompson et al., 2004; Yong et al., 2006), *hsp* 60 (Jesser & Noble 2018; King et al., 2019), *dnaJ* (Nhung et al., 2007; Zhou et al., 2007; Tall et al., 2012), *gyrB* (Lou & Hu, 2008; Cai et al., 2010a; Reilly et al., 2011), the general *Vibrio* pathogenicity gene *ToxR* (Fu et al., 2016; Yin et al., 2018; Dong et al., 2020), and the *V. alginolyticus* gene for collagenase (Di Pinto et al., 2005; Di pinto et al., 2006). For specific detection of *V. alginolyticus*, direct PCR-based methods (endpoint PCR, qPCR, etc.) are generally preferred over sequencing due to the decreased cost and ease of sample processing. Clinical detection has favored the use of quantitative PCR (qPCR) or multiplex PCR to target one or more of these genes and is most often used to test samples against a panel of pathogenic vibrios (typically *V. alginolyticus, V. parahaemolyticus, V. vulnificus,* and *V. cholerae*) to identify the putative agent of disease (Di Pinto et al., 2005; Nhung et al., 2007; Reilly et al., 2011; Yin et al., 2018). Efforts to detect *V. alginolyticus* from environmental water and/or food samples is most often associated

with the monitoring of mariculture facilities. Surveillance methods have been developed utilizing end-point PCR (Lou & Hou, 2008), qPCR (Zhou et al., 2007; Tall et al., 2012), loop-mediated isothermal amplification (LAMP) (Fu et al., 2016; Yin et al., 2018), and isothermal recombinase polymerase amplification with lateral flow dipsticks (RPA-LFD) (Dong et al., 2020). It should be noted that several of these assays have cross usage for both clinical and environmental samples. Sequencing-based methods, while valid for the identification of *V. alginolyticus*, are typically employed broadly for the determination of *Vibrio* community structure rather than the specific identification of *V. alginolyticus*. Common methods of *Vibrio* community sequencing include amplicon sequencing of the 16Sr RNA gene (Thompson et al., 2004; Yong et al., 2006), the *hsp* 60 gene (Jesser & Noble, 2018; King et al., 2019), and the *dnaJ* gene (Nhung et al., 2019). Approaches using shotgun sequencing are most often reserved for the determination of whole genomes for specific strains of *V. alginolyticus* rather than species-level identification (Liu et al., 2015; Deb et al., 2020).

Habitat and Ecology. Geographically, *V. alginolyticus* is a ubiquitous member of coastal and estuarine habitats with reports of the bacterium off every continent, excluding Antarctica (Miyamoto et al., 1961; Prociv, 1978; Schmidt et al., 1979; Reilly et al., 2011; Baker-Austin et al., 2018; Abyoie et al., 2021). Consistent with other salt-requiring *Vibrio* spp., the distribution and abundance of *V. alginolyticus* is limited primarily by temperature in salinity where optimal salinity conditions (near 35) and warm surface waters drive increased seasonal abundance of the bacterium (Maeda et al., 2003; Böer et al., 2013, Takemura et al., 2014). Other environmental correlates (chlorophyll A, nitrogen, phosphorus, zooplankton/phytoplankton presence, pH, iron content, dissolved organic carbon, dissolved oxygen, and turbidity) have been shown to influence total *Vibrio* communities to a lesser degree in regional studies, however the

influence(s) of these factors has not been established for *V. alginolyticus* directly and may be location/community-specific (Thompson et al., 2004; Eiler et al., 2006; Hsieh et al., 2007; Turner et al., 2009; Asplund et al., 2011; Oberbeckmann et al., 2011a; Takemura et al., 2014). Studies examining the total *Vibrio* community composition in environmental samples frequently rate *V. alginolyticus* as one of the most abundant species detected suggesting that this bacterium may be a dominant member of the *Vibrio* community in natural systems (Maeda et al., 2003; Asplund et al., 2011; Oberbeckmann et al., 2011b; Oberbeckmann et al., 2011c; Böer et al., 2013, Xu et al., 2020).

Within the water column, *V. alginolyticus* is known to exist in both the free-living (planktonic) and particle-associated (attached to suspended particles or plankton) fractions of pelagic bacterioplankton (Carli et al., 1993; Baffone et al., 2006; Asplund et al., 2011; Oberbeckmann et al., 2011c; Takemura et al., 2014; Jesser & Noble, 2018; Clinton et al., 2020). It remains unclear what environmental or genetic factors contribute to the adoption of one lifestyle over another however, prior research investigating total *Vibrio* or other *Vibrio* spp. has suggested that stressful environmental/nutritional conditions (Hood & Winter, 1997; Worden et al., 2006; Takemura et al., 2014; Liang et al., 2019), avoidance of protozoan predators (Worden et al., 2006; Asplund et al., 2011; Main et al., 205), and/or the presence of exploitable biological compounds such as chitin (Pruzzo et al., 1996; Zhang et al., 2018) may influence adoption of particle-association. In addition to pelagic waters, *V. alginolyticus* is also found in association with marine and estuarine sediments. Several prior studies have suggested that sediment is an important reservoir for this bacterium, and that colonization of this habitat may enhance survivability during harsh environmental conditions such as wintering (Dumontet et al., 2000; Harriague et al., 2008; Böer et al., 2013) . Furthermore, Böer et al. (2013) found that culturable

levels of *V. alginolyticus* (as well as *V. parahaemolyticus* and *V. vulnificus*) were several orders of magnitude greater in sediment than the overlying water in summer months suggesting that sediment may represent an important habitat for these *Vibrio* spp. beyond wintering persistence.

Associations with Plankton. Beyond the ambient environment, *V. alginolyticus* is known to commonly associate with plankton. Planktonic colonization is hypothesized to provide similar selective advantages to abiotic particle attachment and thus the two are typically discussed in combination as the particle-associated fraction (Takemura et al., 2014). It has been well documented that zooplankton can serve as an environmental reservoir for *Vibrio* spp. and that increased zooplankton abundance is correlated with increased particle-associated *Vibrio* (Huq et al., 1996; Colwell et al., 2003; Turner et al., 2009; Sampaio et al., 2022). Studies examining this relationship for *V. alginolyticus* specifically have shown that the bacterium can colonize the exoskeleton and/or gastrointestinal tract of chitinous zooplankton (Carli et al., 1993; Pruzzo et al., 1996; Montanari et al., 1999; Clinton et al., 2020; Norfolk et al., 2022). Exoskeletal attachment has been described in the works of Carli et al. (1993) and Pruzzo et al. (1996) and is mediated by a membrane protein system capable of recognizing and binding to chitin. This system in combination with *V. alginolyticus* chitinases (Murao et al., 1992; Ohishini et al., 1996) suggests that exoskeletal association provides a nutritional advantage to this bacterium through utilization of chitin as a substrate (Pruzzo et al., 1996; Erken et al., 2015). The rationale behind gastrointestinal colonization of zooplankton remains poorly understood. Recent work by Norfolk et al. (2022) demonstrated that *Artemia* spp. will accumulate *V. alginolyticus* within the gastrointestinal tract following waterborne exposure to the elevated levels of the bacterium however, it is unknown if this colonization is due to incidental ingestion, proliferation of the bacterium within the gastrointestinal tract, and/or purposeful chemotaxis. Regardless of the

location of colonization, studies have shown that ingestion of *Vibrio*-colonized (*V. cholerae* [Huq et al., 1996; Nelson et al., 2009], *V. alginolyticus* [Norfolk et al., 2022], and *V. owensii* [Goulden et al., 2012]) zooplankton can facilitate receipt of a potentially pathogenic dose in susceptible hosts suggesting that this ecological adaptation may play a role in the transmission of *Vibrio*-diseases.

Phytoplankton are similarly known to be colonized by *Vibrio* spp. and make up a significant portion of the particle-associated community (Turner et al., 2009; Takemura et al., 2014; Main et al., 2015). *Vibrio* community studies have suggested that phytoplankton abundance may have species-specific effects on *Vibrio* abundance with some studies showing a positive correlation (Asplund et al., 2011; Main et al., 2015) and other showing a negative correlation (Turner et al., 2009). This disagreement can potentially be explained by the location-specific composition of the phytoplankton and *Vibrio* communities where prior research has shown that some *Vibrio* spp. may be able to synergistically utilize algal exudates whereas other species combinations may be antagonistic (Turner et al., 2009; Takemura et al., 2014; Main et al., 2015). These relationships have been observed specifically for *V. alginolyticus* where attractive chemotactic responses were observed in relation the algal exudates of *Synechococcus* and *Prochlorococcus* (Seymour et al., 2010) as well as glycolic acid, acrylic acid, and dimethyl sulfide (Sjoblad & Mitchell, 1979). *V. alginolyticus* antagonism has been documented in association with the microalgae *Chlorella minutissima*, *Tetraselmis chui*, *Nannochloropsis*, *Arthrospira platensis*, *Isochrysis*, and *Chaetoceros calcitrans* (Kokou et al., 2012; Interaminense et al., 2014; Molina-Cárdenas et al., 2014). Though the mechanism(s) of this antagonism are unknown, researchers hypothesize that secondary metabolites such as fatty acids produced by these microalgae exhibit antibacterial properties (Kokou et al., 2012; Molina-Cárdenas et al.,

2014). Use of antagonistic species has been recommended as a method of biological control to promote reduction of *V. alginolyticus* in aquaculture facilities (Interaminense et al., 2014; Molina-Cárdenas et al., 2017).

Associations with Animals. In addition to plankton, *V. alginolyticus* is known to colonize and/or concentrate on/within marine and estuarine macrofauna. While the majority of research regarding this bacterium and larger organisms has focused on pathogenic relationships (discussed below in "Pathogenicity in Animals"), here we discuss examples of commensal and mutualistic association. It should be noted that some of these relationships have only been described casually thus, the full extent of their symbioses may not yet be understood.

One of the more curious examples of *V. alginolyticus* animal associations is the relationship between this bacterium and tetrodotoxin- (TTX) containing organisms. There is strong evidence to suggest that TTX is produced through mutualistic or commensal bacterial symbiosis (reviewed by Chau et al., 2011, Pratheepa & Vasconcelos, 2013 and Magarlamov et al., 2017). While it has been suggested that different bacterial species may be involved in TTX production, several studies have found *V. alginolyticus* in association with TTX-containing puffer fish (Noguchi et al., 1987; Yu et al., 2004), horseshoe crabs (Kungsuwan et al., 1988), marine worms (Thuesen & Kogure, 1989), sea stars (Narita et al., 1987), and mollusks (Cheng et al., 1995). Despite this association, the biosynthetic pathway of TTX production remains unknown. Efforts to replicate bacterial TTX synthesis has produced mixed results with low levels of toxin produced compared to those measured within wild hosts (Pratheepa & Vasconcelos, 2013). These data suggest that TTX accumulation may require a host-mediated enhancer or inducer that promotes increased toxin production and/or may be the result of biomagnification of toxin-producing microorganisms in higher trophic-level hosts (Chau et al.,

2011; Pratheepa & Vasconcelos, 2013). It should be noted that studies have questioned the validity of *V. alginolyticus* as a TTX-producing bacterium suggesting that detection of the toxin may be a false positive result (Matsumura, 1995; Strand et al., 2016). Recent work by Bacchiocchi et al. (2021) investigated *V. alginolyticus* TTX production in relation to nonribosomal peptidesynthetase (NRPS) and polyketide synthase (PKS) genes; two genes hypothesized to involved in TTX biosynthesis (Chau et al., 2011). While NRPS and PKS positive *V. alginolyticus* strains were detected, TTX was not detected in any samples collected throughout this study (Bacchiocchi et al., 2021). Further research is needed to corroborate the role of *V. alginolyticus* in the bacterial biosynthesis of TTX.

Beyond TTX-organisms, *V. alginolyticus* has been found in casual association with several species of aquatic macrofauna. Environmental sampling studies have detected *V. alginolyticus* in commensal association with bivalves (Beleneva et al., 2004; González-Escalona et al., 2006; Miller et al., 2006; Schets et al., 2010), benthic worms (Miller et al., 2006), corals (Ducklow & Mitchell, 1979; Hörmansdorfer et al., 2000; Alves et al., 2010), echinoderms (Beleneva et al., 2004), crustaceans (Beleneva et al., 2004; Miller et al., 2006), and sponges (Hoffmann et al., 2010). Under the scope of these studies, it is unclear if the detection of *V. alginolyticus* within these organisms is due to purposeful colonization or incidental association due to presence in the ambient seawater and/or suspended particulates. Seafood surveillance frequently detects *V. alginolyticus* in association with various species of marine fishes (Chan et al., 1986; Baffone et al., 2000; Buck, 2008; Oh et al., 2011; Lucero-Mejía et al., 2020; Neetoo et al., 2022) and mollusks (Vasconcelos et al., 1975; Molitoris et al., 1985; Chan et al., 1986; Buck, 2008; Vu et al., 2018; Song et al., 2020; Lucero-Mejía et al., 2020; Neetoo et al., 2022). Collection of surveillance samples are typically acquired from seafood processing facilities,

mariculture facilities, or seafood markets thus the mechanisms and/or rational for *V. alginolyticus* colonization of these species is often unknown. Furthermore, research on cartilaginous fishes has suggested that *Vibrio* spp. are common bacterial flora of shark oral, gastrointestinal, and organ tissues (Grimes et al., 1985; Grimes et al., 1993). Specifically, *V. alginolyticus* has was found to be strongly associated with the eyes, mouth, and stomach of sharks suggesting that exposure to the ambient water may facilitate colonization (Grimes et al., 1985).

Associations with Plants. In contrast to fauna, the relationship between *V. alginolyticus* and aquatic plants is vastly understudied. It is known that *Vibrio* spp. can be found in association with the epiphytic communities of marine plants such as seagrasses (Kurilenko et al., 2001; Cai et al., 2021) and macroalgae (Beleneva & Zhukova, 2006; Wang et al., 2009; Barberi et al., 2019; Selvarajan et al., 2019) however, little is known about the roles(s) that specific *Vibrio* spp. play in the ecology of these communities. Research has suggested that epiphytic colonization may enhance survivability of *Vibrio* spp. during harsh conditions (similar to sediment colonization) (Islam et al., 1994) however, further research is needed to corroborate this hypothesis for *V. alginolyticus* specifically. A recent study by Reusch et al. (2021) demonstrated that decreased abundance of eelgrass (*Zostera marina*) coverage was correlated with increased abundance of pathogenic *Vibrio* spp. (including *V. alginolyticus*) in the water column suggesting that these communities have an inhibitory effect on the abundance of *Vibrio* population. The authors hypothesize that this decrease is likely associated with improved general water quality characteristics (i.e., increased sedimentation, presence of filter feeding organisms, etc.) of grass beds that are known to facilitate a reduction in waterborne bacteria (Lamb et al., 2017).

Pathogenicity in Animals. *V. alginolyticus* pathogenicity has been described in several species of aquatic animals with infection severity ranging from mild lesions to total mortality of the individual. Infections can be loosely characterized by the major groups of host species and primarily affect marine invertebrates and bony fishes with a few instances of disease occurrence in larger organisms such as marine mammals, sea turtles, and cartilaginous fishes. A summary of the susceptible animal hosts of *V. alginolyticus* can be found in Table 1.

Invertebrate and bony fish infections have been widely described in association with aquaculture facilities. Facility-level outbreaks of vibriosis (a term for non-Cholera vibrio infections) has fueled a large body of research interest to ameliorate the economic losses associated with these mortality/morbidity events. Reports of these outbreaks occur in facilities worldwide with the majority of cases centered in Asia, India, and countries bordering the Mediterranean or Red Sea (Colorini et al., 1981; Balebona et al., 1998; Selvin & Lipton, 2003; Liu et al., 2004). While our understanding of the mechanisms of *V. alginolyticus* transmission/exposure varies from study to study; typically, these outbreaks are associated with opportunistic infection where the host species becomes stressed due to suboptimal rearing conditions (i.e., poor water quality, overcrowding, injury, etc.) (Mohney et al., 1994; Liu et al., 2004; Austin & Austin 2012). This stress combined with water conditions favorable for the proliferation of *V. alginolyticus* (and similar *Vibrio* spp.) creates a situation optimal for the onset of infection (Mohney et al., 1994; Sung et al., 2001). It should be noted that many outbreaks are associated with multiple *Vibrio* spp. and/or additional microorganisms as co-infectors and thus *V. alginolyticus* may not be the sole pathogen in all instances of disease (Colorni et al., 1981; Li et al., 1999; Kumar et al., 2017; Xue et al., 2017).

While the effects of aquaculture outbreaks can adversely impact numerous host species, facilities targeting the growth of Penaeid shrimp/prawns (Penaeidae) and seabreams (Sparidae) are some of the most heavily impacted (Colorni et al., 1981; Selvin & Lipton, 2003; Lui et al., 2004; Abdel-Aziz et al., 2013). Penaeid shrimp/prawns are economically important shellfish species that are widely cultured in facilities worldwide (Boyd & Jescovitch, 2020). Gross signs of penaeid infection typically manifest as discoloration of the body, lethargy, and anorexia. Pathologic examination typically reveals damage to the hepatopancreas, bacterial septicemia, and hemolymph dysfunction often resulting in mass mortality of the affected species (Lightner & Lewis, 1975; Selvin & Lipton, 2003; Abdel-Aziz et al., 2013). Similar disease signs have been reported in outbreaks of aquaculture-reared lobsters (*Panulirus* spp.) (Abraham et al., 1996; Bourne et al., 2007) and swimming crabs (Wang et al., 2006) suggesting that these signs may be characteristic of systemic *V. alginolyticus* infection in crustaceans. Several studies also identify *V. alginolyticus* as a potential contributing pathogen to shell disease syndrome, a disease characterized by degradation of the chitinous exoskeleton of aquatic arthropods by chitinolytic bacteria (Vogan et al., 2002; Mancuso et al., 2010). Descriptions of shell disease are characterized by multifocal lesions on the carapace suggesting that development of this disease may differ from systemic infection and is linked to the ability of *V. alginolyticus* to opportunistically attach to and degrade the exoskeleton (Mancuso et al., 2010). However, continual degradation at the lesion site can result in breach of the carapace leading to infiltration of the bacterium into tissues facilitating the onset of disease signs consistent with systemic infection (Mancuso et al., 2010).

Seabreams (Sparidae) known commonly as porgies, are broadly cultivated in aquaculture due to their high survivability, cultivation ease, and market price (Cardia & Lovatelli, 2007).

Seabream aquaculture is concentrated in countries bordering the Mediterranean or Red Sea and often targets the cultivation of gilthead seabream (*Sparus aurata*) (Arechavala-Lopez et al., 2017; Rigos et al., 2020). Gross signs of *V. alginolyticus* infection of these fishes typically present as discoloration, lesions (often hemorrhagic), abdominal swelling, and eye damage. Pathological signs include organ damage (swelling, congestion, and dysfunction), hemorrhage, and accretion of ascitic fluid often leading to mortality (Colorni et al., 1981; Balebona et al., 1998; Zorrilla et al., 2003; Abdel-Aziz et al., 2013). Similar disease signs have been described in aquaculture facilities targeting other species of bony fish including flatfish (Austin et al., 1993; Zorrilla et al., 2003), grouper (Lee, 1995; Mohamad et al., 2019), tilapia (El-Sayed et al., 2019), sea bass (Zorrilla et al., 2003; Abdel-Aziz et al., 2013; Ragab et al., 2022), milkfish (Muroga et al., 1984), snapper (Cai et al., 2010), and seahorses (Martins et al., 2010; Xie et al., 2020) suggesting that these symptoms are broadly characteristic of *V. alginolyticus* infection in bony fishes. Collectively, these outbreaks are commonly referred to as vibriosis, hemorrhagic septicemia, and/or bacterial septicemia in aquaculture literature.

In addition to crustaceans and bony fishes, *V. alginolyticus* has also been implicated in aquaculture outbreaks of mollusks, sea cucumbers, as well as captive-reared cartilaginous fishes, marine mammals, and sea turtles. Mollusk infection, often referred to as bacillary necrosis, is characterized by reduced swimming ability, lethargy, weakness of the adductor muscle or foot (gastropods and bivalves), epidermal lesions (cephalopods) and tissue necrosis (Luna-González et al., 2002; Sangster & Smolowitz, 2003; Gómez-León et al., 2005; Cai et al., 2006; Kua et al., 2011). Sea cucumber infection has been described in *Holothuria* spp. and *Apostichopus* spp. and presents with epidermal lesions followed by visceral ejection and often mortality (Zhang et al., 2015; Rafidah et al., 2017; Fahmy & Hamed, 2022). Infections of captive-reared cartilaginous

fishes, marine mammals, and sea turtles, while rare, have been described in several instances. Emam et al. (2019) describes an outbreak in captive-reared rays (*Himantura* spp.) where infection presented with epidermal lesions, lethargy, myolysis, and organ damage progressing to mortality in 25% of infected individuals. Schroeder et al. (1985) reports an incidence of infection in an Atlantic bottlenose dolphin (*Tursiops truncatus*) presenting as reoccurring epidermal lesions requiring antibiotic treatment. Glazebrook & Campbell (1990a & 1990b) report occurrences of infections in captive-raised sea turtles (*Caretta caretta, Chelonia mydas,* and *Eretmochelys imbdcata*) presenting as epidermal lesions, ulcerative stomatitis, and bronchopneumonia leading to high juvenile mortality. In all cases, *V. alginolyticus* infection presents primarily as epidermal and/or oral lesions suggesting that infections in larger animals is associated with opportunistic exposure via seawater.

Compared to aquaculture outbreaks, instances of environmental infection (non-aquaculture associated) are seldom reported in scientific literature and have been restricted to highly monitored species including, corals, sea urchins, sea turtles, and marine mammals. Coral infection has been described as two distinct tissue loss diseases, *Porites andrewsi* white syndrome (PAWS) where *V. alginolyticus* is the primary pathogen and yellow band disease (YBD) where *V. alginolyticus* is a member of a disease consortium (Cervino et al., 2008; Zhenyu et al., 2013). In both cases, infection is characterized by death of the coral tissue progressing from one or multiple origin points of the disease. PAWS is characterized by a progressively advancing margin of tissue loss resulting in a stark white appearance of the infected coral and has only been described in the species *P. andrewsi* (Zhenyu et al., 2013). YBD is a broad disease affecting several boulder coral species in the Caribbean and Indo-Pacific. Disease signs of YBD consist of characteristic “blotch” lesions were an advancing ring of yellow-white necrosis and

zooxanthellae damage expands from the point of origin (Cervino et al., 2008). Urchin infections present similarly to aquaculture reports of sea cucumber infection and are characterized by epidermal lesions, loss of spines/tube feet, and disruption of the water vascular system leading to direct or indirect (susceptible to predation) mortality (Clemente et al., 2014). Environmental reports of infection in sea turtles and marine mammals have been described predominately from incidences of strandings thus, it is often difficult to discern the role of *V. alginolyticus* in these cases. However, many stranding events include clinical signs that are characteristic of traditional *V. alginolyticus* infection such as epidermal and oral lesions (Tangredi, 1980; Orós et al., 2005; Di Renzo et al., 2017). While reporting of environmental *V. alginolyticus* is uncommon, it is reasonable to posit that susceptible host species reported from aquaculture studies may also be vulnerable to environmental infection if the ambient conditions become favorable.

Pathogenicity in Humans. Human pathogenicity of *V. alginolyticus* has been well documented. Casual reports of human infection date back to the discovery of the bacterium with the first reported clinical cases occurring in the late 1960s and early 1970s (Twedt et al., 1969; Baumann et al., 1973; Von Graevenitz & Currington, 1973; Zen-Yoji et al., 1973; Jo Rubin & Tilton, 1975). Predominately, infections with this bacterium present as opportunistic extraintestinal infections of the ears and preexisting or sustained wounds following exposure to marine or estuarine water (Slifka, et al., 2017). Human infections have been documented worldwide with the majority of cases reported in warm coastal regions and are almost always linked to direct (swimming, diving, wading, etc.) or indirect (boating, fishing, seafood processing, etc.) seawater exposure (Prociv, 1978; Hornstrup & Gahrn-Hansen, 1993; Dechet et al., 2008; Weis et al., 2011; Slifka et al., 2017). Treatment of infections varies by case but, typically includes administration of oral and/or topical antibiotics often ciprofloxacin, tetracycline, or their

derivatives (Pien et al., 1977; Pezzlo et al., 1979; Dechet et al., 2008; Reilly et al., 2011). Mortality associated with *V. alginolyticus* infection is low compared to other non-cholera vibrios with fatal infections typically restricted to severely immunocompromised individuals or victims of severe seawater-associated accidents (English & Lindberg, 1977; Bonner et al., 1983; Janda et al., 1986; Lee et al., 2008). Broad demographic patterns of infection show increased incidence in males as well as a median infection age of 33-36 (Dechet et al., 2008; Weis et al., 2011; Slifka, et al., 2017). These incidence patterns are hypothesized to be associated with increased recreational and/or occupational seawater exposure associated with younger male populations (Slifka, et al., 2017). A summary of common infection case reports can be found in Table 2 and a summary of broad infection surveys can be found in Table 3.

Of the typical *V. alginolyticus* infection types, wound infections remain the most frequently described. Two recent infection surveys from the United States by Weis et al. (2011) and Slifka, et al. (2017) found wound infections to account for 71.40% and 81.00% of the total *V. alginolyticus* cases surveyed, respectively. Of these cases, infections of the lower extremities appear most frequently and correlate strongly with the exposure of preexisting or sustained wounds to seawater (Schets et al., 2006; Slifka et al., 2017). Common symptoms of wound infections typically manifest as cellulitis (swelling, redness, pain) with wound discharge and a foul odor (Hlady & Klontz, 1996; Royle et al., 1997; Schets et al., 2006). Severe infections or cases in immunocompromised patients may progress to bacteremia, septicemia, and/or necrotizing fasciitis (discussed below) (Ho et al., 1998; Gomez et al., 2003). Treatment of infected wounds typically involves a combination of wound irrigation, cleaning, tissue debridement, and the administration of topical or oral antibiotics (Pien et al., 1977; Howard & Bennett, 1993; Slifka, et al., 2017).

The second most common type of *V. alginolyticus* human infections are ear infections. Ear infections are strongly linked to seawater exposure, particularly activities like swimming or diving where head submersion is common (Hornstrup & Gahrn-Hansen,1993). Symptoms of these infections typically present as otitis externa, otitis media, and/or damage to the tympanic membrane (Hornstrup & Gahrn-Hansen, 1993; Weis et al., 2011; Slifka et al., 2017). Unlike wound infections, preexisting or sustained injuries to the ear are not necessarily required to facilitate infection (Pien et al., 1977; Hornstrup & Gahrn-Hansen, 1993); though cases have been reported in patients with pressure-equalizing tubes (Feingold & Kumar, 2004) and in instances of accidental eardrum perforation (McSweeney et al., 1977) suggesting that injury may enhance the development and/or severity of infection. In many cases, ear infections can clear naturally but are often treated through the use of oral antibiotics and eardrops (Hornstrup & Gahrn-Hansen, 1993; Feingold & Kumar, 2004). Complications associated with ear infections are uncommon but have been reported to cause hearing damage or loss (Slifka et al., 2017). Progression of ear infections to an invasive infection has not been described suggesting a low risk of life-threatening complications with these cases.

To a lesser extent, *V. alginolyticus* has also been linked intermittently to cases of eye infection and gastrointestinal illness. Eye infections typically present as mild cases of conjunctivitis associated with individuals with frequent seawater exposures such as fishermen (Schmidt et al., 1979; Lessner et al., 1985; Penland et al., 2000). Treatment of these infections can typically be cleared using a combination of oral antibiotics and eyedrops (Schmidt et al., 1979; Lessner et al., 1985). It is uncommon for eye infections to progress to severe conditions however, complications have been observed in association with cases of traumatic eye damage such as in Li et al. (2009) where a patient developed endophthalmitis following injury to the eye

with a fishing hook. Gastrointestinal infections predominately present as mild to moderate cases of gastroenteritis following ingestion of seafood, most often raw or undercooked dishes (Hlady & Klontz, 1996; Uh et al., 2001; Slifka et al., 2017). Unlike other non-Cholera vibrios such as *V. parahaemolyticus* and *V. vulnificus*, gastrointestinal infection represents a minor proportion of the total disease burden of *V. alginolyticus* (Weis et al., 2011; Slifka et al., 2017). Slifka et al. (2017) reports that gastrointestinal infection accounted for 62 of the 1,331 (4.7%) *V. alginolyticus* infection cases reported in the United States from 1988-2012. This low incidence suggests that while possible, gastrointestinal infection may be restricted to incidences where a very high dose of the bacterium is ingested and/or a specific virulent strain is present in the seafood. It should be noted that while the clinically reported incidence of these cases is low, these infections are likely underreported due to the mild nature of their presentation.

Invasive and atypical *V. alginolyticus* infections are uncommon and have been largely restricted to cases where the patient is immunocompromised and/or suffered a traumatic injury associated with seawater exposure (Table 4). The most common type of invasive infection reported is bacteremia (Howard & Lieb, 1988; Howard & Bennett, 1993; Slifka et al., 2017). Bacteremia has been described in instances of wound and gastrointestinal infection where *V. alginolyticus* spreads from the infection site to the bloodstream (Janda et al., 1986; Ruiz & Agraharkar, 2003 Nadkarni & Shah, 2007; Lee et al., 2008; Oksuz & Gurler, 2013). Once established, bacteremia cases become life-threatening requiring hospitalization, tissue debridement, and antibiotic treatment to clear (Nadkarni & Shah, 2007; Lee et al., 2008; Oksuz & Gurler, 2013). Serious cases of bacteremia can lead to the onset of sepsis, greatly increasing the risk of death (Janda et al., 1986; Oksuz & Gurler, 2013; Gaüzère et al., 2016). Furthermore, severe wound infection cases can also lead to the development of necrotizing fasciitis which can

further exacerbate complications associated with bacteremia and has been reported in cases of fatal infection (Bonner et al., 1983; Ho et al., 1998; Gomez et al., 2003). Atypical infections are cases that produce unusual symptoms or instances where *V. alginolyticus* is isolated from an infection site that is uncharacteristic of common exposures. In all reported instances, atypical infections present in patients with an underlaying medical condition, treatment, or injury that appears to enable *V. alginolyticus* infiltration into the infection site (Table 4). Atypical cases have been reported to cause peritonitis (Taylor et al., 1981), sinusitis (Wagner et al., 1981), intercranial infection (Opal & Saxon, 1986), pleural empyema (Chien et al., 2002), respiratory distress syndrome (Gaüzère et al., 2016), osteomyelitis (Barbarossa et al., 2002), and infection associated with an implanted medical device (pacemaker) (Floch & Boutoille, 2008). These cases range in severity but were all successfully treated using the treatment regimens listed in Table 4.

Virulence Mechanisms. Similar to other non-Cholera vibrios, *V. alginolyticus* has a variety of virulence mechanisms that enhance its pathogenicity to humans and animals. As an indigenous microorganism, many of these virulence factors are derived from natural adaptations the bacterium possesses to improve survivability in seawater environments. The major mechanisms that contribute to *V. alginolyticus* virulence are 1) iron acquisition systems, 2) effectors and secretion systems, 3) biofilm formation, 4) flagellar systems, 5) quorum sensing, and 6) antibiotic resistance. Prior work by Ruwandeepika et al. (2012), Cai et al. (2022), and Johnson (2013) provides a detailed review of *Harveyi*-clade virulence, *V. alginolyticus* virulence, and *Vibrio* spp. fitness, respectively. Here we summarize the major mechanisms with emphasis on the ecological and pathological roles of each. A summary of significant virulence genes detected in *V. alginolyticus* can be found in Table 5.

Iron acquisition systems. It is well accepted that iron is a critical macronutrient required for bacterial metabolism. In pelagic seawater environments, biologically available iron is scare; thus, bacteria have developed specialized acquisition systems collect available iron and compete for uptake (Kuehl & Crosa, 2010). The two main systems present in *V. alginolyticus* are siderophores and the TonB energy transduction system which work in concert to scavenge and internalize available iron from the ambient environment (Wang et al., 2008; Kuehl & Crosa, 2010). Siderophores are small molecular weight compounds that have a high affinity to chelate ferric iron (Fe^{3+}). In iron-limiting systems, siderophores are secreted into the ambient environment to bind ferric iron which are then recognized by outer membrane proteins (Escolar et al., 1999; Kuehl & Crosa, 2010). In Gram negative bacteria, the outer membrane is separated from the inner membrane by the periplasmic space. Energy produced along the inner membrane by proton motive force is transferred to the outer membrane proteins by means of the TonB energy transduction system. This energy transfer allows the ferrisiderophore complex to be transferred across both membranes into the cytosol (Wang et al., 2008; Kuehl & Crosa, 2010). Activation and repression of the TonB system is controlled by *fur* gene, specifically the Fur protein and is regulated by a negative feedback loop based on the internal iron concentration (Escolar et al., 1999).

During infection, *V. alginolyticus* gains access to the large pool of iron stored in host fluids. Iron acquisition systems will continually operate effectively 'stealing' iron from the host facilitating proliferation of the bacterium and spread of the infection (Wang et al., 2008; Kustusch et al., 2011). *V. alginolyticus* is known to have two types of TonB systems, TonB1 and TonB2. TonB1 is associated with the assimilation of hemin and hemoglobin which can be directly utilized by the bacterium during infection, whereas TonB2 is thought to be more

promiscuous facilitating the internalization of various ferrisiderophore complexes (Wang et al., 2008; Kuehl & Crosa, 2010). Research on the production of siderophores suggests that *V. alginolyticus* can produce carboxylate (Wang et al., 2007a; Wang et al., 2008), hydroxamate (Gómez-León et al., 2005; Mechri et al., 2017), catechol (Mechri et al., 2017) and catecholate (Poorvin et al., 2011) siderophores under differing environmental conditions suggesting a wide range of adaptivity within the bacterium dependent on the conditions of growth. Furthermore, research has shown that *V. alginolyticus* has the capacity to utilize exogenous siderophores further improving the competitiveness of this bacterium in mixed communities (Wang et al., 2008; Kuehl & Crosa, 2010). The combined efficacy of iron acquisition systems is further exacerbated during infection in concert with bacterial effectors (hemolysins, proteases, etc.) which directly attack host infrastructure releasing iron where it can be scavenged by the bacterium (Hernández-Robles et al., 2016; Cai et al., 2022).

Effectors and Secretion Systems. Bacterial effectors are extracellular proteins produced by pathogenic bacteria that damage or destroy host cells. Effectors work in concert with bacterial secretion systems which transfer these proteins from the cytosol to the extracellular space and/or directly inject them into the cytoplasm of adjacent host cells (Schroeder et al., 2021). *V. alginolyticus* is known to have a broad capacity for the production of effectors with hemolysins and proteases representing the best studied in relation to pathogenicity. Research has shown that *V. alginolyticus* strains can produce two major hemolysins, the pore-forming toxin thermostable direct hemolysin (TDH) and the phospholipase thermolabile hemolysin (TLH) (Cai et al., 2007a; Jia et al. 2010; Wong et al., 2012). During infection, these exotoxins are released where they lyse the cell membrane of host blood cells. Lysis primarily affects erythrocytes but is also known to effect other blood cells such as leukocytes and neutrophils (Cai et al., 2022). Hemolysis

disrupts the nutritional immunity releasing host sequestered iron in hemoglobin, transferrin, and lactoferrin (Cai et al., 2022). Subsequent uptake of this iron fuels bacterial metabolism and proliferation (Kuehl & Crosa, 2010). Proteases are enzymes that hydrolyze proteins contributing to the degradation of host tissues and immune defenses during infection (Culp & Wright, 2017 Matkawala et al., 2021). While *V. alginolyticus* is known to produce several different types of proteases such as collagenase (Hare et al., 1983; Takeuchi et al., 1992) and gelatinase (Hörmansdorfer et al., 2000; Sadok et al., 2013), alkaline serine protease has been widely associated with increased virulence of this bacterium (Hare et al., 1983; Chen et al., 2000; Cai et al., 2007b; Rui et al., 2008; Rui et al., 2009). Research has shown that alkaline serine protease can be lethal when injected into marine fishes (Cai et al., 2007b) and crustaceans (Lee et al., 1997; Chen et al., 2000) specifically eliminating the clotting ability of hemolymph in *P. japonicus* (Lee et al., 1997a; Lee et al., 1997b). Host disruption by proteases and the subsequent release of biologically available macronutrients enhances the dissemination and metabolism of the invading bacterium thus, facilitating proliferation of the infection (Supuran et al., 2001).

Transfer of effectors from *V. alginolyticus* to the extracellular environment is mediated by secretion systems. Of the six major types of bacterial secretion systems, type 3 (T3SS) systems are believed to play a major role in the pathogenicity of *V. alginolyticus* (Zhao et al., 2010; Zhao et al., 2011). T3SS, also called “injectosomes’ are transmembrane protein complexes that transfer effectors from the bacterial cytosol directly to the cytoplasm of the host cell using a needle-like injection mechanism (Green & Mecsas, 2016). Prior research has demonstrated that the T3SS induce cytolysis in both fish (Zhao et al., 2010) and mammalian (Zhao et al., 2011) cells suggesting that these mechanisms are key indicators of broad virulence of the bacterium.

Biofilm Production. It has been well established that the production of biofilms enhances the pathogenicity of bacteria through improved host colonization and survivability (Hall-Stoodley et al., 2004). Biofilms are formed through the secretion of extracellular polymeric substances (EPS) which provide a substrate for the colonization of cells into a suspended matrix. Suspended cells lose their motility and gain increased fitness through improved access to nutritional resources and increased resistance to external stressors, including antibiotics (Donlan & Costerton, 2002; Yildiz & Visick, 2009; Cai et al., 2022). The process of *V. alginolyticus* biofilm formation occurs in four distinct stages 1) initial chemotaxis and attachment to a substrate, 2) loss of motility and EPS production, 3) biofilm thickening, and 4) biofilm dispersal, or the release of cells from a mature film (Cai et al., 2022). While the formation process is well understood, progression through these steps is dependent on the combined effort of multiple genes related to motility/chemotaxis, adhesion, and EPS production (summarized in Table 6). Master regulation of the collaborative efforts of biofilm production are maintained through quorum sensing-dependent transcriptional cascades (discussed below) (Ye et al., 2008; Gu et al., 2016a; Ball et al., 2017; Gao et al., 2018). Once established, *V. alginolyticus* can produce a lose slime biofilm composed of a base exopolysaccharide matrix that accretes additional organic molecules such as proteins, carbohydrates, and glycoproteins as the biofilm matures (Ruwandeepika et al., 2012; Cai et al., 2022). Compositional analysis of the exopolysaccharides produced by a *V. alginolyticus* strain isolated in the Bay of Bengal, India showed that the matrix was composed of glucose, aminoarabinose, aminoribose and xylose in a molar ratio of 2:1:9:1 (Muralidharan & Jayachandran, 2003).

While biofilms can contribute to the pathogenicity of all *Vibrio* spp. infections, outbreaks occurring in aquaculture facilities are particularly susceptible to issues associated with their

formation. Studies have shown that biofilms can act as reservoirs for pathogenic *Vibrio* spp. in aquaculture infrastructure (Bourne et al., 2006; Snoussi et al., 2009; Arunkumar et al., 2020; Mougin et al., 2021). *Vibrio* spp. harbored within these biofilms can serve as a continuous source of pathogenic bacteria and are more resistant to treatment with antibiotics and ultraviolet light (Snoussi et al., 2009; Arunkumar et al., 2020). To combat this in *V. alginolyticus*, researchers have explored the use of several methods of biocontrol including anti-biofilm bacteriophages (Sasikala & Srinivasan, 2016; Kim et al., 2019), vanillic acid (Liu et al., 2021), citral (Liu et al., 2020a), *Moringa oleifera* leaf extract (Suhartono et al., 2019), and biofilm oral immunostimulation (Sharma et al., 2010; Sharma et al., 2011). Use of these biocontrol methods has shown success in the reduction of *V. alginolyticus* and/or increased host resistance to infection.

Flagellar System. Quite simply, flagellar systems are important virulence factors because they allow bacteria to move (motility) and respond directionally to environmental signals (chemotaxis). These advantages enable host invasion and allows the bacterium to be more competitive for the acquisition of extracellular resources (Josenhans & Suerbaum, 2002). *V. alginolyticus* movement is accomplished using two flagellar systems, a single polar sheathed flagellum or multiple non-sheathed lateral flagella. The polar flagellum allows for rapid movement in a liquid medium and is essential for chemotaxis and competition for limiting resources (Kawagishi et al., 1995; Atsumi et al., 1996). Lateral flagella are adapted for a more sessile lifestyle and confer traits essential for substrate adhesion, cell-to-cell aggregation, and biofilm formation (Kawagishi et al., 1995; Atsumi et al., 1996; Böttcher et al., 2016). This dual flagellar system allows *V. alginolyticus* to be highly adaptable to changing environmental conditions which contributes to the ability of this bacterium to act as an opportunistic pathogen

by allowing *V. alginolyticus* to switch between optimal motility states best adapted to capitalize on newly available nutrients derived from the infected host.

Quorum Sensing. Of all the virulence characteristics of *V. alginolyticus*, quorum sensing (QS) is arguably the most important serving as the master regulator for transcriptional cascades that activate and deactivate many pathways associated with the traits discussed above. QS is a form of concentration-dependent bacterial "communication" which controls the transcriptional activation of various genes. Activation is based on the presence of autoinducers, or small extracellular signaling molecules that are secreted by sister bacterial cells in an area. As the concentration of cells increases, the concentration of autoinducers also increases until it reaches a threshold which triggers a transcriptional cascade (Ng & Bassler, 2009; Prescott & Decho, 2020). This concentration-based activation allows *V. alginolyticus* to display sophisticated collaborative behaviors through the synchronization of gene expression.

Vibrio QS is controlled by two master regulators the AphA and LuxR transcription factors which modulate expression at low cell densities and high cell densities, respectively (Rutherford et al., 2011). Reciprocal activation of these transcription factors is controlled via phosphorylation cascade that moderates the production of small non-coding RNAs (sRNA) called Qrr sRNAs and the response regulator LuxO (Freeman & Bassler, 1999; Lenz et al., 2004; Tu & Bassler, 2007; Rutherford et al., 2011; Liu et al., 2020b). At low cell densities, LuxO activates the transcription of the Qrr sRNAs which repress the translation of LuxR and activate AphA (Tu & Bassler, 2007; Rutherford et al., 2011; Liu et al., 2020b). At high cell densities, the opposite occurs where LuxO is deactivated arresting transcription of the Qrr sRNAs allowing activation of the LuxR pathway (Neiditch et al., 2006; Rutherford et al., 2011). Additional regulators such as the sRNA chaperone Hfq and alternative sigma (σ) factors, which modulate

transcriptional response to stress conditions, can interact with QS cascades allowing for fine scale tuning of the expressed genes based on the survival needs of the bacterium (Tian et al., 2008a; Liu et al., 2011a; Sheng et al., 2012; Gu et al., 2016b; Gu et al., 2019; Zhang et al., 2021a). QS in *V. alginolyticus* has been shown to be critical for the expression of virulence factors including biofilm production (Rui et al., 2008; Gu et al., 2016a), bacterial adhesion (Zhang et al., 2022), secretion of effectors (Wang et al., 2007b; Rui et al., 2009, Gu et al., 2016b), siderophore production (Wang et al., 2007b), and motility (Rui et al., 2008; Cao et al., 2011; Gu et al., 2016b). Gene knockout studies of strains lacking one or more elements of the *lux*, *aph*, *hfq*, and/or *rpo* systems demonstrated substantial reduction in *V. alginolyticus* pathogenicity and/or survivability suggesting that proper quorum sensing is critical for the maintenance of virulence (Tian et al., 2008a; Ye et al., 2008; Liu et al., 2011a; Gu et al., 2016a).

Antibiotic Resistance. In addition to virulence adaptations, *V. alginolyticus* can also be resistant to various antibiotics further adding to its potential pathogenicity. Susceptibility studies conducted at the CDC described in Farmer & Janda (2005) demonstrate strong resistance to beta-lactam antibiotics with total resistance to penicillin D, ampicillin and carbenicillin and near total resistance cephalosporin. Strong resistance was also observed to colistin and sulfadiazine, the latter of which was broadly resisted among all tested *Vibrio* spp. Moderate susceptibility was observed towards the aminoglycoside antibiotics, streptomycin and kanamycin. Strong susceptibility was observed to nalidixic acid, tetracycline, chloramphenicol, and gentamicin the latter two of which demonstrated complete susceptibility (Farmer & Janda, 2005). These resistance patterns are supported by reported cases of human infection (Pien et al., 1977; Spark et al., 1979; Janda et al., 1986; Opal & Saxon, 1986) and environmental sampling (Oh et al., 2011; Hernández-Robles et al., 2016) where isolates with similar resistance profiles have been

identified. Modern cases of clinical *V. alginolyticus* infection are typically treated successfully with the administration of antibiotics from the tetracycline and/or quinoline families the latter of which is widely employed for the treatment of serious non-Cholera *Vibrio* infections (Pezzlo et al., 1979; Ho et al., 1998; Dechet et al., 2008; Wong et al., 2015). While the intrinsic resistance profile is of concern for the treatment of infections, acquisition of multidrug resistance by means of horizontal gene transfer is of high concern, particularly to aquaculture facilities where prophylactic use of antibiotics has been employed. Several studies have suggested that aquaculture facilities may promote and/or harbor antibiotic resistant *Vibrio* strains (Akinbowale et al., 2006; Igbinosa, 2016; Loo et al., 2020). Thus, there is a regulatory push to monitor the use of antibiotics and to develop affordable alternative means of *Vibrio* control to reduce/eliminate their use during the rearing process (Reverter et al., 2020; Schar et al., 2020). No instances of extensively drug resistant (XDR) clinical *V. alginolyticus* infections have been described suggesting that infection with these strains and nosocomial-acquired antibiotic resistance is unlikely.

While studies on *V. alginolyticus* virulence mechanisms are ongoing, research to date has clearly demonstrated that this bacterium has a broad genomic capacity for virulence traits (Table 6). This ubiquity has led researchers to suggest that *V. alginolyticus* may severe as an environmental reservoir for *Vibrio* virulence genes (Xie et al., 2005; Gennari et al., 2012; Khouadja et al., 2022). Maintenance of these genes within *V. alginolyticus* populations allows traits to persist within the microbial community where they can then be transferred horizontally to other *Vibrio* spp. (Xie et al., 2005; Hoffmann et al., 2012). Specifically, the genes associated with cholera toxicity (Xie et al., 2005; Gennari et al., 2012) and hemolytic activity (*tdh, trh*, and *tlh*) (González-Escalona et al., 2006; Gargouti et al., 2015) have been of great interest to

researchers as horizontal transfer of these traits to *V. cholerae* and *V. parahaemolyticus* may stoke pathogenicity in avirulent strains (Xie et al., 2005; Gennari et al., 2012). Continued research on the mechanisms of *Vibrio* virulence and the impacts of community-level horizontal gene transfer are needed to better understand how pathogenicity traits are maintained and spread within the *Vibrio* community.

Implications for Public Health in the United States. It is clear that *V. alginolyticus* poses a substantial threat to public health. In the United States, human vibriosis infections are tracked through the Cholera and Other Vibrio Illness Surveillance System (COVIS). This program first established *Vibrio* infections as notifiable diseases in Gulf Coast states (Alabama, Florida, Louisiana, and Texas) in 1989 and was then applied nationally in 2007, with most states voluntarily reporting by the early 2000s (Wies et al., 2011; CDC, 2022). Despite this reporting system, public health concern for *V. alginolyticus* infections has been less than ideal with most of the research focus directed at *V. vulnificus* and *V. parahaemolyticus* infections. While it is important to consider that *V. alginolyticus* infections are not as deadly as *V. vulnificus* or as abundant as *V. parahaemolyticus*, these infections still impose a substantial economic and morbidity burden to the country. Ralston et al. (2011) reports an annual cost in excess of 1 million dollars for the treatment of *V. alginolyticus* infections in the United States.

To demonstrate the importance of *V. alginolyticus* as a public health concern, we analyzed reporting data collected through COVIS to highlight the current status of infections with this bacterium in the Unites States (CDC, 2022). Data analysis focused on the three major causes of vibriosis infections *V. alginolyticus*, *V. parahaemolyticus*, and *V. vulnificus*. Total case analysis included all cases where *V. alginolyticus*, *V. parahaemolyticus*, or *V. vulnificus* were identified as the causative agent and included metadata on the date and state of reporting from

cases spanning 1988-2019. Specific analysis of *V. alginolyticus* cases included reports from 1988-2019 where *V. alginolyticus* was identified as the causative agent and included metadata on the date, state, and site of *V. alginolyticus* isolation from the patient. Analysis was performed using Rstudio statistical analysis software using the packages 'tidyverse' and 'readxl' (R Core Team, 2022).

Analysis of the total reported cases of *V. alginolyticus*, *V. parahaemolyticus*, and *V. vulnificus* infections indicate that the incidence of vibriosis is increasing steadily in the United States. As of 2019, *V. parahaemolyticus* represented the most common type of infection with 656 (60.2%) total cases, *V. alginolyticus* in second with 277 (25.4%) cases, and *V. vulnificus* in third with 157 (14.4%) cases (Figure 1). This case level represents a 70.0%, 114.7%, and 42.7% increase in reported cases of *V. parahaemolyticus*, *V. alginolyticus*, and *V vulnificus*, respectively compared to levels recorded 10 years earlier (2009). This increase can be attributed to anthropogenically-driven environmental changes favoring an increase in the abundance of *Vibrio* spp. and increases in interactions with these bacteria (Froelich & Daines, 2020). Furthermore, in 2007 *V. alginolyticus* overtakes *V. vulnificus* as the second most common cause of vibriosis. From this year onward, the gap between *V. alginolyticus* and *V. vulnificus* has steadily widened. This widening plus the 10 year percent change in reported cases suggests that *V. alginolyticus* infections may be increasing at a greater rate. This increase is even more influential considering the likely underreporting of *V. alginolyticus* cases compared to more serious *V. vulnificus* cases. While it is clear that vibriosis is increasing, it should be noted that enhancements in detection methodologies have also improved reporting capacity and thus likely influenced the total reported cases in more recent years.

While *V. alginolyticus* is currently the second most common cause of vibriosis in the United States, it is important to consider the route of exposure for this bacterium. Unlike *V. parahaemolyticus* and *V. vulnificus* which are largely foodborne, *V. alginolyticus* predominately manifests as extraintestinal infections thus limiting major risk to regions where water exposure is common. State-level examination of cases demonstrates that *V. alginolyticus* represents a minor burden of disease in non-coastal states with an average annual incidence of 33.25 cases compared to 239.00 cases in coastal states for cases reported 2016-2019 (Figure 2). Among coastal states, the highest incidence of *V. alginolyticus* is reported in Florida, California, Massachusetts, Hawaii, and Texas with an average annual case rate of 64.50, 38.75, 23.75, 15.25, and 15.12, respectively (cases reported 2016-2019). Increased incidence in Florida, Hawaii, and Texas is likely associated with increased surface water temperature in these states. While less optimal environments, we hypothesize that high *V. alginolyticus* incidence in California and Massachusetts may be the result of disproportionate reporting/exposure in these states due to the length of California's coastline and the large fishing industry in Massachusetts. Specific examination of Florida and Hawaii, demonstrates that *V. alginolyticus* is the dominant cause of vibriosis in these states suggesting that regions with tropical/subtropical climates and high recreational or occupational seawater exposure are at greater risk of infection with this bacterium. This elevated incidence supports prior hypotheses suggesting that warmer sea surface temperatures increase the risk of exposure to this bacterium (Weis et al., 2010; Schets et al., 2011; Baker-Austin et al., 2017). Continued research exploring the environmental parameters favorable to *V. alginolyticus* proliferation and surveillance of warming coastal regions is needed to mitigate future outbreaks of this bacterium in the United States.

Of the 3,091 total *V. alginolyticus* cases recorded in COVIS from 1988-2019, 2,913 included information on the site of infection. This site information represents the location(s) where *V. alginolyticus* was isolated from the patient. For analysis purposes, the primary isolation source was used for patients with multiple isolation sites. Examination of these infection sites demonstrates seven major locations of *V. alginolyticus* isolation wound, ear, gastrointestinal, blood, respiratory, urine, and eye (Figure 4).

Consistent with prior surveys of *V. alginolyticus* and non-Cholera vibrios (Weis et al., 2011; Silfka et al., 2017), wound and ear infections represent the most common sites for the isolation of this bacterium with 1,515 (52.0%) and 1,089 (37.4%), respectively. Gastrointestinal and blood infections were near equivalent representing a small but significant burden of disease with 101 (3.5%) and 100 (3.4%) cases, respectively. It should be noted that these designations include any cases where *V. alginolyticus* was isolated from stool, bile, appendix, rectum, gall bladder, or colon for the "gastrointestinal" designation and blood, cerebrospinal fluid, peritoneal fluid, lumbar disc fluid, lymph node or bullae for the "blood" designation. Thus, these cases may represent a range of exposures and patient symptoms. Respiratory infections represent cases where *V. alginolyticus* was isolated from patient sinus, sputum, nose, throat, trachea, or lungs. Prior surveys of *V. alginolyticus* infections have not highlighted the importance of these types of cases often classifying them as "other" infections due to their atypical presentation. Here we show that while uncommon, respiratory infections represent an important part of *V. alginolyticus* epidemiology accounting for 79 (2.7%) of the described cases. We hypothesize that these infections likely are the result of exposures where seawater is inadvertently inhaled or swallowed, such as in the case of a near drowning victim or if water enters the nasal cavity/sinus accidently (i.e., water up the nose) or due to injury. Prior research has shown that *V.*

alginolyticus respiratory infection can progress to severe disease in immunocompromised patients (Chien et al., 2002) suggesting that infections at this site may present increased risk of complication. This hypothesis is supported by the work of Liu et al. (2014) who demonstrated that *V. alginolyticus* infection causes severe lung damage in a mouse model. Further research is needed to investigate the pathogenicity and exposure pathways required to facilitate disease onset and progression for respiratory infections for this bacterium. Isolation of *V. alginolyticus* from urine samples also represents an atypical presentation for this bacterium accounting for 16 (0.5%) reported cases. While exceedingly uncommon, we hypothesize that these cases are likely the result of opportunistic urinary tract infections associated with exposure to seawater. Similar to ear infections, we posit that these infections may not require injury to establish but, preexisting injuries or conditions such as catheter use may facilitate their onset. Lastly, eye infections represent just 13 (0.4%) of the total *V. alginolyticus* cases surveyed. Despite frequent discussion in the literature, this low incidence suggests that the risk of infection at this site is low and likely restricted to cases where eye injury is sustained in associated with seawater.

Since 1988, there have been 3,091 reported cases of *V. alginolyticus* infection in the United States. This incidence disproportionally affects coastal states and imposes a substantial economic and morbidity burden to the country. With the increasing frequency of annual *V. alginolyticus* cases, continued research and surveillance of this pathogen is imperative to the management of disease. Specific attention should be given to tropical/subtropical states as well as states where coastal water temperatures are increasing due to climate change. Furthermore, we recommend continued research on the nature of *V. alginolyticus* infections, specifically infections of the blood, respiratory lumen, and severe wound infections to better our understanding of how cases progress to invasive conditions. Lastly, appropriate recognition of

V. alginolyticus as a significant contributor to vibriosis is imperative for the continued management of future outbreaks.

Conclusion. In summation, *V. alginolyticus* is an important bacterial pathogen of both human and animal populations. To date, summary reviews of *Vibrio* infections often dismiss *V. alginolyticus* cases as "other *Vibrio*" infections when discussing the burden of vibriosis and impacts to public health. Based on the research summarized in this work, it is clear that *V. alginolyticus* warrants equivalent attention as is given to other major *Vibrio* pathogens such as *V. cholerae*, *V. parahaemolyticus*, and *V. vulnificus*. Specifically, there is a need for continued investigation of the pathogenicity of this bacterium in relation to aquaculture and human extraintestinal infections. Special attention should be given to aquaculture facilities targeting the cultivation of crustaceans and marine fishes as well as human infections associated with immunocompromised or sensitive populations. Furthermore, as a ubiquitous opportunistic pathogen, characterization of the environmental determinants that contribute to the proliferation and dispersal is a critical area of research need for the management of *V. alginolyticus*. Understanding of the roles of abiotic factors such as temperature, salinity, and biologically available iron as well as biotic factors such as zooplankton association, biofilm production, and macrofauna presence can improve our understanding of *V. alginolyticus* ecology. These data can be used to better assess risk of infection and identify critical transmission pathways that can be used to improve management of these outbreaks.

Literature Cited

Abdel-Aziz M, Eissa AE, Hanna M, and Okada MA. 2013. Identifying some pathogenic

Vibrio/Photobacterium species during mass mortalities of cultured Gilthead seabream (*Sparus aurata*) and European seabass (*Dicentrarchus labrax*) from some Egyptian coastal provinces. *International Journal of Veterinary Science and Medicine.* 1(2): 87-95.

Abdelsalam M, Ewiss MAZ, Khalefa HS, Mahmoud MA, Elgendy MY, and Abdel-Moneam DA. 2021. Coinfections of *Aeromonas* spp., *Enterococcus faecalis,* and *Vibrio alginolyticus* isolated from farmed Nile tilapia and African catfish in Egypt, with an emphasis on poor water quality. *Microbial Pathogenesis*. 160: 105213.

Abioye OE, Osunla AC, and Okoh AI. 2021. Molecular detection and distribution of six medically important *Vibrio* spp. in selected freshwater and brackish water resources in Eastern Cape Province, South Africa. *Frontiers in Microbiology.* 12: 617703. https://doi.org/10.3389/fmicb.2021.617703.

Abraham TJ, Rahman MK, and Joseph MTL. 1996. Bacterial disease in cultured spiny lobster, *Panulirus homarus* (Linnaeus). *Journal of Aquaculture in the Tropics.* 11(3): 187-192.

Aggarwal P, Singh M, Kumari S. 1986. Isolation of *Vibrio alginolyticus* from two patients of acute gastroenteritis. *Journal of Diarrhoeal Diseases Research.* 4(1): 30.

Akinbowale OL, Peng H, and Barton MD. 2006. Antimicrobial resistance in bacteria isolated from aquaculture sources in Australia. *Journal of Applied Microbiology.* 100(5): 1103-1113.

Alves N, Neto OSM, Silva BSO, De Moura RL, Francini-Filho RB, Barreira e Castro C, Paranhos R, Bitner-Mathé BC, Kruger RH, Vicente ACP, Thompson CC, and Thompson FL. 2010. Diversity and pathogenic potential of vibrios isolated from Abrolhos Bank corals. *Environmental Microbiology Reports*. 2: 90-95. https://doi.org/10.1111/j.1758-2229.2009.00101.x

Anguiano-Beltrán C, Searcy-Bernal R, and Lizárraga-Partida ML. 1998. Pathogenic effects of *Vibrio alginolyticus* on larvae and postlarvae of the red abalone *Haliotis rufescens. Diseases of Aquatic Organisms.* 33: 119-122.

Anguiano-Beltrán C, Lizárraga-Partida ML, and Searcy-Bernal R. 2004. Effect of *Vibrio alginolyticus* on larval survival of the blue mussel *Mytilus galloprovincialis. Diseases of Aquatic Organisms.* 59: 119-123.

Arechavala-Lopez P, Toledo-Guedes K, Izquierdo-Gomez D, Šegvić-Bubić T, and Sanchez-Jerez. 2017. Implications of sea bream and sea bass escapes for sustainable aquaculture management: r review of interactions, risks and consequences. *Reviews in Fisheries Science & Aquaculture.* 26(2): 214-234.

Arunkumar M, LewisOscar F, Thajuddin N, Pugazhendhi A, and Nithya C. 2020. *In vitro* and *in vivo* biofilm forming *Vibrio* spp: A significant threat in aquaculture. *Process Biochemistry.* 94: 213-223.

Asai Y, Kojima S, Kato H, Nishioka N, Kawagishi I, and Homma M. 1997. Putative channel components for the fast-rotating sodium-driven flagellar motor of a marine bacterium. *Journal of Bacteriology.* 176(16): 5104-5110.

Asplund ME, Rehnstam-Holm AS, Atnur V, Raghunath P, Saravanan V, Härnström K, Collin B, Karunasagar I, and Godhe. 2011. Water column dynamics of *Vibrio* in relation to phytoplankton community composition and environmental conditions in a tropical coastal area. *Environmental Microbiology.* 13(10): 2738-2751.

Atsumi T, Maekawa Y, Yamada T, Kawagishi I, Imae Y, and Homma M. 1996. Effect of viscosity on swimming by the lateral and polar flagella of *Vibrio alginolyticus*. *Journal of Bacteriology.* 178(16): 5024-5026.

Austin B, Stobie M, Robertson PAW, Glass HG, Stark JR, and Mudarris M. 1993. *Vibrio alginolyticus*: the cause of gill disease leading to progressive low-level mortalities among juvenile turbot, *Scophthalmus maximus* L., in a Scottish aquarium. *Journal of Fish Diseases.* 16(3): 277-280.

Austin B and Austin DA. 2012. Vibrios. In: *Bacterial Fish Pathogens: Disease of Farmed and Wild Fish*. Springer, UK. 499-601.

Bacchiocchi S, Campacci D, Siracusa M, Dubbini A, Leoni F, Tavoloni T, Accoroni S, Gorbi S, Giuliani ME, Stramenga A, and Piersanti. 2021. Tetrodotoxins (TTXs) and *Vibrio alginolyticus* in mussels from Central Adriatic Sea (Italy): Are they closely related? *Marine Drugs.* 19(6): 304. https://doi.org/10.3390/md19060304.

Baffone W, Pianetti A, Bruscolini F, Barbieri E, and Citterio B. 2000. Occurrence and expression of virulence-related properties of *Vibrio* species isolated from widely consumed seafood products. *International Journal of Food Microbiology.* 54(1-2): 9-18.

Baffone W, Tarsi R, Pane L, Campana R, Repetto B, Mariottini GL, and Pruzzo C. 2006. Detection of free-living and plankton-bound vibrios in coastal waters of the Adriatic Sea (Italy) and study of their pathogenicity-associated properties. *Environmental Microbiology.* 8(7): 1299-1305.

Baker-Austin C, Trinanes J, Salmenlinna S, Löfdahl M, Siitonen A, Taylor NGH, and Martinez-Urtaza J. 2016. Heat wave–associated vibriosis, Sweden and Finland, 2014. *Emerging Infectious Diseases.* 22(7): 1216-1220.

Baker-Austin C, Trinanes J, Gonzalez-Escalona N, and Martinez-Urtaza J. 2017. Non-Cholera vibrios: the microbial barometer of climate change. *Trends in Microbiology.* 25(1): 76-84.

Baker-Austin C, Oliver JD, Alam M, Ali A, Waldor MK, Qadri F, and Martinez-Urtza. 2018. *Vibrio* spp. infections. *Nature Reviews Disease Primers*. 4:1-19. https://doi.org/10.1038/s41572-018-0005-8.

Balcázar JL, Gallo-Bueno A, Planas M, and Pintado J. 2010. Isolation of *Vibrio alginolyticus* and *Vibrio splendidus* from captive-bred seahorses with disease symptoms. *Antonie van Leeuwenhoek*. 97: 207-210.

Balebona MC, Andreu MJ, Bordas MA, Zorrilla I, Moriñigo MA, and Borrego JJ. 1998. Pathogenicity of *Vibrio alginolyticus* for Cultured Gilt-Head Sea Bream (*Sparus aurata*L.). *Applied and Environmental Microbiology.* 64(11): 4269-4275.

Ball AS, Chaparian RR, and Van Kessel JC. 2017. Quorum sensing gene regulation by LuxR/HapR master regulators in Vibrios. *Journal of Bacteriology.* 199(19): https://doi.org/10.1128/JB.00105-17.

Baran I, Acar A, Genç Y, and Aksu N. 2016. Case report: A case of otitis externa due to *Vibrio alginolyticus. Turkish Bulletin of Hygiene and Experimental Biology.* 73(1): 49-54.

Barbarossa V, Kuèišec-Tepeš N, Aldova E, Matek D, and Stipoljev F. 2002. Ilizarov technique in the treatment of chronic osteomyelitis caused by *Vibrio alginolyticus. Croatian Medical Journal*. 43(3): 346-349.

Barberi ON, Byron CJ, Burkholder KM, St. Gelais AT, and Williams AK. 2019. Assessment of bacterial pathogens on edible macroalgae in coastal waters. *Journal of Applied Phycology*. 32: 683-696.

Bauer JC and Young CM. 2000. Epidermal lesions and mortality caused by vibriosis in deep-sea Bahamian echinoids: a laboratory study. *Diseases of Aquatic Organisms.* 39: 193-199.

Baumann P, Baumann L, and Mandel M. 1971. Taxonomy of marine bacteria: the genus

Beneckea. *Journal of Bacteriology.* 107(1): 268-294.

Baumann P, Baumann L, Bang SS, and Woolkalis MJ. 1980. Reevaluation of the taxonomy of *Vibrio, Beneckea,* and *Photobacterium*: abolition of the genus *Beneckea*. *Current Microbiology.* 4: 127-132.

Bean NH, Maloney EK, Potter ME, Korazemo P, Ray B, Taylor JP, Seigler S, and Snowden J. 1998. Crayfish: A newly recognized vehicle for vibrio infections. *Epidemiology & Infection*. 121(2): 269-273.

Beleneva IA, Maslennikova EF, and Magarlamov. 2004. Physiological and biochemical characteristics of the halophilic bacteria *Vibrio parahaemolyticus* and *V. alginolyticus* isolated from marine invertebrates of Peter the Great Bay, Sea of Japan. *Russian Journal of Marine Biology.* 30: 96-100. https://doi.org/10.1023/B:RUMB.0000025985.38429.11

Beleneva IA and Zhukova NV. 2006. Bacterial communities of some brown and red algae from Peter the Great Bay, the Sea of Japan. *Microbiology.* 73(3): 348-357.

Böer SI, Heinemeyer EA, Luden K, Erler R, Gerdts G, Janssen F, and Brennholt N. 2013. Temporal and spatial distribution patterns of potentially pathogenic *Vibrio* spp. at recreational beaches of the German North Sea. *Environmental Microbiology.* 65: 1052-1067.

Bonner JR, Coker AS, Berryman CR, and Pollock HM. 1983. Spectrum of Vibrio infections in a Gulf coast community. *Annals of Internal Medicine.* 99(4): 464-469.

Böttcher T, Elliott HL, and Clardy J. 2016. Dynamics of snake-like swarming behavior of *Vibrio alginolyticus*. *Biophysical Journal.* 110(4): 981-992.

Bourne DG, Høj L, Webster NS, Swan J, and Hall MR. 2006. Biofilm development within a

larval rearing tank of the tropical rock lobster, *Panulirus ornatus*. *Aquaculture.* 260(1-4): 27-38.

Bourne DG, Høj L, Webster NS, Payne M, Skindersøe M, Givskov M, and Hall MR. 2007. Microbiological aspects of phyllosoma rearing of the ornate rock lobster *Panulirus ornatus. Aquaculture*. 268(1-4): 274-287.

Boyd CE and Jescovitch LN. 2020. Penaeid shrimp aquaculture. In: Lovrich G and Thiel M (eds). *Fisheries and Aquaculture.* Oxford University Press, USA.

Buck JD. 2008. Potentially pathogenic *Vibrio* spp. in market seafood and natural habitats from Southern New England and Florida. *Journal of Aquatic Food Product Technology.* 7(4): 53-61.

Bunpa S, Chaichana N, Teng JLL, Lee HH, Woo PCY, Sermwittayawong D, Sawangjaroen N, and Sermwittayawong N. 2019. Outer membrane protein A (OmpA) is a potential virulence factor of *Vibrio alginolyticus* strains isolated from diseased fish. *Journal of Fish Diseases.* 43(2): 275-284.

Burke J, and Rodgers L. 1981. Identification of pathogenic bacteria associated with the occurrence of 'red spot' in sea mullet, *Mugil cephalus* L., in south-eastern Queensland. *Journal of Fish Diseases*. 4(2): 153-159.

Caccamese SM and Rastegar DA. 1999. Chronic diarrhea associated with *Vibrio alginolyticus* in an immunocompromised patient. *Clinical Infectious Diseases*. 29(4): 946-947.

Cai J, Han H, Song Z, Li C, and Zhou J. 2006. Isolation and characterization of pathogenic *Vibrio alginolyticus* from diseased postlarval abalone, *Haliotis diversicolor supertexta* (Lischke). *Aquaculture Research*. 37: 1222-1226.

Cai SH, Wu ZH, Jian JC, and Lu YS. 2007a. Cloning and expression of gene encoding the

thermostable direct hemolysin from *Vibrio alginolyticus* strain HY9901, the causative agent of vibriosis of crimson snapper (*Lutjanus erythopterus*). *Journal of Applied Microbiology.* 103(2): 289-296.

Cai SH, Wu ZH, Jian JC, and Lu YS. 2007b. Cloning and expression of the gene encoding an extracellular alkaline serine protease from *Vibrio alginolyticus* strain HY9901, the causative agent of vibriosis in *Lutjanus erythopterus* (Bloch). *Journal of Fish Diseases.* 30: 493-500.

Cai SH, Lu YS, Wu ZH, Jian JC, Wang B, and Huang YC. 2010a. Loop-mediated isothermal amplification method for rapid detection of *Vibrio alginolyticus*, the causative agent of vibriosis in mariculture fish. *Letters in Applied Microbiology.* 50(5): 480-485.

Cai SH, Yao SY, Lu YS, Wu ZH, Jian JC, and Wang B. 2010b. Immune response in *Lutjanus erythropterus* induced by the major outer membrane protein (OmpU) of *Vibrio alginolyticus. Diseases of Aquatic Organisms.* 90: 63-68.

Cai SH, Lu YS, Jian JC, Wang B, Huang YC, Tang JF, Ding Y, and Wu ZH. 2013. Protection against *Vibrio alginolyticus* in crimson snapper *Lutjanus erythropterus* immunized with a DNA vaccine containing the *ompW* gene. *Diseases of Aquatic Organisms.* 106: 39-47.

Cai S, Cheng H, Pang H, Jian J, and Wu Z. 2018. AcfA is an essential regulator for pathogenesis of fish pathogen *Vibrio alginolyticus. Veterinary Medicine.* 213: 35-41.

Cai Z, Zhou L, Liu L, Wang D, Ren W, Long H, Zhang X, and Xie Z. 2021. Bacterial epiphyte and endophyte communities of seagrass *Thalassia hemprichii*: the impact of feed extract solution. *Environmental Microbiology Reports.* 13(6): 757-772.

Cai H, Yu J, Li Q, Zhang Y, and Huang L. 2022. Research progress on virulence factors of

Vibrio alginolyticus: A key pathogenic bacteria of sepsis. In Huang L, Zhang Y, and Sun L (eds). *Sepsis – New Perspectives*. IntechOpen. https://doi.org/10.5772/intechopen.108206.

Campanelli A, Sanchez-Politta S, and Saurat JH. 2008. Cutaneous ulceration after an octopus bite: Infection due to *Vibrio alginolyticus*, an emerging pathogen. *Annales de Dermatologie et de Vénéréologie*. 135(3): 225-227.

Cao X, Wang Q, Liu Q, Liu H, He H, and Zhang Y. 2010. *Vibrio alginolyticus* MviN is a LuxO-regulated protein and affects cytotoxicity towards epithelioma papulosum cyprini (EPC) cells. *Journal of Microbiology and Biotechnology*. 20(2): 271-280.

Cao X, Wang Q, Liu Q, Rui H, Liu H, and Zhang Y. 2011. Identification of a *luxO*-regulated extracellular protein Pep and its roles in motility in *Vibrio alginolyticus*. *Microbial Pathogenesis.* 50(2): 123-131.

Carli A, Pane L, Casareto L, Bertone S, and Pruzzo C. 1993. Occurrence of *Vibrio alginolyticus* in Ligurian coast rock pools (Tyrrhenian Sea, Italy) and its association with the copepod *Tigriopus fulvus* (Fisher 1860). *Applied and Environmental Microbiology.* 59(6): 1960-1962.

Cardia F and Lovatelli A. 2007. A review of cage aquaculture: Mediterranean Sea. In: Halwart M, Soto D, and Arthur JR (eds) *Cage Aquaculture: Regional Reviews and Global Overview*. FAO Fisheries Technical Paper, Rome, FAO 156-187.

Cervino JM, Thompson FL, Gomez-Gil B, Lorence EA,Goreau TJ, Hayes RL, Winiarski-Cervino KB, Smith GW, Hughen K, and Bartels E. 2008. The *Vibrio* core group induces yellow band disease in Caribbean and Indo-Pacific reef-building corals. *Journal of Applied Microbiology.* 105(5): 1658-1671.

Centers for Disease Control and Prevention (CDC). 2022. Cholera and Other Vibrio Illness Surveillance (COVIS), summary data, 1988–2019. Atlanta, GA: US Department of Health and Human Services. Accessed 14 June 2022.

Chan KY, Woo ML, Lam LY, and French GL. 1986. *Vibrio parahaemolyticus* and other halophilic vibrios associated with seafood in Hong Kong. *Journal of Applied Bacteriology.* 66(1): 57-64.

Chang CI, Lee CF, Wu CC, Cheng TC, Tsai JM, and Lin KJ. 2011. A selective and differential medium for *Vibrio alginolyticus*. *Journal of Fish Diseases*. 34(3):227-234.

Chau R, Kalaitzis JA, and Neilan BA. 2011. On the origins and biosynthesis of tetrodotoxin. *Aquatic Toxicology*. 104(1-2): 61-72.

Chen FR, Liu PC, and Lee KK. 2000. Lethal attribute of serine protease secreted by *Vibrio alginolyticus* strains in Kuruma Prawn *Penaeus japonicus*. *Zeitschrift für Naturforschung C*. 55(1-2): 94-99.

Chen C, Wang QB, Liu ZH, Zhao JJ, Jiang X, Sun HY, Ren CH, and Hu CQ. 2012. Characterization of role of the *toxR* gene in the physiology and pathogenicity of *Vibrio alginolyticus. Antonie van Leeuwenhoek.* 101: 281-288.

Chen X, Li J, Pang H, Chang Y, Huang Y, Wu Z, and Jian J. 2017. Molecular cloning, bioinformatics analysis and expression analysis of type III secretion system (T3SS) injectisome gene *vscX* from *Vibrio alginolyticus*. *Agricultural Biotechnology.* 6(1): 41-45.

Chen Y, Wu F, Pang H, Tang J, Cai S, and Jian J. 2019. Superoxide dismutase B (*sodB*), an

important virulence factor of *Vibrio alginolyticus*, contributes to antioxidative stress and its potential application for live attenuated vaccine. *Fish and Shellfish Immunology.* 89: 354-360.

Chen Y, Wu F, Wang Z, Tang J, Cai S, and Jian J. 2020. Construction and evaluation of *Vibrio alginolyticus* Δ*clpP* mutant, as a safe live attenuated vibriosis vaccine. *Fish & Shellfish Immunology.* 98: 917-922.

Cheng CA, Hwang DF, Tsai YH, Chen HC, Jeng SS, Noguchi T, Ohwada K, and Hasimoto K. 1995. Microflora and tetrodotoxin-producing bacteria in a gastropod, *Niotha clathrata*. *Food and Chemical Toxicology.* 33(11): 929-934.

Cheng AC, Cheng SA, Chen YY, and Chen JC. 2009. Effects of temperature change on the innate cellular and humoral immune responses of orange-spotted grouper *Epinephelus coioides* and its susceptibility to *Vibrio alginolyticus. Fish & Shellfish Immunology.* 26(5): 768-772.

Chien JY, Shih JT, Hsueh PR, Yang PC, and Luh KT. 2002. *Vibrio alginolyticus* as the cause of pleural empyema and bacteremia in an immunocompromised patient. *European Journal of Clinical Microbiology and Infectious Disease.*21: 401-403.

Citil BE, Derin S, Sankur F, Sahan M, and Citil MU. 2015. *Vibrio alginolyticus* associated chronic myringitis acquired in Mediterranean waters of Turkey. *Case Reports in Infectious Diseases.* 187212. https://doi.org/10.1155/2015/187212.

Ciufecu C, Năcescu N, and Florescu D. 1979. Middle ear infection due to vibrio alginolyticus. Bacteriological characterization. *Acta Microbiologica Academiae Scientiarum Hungaricae.* 26(1): 95-98.

Clemente S, Lorenzo-Morales J, Mendoza JC, López C, Sangil C, Alves F, Kaufmann M, and

Hernández JC. 2014. Sea urchin *Diadema africanum* mass mortality in the subtropical eastern Atlantic: role of waterborne bacteria in a warming ocean. *Marine Ecology Press Series.* 506(1-14). https://doi.org/10.3354/meps10829.

Clinton M, Kintner AH, Delannoy CMJ, Brierley AS, and Ferrier DEK. 2020. Molecular identification of potential aquaculture pathogens adherent to cnidarian zooplankton. *Aquaculture*. 518: 734801. https://doi.org/10.1016/j.aquaculture.2019.734801

Colorni A, Paperna I, and Gordin H. 1981. Bacterial infections in gilt-head sea bream *Sparus aurata* cultured at Elat. *Aquaculture.* 23(1-4): 257-267.

Colwell RR, Huq A, Islam MS, Aziz KMA, Yunus M, Khan NH, Mahmud A, Sack RB, Chakraborty J, Sack DA, and Russek-Cohen E. 2003. Reduction of cholera in Bangladeshi villages by simple filtration. *PNAS.* 100(3): 1051-1055.

Culp E and Wright GD. 2016. Bacterial proteases, untapped antimicrobial drug targets. *The Journal of Antibiotics*. 70: 366-377.

Deane SM, Robb FT, Robb SM, and Woods DR. 1989. Nucleotide sequence of the *Vibrio alginolyticus* calcium-dependent, detergent-resistant alkaline serine exoprotease A. *Gene*. 76(2): 281-288.

Deb S, Badhai J, and Das SK. 2020. Draft genome sequences of *Vibrio alginolyticus* strain S6-61 and *Vibrio diabolicus* strain S7-71, isolated from corals in the Andaman Sea. *Microbiology Resource Announcements.* 9(8): e01465-19.

Dechet AM, Yu PA, Koram N, and Painter J. 2008. Nonfoodborne *Vibrio* infections: An important cause of morbidity and mortality in the United States, 1997–2006. *Clinical Infectious Diseases.* 46(7): 970-976.

De Vos, P, Vanlandschoot A, Segers P, Tytgat R, Gillis M, Bauwens M, Rossau R, Goor M, Pot

B, Kersters K Lizzaraga P, and Deley J. 1989. Genotypic relationships and taxonomic localization of unclassified *Pseudomonas* and *Pseudomonas*-like strains by deoxyribonucleic acid:ribosomal ribonucleic acid hybridizations. *International Journal of Systematic Bacteriology*. 39:35-49.

Di Pinto A, Ciccarese G, Tantillo G, Catalano D, and Forte VT. 2005. A collagenase-targeted multiplex PCR assay for identification of *Vibrio alginolyticus*, *Vibrio cholerae*, and *Vibrio parahaemolyticus*. *Journal of Food Protection*. 68(1): 150-153.

Di Pinto A, Ciccarese G, Fontanarosa M, Terio V, and Tantillo G. 2006. Detection of *Vibrio alginolyticus* and *Vibrio parahaemolyticus* in shellfish samples using collagenase-targeted multiplex-PCR. *Journal of Food Safety*. 26(2): 150-159.

Di Renzo L, Di Francesco G, Profico C, Di Francesco CE, Ferri N, Averaimo D, and Di Guardo G. 2017. *Vibrio parahaemolyticus*- and *V. alginolyticus*-associated meningo-encephalitis in a bottlenose dolphin (*Tursiops truncatus*) from the Adriatic coast of Italy. *Research in Veterinary Science.* 115: 363-365.

Doh YJ, Kim MH, and Kim ES. 1997. A case of Vibrio alginolyticus isolated from otorrhea of chronic otitis media. *Korean Journal of Infectious Diseases.* 29:153-157.

Donlan RM and Costerton JW. 2002. BiofilmsL Survival mechanisms of clinically relevant microorganisms. *Clinical Microbiology Reviews.* 15(2): 167-193.

Dong Y, Zhao P, Chen L, Wu H, Si X, Shen X, Shen H, Qiao Y, Zhu S, Chen Q, Jia W, Dong J, Li J, and Gao S. 2020. Fast, simple and highly specific molecular detection of *Vibrio alginolyticus* pathogenic strains using a visualized isothermal amplification method. *BMC Veterinary Research*. 16(76): https://doi.org/10.1186/s12917-020-02297-4.

Ducklow HW and Mitchell R. 1979. Bacterial populations and adaptations in the mucus layers of

living corals. *Limnology and Oceanography.* 24(4): 715-725.

Dumontet S, Krovacek K, Svenson SB, Pasquale V, Baloda SB, and Figliuolo G. 2000. Prevalence and diversity of *Aeromonas* and *Vibrio* spp. in coastal waters of Southern Italy. *Comparative Immunology, Microbiology and Infectious Diseases.* 23(1): 53-72.

Eiler A, Johansson M, and Bertilsson S. 2006. Environmental influences on *Vibrio* populations in northern temperate and boreal coastal waters (Baltic and Skagerrak Seas). *Applied and Environmental Microbiology.* 72(9): 6004-6011.

El-Sayed ME, Algammal AM, Abouel-Atta ME, Mabrok M, and Emam AM. 2019. *Revue de Medecine Veterinaire*. 170(4-6): 80-86.

Emam AM, Hashem M, Gadallah AO, and Haridy M. 2019. An outbreak of *Vibrio alginolyticus* infection in aquarium-maintained dark-spotted (*Himantura uarnak*) and Tahitian (*H. fai*) stingrays. *The Egyptian Journal of Aquatic Research.* 45(2): 153-158.

English VL and Lindberg RB. 1997. Isolation of *Vibrio alginolyticus* from wounds and blood of a burn patient. *American Journal of Medical Technology.* 43(10): 989-993.

Erken M, Lutz C, and McDougald D. 2015. Interactions of *Vibrio* spp. with zooplankton. *Microbiology Spectrum*. 3(3): 3.3.02. https://doi.org/10.1128/microbiolspec.VE-0003-2014.

Escolar L, Pérez-Martín J, and De Lorenzo V. 1999. Opening the iron box: Transcriptional metalloregulation by the Fur protein. *Journal of Bacteriology.* 181(20): 6223-6229.

Fahmy NM and Hamed ESAE. 2022. Isolation and characterization of *Vibrio alginolyticus* strain HAT3 causing skin ulceration disease in cultured sea cucumber *Holothuria atra* (Jaeger, 1833). *The Egyptian Journal of Aquatic Research.* 48(1): 75-81.

Farid AF and Larsen JL. 1981. Growth of *Vibrio alginolyticus*: Interacting effects on pH,

temperature, salt concentration, and incubation time. *Zentralblatt für Bakteriologie Mikrobiologie und Hygiene: I. Abt. Originale C: Allgemeine, angewandte und ökologische Mikrobiologie.* 3(4): 68-75.

Farmer JJ and Janda JM. 2005. Order XI. "Vibrionales" In: Brenner DJ, Kreig NR, and Staley JT (eds). *Bergey's manual of systematic bacteriology. Vol. 2. The Proteobacteria. Part B, the Gammaproteobacteria*. Springer, New York, NY. 491-556.

Feingold MH and Kumar ML. 2004. Otitis media associated with *Vibrio alginolyticus* in a child with pressure-equalizing tubes. *The Pediatric Infectious Disease Journal*. 23(5): 475-476.

Fichi G, Cardeti G, Perrucci S, Vanni A, Cersini A, Lenzi C, De Wolf T, Fronte B, Guarducci M, and Susini F. 2015. Skin lesion-associated pathogens from Octopus vulgaris: first detection of *Photobacterium swingsii*, *Lactococcus garvieae* and betanodavirus. *Diseases of Aquatic Organisms.* 115: 147-156.

Floch F and Boutoille D. 2008. Pacemaker infection due to *Vibrio alginolyticus*. *European Journal of Internal Medicine.* 19(8): e109-e110.

Freeman JA and Bassler BL. 1999. A genetic analysis of the function of LuxO, a two-component response regulator involved in quorum sensing in *Vibrio harveyi*. *Molecular Microbiology.* 31(2): 665-677.

Froelich BA and Daines DA. 2020. In hot water: effects of climate change on *Vibrio*–human interactions. *Environmental Microbiology.* 22(10): 4101-4111.

Fu K, Li J, Wang Y, Liu J, Yan H, Shi, and Zhou L. 2016. An innovative method for rapid identification and detection of Vibrio alginolyticus in different infection models. *Frontiers in Microbiology.* 7: 10.3389/fmicb.2016.00651.

Fujino T, Okuno Y, Nakada D, Aoyama A, Fukai K, Mukai T, and Ueho T. 1953. On the

bacteriological examination of Shirasu-food poisoning. *Medical Journal of Osaka University*. 4:299.

Gao X, Wang Q, Liu Q, Rui H, Liu H, and Zhang Y. 2011. Identification of a *luxO*-regulated extracellular protein Pep and its roles in motility in *Vibrio alginolyticus. Microbial Pathogenesis.* 50(2): 123-131.

Gao X, Wang X, Mao Q, Xu R, Zhou X, Ma Y, Liu Q, Zhang Y, and Wang Q. 2018. VqsA, a novel LysR-type transcriptional regulator, coordinates quorum sensing (QS) and is controlled by QS to regulate virulence in the pathogen *Vibrio alginolyticus. Applied and Environmental Microbiology.* 84(2): e00444-18.

Gargouti AS, Ab-Rashid MNK, Ghazali MF, Mitsuaki N, Haresh KK, and Radu S. 2015. Detection of *tdh* and *trh* toxic genes in *Vibrio Alginolyticus* strain from mantis shrimp (*Oratosquilla oratoria*). *Journal of Nutrition & Food Sciences.* 5(5): 1000405.

Gaüzère BA, Chanareille P, and Vandroux D. 2016. Post nearly Drowning *Vibrio alginolyticus* Septicemia Acquired in Reunion (Indian Ocean). *Bulletin de la Société de Pathologie Exotique*. 109: 151-154.

Gennari M, Ghidini V, Caburlotto G, and Lleo MM. 2012. Virulence genes and pathogenicity islands in environmental *Vibrio* strains nonpathogenic to humans. *FEMS Microbial Ecology.* 82: 563-573.

Ghosh HK, and Bowen TE. 1980. Halophilic vibrios from human tissue infections on the Pacific coast of Australia. *Pathology.* 12: 397-402.

Gil Gomez B and Roque A. 2006. Isolation, Enumeration, and Preservation of the Vibrionaceae. In: Thompson FL, Austin B, and Swings J (eds). *The Biology of Vibrios*. ASM Press, Washington DC. 15-26.

Glazebrook JS and Campbell RSF. 1990a. A survey of the diseases of marine turtles in northern Australia. I. Farmed turtles. *Diseases of Aquatic Organisms.* 9: 93-95.

Glazebrook JS and Campbell RSF. 1990b. A survey of the diseases of marine turtles in northern Australia. 1I. Oceanarium-reared and wild turtles. *Diseases of Aquatic Organisms.* 9: 97-104.

Gomez JM, Fajardo R, Patiño JF, and Arias CA. 2003. Necrotizing fasciitis due to *Vibrio alginolyticus* in an immunocompetent patient. *Journal of Clinical Microbiology.* 41(7): 3427-3429.

Gómez-León J, Villamil L, Lemos ML, Novoa B, and Figueras A. 2005. Isolation of *Vibrio alginolyticus* and *Vibrio splendidus* from aquacultured Carpet Shell Clam (*Ruditapes decussatus*) larvae associated with mass mortalities. *Applied and Environmental Microbiology.* 71(1): https://doi.org/10.1128/AEM.71.1.98-104.2005.

González-Escalona N, Blackstone GM, and DePaola A. 2006. Characterization of a *Vibrio alginolyticus* strain, isolated from Alaskan oysters, carrying a hemolysin gene similar to the thermostable direct hemolysin-related hemolysin gene (*trh*) of *Vibrio parahaemolyticus. Applied and Environmental Microbiology.* 72(12): https://doi.org/10.1128/AEM.01548-06.

Goulden EF, Hall MR, Bourne DG, Pereg LL, and Høj L. 2021. Pathogenicity and infection cycle of *Vibrio owensii* in larviculture of the Ornate Spiny Lobster (*Panulirus ornatus*). *Applied and Environmental Microbiology.* 78(8): 2841-2849.

Green ER and Mecsas J. 2016. Bacterial secretion systems – An overview. *Microbiology Spectrum*. 4(1): 10.1128/microbiolspec.VMBF-0012-2015.

Grimes DJ, Brayton P, Colwell RR, and Gruber SH. 1985. Vibrios as autochthonous flora of

neritic sharks. 1985. *Systematic and Applied Microbiology.* 6(2): 221-226.

Grimes DJ, Jacobs D, Schwartz DG, Brayton PR, and Colwell RR. 1993. Numerical taxonomy of Gram-negative, oxidase-positive rods from Carcharhinid sharks. *International Journal of Systematic and Evolutionary Microbiology.* 43(1): 88-98.

Gu D, Liu H, Yang Z, Zhang Y, and Wang Q. 2016a. Chromatin immunoprecipitation sequencing technology reveals global regulatory roles of low-cell-density quorum-sensing regulator AphA in the pathogen *Vibrio alginolyticus. Journal of Bacteriology.* 198(21): 2985-2999.

Gu D, Guo M, Yang M, Zhang Y, Zhou X, and Wang Q. 2016b. A σ^E-mediated temperature gauge controls a switch from LuxR-mediated virulence gene expression to thermal stress adaptation in *Vibrio alginolyticus. PLoS Pathogens*. 12(6): e1005645.

Gu D, Zhang J, Hao Y, Xu R, Zhang Y, Ma Y, and Wang Q. 2019. Alternative sigma factor RpoX is a part of the RpoE regulon and plays distinct roles in stress responses, motility, biofilm formation, and hemolytic activities in the marine pathogen *Vibrio alginolyticus. Applied and Environmental Microbiology.* 85(4): e00234-19.

Hall-Stoodley L, Costerton JW, and Stoodley P. 2004. Bacterial biofilms: from the Natural environment to infectious diseases. *Nature Reviews Microbiology.* 2: 95-108.

Hanlon RT, Forsythe JW, Cooper KM, Dinuzzo AR, Folse DS, and Kelly MT. 1984. Fatal penetrating skin ulcers in laboratory-reared octopuses. *Journal of Invertebrate Pathology.* 44(1): 67-83.

Hare P, Scott-Burden T, and Woods DR. 1983. Characterization of extracellular alkaline proteases and collagenase induction in *Vibrio alginolyticus*. *Journal of General Microbiology.* 129: 1141-1147.

Harlock M, Quinn S, and Turnbull AR. 2022. Emergence of non-choleragenic *Vibrio* infections in Australia. *Communicable Diseases Intelligence*. 46: https://doi.org/10.33321/cdi.2022.46.8

Harikrishnan R, Kim JS, Balasundaram C, and Heo MS. 2012. Immunomodulatory effects of chitin and chitosan enriched diets in *Epinephelus bruneus* against *Vibrio alginolyticus* infection. *Aquaculture.* 326-329: 46-52.

Harriague AC, Di Brino M, Zampini M, Albertelli G, Pruzzo C, and Misic C. 2008. Vibrios in association with sedimentary crustaceans in three beaches of the northern Adriatic Sea (Italy). *Marine Pollution Bulletin*. 56(3): 574-579.

He H, Wang Q, Sheng L, Liu Q, and Zhang Y. 2010. Functional characterization of *Vibrio alginolyticus* twin-arginine translocation system: its roles in biofilm formation, extracellular protease activity, and virulence towards fish. *Current Microbiology*. 62: 1193-1199.

Hernández-Robles MF, Álvarez-Contreras AK, Juárez-García P, Natividad-Bonifacio I, Curiel-Quesada E, Vázquez-Salinas C, and Quiñones-Ramírez EI. 2016. Virulence factors and antimicrobial resistance in environmental strains of *Vibrio alginolyticus*. *International Microbiology.* 19(4): 191-198.

Hiratsuka M, Saitoh Y, and Yamane N. 1980. The isolation of *Vibrio alginolyticus* from a patient with acute entero-colitis. *Tohoku Journal of Experimental Medicine.* 132: 469-472.

Hlady WG and Klontz KC. 1996. The epidemiology of *Vibrio* infections in Florida, 1981-1993. *The Journal of Infectious Diseases.* 173: 1176-1183.

Ho PL, Tang WM, Lo KS, and Yuen KY. 1998. Necrotizing fasciitis due to Vibrio alginolyticus

following an injury inflicted by a stingray. *Scandinavian Journal of Infectious Diseases.* 30(2): 192-193.

Hoffman M, Fischer M, Ottesen A, McCarthy PJ, Lopez JV, Brown EW, and Monday SR. 2010. Population dynamics of Vibrio spp. associated with marine sponge microcosms. *The ISME Journal*. 4: 1608-1612. https://doi.org/10.1038/ismej.2010.85.

Hoffmann M, Monday SR, McCarthy PJ, Lopez JV, Fischer M, and Brown EW. 2012. Genetic and phylogenetic evidence for horizontal gene transfer among ecologically disparate groups of marine *Vibrio. Cladistics*. 29(1): 46-64.

Hood MA and Winter PA. 1997. Attachment of *Vibrio cholerae* under various environmental conditions and to selected substrates. *FEMS Microbiology Ecology.* 22(3): 215-223. https://doi.org/10.1111/j.1574-6941.1997.tb00373.x.

Horii T, Morita M, Muramatsu H, Monji A, Miyagishima D, Kanno T, Maekawa M. 2005. Antibiotic resistance in *Aeromonas hydrophila* and *Vibrio alginolyticus* isolated from a wound infection: a case report. *Journal of Trauma: Injury, Infection, and Critical Care.* 58(1): 196-200.

Hörmansdorfer S, Wentges H, Neugebaur-Büchler K, and Bauer J. 2000. Isolation of *Vibrio alginolyticus* from seawater aquaria. *International Journal of Hygiene and Environmental Health.* 203: 169-175.

Hornstrup MK and Gahrn-Hansen B. 1993. Extraintestinal infections caused by *Vibrio parahæmolyticus* and *Vibrio alginolyticus* in a Danish County, 1987–1992. *Scandinavian Journal of Infectious Diseases.* 25(6): 735-740.

Howard RJ and Lieb S. 1988. Soft-tissue infections caused by halophilic marine vibrios. *Archives of Surgery.* 123(2): 245-249.

Howard RJ and Bennett NT. 1993. Infections caused by halophilic marine Vibrio bacteria. *Annals of Surgery.* 217(5): 525-531.

Hsieh JL, Fries S, and Noble RT. 2007. Dynamics and predictive modelling of Vibrio spp. in the Neuse River Estuary, North Carolina, USA. *Environmental Microbiology.* 10(1): 57-64. https://doi.org/10.1111/j.1462-2920.2007.01429.x.

Huang L, Gou L, Xu X, Quin Y, Zhao L, Su Y, and Yan Q. 2018. The role of *rpoS* in the regulation of *Vibrio alginolyticus* virulence and the response to diverse stresses. *Journal of Fish Diseases.* 42(5): 703-712.

Hunt DE, David LA, Gevers D, Preheim SP, Alm EJ, and Polz MF. 2008. Resource partitioning and sympatric differentiation among closely related bacterioplankton. *Science*. 320(5879): 1081-1085. https://www.science.org/doi/10.1126/science.1157890.

Huq A, Xu B, Chowdhury MAR, Islam MS, Montilla R, and Colwell RR. 1996. A simple filtration method to remove plankton-associated *Vibrio cholerae* in raw water supplies in developing countries. *Applied and Environmental Microbiology.* 62(7): 2508-2512.

Igbinosa EO. 2016. Detection and antimicrobial resistance of *Vibrio* isolates in aquaculture environments: Implications for public health. *Microbial Drug Resistance.* 22(3): 238-245.

Interaminense JA, Calazans NF, do Valle BC, Vogeley JL, Peixoto S, Soares R, and Filho JVL. 2014. *Vibrio* spp. control at brine shrimp, *Artemia*, hatching and enrichment. *Journal of the World Aquaculture Society.* 45(1): 65-74.

Islam MS, Drasar BS, and Sack RB. 1994. The aquatic flora and fauna as reservoirs of *Vibrio cholerae*: A review. *Journal of Diarrhoeal Diseases Research.* 12(2): 87-96.

Issack MI, Appiah D, Rassoul A, Unuth MN, and Unith-Lutchun N. 2008. Extraintestinal *Vibrio* infections in Mauritius. *Journal of Infection in Developing Countries*. 2(5): 397-399.

Iwata K, Yanohara Y, and Ishibashi O. 1978. Studies on factors related to mortality of young Red Seabream (*Pagrus major*) in the artificial seed production. *Fish Pathology*. 13(2): 97-102.

Janda JM, Brenden R, DeBenedetti JA, Constantino MO, and Robin T. 1986. *Vibrio alginolyticus* bacteremia in an immunocompromised patient. *Diagnostic Microbiology and infectious Disease*. 5:337-340.

Jayaprakash NS, Pai SS, Phillip R, and Singh ISB. 2006. Isolation of a pathogenic strain of *Vibrio alginolyticus* from necrotic larvae of *Macrobrachium rosenbergii* (de Man). *Journal of Fish Diseases.* 29(3): 187-191.

Jayasree L, Janakiram P, and Madhavi R. 2006. Characterization of *Vibrio* spp. associated with diseased shrimp from culture ponds of Andhra Pradesh (India). *Journal of the World Aquaculture Society.* 37(4): 523-532.

Jesser KJ and Noble RT. 2018. *Vibrio* ecology in the Neuse River Estuary, North Carolina, characterized by next-generation amplicon sequencing of the gene encoding heat shock protein 60 (*hsp60*). *Applied and Environmental Microbiology.* 84(13): e00333-18.

Jia A, Woo NYS, Zhang XH. 2010. Expression, purification, and characterization of thermolabile hemolysin (TLH) from *Vibrio alginolyticus. Diseases of Aquatic Organisms.* 90:121-127.

Johnson CN. 2013. Fitness factors in vibrios: a mini-review. *Microbial Ecology.* 65: 826-851.

Jo Rubin S and Tilton RC. 1975. Isolation of *Vibrio alginolyticus* from wound infections. *Journal of Clinical Microbiology.* 2(6): 556-558.

Josenhans C and Suerbaum S. 2002. The role of motility as a virulence factor in bacteria. *International Journal of Medical Microbiology.* 291: 605-614.

Kahla-Nakbi AB, Chaieb K, Bakhrouf A. 2009. Investigation of several virulence properties among *Vibrio alginolyticus* strains isolated from diseased cultured fish in Tunisia. *Diseases of Aquatic Organisms.* 86: 21-28.

Kawagishi I, Maekawa Y, Atsumi T, Homma M, and Imae Y. 1995. Isolation of the polar and lateral flagellum-defective mutants in *Vibrio alginolyticus* and identification of their flagellar driving energy sources. *Journal of Bacteriology.* 177(17): 5158-5160.

Khouadja S, Roque A, Gonzalez M, and Furones D. 2022. *Vibrio* pathogenicity island and phage *CTX* genes in *Vibrio alginolyticus* isolated from different aquatic environments. *Journal of Water & Health.* 20(10): 1469-1478.

Kim KH, Hwang YJ, Bai SC. 1999. Resistance to *Vibrio alginolyticus* in juvenile rockfish (*Sebastes schlegeli*) fed diets containing different doses of aloe. *Aquaculture.* 180(1-2): 13-21.

Kim SG, Jun JW, Giri SS, Yun S, Kim HJ, Kim SW, Kang JW, Han SJ, Jeong D, and Park SC. 2019. Isolation and characterization of pVa-21, a giant bacteriophage with anti-biofilm potential against *Vibrio alginolyticus*. *Scientific Reports.* 9: 6284.

King WL, Siboni N, Khalke T, Green TJ, Labbate M, and Seymour JR. 2019. A new high throughput sequencing assay for characterizing the diversity of natural *Vibrio* communities and its application to a Pacific oyster mortality event. *Frontiers in Microbiology.* 10: 10.3389/fmicb.2019.02907.

Kojima M, Kubo R, Yakushi T, Homma M, and Kawagishi I. 2007. The bidirectional polar and unidirectional lateral flagellar motors of *Vibrio alginolyticus* are controlled by a single CheY species. *Molecular Microbiology.* 64(1): 57-67.

Kokou F, Makridis P, Kentouri M, and Divanach P. 2012. Antibacterial activity in microalgae

cultures. *Aquaculture Research*. 43: 1520-1527.

Kua BC, Ramly R, Devakie M, Groman D, Berthe CJF. Investigating a mortality in hatchery cultured tropical abalone, *Haliotis asinina* Linnaeus, 1758 in Malaysia. *Diseases in Asian Aquaculture.* 7: 103-109.

Kuehl CJ and Crosa JH. 2010. The TonB energy transduction systems in *Vibrio* species. *Future Microbiology.* 5(9): 1403-1412.

Kumar TS, Vidya R, Kumar S, Slavandi SV, and Vijayan KK. 2017. Zoea-2 syndrome of *Penaeus vannamei* in shrimp hatcheries. *Aquaculture.* 479: 759-767.

Kungsuwan A, Noguchi T, Arakawa O, Simidu U, Tsukamoto K, Shida Y, and Hashimoto K. 1988. Tetrodotoxin-producing bacteria from the horseshoe crab *Carcinoscorpius rotundicauda*. *Nippon Suisan Gakkaishi*. 54(10): 1799-1802.

Kurilenko VV, Ivanova EP, and Mikhailov VV. 2001. Zonal distribution of epiphytic microorganisms on the eelgrass *Zostera marina*. *Microbiology.* 70(3): 372-373.

Kustusch RJ, Kuehl CJ, and Crosa JH. 2011. Power plays: iron transport and energy transduction in pathogenic vibrios. *Biometals*. 24(3): 559-566.

Kusuda R, Yokoyama J, and Kawai K. 1986. Bacteriological study on cause of mass mortalities in cultured Black Sea Bream fry. *Bulletin of the Japanese Society of Scientific Fisheries*. 50(1): 1745-1751.

Kusumoto A, KAmisaka K, Yakushi T, Terashima H, Shinohara A, and Homma M. 2006. Regulation of polar flagellar number by the *flhF* and *flhG* Genes in *Vibrio alginolyticus. The Journal of Biochemistry.* 139(1): 113-121.

Laith AA, Ros-Amira MK, Sheikh HI, Effendy AWM, and Najiah M. 2021. Histopathological

and immunological changes in green mussel, *Perna viridis*, challenged with *Vibrio alginolyticus. Fish & Shellfish Immunology*. 118: 169-179.

Lamb JB, Van de Water JJM, Bourne DG, Altier C, Hein M, Fiorenza EA, Abu N, Jompa J, and Harvell D. 2017. Seagrass ecosystems reduce exposure to bacterial pathogens of humans, fishes, and invertebrates. *Science.* 355(6326): 731-733.

Leamaster BR and Ostrowski AC. 1988. Vibriosis in captive dolphins. *The Progressive Fish-Culturist.* 50(4): 251-254.

Lee KK. 1995. Pathogenesis studies on *Vibrio alginolyticus* in the grouper, *Epinephelus malabaricus*, Bloch et Schneider. *Microbial Pathogenesis.* 19(1): 39-48.

Lee KK, Yu SR, Chen FR, Yang TI, and Liu PC. 1996a. News & Notes: Virulence of *Vibrio alginolyticus* isolated from diseased Tiger Prawn, *Penaeus monodon*. *Current Microbiology*. 32: 229-231.

Lee KK, Yu SR, Yang TI, Liu PC, and Chen FR. 1996b. Isolation and characterization of *Vibrio alginolyticus* isolated from diseased kuruma prawn, *Penaeus japonicus*. *Letters in Applied Microbiology.* 22: 111-114.

Lee KK, Chen FR, Yu SR, Yang TI, and Liu PC. 1997a. Effects of extracellular products of *Vibrio alginolyticus* on penaeid prawn plasma components. *Letters in Applied Microbiology.* 24: 98-100.

Lee KK, Yu SR, Liu PC. 1997b. Alkaline serine protease is an exotoxin of *Vibrio alginolyticus* in Kuruma Prawn, *Penaeus japonicus*. *Current Microbiology.* 34: 110-117.

Lee DY, Moon SY, Lee SO, Yang HY, Lee HJ, and Lee MS. 2008. Septic shock due to *Vibrio alginolyticus* in a cirrhotic patient: The first case in Korea. *Yonsei Medical Journal*. 49(2): 329-332.

Lenz DH, Mok KC, Lilley BN, Kulkarni RV, Wingreen NS, and Bassler BL. 2004. The small RNA chaperone Hfq and multiple small RNAs control quorum sensing in *Vibrio harveyi* and *Vibrio cholerae*. *Cell.* 118(1): 69-82.

Lessner AM, Webb RM, and Rabin B. 1985. *Vibrio alginolyticus* conjunctivitis first reported case. *Archives of Ophthalmology*. 103(2): 229-230.

Leveine WC, Griggin PM, and Gulf Coast Vibrio Working Group. 1993. *Vibrio* infections on the Gulf Coast: Results of first year of regional surveillance. *The Journal of Infectious Diseases.* 167(2): 479-483.

Li J, Yie J, Foo RWT, Ling JML, Xu H, and Woo NYS. 1999. Antibiotic resistance and plasmid profiles of Vibrio isolates from cultured Silver Sea Bream, *Sparus sarba*. *Marine Pollution Bulletin*. 39(1-12): 245-249.

Li J, Zhou L, and Woo NYS. 2003. Invasion route and pathogenic mechanisms of *Vibrio alginolyticus* to Silver Sea Bream *Sparus sarba. Journal of Aquatic Animal Health.* 15(4): 302-313.

Li XC, Xiang ZY, Xu XM, Yan WH, and Ma JM. 2009. Endophthalmitis caused by *Vibrio alginolyticus. Journal of Clinical Microbiology.* 47(10): 3379-3381.

Liang HY, Wu ZH, Jian JC, and Huang YC. 2010a. Protection of red snapper (*Lutjanus sanguineus*) against *Vibrio alginolyticus* with a DNA vaccine containing flagellin *flaA* gene. *Letters in Applied Microbiology.* 52(2): 156-161.

Liang H, Xia L, Wu Z, Jian J, and Lu Y. 2010b. Expression, characterization and immunogenicity of flagellin FlaC from *Vibrio alginolyticus* strain HY990. *Fish & Shellfish Immunology.* 29(2): 343-348.

Liang J, Liu J, Wang X, Lin H, Liu J, Zhou S, Sun H, and Zhang XH. 2019. Spatiotemporal

dynamics of free-living and particle-associated Vibrio communities in the Northern Chinese marginal seas. *Applied and Environmental Microbiology*. 85(9): e00217-19.

Lightner DV and Lewis DH. 1975. A septicemic bacterial disease syndrome of Penaeid shrimp. *Marine Fisheries Review.* 37(5-6): 25-28.

Liu CH, Cheng W, Hsu JP, and Chen JC. 2004a. *Vibrio alginolyticus* infection in the white shrimp *Litopenaeus vannamei* confirmed by polymerase chain reaction and 16S rDNA sequencing. *Diseases of Aquatic Organisms.* 61: 169-174.

Liu PC, Lin JY, Hsiao PT, and Lee KK. 2004b. Isolation and characterization of pathogenic *Vibrio alginolyticus* from diseased cobia *Rachycentron canadum. Journal of Basic Microbiology.* 44(1): 23-28.

Liu H, Wang Q, Cao X, Shi C, and Zhang Y. 2011a. Roles of Hfq in the stress adaptation and virulence in fish pathogen *Vibrio alginolyticus* and its potential application as a target for live attenuated vaccine. *Applied Microbiology and Biotechnology*. 91: 353-364.

Liu H, ,Wang Q, Cao X, Shi C, and Zhang Y. 2011b. Roles of Hfq in the stress adaptation and virulence in fish pathogen *Vibrio alginolyticus* and its potential application as a target for live attenuated vaccine. *Applied Microbiology and Biotechnology*. 91: 353-364.

Liu XF, Zhang H, Liu X, Gong Y, Chen Y, Cao Y, and Hu C. 2014. Pathogenic analysis of *Vibrio alginolyticus* infection in a mouse model. *Folia Microbiologica*. 59: 167-171.

Liu XF, Cao Y, Zhang HL, Chen YJ, and Hu CJ. 2015. Complete genome sequence of *Vibrio alginolyticus* ATCC 17749^{T}. *Genome Announcements.* 3(1): e01500-14.

Liu W, Huang L, Su Y, Quin Y, Zhao L, and Yan Q. 2017. Contributions of the oligopeptide permeases in multistep of *Vibrio alginolyticus* pathogenesis. *MicrobiologyOpen.* 6(5): e00511.

Liu CH, Wu K, Chu TW, and Wu TM. 2018. Dietary supplementation of probiotic, *Bacillus subtilis* E20, enhances the growth performance and disease resistance against *Vibrio alginolyticus* in parrot fish (*Oplegnathus fasciatus*). *Aquaculture International.* 26: 63-74.

Liu H, Wang Y, Cao J, Jiang H, Yao J, Gong G, Chen X, Xu W, and He X. 2020a. Antimicrobial activity and virulence attenuation of citral against the fish pathogen *Vibrio alginolyticus. Aquaculture.* 515: 734578.

Liu H, Liu W, He X, Chen X, Yang J, Wang Y, Li Y, Ren J, Xu W, and Zhao Y. 2020b. Characterization of a cell density-dependent sRNA, Qrr, and its roles in the regulation of the quorum sensing and metabolism in *Vibrio alginolyticus*. *Applied Microbiology and Biotechnology.* 104: 1707-1720.

Liu H, Xiao M, Zuo J, He X, Lu P, Li Y, Zhao Y, and Xia F. 2021. Vanillic acid combats *Vibrio alginolyticus* by cell membrane damage and biofilm reduction. *Journal of Fish Diseases.* 44(11): 1799-1809.

Loo KY, Letchumanan V, Law JWF, Pusparajah P, Goh BH, Ab Mutalib NS, He YW, and Lee LH. 2020. Incidence of antibiotic resistance in *Vibrio* spp. *Reviews in Aquaculture.* 12(4): 2590-2608.

Lopes CM, Rabadão EM, Ventura C, Da Cunha S, Côrte-Real R, and Meliço-Silvestre AA. 1993. A case of *Vibrio alginolyticus* bacteremia and probable sphenoiditis following a dive in the sea. *Clinical Infectious Diseases*. 17(2): 299-300.

Lou P and Hu C. 2008. *Vibrio alginolyticus gyrB* sequence analysis and *gyrB*-targeted PCR identification in environmental isolates. *Diseases of Aquatic Organisms.* 82: 209-216.

Lou G, Huang L, Su Y, Quin Y, Xu X, Zhao L, and Yan Q. 2016. *flrA*, *flrB* and *flrC* regulate

adhesion by controlling the expression of critical virulence genes in *Vibrio alginolyticus.* *Emerging Microbes & Infections.* 5(1): 1-11.

Lucero-Mejía JE, Romero-Gómez SdJ, and Hernández-Iturriaga M. 2020. A new classification criterion for the biofilm formation index: A study of the biofilm dynamics of pathogenic *Vibrio* species isolated from seafood and food contact surfaces. *Journal of Food Science.* 85(8): 2491-2497.

Luna-González A, Maeda-Martínez AN, Sainz JC, and Ascencio-Valle F. 2002. Comparative susceptibility of veliger larvae of four bivalve mollusks to a *Vibrio alginolyticus* strain. *Diseases of Aquatic Organisms.* 49: 221-226.

Maeda T, Matsuo Y, Furushita M, and Shiba T. 2003. Seasonal dynamics in a coastal Vibrio community examined by a rapid clustering method based on 16S rDNA. *Fisheries Science.* 69: 385-394.

Magarlamov TY, Melnikova DI, and Chernyshev AV. 2017. Tetrodotoxin-producing bacteria: Distribution and migration of the toxin in aquatic systems. *Toxins.* 9(5): 166. https://doi.org/10.3390/toxins9050166.

Main CR, Salvitti LR, Whereat EB, and Coyne KJ. 2015. Community-level and species-specific associations between phytoplankton and particle-associated *Vibrio* species in Delaware's inland bays. *Applied and Environmental Microbiology.* 81(17): 5703-5713.

Mancuso M, Constanzo MT, Maricchiolo G, Gristina M, Zaccone R, Cuccu D, and Genovese L. 2010. Characterization of chitinolytic bacteria and histological aspects of shell disease syndrome in European spiny lobsters (*Palinurus elephas*) (Fabricius 1787). *Journal of Invertebrate Pathology.* 104: 242-244.

Mancuso M, Zaccone R, Carella F, Maiolino P, and De Vico G. 2013. First episode of shell

disease syndrome in *Carcinus aestuarii* (Crustacea:Decapoda: Portunidae) in the Volturno River. *Journal of Aquaculture Research and Development.* 4(5): 1000191.

Martins ML, Mouriño JLP, Fezer GF, Buglione Neto CC, Garcia P, Silva BC, Jatobá A, and Vieira FN. 2010. Isolation and experimental infection with *Vibrio alginolyticus* in the sea horse, *Hippocampus reidi* Ginsburg, 1933 (Osteichthyes: Syngnathidae) in Brazil. *Brazilian Journal of Biology*. 70(1): 205-209.

Martocello DE, Morel FMM, and McRose DL. 2019. H-Aquil: a chemically defined cell culture medium for trace metal studies in *Vibrios* and other marine heterotrophic bacteria. *Biometals*. 32:819-828.

Matkawala F, Nighojkar S, Kumar A, and Nighojkar A. 2021. Microbial alkaline serine proteases: Production, properties and applications. *World Journal of Microbiology and Biotechnology*. 37: 63. https://doi.org/10.1007/s11274-021-03036-z.

Matsiota-Bernard P and Nauciel C. 1993. *Vibrio alginolyticus* wound infection after exposure to sea water in an air crash. *European Journal of Clinical Microbiology & Infectious Diseases.* 12(6): 474-475.

Matsumura K. 1005. Reexamination of tetrodotoxin production by bacteria. *Applied and Environmental Microbiology.* 61(9): 3468-3470.

McSweeney RJ and Forgan-Smith WR. 1997. Wound infections in Australia from halophilic vibrios. *Medical Journal of Australia.* 1(24): 896-897.

Mechri B, Monastiri A, Medhioub A, Medhioub MN, and Aouni A. 2017. Molecular characterization and phylogenetic analysis of highly pathogenic *Vibrio alginolyticus* strains isolated during mortality outbreaks in cultured *Ruditapes decussatus* juvenile. *Microbial Pathogenesis.* 111: 487-496.

Miyamoto Y, Nakamuma K, and Takizawa K. 1961. Pathogenic halophiles. Proposals of a new genus "*Oceanomonas*" and the amended species names. *Japanese Journal of Microbiology.* 5(4): 477-486.

Miyamoto Y, Nakamura K, Takizawa K, and Kodama T. 1960. Mackerel poisoning I. Japanese Journal of Public Health 7: 587.

Miyamoto Y, Nakamura K, Takizawa K, and Kodama T. 1961a. Mackerel poisoning II. Japanese Journal of Public Health 8: 673.

Miyamoto Y, Nakamura K, Takizawa K, Osumi T, and Kodama T. 1961b. Mackerel poisoning III. Japanese Journal of Public Health 8: 703.

Mohamed NA, Joseph PG, Hussin H, and Hashim R. 2016. A cat-bite wound infected with *Vibrio alginolyticus* following use of sea cucumber oil. *Southeast Asian Journal of Tropical Medicine and Public Health.* 47(5): 967-969.

Mohamad N, Roseli FAM, Azmai MNA, Saad MZ, Yasin ISM, Zulkiply NA, and Nasruddin NS. 2019. Natural concurrent infection of *Vibrio harveyi* and *V. alginolyticus* in cultured hybrid groupers in Malaysia. *Journal of Aquatic Animal Health*. 31:88-96.

Mohney LL, Lightner DV, and Bell TA. 1994. An epizootic of vibriosis in Ecuadorian pond-reared *Penaeus vannamei* Boone (Crustacea: Decapoda). *Journal of the World Aquaculture Society.* 25(1): 116-125.

Molina-Cárdenas CA, Sánchez-Saavedra MDP, and Lizárraga-Partida ML. 2014. Inhibition of pathogenic *Vibrio* by the microalgae *Isochrysis galbana*. *Journal of Applied Phycology.* 26: 2347-2355.

Molina-Cárdenas CA and Sánchez-Saavedra MdP. 2017. Inhibitory effect of benthic diatom species on three aquaculture pathogenic vibrios. *Algal Research*. 27: 131-139.

Molitoris E, Joseph SW, Krichevsky MI, Sindhuhardja W, and Colwell RR. 1985. Characterization and distribution of *Vibrio alginolyticus* and *Vibrio parahaemolyticus* isolated in Indonesia. *Applied and Environmental Microbiology.* 50(6): 1388-1394.

Montanari MP, Pruzzo C, Pane L, and Colwell RR. 1999. Vibrios associated with plankton in a coastal zone of the Adriatic Sea (Italy). *FEMS Microbiology Ecology.* 29(3): 241-247.

Moreira R, Milan M, Balseiro P, Romero A, Babbucci M, Figueras A, Bargelloni L, and Novoa B. 2014. Gene expression profile analysis of Manila clam (*Ruditapes philippinarum*) hemocytes after a *Vibrio alginolyticus* challenge using an immune-enriched oligo-microarray. *BMC Genomics.* 15: 267. https://doi.org/10.1186/1471-2164-15-267.

Mougin J, Roquigny R, Flahaut C, Bonnin-Jusserand M, Grard T, and Le Bris C. 2021. Abundance and spatial patterns over time of Vibrionaceae and *Vibrio harveyi* in water and biofilm from a seabass aquaculture facility. *Aquaculture.* 542: 736862.

Mukherji A, Schroeder S, Deyling C, and Procop GW. 2000. An unusual source of *Vibrio alginolyticus*-associated otitis prolonged colonization or freshwater exposure? *Archives of Otorhinolaryngology-Head & Neck Surgery.* 126(6): 790-791.

Muralidharan J and Jayachandran S. 2003. Physicochemical analyses of the exopolysaccharides produced by a marine biofouling bacterium, *Vibrio alginolyticus*. *Process Biochemistry.* 38(6): 841-847.

Murao S, Kawada T, Itoh H, Oama H, and Shin T. 1992. Purification and characterization of a novel type of chitinase from *Vibrio alginolyticus* TK-22. *Bioscience, Biotechnology, and Biochemistry.* 56(2): 368-369.

Muroga K, Lio-Po G, Pitogo C, and Imada R. 1984. *Vibrio* sp. isolated from milkfish (*Chanos chanos*) with opaque eyes. *Fish Pathology.* 19(2): 81-87.

Musgrove RJ, Geddes MC, and Thomas C. 2005. Causes of tail fan necrosis in the southern rock lobster, *Jasus edwardsii*. *New Zealand Journal of Marine and Freshwater Research.* 39(2): 293-304.

Nadkarni AS and Shah MK. 2007. Concomitant bacteremia caused by *Vibrio fluvialis* and *Vibrio alginolyticus* in a patient on . emodialysis a first case report and review of literature. *Infectious Diseases in Clinical Practice.* 15(2): 129-131.

Narita H, Matsubara S, Miwa N, Akahane S, Murakami M, Goto T, Nara M, Noguchi T, Saito T, Shida Y, and Hashimoto K. 1987. *Vibrio alginolyticus,* a TTX-producing bacterium isolated from the starfish *Astropecten polyacanthus*. *Nippon Suisan Gakkaishi.* 53(4): 617-621.

Neetoo H, Reega K, Manoga ZS, Nazurally N, Bhoyroo V, Allam M, Jaufeerally-Fakim Y, Ghoorah AW, Jaumdally W, Hossen AM, Mayghun F, Ismail A, and Hosenally M. 2022. Prevalence, genomic characterization and risk assessment of human pathogenic *Vibrio* species in seafood. *Journal of Food Protection.* 85(11): 1553-1565.

Neiditch MB, Federle MJ, POmpeani AJ, Kelly RC, Swem DL, Jeffery PD, Bassler BL, and Hughson FM. 2006. Ligand-induced asymmetry in histidine sensor kinase complex regulates quorum sensing. *Cell*. 126(6): 1095-1108.

Nelson EJ, Harris JB, Morris JG Jr, Calderwood SB, Camilli A. 2009. Cholera transmission: the host, pathogen and bacteriophage dynamic. *Nature Reviews Microbiology*. 7:693-702.

Ng WL and Bassler BL. 2009. Bacterial quorum-sensing network architectures. *Annual Review of Genetics.* 43:197-222.

Nhung PH, Shah MM, Ohkusu K, Noda M, Hata H, Sun XS, Iihara H, Goto K, Masaki T,

Miyasaka J, and Ezaki T. 2007. The *dnaJ* gene as a novel phylogenetic marker for identification of *Vibrio* species. *Systematic and Applied Microbiology*. 30(4): 309-315.

Nishibuchi M. 2006. Miscellaneous Human Pathogens. In: Thompson FL, Austin B, and Swings J (eds). *The Biology of Vibrios*. ASM Press, Washington DC. 367-384.

Noguchi T, Hwang DF, Arakawa O, Sugita H, Deguchi Y, Shida Y, and Hashimoto K. 1987. *Vibrio alginolyticus*, a tetrodotoxin-producing bacterium, in the intestines of the fish *Fugu vermicularis vermicularis*. *Marine Biology.* 94: 625-630.

Norfolk WA and Lipp EK. 2022. Use an evaluation of a pES213-derived plasmid for the constitutive expression of *gfp* protein in pathogenic vibrios: a tagging tool for *in vitro* studies. *Microbiology Spectrum.* e02490-22.

Nottage AS, and Brikbeck TH. 1987. Production of proteinase during experimental infection of *Ostrea edulis* L. larvae with *Vibrio alginolyticus* NCMB 1339 and the antigenic relationship between proteinases produced by marine vibrios pathogenic for fish and shellfish. *Journal of Fish Diseases.* 10(4): 265-273.

Oberbeckmann S, Fuchs BM, Meiners M, Wichels A, Wiltshire KH, and Gerdts G. 2011a. Seasonal dynamics and modeling of a *Vibrio* community in coastal waters of the North Sea. *Environmental Microbiology.* 63: 543-551. https://doi.org/10.1007/s00248-011-9990-9.

Oberbeckmann S, Wichels A, Maier T, Kostrzewa M, Raffelberd S, and Gerdts G. 2011b. A polyphasic approach for the differentiation of environmental *Vibrio* isolates from temperate waters. *FEMS Microbiology Ecology.* 75(1): 145-162.

Oberbeckmann S, Wichels A, Wiltshire KH, and Gerdts G. 2011c. Occurrence of *Vibrio*

parahaemolyticus and *Vibrio alginolyticus* in the German Bight over a seasonal cycle. *Antonie van Leeuwenhoek*. 100: 291-307.

Oh EG, Son KT, Yu H, Lee TS, Lee HJ, Shin S, Kwon JY, Park K, and Kim J. 2011. Antimicrobial resistance of *Vibrio parahaemolyticus* and *Vibrio alginolyticus* strains isolated from farmed fish in Korea from 2005 through 2007. *Journal of Food Protection.* 74(3): 380-386.

O'Hara CM, Sowers EG, Bopp CA, Duda SB, and Strockbine NA. 2003. Accuracy of six commercially available systems for identification of members of the family *Vibrionaceae*. *Journal of Clinical Microbiology.* 41(12): 5654-5659.

Ohishi K, Yamagishi M, Ohta T, Suzuki M, Izumida H, Sano H, Nishijima M, and Miwa T. 1996. Purification and properties of two chitinases from *Vibrio alginolyticus* H-8. *Journal of Fermentation and Bioengineering*. 82(6): 598-600.

Oksuz L and Gurler N. 2013. Sepsis due to *Vibrio alginolyticus* isolated from catheter of young patient with hypercholesterolemy: the first case from Turkey. *Clinical Medical Research.* 2(3): 37-39.

Okunishi I, Kawagishi I, and Homma M. 1996. Cloning and characterization of *motY*, a gene coding for a component of the sodium-driven flagellar motor in *Vibrio alginolyticus.* *Journal of Bacteriology.* 178(8): 2409-2415.

O'Neill TB, Drisko RW, and Hochman H. 1961. *Pseudomonas creosotensis* sp. n., a creosote-tolerant marine bacterium. *Applied Microbiology.* 6:472-474.

Opal SM and Saxon JR. 1986. Intracranial infection by *Vibrio alginolyticus* following injury in salt water. *Journal of Clinical Microbiology.* 23(2): 373-374.

Orós J, Torrent A, Calabuig P, and Déniz S. 2005. Diseases and causes of mortality among sea

turtles stranded in the Canary Islands, Spain (1998–2001). *Diseases of Aquatic Organisms.* 63: 13-24.

Overman TL, Kessler JF, and Seabolt JP. 1985. Comparison of API 20E, API rapid E, and API rapid NFT for identification of members of the family Vibrionaceae. *Journal of Clinical Microbiology.* 22(5): 778-781.

Patterson TF, Bell SR, and Bia FJ. 1988. *Vibrio alginolyticus* cellulitis following coral injury. *The Yale Journal of Biology and Medicine.* 61: 507-512.

Penland R, Boniuk M, and Wilhelmus K.2000. *Vibrio* ocular infections on the U.S. Gulf Coast. *Cornea*. 19(1): 26-29.

Pezzlo M, Valter MA, and Burns MJ. 1979. Wound infection associated with *Vibrio alginolyticus*. *American Journal of Clinical Pathology.* 71(4): 476-478.

Pien F, Lee, K, and Higa. 1977. *Vibrio alginolyticus* infections in Hawaii. *Journal of Clinical Microbiology.* 5(6): 670-672.

Pien FD, Ang KS, Nakashima NT, Evans DG, Grote JA, Hefley ML, and Kubota EA. 1983. Bacterial flora of marine penetrating injuries. *Diagnostic Microbiology and Infectious Disease.* 1(3): 229-232.

Poorvin L, Sander SG, Velasquez I, Ibisanmi E, LeClair GR, and Wilhelm SW. 2011. A comparison of Fe bioavailability and binding of a catecholate siderophore with virus-mediated lysates from the marine bacterium *Vibrio alginolyticus* PWH3a. *Journal of Experimental Marine Biology and Ecology.* 399(1): 43-47.

Pratheepa V and Vasconcelos V. 2013. Microbial diversity associated with tetrodotoxin production in marine organisms. *Environmental Toxicology and Pharmacology.* 36(3): 1046-1054.

Prescott RD and Decho AW. 2020. Flexibility and adaptability of quorum sensing in nature. *Trends in Microbiology.* 28(6): 436-444.

Prociv P. 1978. *Vibrio alginolyticus* in Western Australia. *Medical Journal of Australia*. 2(7): 296-296.

Pruzzo C, Crippa A, Bertone S, Pane L, and Carli A. 1996. Attachment of *Vibrio alginolyticus* to chitin mediated by chitin-binding proteins. *Microbiology.* 142(8): 2181-2186. https://doi.org/10.1099/13500872-142-8-2181.

Qian R, Chu W, Mao Z, Zhang C, Wei Y, and Yu L. 2007. Expression, characterization and immunogenicity of a major outer membrane protein from *Vibrio alginolyticus*. *Acta Biochimica et Biophysica Sinica*. 39(3): 194-200.

R Core Team. 2022. R: A language and environment for statistical computing. R Foundation for Statistical Computing, Vienna, Austria. https://www.R-project.org/.

Radhakrishnan EV and Kizhakudan JK. 2019. Health management in lobster aquaculture. In: Radhakrishnan, E., Phillips, B., Achamveetil, G. (eds) *Lobsters: Biology, Fisheries and Aquaculture*. Springer, Singapore. https://doi.org/10.1007/978-981-32-9094-5_13.

Rafidah O, Firdaus-Nawi M, Sitti Raehanah MS, Ina-Salwany MY, Ching FF, Abidin NA, and Zamri-Saad M. 2017. An outbreak of *Vibrio alginolyticus* in juvenile sea cucumbers *Holothuria scabra* in Sabah, Malaysia. *Pertanika Tropical Agriculture Science.* 40(4): 691-696.

Ragab RH, Elgendy MY, Sabry NM, Sharaf MS, Attia MM, Korany RMS, Abdelsalam M, Ethahan AS, Eldessouki EA, El-Demerdash GO, and Khalil RH. 2022. Mass kills in hatchery-reared European seabass (*Dicentrarchus labrax*) triggered by concomitant

infections of *Amyloodinium ocellatum* and *Vibrio alginolyticus. International Journal of Veterinary Science and Medicine.* 10(1): 33-45.

Ralston EP, Kite-Powell H, and Beet A. 2011. An estimate of the cost of acute food and water borne health effects from marine pathogens and toxins in the United States. *Journal of Water & Health.* 9(4): 680-694.

Reilly GD, Reilly CA, Smith EG, and Baker-Austin C. 2011. *Vibrio alginolyticus*-associated wound infection acquired in British waters, Guernsey, July 2011. *Eurosurveillance.* 16(42): https://doi.org/10.2807/ese.16.42.19994-en.

Reina J, Fernandez-Baca V, and Lopez A. 1995. Acute gastroenteritis caused by *Vibrio alginolyticus* in an immunocompetent patient. *Clinical Infectious Diseases.* 21(4): 1044-1045.

Reusch TBH, Schubert PR, Marten SM, Gill D, Karez R, Busch K, and Hentschel U. 2021. Lower *Vibrio* spp. abundances in *Zostera marina* leaf canopies suggest a novel ecosystem function for temperate seagrass beds. *Marine Biology.* 68: 149. https://doi.org/10.1007/s00227-021-03963-3.

Reverter M, Sarter S, Caruso D, Avarre JC, Combe M, Pepey E, Pouyaud L, Vega-Heredía S, De Verdal H, and Gozlan RE. 2020. Aquaculture at the crossroads of global warming and antimicrobial resistance. *Nature Communications.* 11: 1870.

Rigos G, Kogiannou D, Padrós F, Cristòfol C, Florio D, Fioravanti M, and Zarza C. 2020. Best therapeutic practices for the use of antibacterial agents in finfish aquaculture: a particular view on European seabass (*Dicentrarchus labrax*) and gilthead seabream (*Sparus aurata*) in Mediterranean aquaculture. *Reviews in Aquaculture*. 13(3): 1285-1323.

Riquelme C, Toranzo AE, Barja JL, Vergara N, and Araya R. 1996. Association of *Aeromonas*

hydrophila and *Vibrio alginolyticus* with larval mortalities of scallop (*Argopecten purpuratus*). *Journal of Invertebrate Pathology.* 67: 213-218.

Robert R, Grollier G, Malin F, Doré P, and Pourrat O. 1991. Isolation of *Vibrio alginolyticus* from blood cultures in a leukaemic patient after consumption of oysters. *European Journal of Clinical Microbiology & Infectious Diseases.* 10(11): 987-988.

Royle JA, Isaacs D, Eagles G, Cass D, Gilroy N, Chen S, Malouf D, and Griffiths C. 1997. Infections after shark attacks in Australia. *The Pediatric Infectious Disease Journal.* 16(5): 531-532.

Rui H, Liu Q, Ma Y, Wang Q, and Zhang Y. 2008. Roles of LuxR in regulating extracellular alkaline serine protease A, extracellular polysaccharide and mobility of *Vibrio alginolyticus*. *FEMS Microbiology Letters.* 285(2): 155-162.

Rui H, Liu Q, Wang Q, Ma Y, Liu H, Shi C, and Zhang Y. 2009. Role of alkaline serine protease, Asp, in *Vibrio alginolyticus* virulence and regulation of its expression by LuxO-LuxR regulatory system. *Journal of Microbiology and Biotechnology*. 19(5): 431-438.

Ruiz CC and Agraharkar M. 2003. Unusual marine pathogens causing cellulitis and bacteremia in hemodialysis patients: Report of two cases and review of the literature. *Hemodialysis International*. 7(4): 356-359.

Rutherford ST, Van Kessel JC, Shao Y, and Bassler BL. 2011. AphA and LuxR/HapR reciprocally control quorum sensing in vibrios. *Genes & Development*. 25: 397-408.

Ruwandeepika HAD, Jayaweera TSP, Bhowmick PP, Karunasagar I, Bossier P, and Defoirdt T. 2012. Pathogenesis, virulence factors and virulence regulation of vibrios belonging to the *Harveyi* clade. *Reviews in Aquaculture.* 4(2): 59-74.

Ryan WJ. 1976. Marine vibrios associated with superficial septic lesions. *Journal of Clinical*

Pathology. 29: 1014-1015.

Sadok K, Mejdi S, Nourhen S, and Amina B. 2013. Phenotypic characterization and RAPD fingerprinting of *Vibrio parahaemolyticus* and *Vibrio alginolyticus* isolated during Tunisian fish farm outbreaks. *Folia Microbiologica*. 58: 17-26.

Sainz JC, Maeda-Martínez AN, and Ascencio F. 1998. Experimental vibriosis induction with *Vibrio alginolyticus* of larvae of the Catarina scallop (*Argopecten ventricosus =circularis*) (Sowerby II, 1842). *Microbial Ecology.* 35: 188-192.

Sakatoku A, Hatano K, Tanaka S, and Isshiki T. 2021. Isolation and characterization of a *Vibrio* sp. strain MA_3 associated with mass mortalities of the pearl oyster *Pinctada fucata. Archives of Microbiology.* 203: 5267-5273.

Sakazaki R, Iwanami S, and Fukumi H. 1963. Studies on the enteropathogenic facultatively halophilic bacteria, Vibrio parahaemolyticus. *Japanese Journal of Medical Science and Biology.* 16: 161-188.

Sakazaki R. 1968. Proposal of *Vibrio alginolyticus* for the biotype 2 of *Vibrio parahaemolyticus*. *Japanese Journal of Medical Science and biology.* 21: 356-362.

Sampaio A, Silva V, Poeta P, and Aonofriesei F. 2022. *Vibrio* spp.: Life strategies, ecology, and risks in a changing environment. *Diversity*. 14(2): 97. https://doi.org/10.3390/d14020097.

Sangster CR and Smolowitz RM. 2003. Description of *Vibrio alginolyticus* infection in cultured *Sepia officinalis*, *Sepia apama*, and *Sepia pharaonic. The Biological Bulletin.* 205(2): 233-234.

Sarathi M, Ahmed I, Venkatesan C, Balasubramanian G, Prabavathy J, and Sahul Hameed AS. 2007. Comparative study on immune response of *Fenneropenaeus indicus* to *Vibrio alginolyticus* and white spot syndrome virus. *Aquaculture*. 271(1-4): 8-20.

Sasikala D and Srinivasan P. 2016. Characterization of potential lytic bacteriophage against *Vibrio alginolyticus* and its therapeutic implications on biofilm dispersal. *Microbial Pathogenesis.* 101: 24-35.

Schar D, Klein EY, Laxminarayan R, Gilbert M, and Van Boeckel TP. 2020. Global trends in antimicrobial use in aquaculture. *Scientific Reports.* 10: 21878.

Schets FM, Van Den Berg HHJL, Demeulmeester AA, Van Dijk E, Rutjes SA, Van Hooijdonk HJP, and De Roda Husman AM. 2006. *Vibrio alginolyticus* infections in the Netherlands after swimming in the North Sea. *Eurosurveillance*. 11(45): 3077. https://doi.org/10.2807/esw.11.45.03077-en.

Schets FM, Van Den Berg HHJL, Rutjes SA, and Husman AMDR. 2010. Pathogenic *Vibrio* species in Dutch shellfish destined for direct human consumption. *Journal of Food Protection*. 73(4): 734-738.

Schets FM, Van Den Berg HHJL, Marchese A, Garbom S, and De Roda Husman AM. 2011. Potentially human pathogenic vibrios in marine and fresh bathing waters related to environmental conditions and disease outcome. *International Journal of Hygiene and Environmental Health.* 214(5): 399-406.

Schmidt U, Chmel H, and Cobbs C. 1979. Vibrio alginolyticus infections in humans. *Journal of Clinical Microbiology.* 10(5): 666-668.

Schroeder JP, Wallace JG, Cates MB, Greco SB, and Moore WB. 1985. An infection by *Vibrio alginolyticus* in an Atlantic Bottlenose Dolphin housed in an open ocean pen. *Journal of Wildlife Diseases.*21(4): 437-438.

Schroeder GN, Pearson JS, and Thurston TLM. 2021. Editorial: Bacterial effectors as drivers of

human disease: Models, methods, mechanisms. *Frontiers in Cellular and Infection Microbiology.* 11: 708228.

Sechi LA, Duprè I, Deriu A, Fadda G, and Zanetti S. 2001. Distribution of *Vibrio cholerae* virulence genes among different *Vibrio* species isolated in Sardinia, Italy. *Journal of Applied Microbiology.* 88(3): 475-481.

Selvarajan R, Sibanda T, Venkatachalam S, Ogola HJO, Obieze C, and Msagati TA. 2019. Distribution, interaction and functional profiles of epiphytic bacterial communities from the rocky intertidal seaweeds, South Africa. *Scientific Reports.* 9: 19835. https://doi.org/10.1038/s41598-019-56269-2.

Selvin J and Lipton AP. 2003. *Vibrio alginolyticus* associated with white spot disease of *Penaeus monodon. Diseases of Aquatic Organism.* 57: 147-150.

Seymour JR, Ahmed T, Durham WM, and Stocker R. 2010. Chemotactic response of marine bacteria to the extracellular products of *Synechococcus* and *Prochlorococcus. Aquatic Microbial Ecology*. 59: 161-168.

Sganga G, Cozza V, Spanu T, Spada PL, and Fadda G. 2009. Global climate change and wound care: case study of an off-season vibrio alginolyticus infection in a healthy man. *Ostomy Wound Management.* 55(4): 60-62.

Shan J, Guoliang W, Quingsong Z, Tianlun Z, ang Yinger C. 2005. Epidemiology of vibriosis in large yellow croaker *Pseudosciaena crocea* (richardson) in marine cage culture. *Fisheries Science.* 24(1): 17-19.

Sharma SRK, Shankar KM, Sathyanarayana ML, Sahoo AK, Patil R, Narayanaswamy HD, and

Rao S. 2010. Evaluation of immune response and resistance to diseases in tiger shrimp, *Penaeus monodon* fed with biofilm of *Vibrio alginolyticus. Fish & Shellfish Immunology.* 25(5): 724-732.

Sharma SRK, Shankar KM, Sathyanarayana ML, Patil RR, Swamy HDN, and Rao S. 2011. Development of biofilm of *Vibrio alginolyticus* for oral immunostimulation of shrimp. *Aquaculture International.* 19: 421-430.

Sharma SRK, Rathore G, Verma DK, Sadhu N, Philipose KK. 2013. *Vibrio alginolyticus* infection in Asian seabass (*Lates calcarifer*, Bloch) reared in open sea floating cages in India. *Aquaculture Research*. 44(1):86-92.

Sheng L, Gu D, Wang Q, Liu Q, and Zhang Y. 2012. Quorum sensing and alternative sigma factor RpoN regulate type VI secretion system I (T6SSVA1) in fish pathogen *Vibrio alginolyticus*. *Archives of Microbiology.* 194: 379-390.

Slifka KM, Newton AE, and Mahon BE. 2017. *Vibrio alginolyticus* infections in the USA, 1988-2012. *Epidemiology & Infection.* 145:1491-1499.

Sjoblad RD and Mitchell R. 1979. Chemotactic responses of *Vibrio alginolyticus* to algal extracellular products. *Canadian Journal of Microbiology*. 25(9): 964-967.

Snoussi M, Noumi E, Usai D, Sechi LA, Zanetti S, and Bakhrouf A. 2008. Distribution of some virulence related-properties of *Vibrio alginolyticus* strains isolated from Mediterranean seawater (Bay of Khenis, Tunisia): investigation of eight *Vibrio cholerae* virulence genes. *World Journal of Microbiology and Biotechnology.* 24: 2133-2141.

Snoussi M, Noumi E, Hajlaoui H, Usai D, Sechi LA, Zanetti S, and Bakhrouf A. 2009. High potential of adhesion to abiotic and biotic materials in fish aquaculture facility by *Vibrio alginolyticus* strains. *Journal of Applied Microbiology.* 106(5): 1591-1599.

Song X, Zhang J, Yu W, Shi X, and Wu Y. 2020. Occurrence and identification of pathogenic *Vibrio* contaminants in common seafood available in a Chinese traditional market in Quingdao, Shandong Province. *Frontiers in Microbiology.* 11:1488. https://doi.org/10.3389/fmicb.2020.01488.

Spark RP, Fried ML, Perry C, and Watkins C. 1979. *Vibrio alginolyticus* wound infection: case report and review. *Annals of Clinical and Laboratory Science.* 9(2): 133-138.

Strand M, Hedström M, Seth H, McEvoy EG, Jacobsson E, Göransson U, Andersson HS, and Sundberg P. 2016. The bacterial (*Vibrio alginolyticus*) production of tetrodotoxin in the ribbon worm *Lineus longissimus*—Just a False Positive? *Marine Drugs.* 14(4): 63. 10.3390/md14040063.

Suhartono S, Ismail YS, Muhayya SR, and Husnah M. 2019. Ethanolic extracts of *Moringa oleifera* leaves inhibit biofilm formation of *Vibrio alginolyticus* in vitro. *IOP Conference Series: Earth and Environmental Science*. 348: 012018.

Sun B, Wang Z, Wang Z, Ma X, and Zhu F. 2017. A proteomic study of proteins from mud crab (*Scylla paramamosain*) infected with white spot syndrome virus or *Vibrio alginolyticus*. *Frontiers in Immunology.* 8:468. https://doi.org/10.3389/fimmu.2017.00468.

Sung HH, Hsu SF, Chen CK, Ting YY, and Chao WL. 2001. Relationships between disease outbreak in cultured tiger shrimp (*Penaeus monodon*) and the composition of *Vibrio* communities in pond water and shrimp hepatopancreas during cultivation. *Aquaculture.* 192(2-4): 101-110.

Supuran CT, Scozzafava A, and Mastrolorenzo A. 2001. Bacterial proteases: current therapeutic use and future prospects for the development of new antibiotics. *Expert Opinion on Therapudic Patents*. 11(2): 221-259.

Takekawa N, Nishikino T, Hori K, Kojima S, Imada K, and Homma M. 2021. ZomB is essential for chemotaxis of *Vibrio alginolyticus* by the rotational direction control of the polar flagellar motor. *Genes to Cells*. 26(11): 927-937.

Takemura AF, Chien DM, and Polz MF. 2014. Associations and dynamics of Vibrionaceae in the environment, from the genus to the population level. *Frontiers in Microbiology*. 5(38). https://doi.org/10.3389/fmicb.2014.00038.

Takeuchi H, Shibano Y, Morihara K, Fukushima J, Inami S, Kiel B, Gilles AM, Kawamoto S, and Okuda K. 1992. Structural gene and complete amino acid sequence of *Vibrio alginolyticus* collagenase. *Biochemical Journal.* 281(3): 703-708.

Takikawa I. 1958. Studies on pathogenic halophilic bacteria. *Yokohama Medical Bulletin*. 9:313.

Tall A, Teillon A, Boisset C, Delesmont R, Touron-Bodilis, and Hervio-Heath. 2012. Real-time PCR optimization to identify environmental *Vibrio* spp. strains. *Journal of Applied Microbiology.* 113(2): 361-372.

Tangredi BP. 1980. Post-mortem isolation of *Vibrio alginolyticus* from and Atlantic white-sided dolphin (*Lagenorynchus acutus*). *Journal of Wildlife Diseases.* 16(3): 329-331.

Taylor R, McDonald M, Russ G, Carson M, and Lulaczynski E. 1981. *Vibrio alginolyticus* peritonitis associated with ambulatory peritoneal dialysis. *British Medical Journal*. 283(6286): 275.

Thompson JR, Randa MA, Marcelino LA, Tomita-Mitchell A, Lim E, and Polz MF. 2004. Diversity and dynamics of a North Atlantic coastal *Vibrio* community. *Applied and Environmental Microbiology.* 70(7): 4103-4110.

Thompson FL and Swings J. 2006. Taxonomy of Vibrios. In: Thompson FL, Austin B, and Swings J (eds). *The Biology of Vibrios*. ASM Press, Washington DC. 29-43.

Thuesen EV and Kogure K. 1989. Bacterial production of tetrodotoxin in four species of *Chaetognatha*. *The Biological Bulletin.* 176(2): 191-194.

Tian Y, Wang Q, Liu Q, Ma Y, Cao X, and Zhang Y. 2008a. Role of RpoS in stress survival, synthesis of extracellular autoinducer 2, and virulence in *Vibrio alginolyticus*. *Archives of Microbiology.* 190: 585-594.

Tian Y, Wang Q, Liu Q, Ma Y, Cao X, Guan L, and Zhang Y. 2008b. Involvement of LuxS in the regulation of motility and flagella biogenesis in *Vibrio alginolyticus. Bioscience, Biotechnology, and Biochemistry*. 72(4): 1063-1071.

Tsakris A, Psifdis A, and Douboyas J. 1995. Complicated suppurative otitis media in a Greek diver due to a marine halophilic *Vibrio* sp. *The Journal of Laryngology and Otology.* 109: 1082-1084.

Tu KC and Bassler B. 2007. Multiple small RNAs act additively to integrate sensory information and control quorum sensing in *Vibrio harveyi*. *Genes & Development.* 21(2): 221-233.

Tubiash HS, Colwell RR, and Sakazaki R. 1970. Marine vibrios associated with bacillary necrosis, a disease of larval and juvenile bivalve mollusks. *Journal of Bacteriology* 103(1): 272-273.

Turner JW, Good B, Cole D, and Lipp EK. 2009. Plankton composition and environmental factors contribute to *Vibrio* seasonality. *The ISME Journal*. 3: 1082-1092.

Twedt RM, Spaulding PL, and Hall HE. 1969. Morphological, cultural, biochemical, and serological comparison of Japanese strains of *Vibrio parahemolyticus* with related cultures isolated in the United States. *Journal of Bacteriology.* 98(2): 511-518.

Uh Y, Park JS, Hwang GY, Yoon KJ, Park HC, and Hwang SO. 2001. *Vibrio alginolyticus* acute gastroenteritis: report of two cases. *Clinical Microbiology and Infection.* 7(2): 103-106.

Ulitzer S. 1975a. The mechanism of swarming of *Vibrio alginolyticus*. *Archives of Microbiology.* 104(1): 67-71.

Ulitzur S. 1975b. Effect of temperature, salts, pH and other factors on the development of peritrichous flagella in *Vibrio alginolyticus*. *Archives of Microbiology.* 104: 285-288.

Vandenberghe J, Verdonck L, Robles-Arozarena R, Rivera G, Bolland A, Balladares M, Gomez-Gil B, Calderon J, Sorgeloos P, and Swings J. 1999. Vibrios associated with *Litopenaeus vannamei* larvae, postlarvae, broodstock, and hatchery probionts. *Applied and Environmental Microbiology.* 65(6): 2592-2597.

Vasconcelos GJ, Stang WJ, and Laidlaw. 1975. Isolation of *Vibrio parahaemolyticus* and *Vibrio alginolyticus* from estuarine areas of Southeastern Alaska. *Applied Microbiology*. 29(4): 557-559.

Vogan CL, Costa-Ramos C, and Rowley AF. 2002. Shell disease syndrome in the edible crab, *Cancer pagurus* – isolation, characterization and pathogenicity of chitinolytic bacteria. *Microbiology.* 148: 743-754.

Von Graevenitz A and Currington GO. 1973. Halophilic vibrios from extraintestinal lesions in man. *Infection*. 1: 54-58.

Vu TTT, Alter T, and Huehn S. 2018. Prevalence of *Vibrio* spp. in retail seafood in Berlin, Germany. *Journal of Food Protection.* 81(4): 593-597.

Wagner KR and Crichton EP. 1981. Marine vibrio infections acquired in Canada. *Canadian Medical Association Journal.* 124(4): 435-436.

Wang GL, Shan J, Chen Y, and Li Z. 2006. Study on pathogens and pathogenesis of emulsification disease of *Portunus trituberculatus*. *Advances in Marine Science*. 24(4): 526-531.

Wang Q, Liu Q, Ma Y, Zhou L, and Zhang Y. 2007a. Isolation, sequencing and characterization of cluster genes involved in the biosynthesis and utilization of the siderophore of marine fish pathogen *Vibrio alginolyticus*. *Archives of Microbiology.* 188: 433-439.

Wang Q, Liu Q, Ma Y, Rui H, and Zhang Y. 2007b. LuxO controls extracellular protease, haemolytic activities and siderophore production in fish pathogen *Vibrio alginolyticus.* *Journal of Applied Microbiology.* 103(5): 1525-1534.

Wang Q, Liu Q, Cao X, Yang M, and Zhang. 2008. Characterization of two TonB systems in marine fish pathogen *Vibrio alginolyticus*: their roles in iron utilization and virulence. *Archives of Microbiology.* 190: 595-603.

Wang Z, Xiao T, Pang S, Liu M, and Yue H. 2009. Isolation and identification of bacteria associated with the surfaces of several algal species. *Chinese Journal of Oceanography and Limnology*. 27(3): 487-492.

Weis KE, Hammond RM, Hutchinson R, and Blackmore CGM. 2011. Vibrio illness in Florida, 1998-2007. *Epidemiology and Infection.* 139: 591-598.

Wong SK, Zhang XH, and Woo NYS. 2012. *Vibrio alginolyticus* thermolabile hemolysin (TLH) induces apoptosis, membrane vesiculation and necrosis in sea bream erythrocytes. *Aquaculture*. 330-333: 29-36.

Wong KC, Brown AM, Luscombe GM, Wong SJ, and Mendis K. 2015. Antibiotic use for *Vibrio* infections: important insights from surveillance data. *BMC Infectious Diseases.* 15:226.

Worden AZ, Seidel M, Smriga S, Wick A, Malfatti F, Bartlett D, and Azam F. 2006. Trophic regulation of *Vibrio cholerae* in coastal marine waters. *Environmental Microbiology*. 8(1): 21-29.

Xia M, Pei F, Mu C, Ye Y, and Wang C. 2018. Disruption of bacterial balance in the gut of

Portunus trituberculatus induced by *Vibrio alginolyticus* infection. *Journal of Oceanology and Limnology*. 36: 1981-1898.

Xie ZY, Hu CQ, Chen C, Zhang LP, and Ren CH. 2005. Investigation of seven *Vibrio* virulence genes among *Vibrio alginolyticus* and *Vibrio parahaemolyticus* strains from the coastal mariculture systems in Guangdong, China. *Letters in Applied Microbiology*. 41(2): 202-207.

Xie J, Bu L, Jin S, Wang X, Zhao Q, Zhou S, and Xu Y. 2020. Outbreak of vibriosis caused by *Vibrio harveyi* and *Vibrio alginolyticus* in farmed seahorse *Hippocampus kuda* in China. *Aquaculture.* 523: 735168.

Xu SL, Wang DL, Jia CY, Jin S, ang CL, and Zou X. 2013a. Effects of *Vibrio alginolyticus* infection on immune-related enzyme activities and ultrastructure of *Charybdis japonica* gills. *Aquaculture.* 396-399: 82-88.

Xu SL, Qui CG, Zhou W, Wang DL, Jia CY, and Wang CL. 2013b. Pathological analysis of hemolymphs of *Charybdis japonica* infected with *Vibrio alginolyticus. Fish & Shellfish Immunology*. 35(5): 1577-1584.

Xu W, Gong L, Yang S, Gao Y, Ma X, Xu L, Chen H, and Lou Z. 2020. Spatiotemporal dynamics of *Vibrio* communities and abundance in Dongshan Bay, South of China. *Frontiers in Microbiology.* 11: 575287. https://doi.org/10.3389/fmicb.2020.575287.

Xue S, Sun J, and Xu W. 2017. Identification and detection of the pathogenic bacteria responsible for swollen abdomen disease in cultured turbot, *Scophthalmus maximus*, and flounder, *Paralichthys olivaceus. Journal of the World Aquaculture Society*. 49(3): 540-550.

Yan Q, Chen Q, Ma S, Zhuang Z, and Wang X. 2007. Characteristics of adherence of

pathogenic *Vibrio alginolyticus* to the intestinal mucus of large yellow croaker (*Pseudosciaena crocea*). *Aquaculture.* 269(1-4): 21-30.

Yang B, Zhai S, Li X, Tian J, Li Q, Shan H, and Liu S. 2021. Identification of *Vibrio alginolyticus* as a causative pathogen associated with mass summer mortality of the Pacific Oyster (*Crassostrea gigas*) in China. *Aquaculture.* 535: 736363.

Ye J, Ma Y, Liu Q, Zhao DL, Wang QY, and Zhang YX. 2008. Regulation of *Vibrio alginolyticus* virulence by the LuxS quorum-sensing system. *Journal of Fish Diseases*. 31(3): 161-169.

Yi X, Xu X, Qi X, Chen Y, Zhu Z, Xu G, Li H, Kraco EK, Shen H, Lin M, Zheng J, Qin Y, and Jiang X. 2022. Mechanisms underlying the virulence regulation of *Vibrio alginolyticus* ND-01 *pstS* and *pstB* with a transcriptomic analysis. *Microorganisms.* 10(11): 2093.

Yildiz FH and Visick KL. 2009. *Vibrio* biofilms: so much the same yet so different. *Trends in Microbiology.* 17(3): 109-118.

Yin JF, Wang MY, Chen YJ, Yin HQ, Wang Y, Lin MQ, Liu AY, and Hu CJ. 2018. Direct detection of *Vibrio vulnificus*, *Vibrio parahaemolyticus*, and *Vibrio alginolyticus* from clinical and environmental samples by a multiplex touchdown polymerase chain reaction assay. *Surgical Infections*. 19(1): https://doi.org/10.1089/sur.2017.203.

Yin WL, Xie ZY, Zeng YH, Zhang J, Long H, Ren W, Zhang X, Cai XN, and Huang AY. 2022. Two (p)ppGpp synthetase genes, *relA* and *spoT*, are involved in regulating cell motility, exopolysaccharides production, and biofilm formation of *Vibrio alginolyticus. Frontiers in Microbiology.* 13: 858559.

Yong L, Guanpin Y, Hualei W, Jixiang C, Xianming S, Guiwei Z, Qiwei W, and Xiuquin S.

2006. Design of *Vibrio* 16S rRNA gene specific primers and their application in the analysis of seawater *Vibrio* community. *Journal of Ocean University of China.* 5(2): 157-164.

Yu CF, Yu PHF, Chan PL, Yan Q, and Wong PK. 2004. Two novel species of tetrodotoxin-producing bacteria isolated from toxic marine puffer fishes. *Toxicon*. 44(6): 641-647.

Zen-Yoji H, Sakai S, Terayama T, Kudo Y, Ito T, Benoki M, and Nagasaki M. 1965. Epidemiology, enteropathogenicity, and classification of *Vibrio parahaemolyticus*. *The Journal of Infectious Diseases*. 115(5): 436-444.

Zen-Yoji H, Le Clair RA, Ohta K, and Montague TS. 1973. Comparison of *Vibrio parahaemolyticus* cultures isolated in the United States with those isolated in Japan. *The Journal of Infectious Diseases.* 127(3): 237-241.

Zhang J, Cao Z, Li Z, Li H, Wu F, Jin L, Li X, Li S, and Xu Y. 2015. Effect of bacteriophages on *Vibrio alginolyticus* infection in the sea cucumber, *Apostichopus japonicus* (Selenka). *Journal of the World Aquaculture Society.* 46(2): 149-158.

Zhang X, Lin H, Wang X, and Austin B. 2018. Significance of *Vibrio* species in the marine organic carbon cycle – A review. *Science China Earth Sciences*. 61(10): 1357-1368.

Zhang S, Wang J, Jiang M, Xu D, Peng B, Peng XX, and Li H. 2019. Reduced redox-dependent mechanism and glucose-mediated reversal in gentamicin-resistant *Vibrio alginolyticus*. *Environmental Microbiology.* 21(12): 4724-4739.

Zhang N, Zhang S, Ren W, Gong X, Long H, Zhang X, Cai X, Huang A, and Xie Z. 2021a. Roles of rpoN in biofilm formation of *Vibrio alginolyticus* HN08155 at different cell densities. *Microbiological Research.* 247: 126728.

Zhang Y, Tan H, Yang S, Huang Y, Cai S, Jian J, Cai J, and Quin Q. 2021b. The role of *dctP*

gene in regulating colonization, adhesion and pathogenicity of *Vibrio alginolyticus* strain HY9901. *Journal of Fish Diseases.* 45(3): 421-434.

Zhang Y, Wu X, Cai J, Chen M, Zhang J, Shao S, Zhang Y, Ma Y, and Wang Q. 2022. Transposon insertion sequencing analysis unveils novel genes involved in *luxR* expression and quorum sensing regulation in *Vibrio alginolyticus*. *Microbiological Research*. *In press*: 127243.

Zhao Z, Chen C, Hu CQ, Ren CH, Zhao JJ, Zhang LP, Jiang X, Luo P, and Wang QB. 2010. The type III secretion system of *Vibrio alginolyticus* induces rapid apoptosis, cell rounding and osmotic lysis of fish cells. *Microbiology*. 156(9): 2864-2872.

Zhao Z, Zhang L, Ren C, Zhao J, Chen C, Jiang X, Luo P, and Hu CQ. 2011. Autophagy is induced by the type III secretion system of *Vibrio alginolyticus* in several mammalian cell lines. *Archives of Microbiology.* 193: 53-61.

Zhao Z, Liu J, Deng Y, Huang W, Ren C, Call DR, and Hu C. 2018. The *Vibrio alginolyticus* T3SS effectors, Val1686 and Val1680, induce cell rounding, apoptosis and lysis of fish epithelial cells. *Virulence*. 9(1): 318-330.

Zhenyu X, Shaowen K, Chaoqun H, Zhixiong Z, Shifeng W, and Youngcan Z. 2013. First characterization of bacterial pathogen, *Vibrio alginolyticus*, for *Porites andrewsi* white syndrome in the South China Sea. *PLoS One* 8:e75425.

Zhou S, Hou Z, Li N, and Qin Q. 2007. Development of a SYBR Green I real-time PCR for quantitative detection of *Vibrio alginolyticus* in seawater and seafood. *Journal of Applied Microbiology.* 103(5): 1897-1906.

Zhou Z, Pang H, Ding Y, Cai J, Huang Y, Jian J, and Wu Z. 2013. VscO, a putative T3SS

chaperone escort of *Vibrio alginolyticus*, contributes to virulence in fish and is a target for vaccine development. *Fish & Shellfish Immunology*. 35(5): 1523-1531.

Zhou S, Tu X, Pang H, Hoare R, Monaghan SJ, Lou J, and Jian J. 2020. A T3SS regulator mutant of *Vibrio alginolyticus* affects antibiotic susceptibilities and provides significant protection to *Danio rerio* as a live attenuated vaccine. *Frontiers in Cellular and Infection Microbiology.* 10: 183.

Zhou K, Tian KY, Liu XQ, Liu W, Zhang XY, Liu JY, and Sun F. 2021, Characteristic and otopathogenic analysis of a Vibrio alginolyticus strain responsible for chronic otitis externa in China. *Frontiers in Microbiology.* 12: 750642.

Zhu F, Qian X, and Ma X. 2018. Comparative transcriptomic analysis of crab hemocytes in response to white spot syndrome virus or *Vibrio alginolyticus* infection. *Fish & Shellfish Immunology*. 80: 165-179.

Zorrilla I, Moriñigo MA, Castro D, Balebona MC, and Borrego JJ. 2003. Intraspecific characterization of *Vibrio alginolyticus* isolates recovered from cultured fish in Spain. *Journal of Applied Microbiology*. 95(5): 1106-1116.

Zuo Y, Zhao L, Xu X, Zhang J, Zhang J, Yan Q, and Huang L. 2019. Mechanisms underlying the virulence regulation of new *Vibrio alginolyticus* ncRNA Vvrr1 with a comparative proteomic analysis. *Emerging Microbes & Infections.* 8(1): 1604-1618.

Tables and Figures.

Table 1: Susceptible animal hosts and common signs of *V. alginolyticus* infection. Citing literature consists of outbreak investigations, experimental infection studies, or a combination of the two.

Host Organism Type	**Host Species**	**Infection Signs**	**Infection Type**	**Location**	**Selected Citations**
Shrimp and Prawns	*Penaeus monodon*	Discoloration, lethargy, hepatopancreas damage, exoskeletal deterioration, mortality	Outbreak	Taiwan	Lee et al., 1996a
				India	Selvin & Lipton, 2003
			Outbreak & Experimental		Jayasree et al., 2006
	Litopenaeus vannamei (*Penaeus vannamei*)	Discoloration, lethargy, bacterial aggregation in tissues, mortality	Outbreak & Experimental	Taiwan	Lui et al., 2004a
		Larval feeding reduction, metamorphosis impairment, mortality	Outbreak	India	Kumar et al., 2017
				Ecuador and Mexico	Vandenberghe et al., 1999
	Penaeus japonicus	Discoloration, bacterial septicemia, mortality	Outbreak & Experimental	Taiwan	Lee et al., 1996b
	Litopenaeus setiferus (*Penaeus setiferus*) *Farfantepenaeus aztecus* (*Penaeus aztecus*)	Discoloration, lethargy, slow hemolymph clotting, mortality	Outbreak & Experimental	United States	Lightner & Lewis, 1975

	Fenneropenaeus indicus	Discoloration, hemocyte infiltration, slow hemolymph clotting	Experimental	India	Sarathi et al., 2007
	Macrobrachium rosenbergii	Anorexia, lethargy, necrotic appendages, mortality	Outbreak	India	Jayaprakash et al., 2006
Crabs	*Portunus trituberculatus*	Hepatopancreas and muscle tissue emulsification, mortality	Outbreak & Experimental	China	Wang et al., 2006
		Gut dysbiosis	Experimental	China	Xia et al., 2018
	Scylla paramamosain	Discoloration, lethargy, hemocyte damage and reduction, mortality	Experimental	China	Sun et al., 2017 Zhu et al., 2018
	Charybdis japonica	Gill damage, hemocyte damage and reduction, mortality	Experimental	China	Xu et al., 2013a Xu et al., 2013b
	Cancer pagurus	Carapace deterioration and breach, mortality	Outbreak	United Kingdom	Vogan et al., 2002
	Carcinus aestuarii			Italy	Mancuso et al., 2013
Lobsters	*Panulirus ornatus*	Hepatopancreas damage, phyllosoma mortality	Outbreak	Australia	Bourne et al., 2007
		Discoloration, mortality		Vietnam & Indonesia	Radhakrishnan & Kizhakudan 2019
	Panulirus longipes				
	Panulirus polyphagus				
	Panulirus homarus				
		Mortality	Outbreak & Experimental	India	Abraham et al., 1996
	Jasus edwardsii	Tail fan necrosis	Experimental	Australia	Musgrove et al., 2005
	Palinurus elephas	Carapace deterioration and breach, mortality	Outbreak	Italy	Mancuso et al., 2010
Urchins	*Paleopneustes cristatus*	Epidermal lesions, mortality	Experimental	Bahamas	Bauer & Young, 2000
	Archaeopneustes hystrix				

	Diadema africanum	Epidermal lesions, loss of spines and tube feet, deterioration of water-vascular system, mortality	Outbreak & Experimental	Madeira Island, Portugal	Clemente et al., 2014
Sea Cucumbers	*Holothuria scabra*	Epidermal lesions, excess mucus production, mortality	Outbreak	Malaysia	Rafidah et al., 2017
	Holothuria atra	Epidermal lesions, discoloration, visceral ejection, mortality	Outbreak & Experimental	Egypt	Fahmy & Hamed, 2022
	Apostichopus japonicus	Epidermal lesions, visceral ejection, mortality	Outbreak & Experimental	China	Zhang et al., 2015
Bivalves	*Argopecten ventricosus*	Reduced swimming ability, ciliar atrophy, necrotic tissue mortality	Experimental	Mexico	Sainz et al., 1997
			Outbreak & Experimental		Luna-González et al. 2002
	Argopecten purpuratus	Larval mortality	Experimental	Chile	Riquelme et al., 1996
	Ruditapes decussatus	Lesions, tissue degradation, hemocyte infiltration, mortality	Outbreak & Experimental	Spain	Gómez-León et al., 2005
	Ruditapes philippinarum	Tissue necrosis, mortality	Experimental	Italy	Moreira et al., 2014
	Nodipecten subnodosus	Reduced swimming ability, ciliar atrophy, necrotic tissue mortality	Experimental	Bolivia	Luna-González et al. 2002
	Atrina maura				
	Crassotrea gigas				
		Adductor muscle weakness, tissue necrosis, enlarged digestive gland tubules, mortality	Outbreak & Experimental	China	Yang et al., 2021
	Crassostrea virginica	Bacillary necrosis, mortality	Outbreak	Unknown	Tubiash et al., 1970
	Mercenaria mercenaria				
	Mytilus galloprovincialis	Abnormal larvae	Experimental	Mexico	Anguiano-Beltrán et al., 2004

	Perna viridis	Discoloration, excess mucus secretion, opened shells, epithelial sloughing, hemocyte infiltration, mortality	Experimental	Malaysia	Laith et al., 2021
	Pinctada fucata	Soft tissue atrophy, discoloration, mortality	Outbreak	Japan	Sakatoku et al., 2021
	Ostrea edulis	Larval mortality	Experimental	Scotland	Nottage & Brikbeck, 1987
Gastropods	*Haliotis diversicolor supertexta*	Discoloration, reduced body muscle, lethargy, mortality	Outbreak	China	Cai et al., 2006
	Haliotis rufescens	Lethargy, weak attachment, mortality	Experimental	Mexico	Anguiano-Beltrán et al., 1998
	Haliotis asinina	Lethargy, loose mantle attachment, discoloration, lesions, hemocyte infiltration, mortality	Outbreak	Malaysia	Kua et al., 2011
Cephalopods	*Sepia officinalis*	Epidermal and reproductive lesions, necrosis, organ damage, mortality	Outbreak	United States	Sangster & Smolowitz, 2003
	Sepia apama				
	Sepia pharaonis				
	Octopus joubini	Epidermal lesions, reduced feeding, lethargy, mortality	Outbreak	United States	Hanlon et al., 1984
	Octopus briareus				
	Octopus vulgaris	Epidermal lesions	Outbreak	Italy	Fichi et al., 2015
Corals	*Porites andrewsi*	Tissue loss, mortality	Outbreak & Experimental	China	Zhenyu et al., 2013
	Diploastrea heliopora,	Zooxanthellae degradation, lesions, tissue loss, mortality	Outbreak	Indonesia	Cervino et al., 2008
	Fungia spp.				
	Herpolitha spp.				
	Montastraea spp.				
Bony Fishes	*Sparus aurata*	Septicemia, discoloration, ulcers, lesions, mortality	Outbreak	Israel	Colorni et al., 1981
			Experimental	Unknown	Balebona et al., 1998

	Sparus sarba	Ulceration, inflammation, fin rot, hemorrhage, mortality	Outbreak	Hong Kong	Li et al., 1999
			Experimental	Hong Kong	Li et al., 2003
	Acanthopagrus schlegeli	Larval mortality	Outbreak	Japan	Kusuda et al., 1986
	Pagrus major	Mortality	Experimental	Unknown	Iwata et al., 1978
	Oplegnathus fasciatus	Mortality	Experimental	Unknown	Liu et al., 2018
	Scophthalmus maximus	Gill fusion, discoloration, muscle liquefaction, fin rot, mortality	Outbreak	Scotland	Austin et al., 1993
	Paralichthys olivaceus	Swollen abdomen, hemorrhagic trunk skin, lethargy, mortality	Outbreak & Experimental	China	Xue et al., 2017
	Solea senegalensis	Discoloration, hemorrhagic fins, epidermal lesions, hemorrhagic liver, mortality	Outbreak & Experimental	Spain	Zorrilla et al., 2003
	Epinephelus malabaricus	Discoloration, exophthalmia, corneal opacity, mortality	Outbreak	Taiwan	Lee, 1995
	Epinephelus fuscoguttatus Epinephelus polyphekadion (hybrid)	Lethargy, excess mucus production, fin rot, septicemic lesions, organ dysfunction, mortality	Outbreak	Malaysia	Mohamad et al., 2019
	Epinephelus coioides	Mortality	Experimental	Taiwan	Cheng et al., 2009
	Epinephelus bruneus	Mortality	Experimental	Unknown	Harikrishnan et al., 2012
	Tilapia zillii	Exophthalmia, corneal opacity, lesions, liver hemorrhage, organ damage, mortality	Outbreak & Experimental	Egypt	El-Sayed et al., 2019
	Oreochromis niloticus		Outbreak	Egypt	Abdelsalam et al., 2021

	Clarias gariepinus	Discoloration, lesions, corneal opacity, liver hemorrhage, mortality			
	Rachycentron canadum	Discoloration, lethargy, abdominal swelling, eye damage, mortality	Outbreak	Taiwan	Liu et al., 2004b
	Mugil cephalus	Lesions (red spot), mortality	Outbreak	Australia	Burke & Rodgers, 1981
	Lates calcarifer	Hemorrhage, ulcers, enlarged organs, mortality	Outbreak	India	Sharma et al., 2013
	Dicentrarchus labrax	Lethargy, discoloration, abdominal swelling, mortality	Outbreak	Egypt	Ragab et al., 2022
	Larimichthys crocea (*Pseudosciaena crocea*)	Lesions, organ dysfunction, mortality	Outbreak	China	Shan et al., 2005
			Experimental	China	Yan et al., 2007
	Sebastes schlegeli	Mortality	Experimental	Korea	Kim et al., 1999
	Lutjanus erythropterus	Bacterial septicemia, lesions, mortality	Experimental	China	Cai et al., 2010b
	Lutjanus sanguineus	Mortality	Experimental	China	Liang et al., 2010a
	Coryphaena hippurus	Epidermal lesions, anorexia, caudal fin erosion, mortality	Outbreak	United States	Leamaster & Ostrowski, 1988
	Chanos chanos	Exophthalmia, corneal opacity, hemorrhagic eyes, mortality	Outbreak & Experimental	Philippines	Muroga et al., 1984
	Hippocampus kuda	Discoloration, lethargy, lesions, disorientation, hepatic necrosis, mortality	Outbreak	China	Xie et al., 2020
	Hippocampus guttulatus	Lethargy, lack of appetite, lesions, tail necrosis	Outbreak	Spain	Balcázar et al., 2010
	Hippocampus hippocampus				
	Hippocampus reidi	Necrosis of mouth epithelium, gill damage, kidney and liver necrosis, mortality	Outbreak & Experimental	Brazil	Martins et al., 2010
	Himantura uarnak		Outbreak	Egypt	Emam et al., 2019

Cartilaginous Fishes	*Himantura fai*	Lethargy, lesions, lack of appetite, myolysis, liver and spleen congestion, mortality			
Sea Turtles	*Caretta caretta* *Chelonia mydas* *Eretmochelys imbdcata*	Epidermal lesions ulcerative stomatitis, bronchopneumonia	Outbreak	Australia	Glazebrook & Campbell, 1990a
		Epidermal lesions ulcerative stomatitis, bronchopneumonia	Outbreak	Australia	Glazebrook & Campbell, 1990b
	Dermochelys coriacea	Epidermal lesions	Outbreak (stranding)	Canary Islands, Spain	Orós et al., 2005
Marine Mammals	*Tursiops truncatus*	Epidermal lesions	Outbreak	United States	Schroeder et al., 1985
		Meningoencephalitis, mortality	Outbreak (stranding)	Italy	Di Renzo et al., 2017
	Lagenorynchus acutus	Oral lesions, congested lungs, fluid in the peritoneal cavity, necrotizing hepatitis, bronchopneumonia, mortality	Outbreak (stranding)	United States	Tangredi, 1980

Table 2: Case reports of common manifestations of *V. alginolyticus* human infections. Reports listed chronologically by site of infection and exposure source.

Site of Infection	Description of Symptoms	Exposure Source (Known or presumed)	Location of Report	Treatment(s) Administered	Citations
Ear	Otitis externa, otitis media, discharge, discomfort, foul odor	Seawater exposure	Connecticut, USA	Erythromycin	Von Graevenitz & Currington, 1973
			England	Unspecified	Ryan, 1976
			Romania	Unspecified	Ciufecu et al., 1979
			Greece	Amoxycillin-clavulanate	Tsakris et al., 1995
			Korea	Ciprofloxacin, ofloxacin	Doh et al., 1997
			Florida, USA[a]	Ofloxacin, amoxicillin-clavulanate	Feingold & Kumar, 2004
			Germany	Amoxicillin-clavulanate	Schets et al., 2006
			Mauritius	Ciprofloxacin	Issack et al., 2008
			Turkey	Ciprofloxacin	Citil et al., 2015
			Turkey	Amoxicillin-clavulanate, ciprofloxacin	Baran et al., 2016
			China	Ciprofloxacin	Zhou et al., 2021
		Ear drum perforation in seawater	Australia	Tetracycline	McSweeney et al., 1977
		Freshwater and seawater exposure	Ohio, USA[b]	Ciprofloxacin	Mukherji et al., 2000
		Unknown	Belgium	Unspecified	Hansen et al., 1979

Eye	Conjunctivitis, discharge, discomfort	Seafood handling (Fish cutter)	New Jersey, USA	Procaine penicillin, sulfisoxazole	Schmidt et al., 1979
		Handling seashells	New York, USA	Gentamicin	Lessner et al., 1985
Wound Infection (Leg)	Cellulitis, foul odor, discharge, pain, tissue necrosis	Injury sustained in/around seawater (Rock laceration)	England	Unspecified	Ryan, 1976
		Injury sustained in/around seawater (Reef laceration)	St. Thomas, USA	Tissue debridement, doxycycline	Patterson et al., 1988
		Injuries sustained in/around seawater (Plane crash)	Senegal	Topical antiseptic, antibiotics (unspecified)	Matsiota-Bernard & Nauciel, 1993
		Injury sustained in/around seawater (Shark bite)	Australia	Gentamicin, metronidazole, ciprofloxacin	Royle et al., 1997
		Exposure of preexisting injury to seawater	New York, USA	Gentamicin	Jo Rubin & Tilton, 1975
			California, USA	Tetracycline	Pezzlo et al., 1979
			New Jersey, USA	Tissue debridement, povidone-iodine	Schmidt et al., 1979
			Canada	Trimethoprim-sulfamethoxazole	Wagner et al., 1981
			Germany	Amoxicillin-clavulanate	Schets et al., 2006
		Injury sustained near coastline (No direct water exposure)	Italy	Levofloxacin	Sganga et al., 2009
		Wrapped an existing injury in seaweed, swimming	United Kingdom	Doxycycline	Reilly et al., 2011

		Applied sea cucumber (*A. japonicus*) oil to existing injury	Malaysia	Cloxacillin, amoxycillin-clavulanate	Mohamed et al., 2016
Wound Infection (Foot)	Cellulitis, pain	Exposure of preexisting injury to seawater	Australia	Tetracycline	McSweeney et al., 1977
		Injury sustained in/around seawater (Seashell laceration)	Alabama, USA	Unspecified	Bonner et al., 1983
Wound Infection (Hand/Fingers)	Cellulitis, pain, necrosis	Injury sustained in/around seawater (Hand laceration)	California, USA	Sodium dicloxacillin monohydrate (oral)	Spark et al., 1979
		Injury sustained in/around seawater (Fishing injury)	England	Tissue excision	Ryan, 1976
		Injuries sustained in/around seawater (Finger amputation)	Japan	Cefazolin, imipenem	Horii et al., 2005
		Injury sustained in/around seawater (Octopus bite)	France	Bacitracin–neomycin, ciprofloxacin	Campanelli et al., 2008
		Exposure of preexisting injury to seawater	Germany	Amoxicillin-clavulanate	Schets et al., 2006
Gastrointestinal	Abdominal pain, diarrhea, nausea, vomiting, fever, blood in stool	Fish roe	Japan	Unspecified	Hiratsuka et al., 1980
		Raw seafood (unspecified)	Florida, USA	Unspecified	Hlady & Klontz, 1996
		Crayfish	Louisiana & Texas, USA	Antibiotics (unspecified)	Bean et al., 1998
		Raw crab	South Korea	Symptomatic treatment of diarrhea	Uh et al., 2001
		Unknown	Spain	Symptomatic treatment of diarrhea	Reina et al., 1995

			India	Rehydration, antibiotics (unspecified)	Aggarwal et al., 1986
			Texas, USA[c]	Symptomatic treatment of diarrhea	Caccamese & Rastegar, 1999

[a]Patient had pressure-equalizing tubes placed in ears at a young age to treat recurrent ear infections.

[b]Patient had a prior eardrum perforation before exposure.

[c]Patient was immunocompromised and experienced chronic gastrointestinal symptoms associated with infection.

Table 3: Broad epidemiological surveys of *V. alginolyticus* human infections.

Types of Infections Surveyed	**Number of *V. alginolyticus* Cases Surveyed**	**Exposure Source (Presumed to known)**	**Treatment(s) Administered**	**Year(s) Surveyed**	**Location of Survey**	**Citation**
Wound, ear	8	Exposure and injuries sustained in/around seawater	Tissue debridement, tetracycline, polymyxin B-neomycin-hyinfection drocortisone, erythromycin,	1972	Hawaii, USA	Pien et al., 1977
Wound	36	Injuries sustained in/around seawater (Reef lacerations)	Natural healing, topical antibiotics (unspecified)	1978	Australia	Prociv, 1978
Wound, ear	10	Exposure of preexisting injuries and injuries sustained in/around seawater, seawater exposure	Natural healing, tetracycline	1976-1979	Australia	Ghosh & Bowen, 1980
Wound	3	Injuries sustained in/around seawater	Wound irrigation, draining, antibiotics (unspecified)	1980-1981	Hawaii, USA	Pien et al., 1983
Wound, bacteremia	51	Injuries sustained in/around water, marine animal exposure	Tissue debridement, antibiotics (unspecified)	1981-1986	Florida, USA	Howard & Lieb, 1988
Wound	7	Exposure of preexisting injuries	Unspecified	1989	Gulf Coast, USA	Leveine et al., 1993

		and injuries sustained in/around seawater				
Ear	17	Seawater exposure	Natural healing, antibiotics (unspecified)	1987-1992	Denmark	Hornstrup & Gahrn-Hansen, 1993
Wound, bacteremia	25	Exposure of preexisting injuries and injuries sustained in/around seawater, seafood ingestion	Tissue debridement, tetracycline, erythromycin, cephalosporin	1979-1991	Florida, USA	Howard & Bennett, 1993
Wound, ear, gastrointestinal, pulmonary	52	Exposure of preexisting injuries and injuries sustained in/around seawater, seafood ingestion	Unspecified	1981-1993	Florida, USA	Hlady & Klontz, 1996
Eye	5	Exposure to seawater and marine animals	Natural healing, sulfisoxazole, gentamicin	1969-1985	Gulf Coast, USA	Penland et al., 2000
Wound, ear, gastrointestinal, bacteremia	356	Exposure of preexisting injuries and injuries sustained in/around seawater, seafood ingestion	Tetracycline, minocycline, doxycycline, ceftazidime, levofloxicin	1997-2006	USA	Dechet et al., 2008
Wound, gastrointestinal	131	Exposure of preexisting injuries and injuries sustained in/around seawater, seafood ingestion	Unspecified	1998-2007	Florida, USA	Weis et al., 2011
Unspecified	3	Seawater exposure	Unspecified	2014	Sweden	Baker-Austin et al., 2016

Wound, ear, eye, gastrointestinal, bacteremia	1331	Exposure of preexisting injuries and injuries sustained in/around seawater, seafood ingestion	Unspecified	1988-2012	USA	Slifka, et al., 2017
Wound, ear	17	Exposure to seawater, exposure of preexisting injuries and injuries sustained in/around seawater	Unspecified	2016-2020	Tasmania	Harlock et al., 2022

Table 4: Case reports of atypical and/or invasive *V. alginolyticus* infections in humans. Most cases of severe *V. alginolyticus* infection are associated with immunocompromised individuals and/or severe accidental injuries associated with seawater exposure.

Presentation of Infection	**Preexisting Conditions**	**Exposure Source (Known or presumed)**	**Location of Report**	**Treatment(s) Administered**	**Outcome**	**Citation**
Bacteremia, sepsis	Burn victim	Burn lesions doused with seawater	Florida, USA	Polymyxin B, clindamycin, cephalothin, carbenicillin, gentamicin, penicillin	Fatal	English & Lindberg, 1977
Bacteremia, sepsis	Metastatic cancer patient	Unknown	New York, NY	Cephalothin, tobramycin, mezlocillin, clindamycin, amikacin	Fatal	Janda et al., 1986
Bacteremia	Leukemia patient	Consumption of raw oysters	France	Ceftazidime, amikacin, ventilator use, blood transfusion	Fatal	Robert et al., 1991
Bacteremia, sphenoiditis	None	Ocean diving	Portugal	Ceftriaxone, chloramphenicol	Recovered	Lopes et al., 1993
Bacteremia	End-stage renal disease patient with subclavian catheter	Catheter exposure while swimming in seawater	New York, USA	Vancomycin, ceftriaxone, doxycycline, gatifloxacin	Recovered	Nadkarni & Shah, 2007
Cellulitis, bacteremia	Late stage renal disease on hemodialysis	Leg injury exposed to coastal flood waters	Texas, USA	Vancomycin, gentamicin	Recovered	Ruiz & Agraharkar, 2003
Bacteremia	Cirrhotic patient with hepatitis B	Consumption of raw fish	South Korea	Vancomycin, ciprofloxacin, doxycycline	Fatal	Lee et al., 2008

Bacteremia, sepsis	Hypercholesterolemia patient with catheter	Unknown (Isolated from catheter)	Turkey	Meropenem, teicoplanin	Recovered	Oksuz & Gurler, 2013
Respiratory distress syndrome, sepsis	Near drowning victim, diabetic, elderly, frequent smoker and drinker	Inhalation of seawater	Réunion Island, France	Ventilation, amoxicillin–clavulanic acid, piperacillin–tazobactam, amikacin	Recovered	Gaüzère et al., 2016
Bacteremia, necrotizing fasciitis	Metastatic leukemia patient receiving chemotherapy	Unknown	Gulf Coast, USA	Unknown	Fatal	Bonner et al., 1983
Necrotizing fasciitis (Leg)	Stingray puncture wound	Exposure of puncture wound to seawater	Hong Kong	Tissue debridement, ciprofloxacin, amoxicillin–clavulanate	Recovered	Ho et al., 1998
Necrotizing fasciitis (Leg)	None	Laceration sustained swimming on a reef	Colombia	Tissue debridement, clindamycin, dicloxacillin, ampicillin-sulbactam, ciprofloxacin	Recovered	Gomez et al., 2003
Peritonitis	End-stage renal disease patient receiving peritoneal dialysis	Changed peritoneal dialysis fluid on beach	Australia	Gentamicin, cephalexin	Recovered	Taylor et al., 1981
Sinusitis	Recent sinus surgery	Ocean swimming	Canada	Cloxacillin	Recovered	Wagner et al., 1981
Intercranial Infection	Sustained a head injury while diving	Exposure of head injury to seawater	Guam, USA	Nafcillin, chloramphenicol, cefotaxime	Recovered	Opal & Saxon, 1986
Pleural empyema, bacteremia	History of cancer, mastectomy	Unknown (Recently ingested raw seafood)	Taiwan	Intubation, fluid drainage, amoxicillin-clavulanate, piperacillin–tazobactam	Recovered	Chien et al., 2002
Chronic osteomyelitis	Recent surgery to repair fractured tibia	Ocean swimming	Croatia	Tissue debridement, ciprofloxacin, tetracycline	Recovered	Barbarossa et al., 2002

Chest	Pacemaker	Ocean swimming	France	Gentamicin, ceftriaxone, rifampin	Recovered	Floch & Boutoille, 2008
Endophthalmitis	Fishhook injury to eye	Injury exposure to seawater	China	Lensectomy, vitrectomy, tobramycin, fluorometholone, ampicillin, dexamethasone	Recovered	Li et al., 2009

Table 5: *Vibrio* virulence genes detected in *V. alginolyticus* and their presumed function(s).

Gene/operon descriptions may represent known or presumed function.

Virulence Mechanism(s)	**Gene/Operon Description(s)**	**Gene/Operon Name(s)**	**Selected Citation(s)**
Bacterial effector	Hemolysin	*tdh, trh, tlh, hylA*	Xie et al., 2005 Cai et al., 2007a Gargouti et al., 2015 Liu et al., 2017
	Collagenase	*clg*	Di Pinto et al., 2009 Yang et al., 2021
	Alkaline serine protease	*asp*, *proA*	Deane et al., 1989 Rui et al., 2009 Yang et al. 2021
	Caseinolytic protease	*clpP*	Chen et al., 2020
	Metalloprotease	*hapA*	Liu et al., 2017
	Cholera toxin	*ctxA, ctxB*	Snoussi et al., 2008 Khouadja et al., 2022
	Cholera accessory toxin	*ace*	Sechi et al., 2001 Kahla-Nakbi et al., 2009
	Zonula occludens toxin	*zot*	Sechi et al., 2001 Snoussi et al., 2008
	Cytotoxin	*val1686, val1680, yopP, mviN*	Zhao et al., 2018 Gennari et al., 2012 Cao et al., 2010
Effector secretion	Type III secretion system injectosome protein	*vscX, vscO*	Zhou et al., 2013 Chen et al., 2017
	Effector secretion regulation	*tyeA*	Zhou et al., 2020
Effector secretion, biofilm formation	Twin-arginine translocation	*tatABC*	He et al., 2010
Effector efficacy	Neuraminidase	*nanH*	Gennari et al., 2012
Motility	Lateral flagella-associated extracellular protease	*pep*	Cao et al., 2011
	Flagellar directional response	*cheY, zomB*	Kojima et al., 2007 Takekawa et al., 2021
	Signal recognition particle receptor (flagella)	*flhF, flfG*	Kusumoto et al., 2006.
	Polar flagella motor component	*motY, motX, pomA, pomB*	Okunishi et al., 1996 Asai et al., 1997

Adhesion, motility	Flagellar assembly	*flrA, flrB, flrC*	Lou et al., 2016
Adhesion, biofilm formation	Outer membrane protein	*ompA, ompW, ompK*	Qian et al., 2007 Cai et al., 2013 Yang et al. 2021
Adhesion, biofilm formation	Accessory colonization factor	*acfA*	Cai et al., 2018
Motility, adhesion, biofilm formation	Flagellar system	*flaA, flab, flaK, lafA, lafK, filS*	Yang et al., 2008 Liang et al., 2010b Yang et al. 2021
Motility, adhesion, biofilm formation	Tripartite ATP-independent periplasmic transporter	*dctP*	Zhang et al., 2021b
Motility, adhesion, biofilm formation	Phosphoenolpyruvate-dependent phosphotransferase system	*ptsS, ptsB*	Yi et al., 2022
Adhesion, biofilm production, effector secretion	Oligopeptide permeases	*oppABCDF*	Liu et al., 2017 Gu et al., 2019
Iron acquisition	TonB operation	*fur*	Wang et al., 2008
Stress response/survivability	Metabolism regulation	*pykF*	Zou et al., 2019
	Alarmone synthase	*relA, spoT*	Yin et al., 2022
	Superoxide dismutase	*sodB*	Chen et al., 2019
Quorum sensing	Master regulators	*luxR, luxO, luxS, luxA, aphA, hapR, vpsR*	Gu et al., 2016 Wang et al., 2007b Ye et al., 2008 Tian et al., 2008b
Quorum sensing, motility, biofilm formation	sRNA binding protein	*hfq*	Liu et al., 2011b
Transcriptional regulation, quorum sensing	Vibrio quorum sensing activator	*vqsA*	Gao et al., 2018
Transcriptional regulator, stress response/survivability	Alternative sigma factor	*rpoS, rpoN, rpoX*	Huang et al., 2018 Zhang et al., 2021a
Transcriptional regulation, biofilm formation, adhesion, effector secretion	Highly conserved *Vibrio* pathogenicity gene	*toxR, toxS, toxRS, toxT*	Sechi et al., 2001 Xie et al., 2005 Snoussi et al., 2008 Kahla-Nakbi et al., 2009 Chen et al., 2012

Pathogenicity cluster	Vibrio pathogenicity island	*VPI*	Sechi et al., 2001 Xie et al., 2005 Snoussi et al., 2008 Kahla-Nakbi et al., 2009 Khouadja et al., 2022

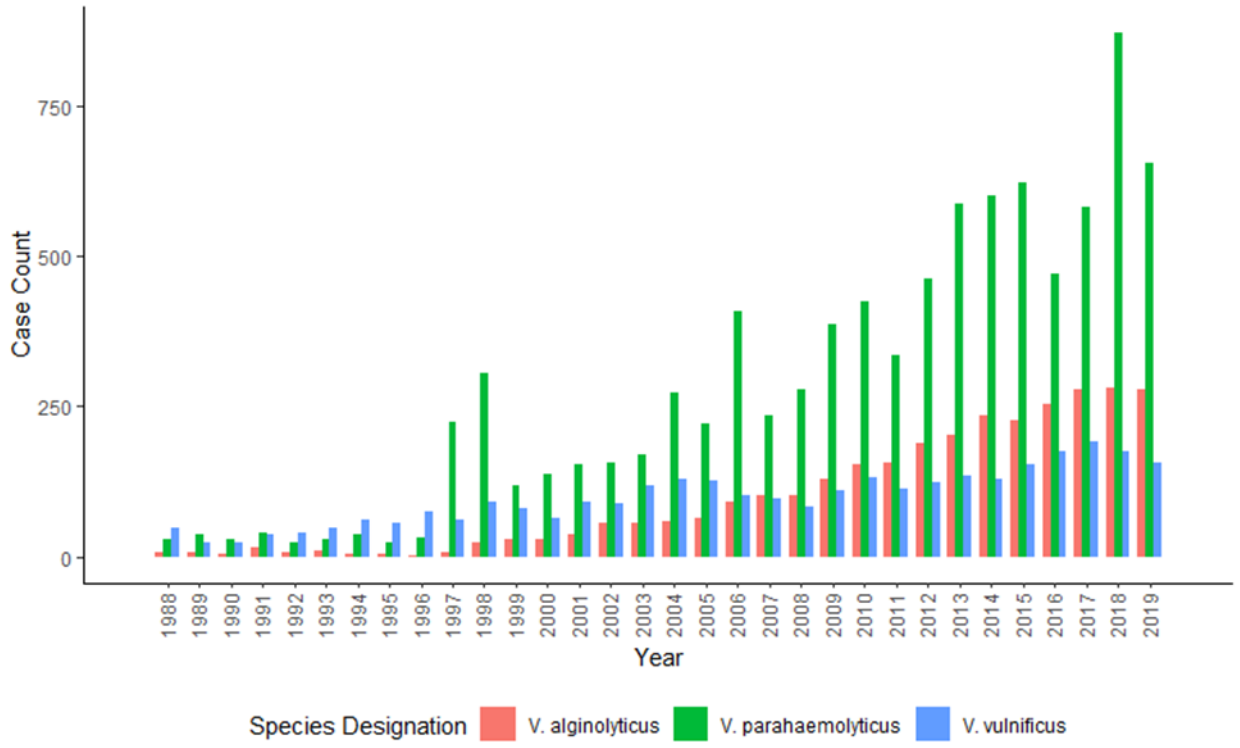

Figure 1: Reported human vibriosis infections from *V. alginolyticus*, *V. parahaemolyticus*, and *V. vulnificus* in the United States from 1988-2019. Reports include all cases where one of the three designated species were identified as the primary agent of disease. Data derived from the CDC's Cholera and Other Vibrio Illness Surveillance System (COVIS).

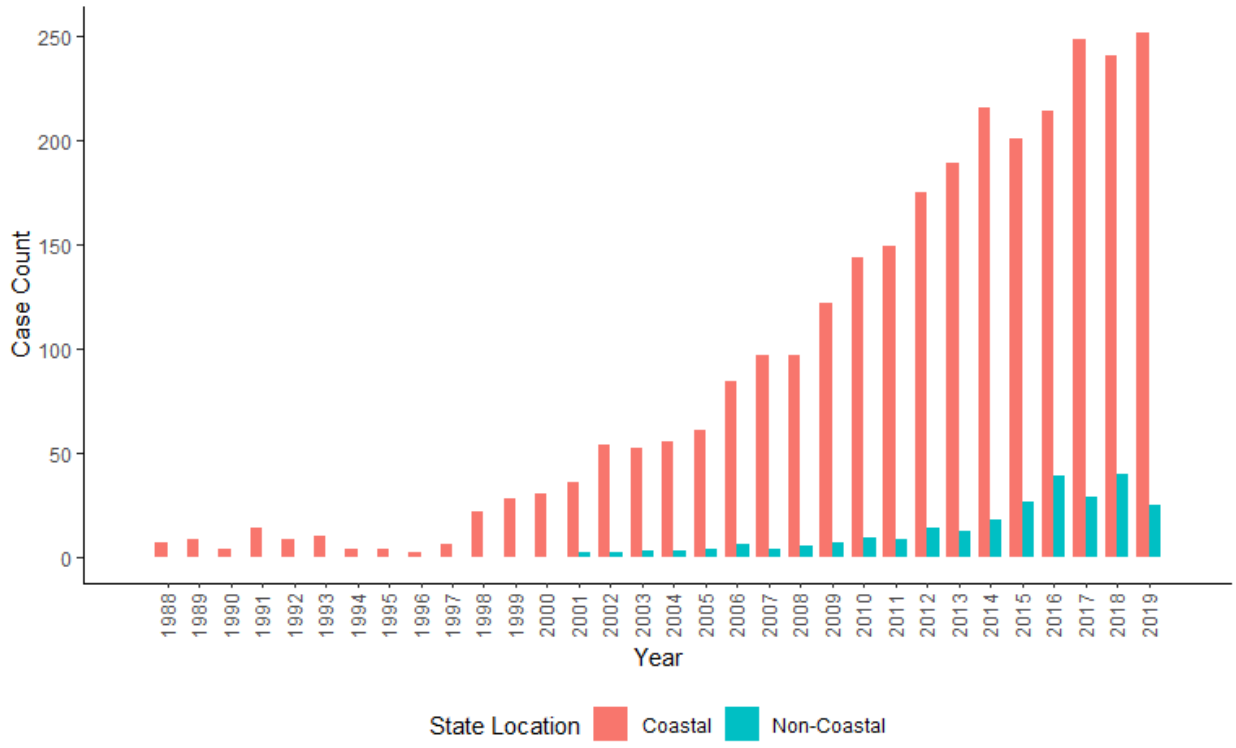

Figure 2: Coastal and non-coastal burden of *V. alginolyticus* infections in the United States from 1988-2019. Coastal state counts include Alabama, Georgia, Florida, Mississippi, Louisiana, Texas, California, North Carolina, South Carolina, Virginia, Maryland, Delaware, New Jersey, New York, Rhode Island, Connecticut, Massachusetts, Maine, Oregon, Washington, Alaska, and Hawaii. Data derived from the CDC's Cholera and Other Vibrio Illness Surveillance System (COVIS).

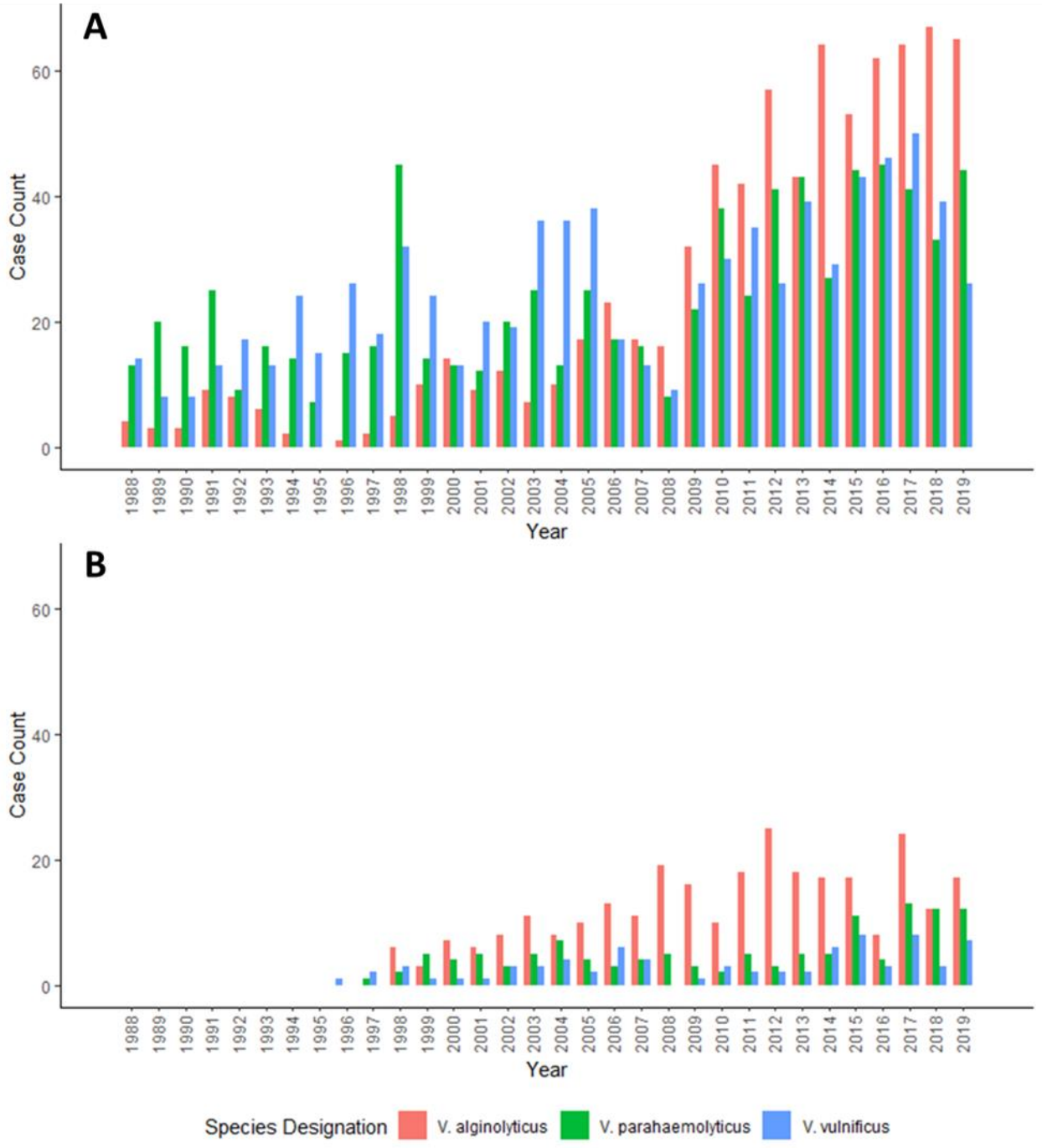

Figure 3: State-level human vibrios infections from *V. alginolyticus*, *V. parahaemolyticus*, and *V. vulnificus* reported in Florida (A) and Hawaii (B) from 1988-2019. Data derived from the CDC's Cholera and Other Vibrio Illness Surveillance System (COVIS).

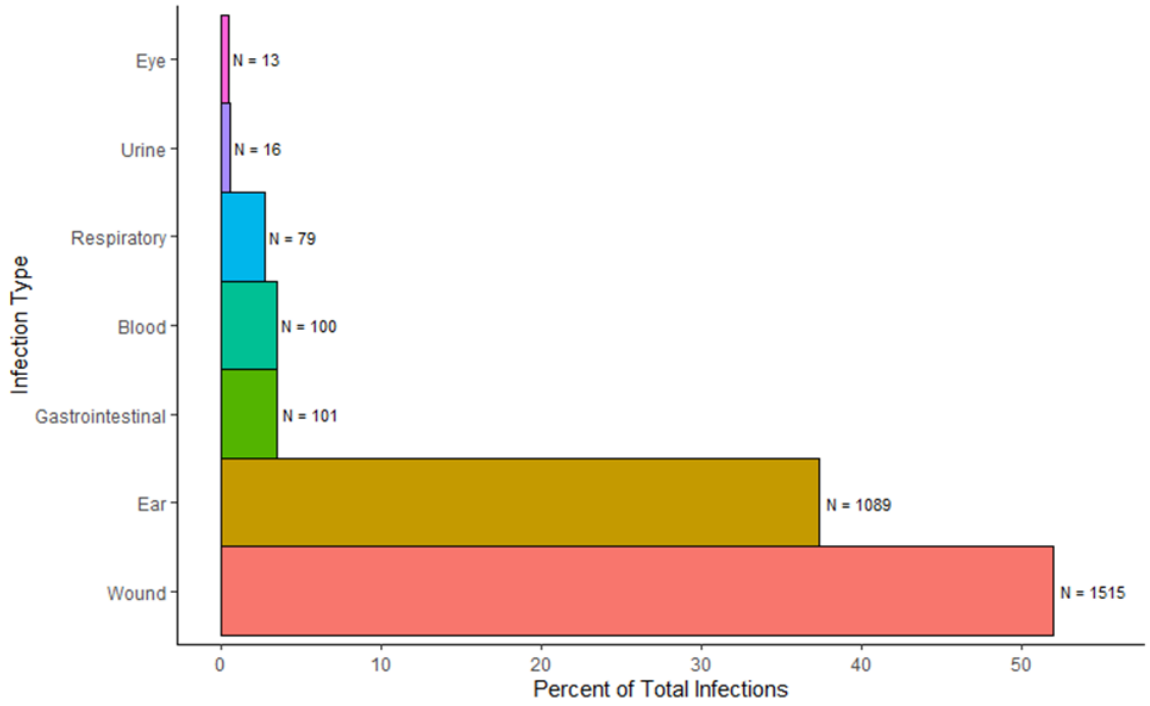

Figure 4: *V. alginolyticus* infection locations from cases reported in the United States from 1988-2019. Sites represent the location were *V. alginolyticus* was cultured from the patient and prioritized the primary site of infection in the event of multiple sites. Wound infections are defined as soft tissue infections from any location on the body (excluding the ears) and represent both preexisting and sustained injures. Ear infections are defined as infections of the outer, middle, and inner ear (including the tympanic membrane). Gastrointestinal infections are defied by isolation from stool, bile, appendix, rectum, gall bladder, or colon. Blood infections are defined as isolation from blood, cerebrospinal fluid, peritoneal fluid, lumbar disc fluid, lymph node or bullae. Respiratory infections are defined as isolation from sinus, sputum, nose, throat, trachea, or lungs. Urine infections are defined as isolation from urine. Eye infections are defined as isolation from either the left or right eye. Data derived from the CDC's Cholera and Other Vibrio Illness Surveillance System (COVIS).

CHAPTER 3

ARDOD: LOW-COST APPLICATION OF AN ARDUINO MICROCONTROLLER BOARD FOR THE REAL-TIME MEASUREMENT OF BACTERIAL GROWTH KINETICS

Norfolk WA and Lipp EK. To be submitted to *PeerJ*

Abstract

Measurement of bacterial growth kinetics is a core assay for the investigation of bacterial physiology and the effects of differing culture conditions. The most common method of growth kinetics quantification is the measurement light scattering to quantify the change in optical density (OD) in a growing culture over a defined timeframe. Here we present and evaluate a low-cost do-it-yourself (DIY) OD meter, called ArdOD (short for Arduino optical density), to continuously measure bacterial growth kinetics over time. This meter was built using an Arduino Uno microcontroller board and is assembled using standard electrical components within a custom 3-D printed housing at a total cost of ~$60 USD. ArdOD is portable and capable of operating under direct electrical connection or battery power. To test the efficacy of this meter, the bacterial growth kinetics of *Escherichia coli*, *Salmonella enterica,* and *Vibrio alginolyticus* were measured in situ for a growing duration of ~6 hours. The resulting growth curves demonstrated that ArdOD effectively measured the growth of all three bacteria allowing for the visualization of lag, log, and stationary phase and the calculation of doubling time. When compared to tandem benchtop spectrophotometer measures, ArdOD produced comparable growth curves with an ArdOD-derived doubling time of 35.78, 55.91, and 46.48 min and a spectrophotometer-derived doubling time of 27.03, 60.58, and 41.55 min for *V. alginolyticus*, *S. enterica*, and *E. coli*, respectively. Biological replicates of each bacterial species showed consistent agreement in the culture kinetics up to the onset of stationary phase with a mean absolute deviation of 0.0153, 0.0101, and 0.0152 for *V. alginolyticus*, *S. enterica,* and *E. coli*, respectively. These results suggest that ArdOD is a cost-effective alternative to benchtop spectrophotometers for the measurement of bacterial growth kinetics.

Importance

Traditionally, OD measurements are collected using benchtop spectrophotometers. While affordable, these meters require continuous direct user input to measure the culture at defined intervals which can lead to increased human error associated with sample disturbance and low sensitivity due to the physical limitations of measurement frequency. High end meters such as plate readers overcome these challenges through the automation of sample measurement however, these machines can be limiting due to cost and are non-portable. Here we present ArdOD, as a low-cost automated alternative for the measurement of OD and evaluate the efficacy compared to benchtop spectrophotometer measures. Use of this meter can improve the measurement efficacy of bacterial growth kinetics in research settings where high-end meters are unavailable or impractical to employ.

Introduction

Assessment of bacterial growth kinetics, or the rate and characteristics of growth under a given set of culture conditions, is a core component of microbiology. Typically applied to characterize the baseline physiology of bacterial species or the physiological changes associated with culture conditions/substrates, these measures provide important information about the growth and replication of species of interest within a controlled setting (Van de Hulst, 1953; Koch, 1970; Koch, 1994). Traditionally, growth kinetics are measured using light scattering to quantify the optical density (OD) of bacterial particles suspended in a liquid medium at specified time points (Van de Hulst, 1953; Koch 1970; Harding, 1986; Lucidi et al., 2019). OD measures are representative of bacterial abundance and are used to quantify growth allowing for the quantification and visualization of lag, log, and stationary phases (Monod, 1949; Van de Hulst, 1953; Koch 1970; Harding, 1986). While additional culture-based methods such as direct counts

(Monod, 1949) and analytical methods such as Fourier-transform infrared spectroscopy (FT-IR) (Zeroual et al., 1994) exist for the quantification of growth kinetics, light scattering remains the most frequently utilized technique due to the relative simplicity of equipment and low-cost per sample.

Using Optical Density to Measure Growth Kinetics. Bacterial OD is measured by passing a continuous or pulsed beam of light through a sample and quantifying the level of transmitted light downstream (Koch, 1970; Sutton, 2011; Mauerhofer et al., 2019). As bacterial abundance increases the level of transmitted light will decrease due to scattering of the light beam by the suspended particles (Van de Hulst, 1953; Koch, 1970; Harding, 1986; Sutton 2011; Mauerhofer et al., 2019). The wavelength of this light beam is optimized to be representative of the growth media color and bacterial cell size; thus, measurement of the change in transmission is illustrative of the change in turbidity (Sutton, 2011; Lucidi et al., 2019; Yallapragada et al., 2019). The level of transmitted light is logarithmically related to the relative abundance of the bacterium in the sample according to Beer-Lampert's Law and can be used to calculate doubling time when measured over a specified growing period (Swinehart, 1962; Harding, 1986; Mauerhofer et al., 2019; Yallapragada et al., 2019).

Typically, growth kinetics are visualized as a bacterial growth curve, where OD values are plotted against time to show the change in relative abundance. From this curve, four critical values can be determined which are used to make predictions about the physiological response of the bacterium in changing abiotic conditions. 1) the onset time of log phase, 2) early log phase OD, 3) late log phase OD, and 4) the onset time of stationary phase. 1) The onset of log phase indicates the time at which the bacterium has successfully acclimated to the given media and entered into logarithmic binary fission (Monod, 1949; Akerlund et al., 1995; Al-Qadiri et al.,

2008). This value is indicative of the adaptivity of the bacterium at the given conditions of the experiment. 2) Early log phase OD and 3) late log phase OD are key measurements that represent the rate of the logarithmic growth phase. Early and late log phase OD values are used to calculate the growth rate constant (*k*) and are indicative of the physiological effects the abiotic conditions have on the growth speed of the bacterium (Monod, 1949; Sutton, 2011). Lastly, 4) the onset of stationary phase is the time at which bacterial abundance reaches carrying capacity within the liquid media. At this phase bacterial growth and death rates are in equilibrium and the viable bacterial abundance is representative of the maximum sustainable population of the given nutritional limitations (Monod, 1949; Akerlund et al., 1995; Al-Qadiri et al., 2008).

Optical Density Meters. While modern OD meters range from simplistic to complex, all meters operate on the foundation of the quantification of light scattering. The most common type of OD meter in use is a standard benchtop spectrophotometer. Benchtop spectrophotometers are discrete OD meters that quantify growth a specific time points dictated by direct user interface (Sutton, 2011; Hall et al., 2013). A small aliquot of the growing sample is transferred to a cuvette then placed between a light source and downstream detector. While satisfactory, this method requires a high level of researcher manipulation and thus is prone to errors in quantification, limited in the number of sampling time points, and laborious complete. Furthermore, cuvette-based spectrophotometers are destructive to the target sample making them impractical for the measurement of extremely rare or expensive to culture bacteria. More advanced OD measurement devices such as well plate readers alleviate many challenges of traditional spectrophotometry however, these devices come at a substantial cost when compared to spectrophotometers (Hall et al., 2013).

In recent years, several DIY meters have been developed by researchers to measure OD using low-cost electronics and 3D printing (Maia et al., 2016; Kutschera & Lamb, 2017; Sasidharan et al., 2018; Deutzmann et al., 2022). Spurred by the limitations of spectrophotometers, these devices are typically designed to mount a commercially available light sensor or miniaturized spectrophotometer to a culture container where growth can be continuously measured. Development of these meters often requires use of a centralized device where the data is collected and the sensors are maintained such as an open source microcontroller board like the Arduino or Raspberry Pi (Kutschera & Lamb, 2017; Sasidharan et al., 2018). Other meters have repurposed existing electronics such as one developed by Yallapragada et al., 2019 which uses a commercially available fitness bracelet to quantify OD coupled with a tandem smartphone application. While robust in their own application, many of these DIY meters require significant electrical knowledge to assemble, lack interchangeable parts, and can be designed around on highly specific methods of culture making them suboptimal for broad application and customization.

To alleviate the challenges associated with spectrophotometer usage and DIY meter design, we developed a prototype OD meter (ArdOD) using the Arduino platform to continuously measure the growth of a bacterium in a liquid medium. Meter design was optimized for easy assembly, minimal user manipulation, low-cost of materials, and the usage of interchangeable parts. Through this research we describe the design of ArdOD and evaluate the efficacy of this prototype through the quantification of bacterial growth kinetics for *Escherichia coli*, *Salmonella enterica,* and *Vibrio alginolyticus.*

Results

The results of this evaluation demonstrate the utility and reproducibility of the ArdOD as a tool for the quantification of bacterial OD. Continuous quantification of OD600 was achieved for all samples (N = 10 each bacterium) up to the onset of stationary phase with little to no user interface beyond setup. *V. alginolyticus* mean growth showed an onset of log phase at 100 minutes, an onset of stationary phase at 200 minutes, an early log phase (130min) OD of 0.0904, a late log phase (180min) OD of 0.238, and a doubling time of 35.78 minutes. *S. enterica* mean growth showed an onset of log phase at 210 minutes, an onset of stationary phase at 340 minutes, an early log phase (240min) OD of 0.113, a late log phase (320min) OD of 0.305, and a doubling time of 55.91 minutes. *E. coli* mean growth showed an onset of log phase at 175 minutes, an onset of stationary phase at 300 minutes, an early log phase (190min) OD of 0.0590, a late log phase (250min) OD of 0.144, and a doubling time of 46.48 minutes (Figure 1).

Comparison to Spectrophotometer Measures. When compared to a standard benchtop spectrophotometer the ArdOD was successful at capturing the overall trends of bacterial growth for all species measured. Similar time values for the onset of log phase, onset of stationary phase, and doubling time were observed across all samples. Direct comparison of OD showed differences in the maximum range of OD based upon meter type. These differences were expected due to structural and component disparities between the ArdOD and spectrophotometer and were normalized using a scaling factor relative to the specific bacterium (x1.55 for *V. alginolyticus,* x1.71 for *S. enterica,* and x1.40 for *E. coli*) (Figures 2-4).

Reproducibility. Technical replicates using the ArdOD showed minimal variation in growth kinetics between samples (Figure 5). *V. alginolyticus*, S. *enterica,* and *E. coli* showed consistent clustering through lag and log phase with a mean absolute deviation up to the onset of stationary

phase of 0.0153, 0.0101, and 0.0152 respectively. Maximum stationary phase OD was variable between technical replicates in all species with the greatest variability seen in *E. coli.*

Discussion

Growth characterization is a quintessential component of microbiology and is crucial to understanding the physiological characteristics of bacteria. Traditional benchtop spectrophotometer-based methods are in dire need of innovation to reduce experimenter burden and sample disturbance throughout measurement. While high-end meters (such as plate readers) overcome the challenges of standard spectrophotometers, these devices are restricted to laboratory usage and can be limiting due to cost. Through this evaluation, we demonstrate the utility of ArdOD as a low-cost DIY substitute for the quantification of bacterial growth kinetics.

Assessment of *E. coli*, *S. enterica*, and *V. alginolyticus* demonstrated that ArdOD can accurately capture the overall growth trends of these bacterial species producing growth curves that are consistent with their expected structure (Zwietering et al., 1990, Hall et al., 2013) and comparable to spectrophotometer-derived curves (Figure 1). Using these data, the bacterial doubling time, duration of lag phase, and the onset of stationary phase could be identified to quantify the physiological response of a bacterium under a given set of culture conditions. When compared to a standard curve created using the same culture conditions, these data can be used to estimate the bacterial concentration of a growing culture in real time.

The design and operation of ArdOD presents several advantages over traditional cuvette-based spectrophotometry. ArdOD stands as a continuous OD meter that requires no sample disturbance to measure, no consumable lab equipment, and no user interface to collect data beyond initial setup. Meter design is portable, and the battery-powered configuration allows for deployment within a shaking incubator or a field environment. Furthermore, the automation of

data collection allows for increased measurement frequency beyond the physical capability of experimenter-directed measurement. While data automation led to increased meter sensitivity, it should be noted that the ArdOD showed a reduced maximum OD when compared to a benchtop spectrophotometer. This disparity is likely due to differences in light source functionality between the two devices and was corrected using a normalization factor derived as the difference between the stationary phase OD for the spectrophotometer and ArdOD. Due to this limitation, we recommend calculation of this scaling factor to compare results between ArdOD and other light scattering meters.

When compared to other existing DIY OD meters (Kutschera & Lamb, 2017; Sasidharan et al., 2018), the ArdOD is designed to be widely practical to a range of experimenter needs and skill levels. Low-cost and user-friendly components were selected to design a meter that was technologically simple to construct and easily customizable to allow for (and encourage) further development and/or modification of the device. Interchangeable components were selected to allow for easy replacement and malfunction diagnosis. This modular design also prevents the need to full meter replacement in the event that a single component is damaged or destroyed. The use of open-source program software allows for individual customization of the ArdOD sampling parameters and allows for additional downstream modification to functionality.

While this evaluation examines the utility of the ArdOD in a research laboratory setting, the scope of the ArdOD's application extends beyond *ex situ* benchtop research. Field-based and remote researchers are highly limited by the availability of laboratory space and analytical equipment. The portability of the ArdOD is optimal for travel and allows for robust sample quantification without the need for large/sophisticated equipment. Furthermore, the modular DIY design allows for easy repair on-site where materials and time may be limiting. Beyond a direct

research application, the ArdOD is also optimal for usage in an educational setting. Bacterial physiology is a core curriculum concept for introductory microbiology courses often taught in conjunction with growth kinetics laboratory activities (Merkel et al., 2012; Wang et al., 2018). Due to budget limitations, these activities are frequently taught using traditional benchtop spectrophotometers which are laborious and prone to errors. Utilization of a DIY meter such as ArdOD for these and other OD-based educational activities would drastically reduce the cost of equipment (even when compared to benchtop spectrophotometers) while also increasing measurement sensitivity and enhancing student experience. Furthermore, the DIY design itself stands as educational tool and could be used to expose students to the design and development of biotechnology.

Conclusion

Through this research we demonstrate the utility and efficacy of ArdOD, a low-cost DIY continuous OD meter designed for the quantification of bacterial growth kinetics. Using this meter, we successfully characterized the growth trends of *V. alginolyticus*, *S. enterica*, and *E. coli* producing growth curves comparable to those derived from a benchtop spectrophotometer. This method eliminates many of the challenges of traditional OD measurement by reducing the need of user input, increasing measurement frequency, and the automation of data collection. This utility coupled with the low material cost, portability, and user-friendly design suggests that the ArdOD can be a valuable tool for the measurement of bacterial growth kinetics in various research and academic settings.

Methods

The ArdOD consists of four primary hardware components, 1) the Arduino board, 2) light source, 3) light detector (lux sensor), and 4) housing. The total cost of components is approximately $60 (USD), a detailed list of materials and cost criteria can be found in table S1.

The Arduino Board. The ArdOD operates using an Arduino Uno microcontroller board augmented with a proto-screwsheild (also called a wingsheild). The Uno is a prefabricated prototyping microcontroller board equipped with prewired "pins" (attachment points for standard jumper wires) for the attachment and operation of electronic components. Components are programmed for use with the board using the open-source Arduino software or Integrated Development Environment (IDE). IDE programs (called sketches) provide the board with instructions of the functions to be performed and allows for the display of quantitative output through the program's serial monitor. The Uno was selected for this project due to the high popularity of the board, ease of customization, and simplicity of usage.

The proto-screwsheild is a supplemental Arduino Uno module that was added to improve the interchangeability of components for the ArdOD. Shields are standard add-ons that plug into the pins of Arduino boards and expand the functionality of the microcontroller. The proto-screwsheild converts all Arduino pins into screw clamp attachments where jumper wires are screwed into place rather than soldered directly into the board. This modification allows for the easy replacement of spent/malfunctioning wires and improves the durability of components during repeated usage.

Light Source. ArdOD operates using a single 600nm water-clear light emitting diode (LED). The LED is wired independently of the microcontroller board and consists of a simple circuit mediated by a 200Ω resistor to attach the LED to an external power source. The ArdOD is

compatible with battery and outlet-supplied power depending on the desired source. For battery configuration a single 9-volt battery is attached to the positive and negative ends of the LED using a simple circuit and a battery clip with wire leads. An outlet supplied configuration requires the usage of a LED adapter with a free wire connector (LEDMO® AC Adapter Model 1250). The trailing wires are soldered to the positive and negative ends of the LED and are clamped into the wall-plugged AC adapter to complete the circuit. Both battery and outlet-supplied power are sufficient for the operation of the ArdOD, however it should be noted that usage of near-depleted batteries will cause the LED to slowly dim during measurement which can misconstrue the data.

Light Detector. Light quantification is accomplished using a BH1750 digital light sensor. The BH1750 is an Arduino compatible sensor that uses Inter-Integrated Circuit (I^2C) communication to quantify light intensity as a measure of lux (lx). The sensor has a resolution range of 0.0-54612.5 lx and is programmable for continuous and one-time light quantification. Using the BH1750 default setting, light is measured continuously at a sampling interval (minimum of 120 milliseconds) designated by the user with a precision of 1 lx. Light quantification is communicated back to the ArdOD microcontroller using the I^2C bus and output as serial data viewable through the IDE serial monitor or serial plotter.

Housing. The ArdOD housing is a custom 3-D printed structure designed to hold meter components, eliminate ambient light intrusion, and stabilize sample tubes for use with a platform shaker. The housing consists of 3-D prints were created using a MakerBot® Replicator® (fifth generation) with 0.07 in diameter polylactide (PLA) filament. All print components were created using Tinkercad® 3-D modeling software.

Software. The ArdOD operates through the Arduino IDE using a set of program libraries and an IDE script adapted from an existing BH1750 code repository (Github user *claws*). Light intensity is quantified and reported to the IDE as serial data. Serial data is stored using a serial port terminal application (CoolTerm) to automate collection and saving throughout the run.

Design. The assembled ArdOD is designed as a large isolation chamber where light from the LED is focused though a glass test tube containing a growing sample onto the light sensor (Figures 6-7). The LED is mounted at the narrow end of the housing inside the "cradle" with the positive and negative leads extending outward to the desired electrical supply. The BH1750 sensor soldered to a blank printed circuit board (PCB) and fitted vertically into the opening at the wide end of the housing. Five 2.54mm pitch Terminal Block Pins (Adafruit ASIN) are attached to the inverse of the PCB aligned with the functional pins of the BH1750. 22-Gauge tinned copper jumper wires (Tuofend 600v) attach the BH1750 to the Arduino via screw terminal blocks. The Arduino Uno and proto-screwsheild are assembled according to the manufacturer's specifications and housed in the microcontroller mount during use. A USB cable connects the Arduino to the measurement computer which also serves as the power supply for the microcontroller.

The ArdOD design uses modular components that are readily replaceable in the event of damage or malfunction. Particular attention was paid to sensitive portions of the device such as wire connections where damage or degradation is common. Soldering was minimized when possible to reduce the need for whole component replacement in the event of malfunction. Furthermore, the ArdOD was designed to be highly portable for remote or field usage. The meter weighs approximately 1 pound and is compact enough to fit in a 15cm x 25cm box for transport. The ArdOD does not require an internet connection to use (assuming all required Arduino

programs have been previously installed) and can operate entirely on battery power limited by the longevity of the user's computer.

Operation. To operate the ArdOD, all components are assembled within the incubation chamber/environment and an uninoculated test tube containing 10 mL of a media appropriate for the bacterium of interest is placed within the sample holder. The BH1750 Arduino sketch is uploaded to the microcontroller and linked to the serial port terminal application (CoolTerm). The ArdOD will immediately begin reporting light data at the specified time interval viewable through the terminal application. A standard inoculum of the bacterium of interest is added to the sample tube and enclosed using the ambient light cover. Following inoculation, no further user interface is required over the course of the growing period. Light data will be automatically collected by the serial port terminal application and can be transferred to any desired data storage software. It should be noted that some serial port terminal applications have a defined limit of raw data that can be stored by the program and may require minor user interface to backup collected data mid experiment dependent on measurement frequency and duration.

Evaluation. To evaluate the efficacy of the ArdOD growth kinetics for *V. alginolyticus, E. coli*, and *S. entercia* were quantified. A 2µL aliquot of the target bacterium (~5.0 x 10^6 cells) was added to 10mL of culture media and incubated at 35^{o}C for >6 hours. Cultures were grown in a shaking incubator at a speed of 100 rpms. All bacteria were cultured in Luria-Bertani Broth (Difco) with *V. alginolyticus* samples amended with additional NaCl to a 3% concentration. Light measurements were taken every 15 seconds and captured using the CoolTerm serial port application. Raw light data was analyzed using Rstudio software to construct growth curves for each bacterial run, quantify the four critical points of kinetics analysis, and calculate the doubling time. Bacterial doubling time was calculated as:

$$k = (OD_2 - OD_1) / T$$

$$dt = ln(2) / k$$

where k is the growth rate constant, OD_1 is the OD at early log phase, OD_2 is the OD at late log phase, T is the total time in minutes between OD_1 and OD_2, dt is the doubling time, and ln is the natural log. ArdOD growth curves were compared to concurrent measurements collected using a standard benchtop spectrophotometer (eppendorf® biophotometer) to monitor meter efficacy. Direct comparison of spectrophotometer and ArdOD data was not possible due to differences in OD maximums between the two meters. To account for this disparity, a bacterial-specific scaling factor was calculated to normalize ArdOD data for direct comparison as:

$$sf = SOD_s / SOD_a$$

where sf is the scaling factor, SOD_s is the stationary phase OD as measured by the spectrophotometer, and SOD_a is the stationary phase optical density as measured by the ArdOD. Technical replicates of ArdOD bacterial curves were compared for reproducibility using mean absolute deviation up to the onset of stationary phase.

Acknowledgements

We would like to thank Andrew Johnson the University of Georgia Science Library Makerspace for their assistance with the 3-D printing required to complete this project. Additionally, we thank Ian Bachli and Olivia Marenda for their assistance with laboratory analysis and component design. We also acknowledge GitHub user *claws* for the initial design of the sensor operational script and Rodger Meier for the design *of CoolTerm* serial output application.

Literature Cited

Akerlund T, Nordstrom K, Bernander R. 1995. Analysis of cell size and DNA content in

exponentially growing and stationary-phase batch cultures of *Escherichia coli. Journal of Bacteriology*. 177(3):6791-6797. 10.1128/jb.177.23.6791-6797.1995.

Al-Qadiri HM, Al-Alami NI, Lin M, Al-Holy M, Cavinato AG, Rasco BA. 2008. Studying of the bacterial growth phases using Fourier transform infrared spectroscopy and multivariate analysis. *Journal of Rapid Methods and Automation in Microbiology*. 16:73-89. 10.1111/j.1745-4581.2008.00117.x.

Deutzmann JS, Callander G, Gu W, Müller AL, McCully AL, Ahn JK, Kracke F, and Spormann AM. 2022. Low-cost clamp-on photometers (ClampOD) and tube photometers (TubeOD) for online cell density determination. *Frontiers in Microbiology.* 12: 790576.

Hall BG, Acar H, Nandipati A, and Barlow M. 2013. Growth rates made easy. *Molecular Biology and Evolution.* 31(1): 232-238.

Harding SE. 1986. Application of light scattering in microbiology. *Biotechnology and Biochemistry.* 8(6):489-509.

Koch AL. 1970. Turbidity measurements of bacterial cultures in some available commercial instruments. *Analytical Biochemistry.* 38(1): 252-259.

Koch AL. 1994. Growth Measurement. Reddy CA, Beverridge TJ, Breznak JA, Marzluf GA, Schmidt TM, and Snyder LR (eds). *Methods for General and Molecular Bacteriology*. American Society for Microbiology, Washington, DC. 172-199.

Kutschera A, Lamb JJ. 2017. Cost-effective live cell density determination of liquid cultured microorganisms. *Current Microbiology.* 75:321-236. https://doi.org/10.1007/s00284-017-1370-3.

Lucidi M, Marsan M, Pudda F, Pirolo M, Frangipani E, Visca P, Cincotti G. 2019. Geometrical-

optics approach to measure the optical density of bacterial cultures using a LED-based photometer. *Biomedical Optical Express*. 10(11):5600-5610.

Maia MRG, Marques S, Cabrita ARJ, Wallace RJ, Thompson G, Fonseca AJM, and Oliveira HM. 2016. Simple and versatile turbidimetric monitoring of bacterial growth in liquid cultures using a customized 3D printed culture tube holder and a miniaturized spectrophotometer: application to facultative and strictly anaerobic bacteria. *Frontiers in Microbiology.* 7: 1381.

Mauerhofer LM, Pappenreiter P, Paulik C, Seifert AH, Bernacchi S, and Rittmann SKMR. 2018. Methods for quantification of growth and productivity in anaerobic microbiology and biotechnology. *Folia Microbiologica.* 64: 321-360.

Merkel S and the ASM Task Force on Curriculum Guidelines for Undergraduate Microbiology. 2012. The development of curricular guidelines for introductory microbiology that focus on understanding. *Journal of Microbiology and Biology Education.* 13(1): https://doi.org/10.1128/jmbe.v13i1.363.

Monod J. 1949. The growth of bacterial cultures. *Annual Review of Microbiology.* 3(1):371-394.

Sasidharan K, Martinez-Vernon AS, Chen J, Fu T, Soyer OS. A low-cost DIY device for high resolution, continuous measurement of microbial growth dynamics. *BioRχiv.* https://doi.org/10.1101/407742.

Sutton, S. 2011. Measurement of microbial cells by optical density. *Journal of Validation Technology.* 17(1):46-50.

Swinehart DF. 1962. The Beer-Lampert law. *Journal of Chemical Education.* 39(7): 333-335.

Van de Hulst, HC. 1953. Basic scattering theory. In: *Light Scattering by Small Particles*. New York: Dover Publications, 1-10.

Wang JTH, Huston WM, Johanesen P, Lloyd M, and Waller KL. 2018. A laboratory competency examination in microbiology. *FEMS Microbiology Letters.* 365(20): fny224.

Yallapragada VVB, Gowda U, Wong D, O'Faolain L, Tangney M, Devarapu GCR. 2019. ODX: A fitness tracker-based device for continuous bacterial growth monitoring. *Analytical Chemistry*. 91:12329-12335. 10.1021/acs.analchem.9b02628.

Zeroual W, Choisy C, Doglia SM, Bobichon H, Angiboust JF, and Manfait M. 1994. Monitoring of bacterial growth and structural analysis as probed by FT-IR spectroscopy. *Biochimica et Biophysica Acta (BBA) - Molecular Cell Research*. 1222(2): 171-178.

Zwietering MH, Jongenburger I, Rombouts FM, and Riet KVT. 1990. Modeling of the bacterial growth curve. *Applied and Environmental Microbiology.* 56(6): 1875-1881.

Tables and Figures

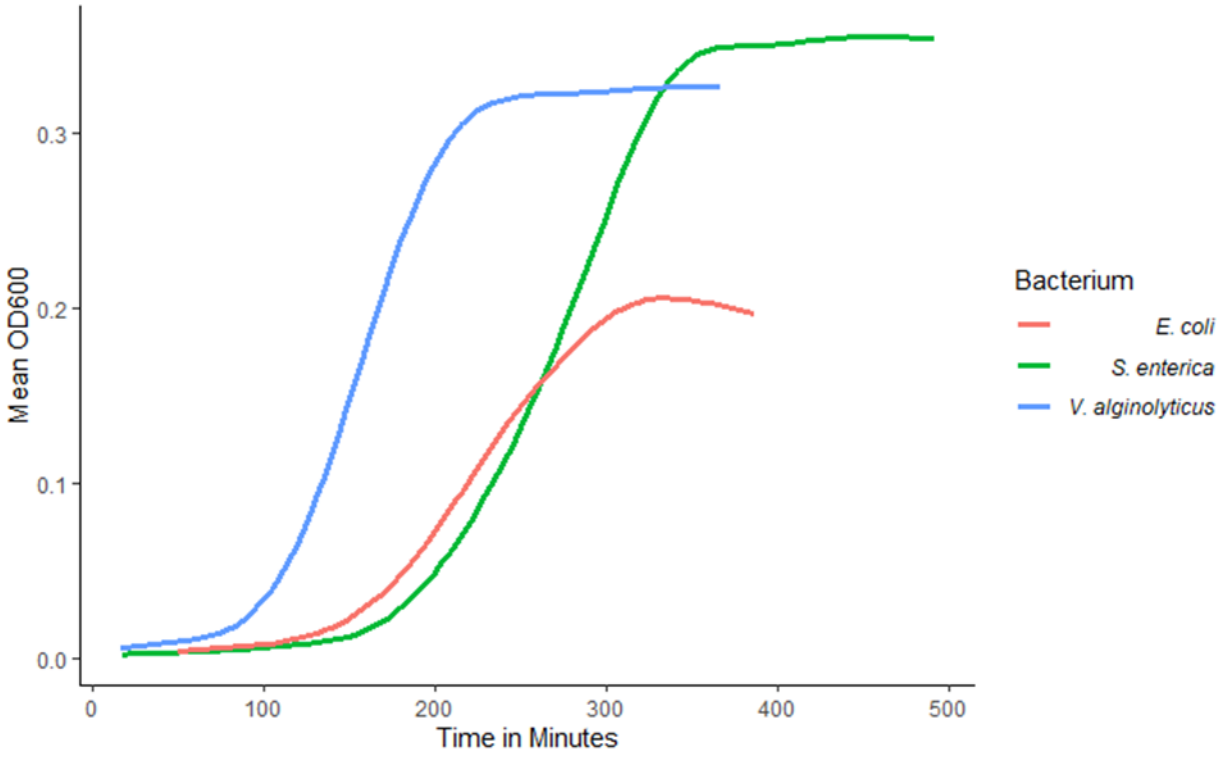

Figure 1: Mean OD600 values for *E. coli, S. enterica,* and *V. alginolyticus* measured using ArdOD. Cultures inoculated with ~5.0 x 10^6 cells into 10mL of liquid media (LB broth *for E. coli* and *S. enterica* and LBS broth for *V. alginolyticus*). Cultures were grown for >6 hours at 35^{o}C with 100rps of shaking agitation. Mean OD600 values were tabulated at N = 10 runs. Early lag phase data (t_0-t_{50}) removed to allow for meter acclimation to the given growth conditions.

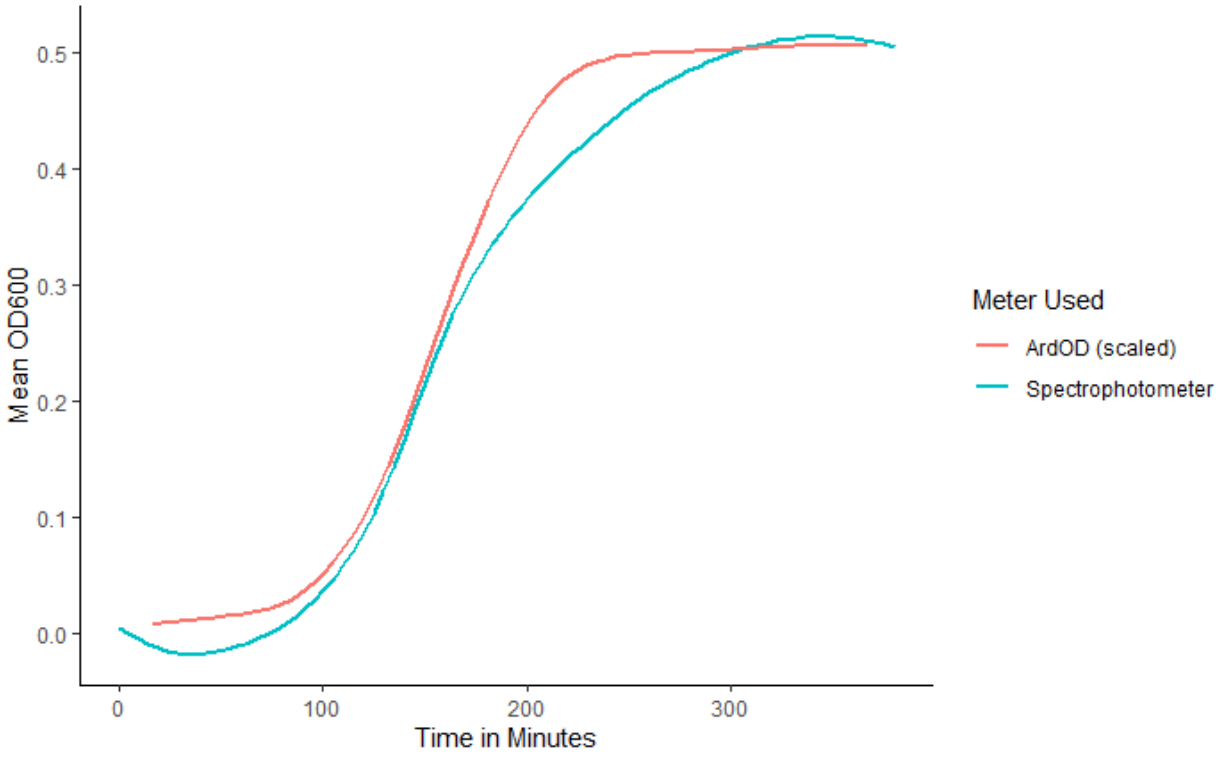

Figure 2: OD comparison of ArdOD and benchtop spectrophotometer-derived measurements for *V. alginolyticus*. Mean OD_{600} tabulated at N = 10 for the ArdOD and N = 3 for benchtop spectrophotometer (Eppendorf® biophotometer). Measurement interval for ArdOD = 15 seconds. Measurement interval for spectrophotometer = 60 minutes. Final ArdOD OD values scaled by a factor of 1.55 to account for differences in LED sensitivity. ArdOD doubling time = 35.78 minutes. Spectrophotometer doubling time = 27.03 minutes.

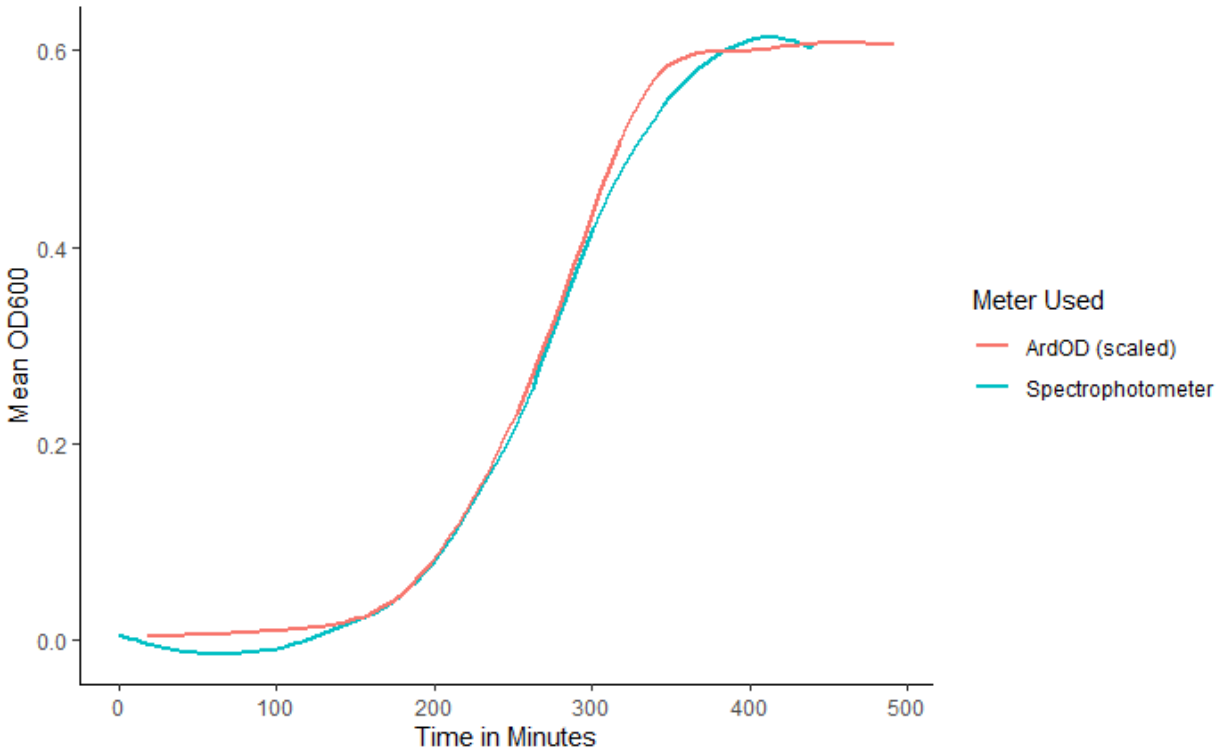

Figure 3: OD comparison of ArdOD and benchtop spectrophotometer-derived measurements for *S. enterica*. Mean OD_{600} tabulated at N = 10 for the ArdOD and N = 3 for benchtop spectrophotometer (Eppendorf® biophotometer). Measurement interval for ArdOD = 15 seconds. Measurement interval for spectrophotometer = 60 minutes. Final ArdOD OD values scaled by a factor of 1.71 to account for differences in LED sensitivity. ArdOD doubling time = 55.91 minutes. Spectrophotometer doubling time = 60.58 minutes.

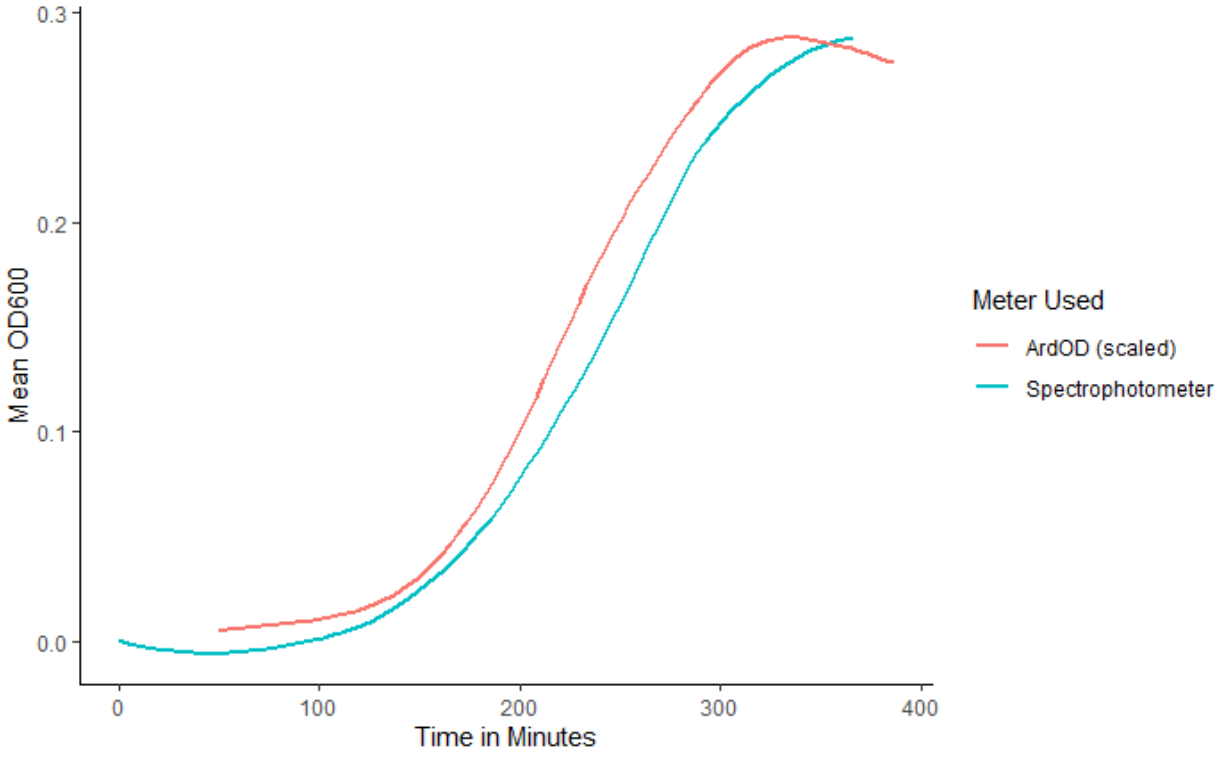

Figure 4: OD comparison of ArdOD and benchtop spectrophotometer-derived measurements for *E. coli*. Mean OD_{600} tabulated at N = 10 for the ArdOD and N = 3 for benchtop spectrophotometer (Eppendorf® biophotometer). Measurement interval for ArdOD = 15 seconds. Measurement interval for spectrophotometer = 60 minutes. Final ArdOD OD values scaled by a factor of 1.40 to account for differences in LED sensitivity. ArdOD doubling time = 46.48 minutes. Spectrophotometer doubling time = 41.55 minutes.

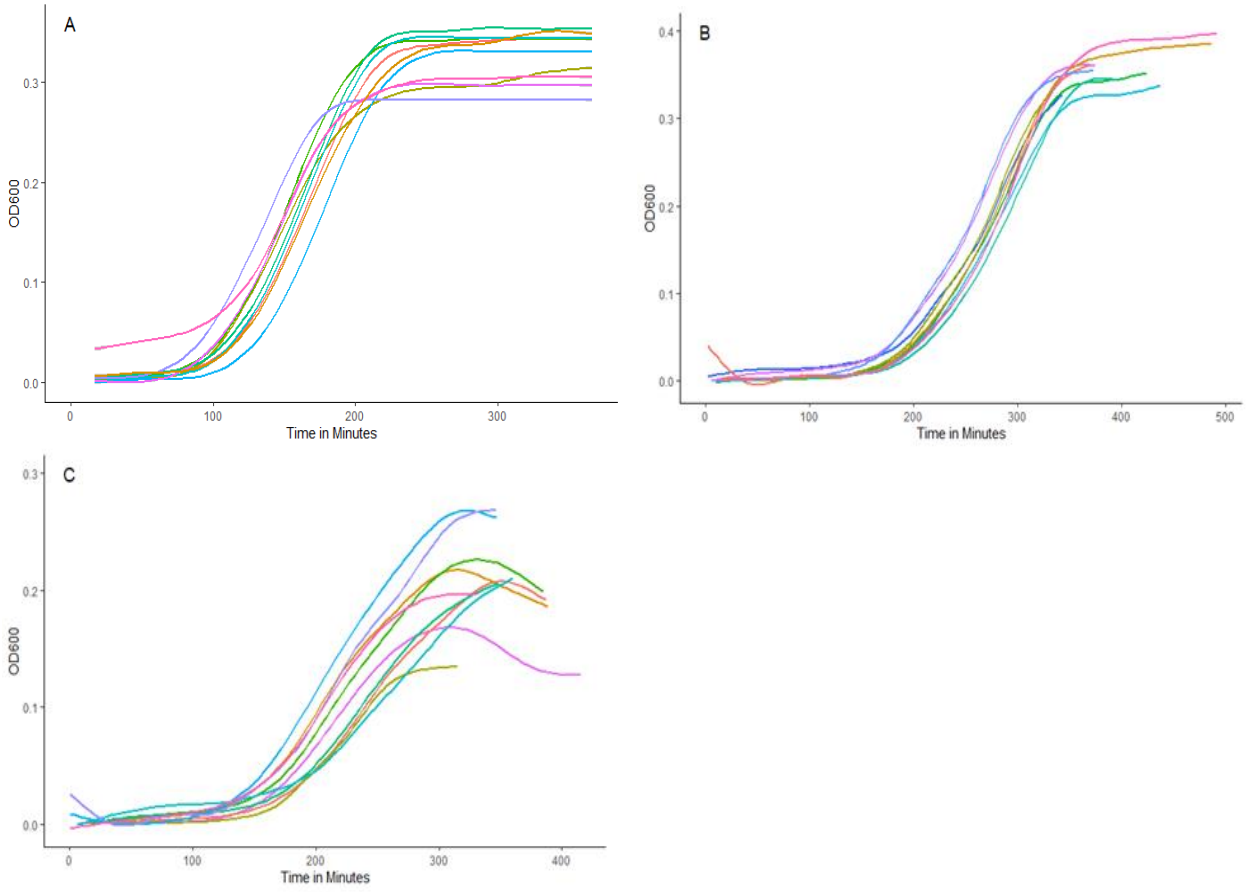

Figure 5: Replicate growth curves for *V. alginolyticus* (A), *S. enterica* (B), and *E. coli* (C) using the ArdOD-derived data. N = 10 curves for each bacterium.

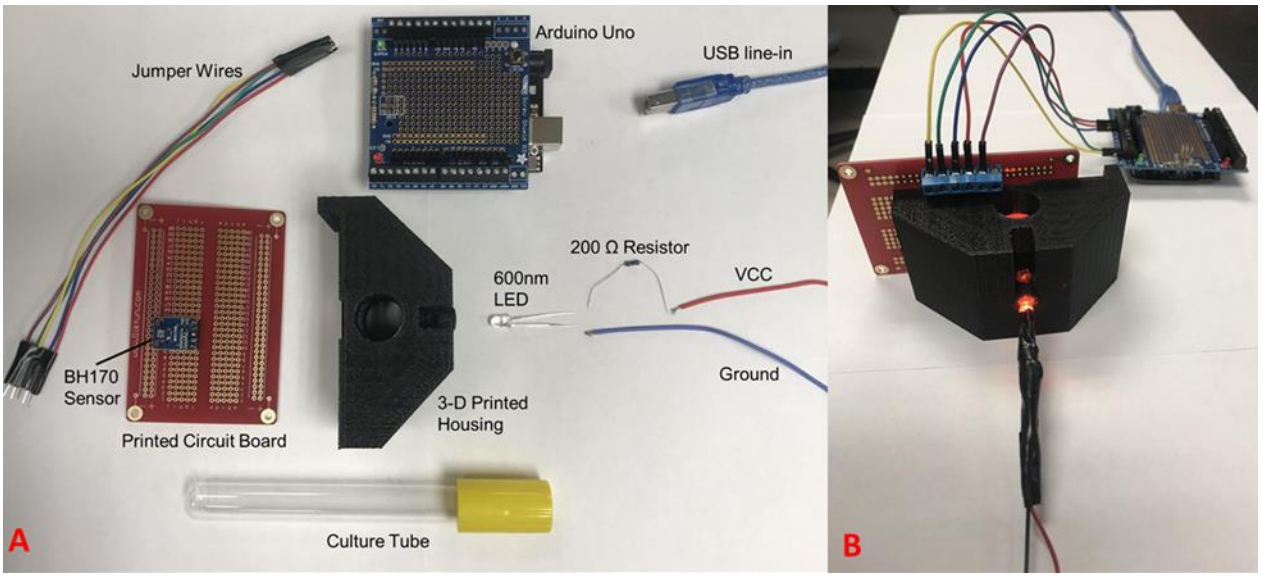

Figure 6: ArdOD design and components. (A) Disassembled ArdOD displaying all major components used to build the meter (excluding computer). (B) Assembled ArdOD illustrating the configuration of the circuit board and LED position within the meter housing. Light shield excluded to show component details.

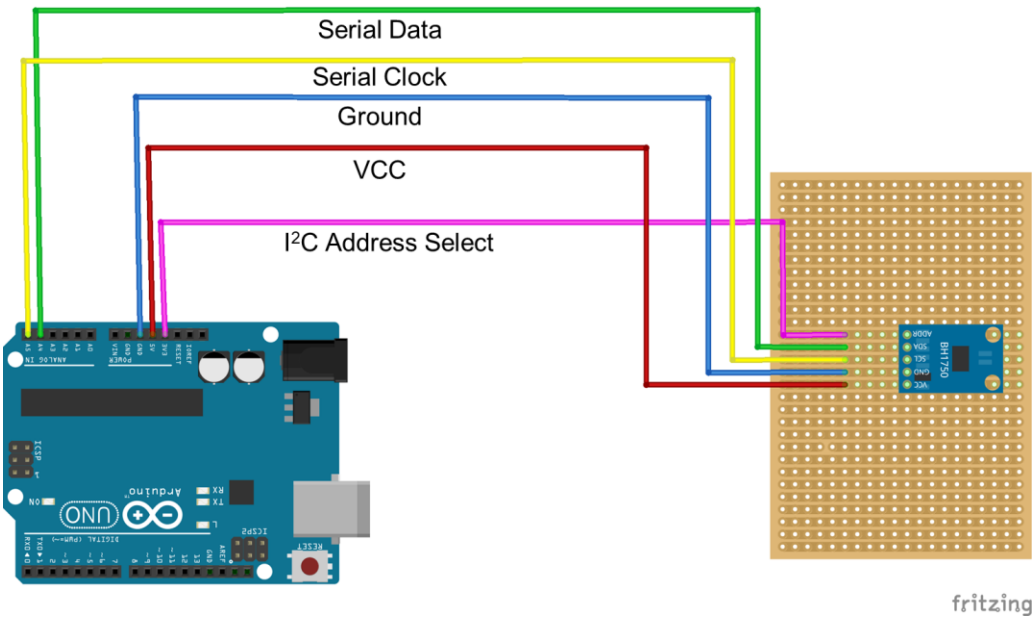

Figure 7: Fritzing wiring diagram of ArdOD. Wires demonstrate the connection of jumper wires between the BH1750 light sensor and the Arduino Uno microcontroller board.

CHAPTER 4

USE AND EVALUATION OF A pES213-DERIVED PLASMID FOR THE CONSTITUTIVE EXPRESSION OF *GFP* PROTEIN IN PATHOGENIC VIBRIOS: A TOOL FOR *IN VITRO* STUDIES

Norfolk WA and Lipp EK. Published in *Microbiology Spectrum*. 2022, e02490-22. Reprinted here with permission of the publisher.

Abstract

Insertion of green fluorescent protein (GFP) into bacterial cells for constitutive expression is a powerful tool for the localization of species of interest within complex mixtures. Here we demonstrate and evaluate the efficacy of the pES213-derived donor plasmid pVSV102 (*gfp* Kn^r) as a conjugative tool for the tagging of *Vibrio* and related species (termed vibrios). Using a tri-parental mating assay assisted by the helper plasmid pEVS104 (*tra trb* Kn^r) we successfully tagged 12 species within the Vibrionaceae family representing 8 of the proposed clades. All transconjugant strains demonstrated bright fluorescence and were readily differentiable within complex mixtures of non-tagged cells. Plasmid retention was assessed using persistence and subculture experimentation. Persistence experiments evaluated plasmid loss over time for non-subcultured samples inoculated into antibiotic-free media and sterile artificial sea water, whereas subculture trials evaluated plasmid loss following one to four subculture passages. Strong plasmid retention (≥80%) was observed in persistence experiments for all transconjugant strains for up to 48 h in both antibiotic-free media and artificial sea water with the exception of *V. cholerae*, which showed a substantial decline in media after 24 h. Subculturing experiments also demonstrated strong plasmid stability with all transconjugant strains showing ≥80% retention after four subculture passages. The results of this research suggest that pVSV102 is a stable GFP plasmid for the tagging of a broad range of vibrios.

Importance

Prior research has suggested that the use of *Aliivibrio fischeri*-derived donor plasmids with the pES213 origin of replication may provide increased plasmid stability for the tagging of vibrios compared to *Escherichia coli*-derived p15A plasmids. Here we present a structured protocol for conjugation-based tagging of vibrios using the pES213-derived plasmid pVSV102 and evaluate

the plasmid stability of tagged strains. These methods and the resulting transconjugant strains provide important standardized tools to facilitate experimentation requiring the use of traceable vibrio strains. Furthermore, the determination of the species-specific plasmid stability provides an estimation of the anticipated level of plasmid loss under the given set of culture conditions. This estimation can be used to reduce the occurrence of experimental biases introduced by plasmid drift.

Introduction

Vibrio spp. (or vibrios, a colloquial term used to describe all members of the family Vibrionaceae) are ubiquitous aquatic bacteria commonly found in marine, coastal, and estuarine habitats worldwide (Thompson et al., 2004). As indigenous members of the aquatic community, vibrios exhibit a diverse range of preferential lifestyles with individuals existing as free-living bacterioplankton, constituents of biofilm communities, or in mutualistic or pathogenic associations with host organisms (Takemura et al., 2014). Through these complex interactions, vibrios play an important role in the ecology of aquatic ecosystems through their contributions to biogeochemical cycling, roles in the food web, beneficial symbioses, and agents of disease (Thompson et al., 2004; Takemura et al., 2014). Vibrios act as pathogens across a broad range of hosts from economically important penaeid shrimps, to critically endangered scleractinian corals, and humans (Chakraborty et al., 1997; Ben-Haim et al., 2003; Thompson et al., 2004; Austin & Zhang, 2006). The ability to localize the physical association of vibrios in their environment or host in a controlled setting is an important tool for investigating their ecology and pathways of transmission.

The use of fluorescent molecules to label bacteria is commonly used to visualize and localize cells or their expressed proteins in systems of interest (Valdivia & Falkow, 1997;

Southward & Surette, 2002; Sawabe et al., 2006; Dunn et al., 2006). While numerous tagging molecules exist, green fluorescent protein (GFP) and its derivatives remain among the most popular due to their intrinsic stability and resistance to photobleaching (Shimomura, 2005, Sawabe et al., 2006; Kong et al., 2020). First isolated from the jellyfish *Aequorea victoria*, GFP is a protein that exhibits a bright green fluorescence when excited with blue/ultraviolet light (Shimomura et al., 1962; Prasher, 1995; Shimomura, 2005, Kong et al., 2020). Since its discovery in 1961 (Shimomura et al., 1962) and adoption for use as a molecular marker in 1992 (Prasher et al., 1992), GFP tagging methods have been optimized for various experimental outcomes ranging from localization of host-pathogen/vector interactions to detection of target gene expression (Valdivia et al., 1996; Stretton et al., 1998; O'Toole et al., 2004; Travers et al., 2008; Drake et al., 2020).

Fluorescent tagging is a particularly useful approach when investigating the environmental or host-associated dynamics of indigenous microorganisms such as vibrios, where it is otherwise impractical to differentiate an introduced experimental strain from the existing population. GFP tagging allows for the visualization of specific strains within complex systems, which can elucidate potentially important inter- and intraspecies interactions with the microbial community, the environment, or within a host (Southward & Surette, 2002; Sawabe et al., 2006; Dunn et al., 2006). When used in conjunction with specialized microscopy techniques and/or histopathology, GFP tags can provide vital spatial information on the colonization of pathogenic or symbiotic bacterial species within a host or movement among host tissues (Ling et al., 2001; O'Toole et al., 2004; Mazzarini et al., 2021). Prior studies have successfully employed GFP-vibrios to model host-pathogen interactions in oysters (Aboubaker et al., 2013; Wang et al., 2021), lobsters (Goulden et al., 2021), corals (Pollock et al., 2015), fishes (O'Toole et al., 2004;

Rekecki et al., 2012), *Caenorhabditis elegans* (as a model for human wound infection) (Durai et al., 2011), as well as host-symbiont interactions in the Hawaiian squid (*Euprymna scolopes*) (Nyholm et al., 2002; Millikan & Ruby, 2002). While these studies demonstrate the utility of GFP tags for vibrio research, there is a need for standardized methods of tagging that can be applied to a range of different vibrios.

Prior research by Dunn et al. (2006) and Sawabe et al. (2006) successfully used conjugation-based methods to tag vibrio species. Dunn et al. (2006) labeled *Aliivibrio fischeri* using a tri-parental mating assay with the helper plasmid pEVS104 (*tra trb* Kn^r) (Stabb & Ruby, 2002) and one of several pES213-derived (Boettcher & Ruby 1994; Dunn et al., 2005) donor plasmids. Shortly after, Sawabe et al. (2006) employed a biparental mating assay using a single *E. coli* strain carrying both the helper plasmid pEVS104 (*tra trb* Kn^r) and a p15A-derived (Stabb & Ruby, 2002) donor plasmid pKV111 (*gfp* Cm^r) or pKV112 (*gfp* Cm^r Er^r) to tag 39 different vibrios. While the work of Sawabe et al. (2006) effectively demonstrated the broad efficacy of conjugation-based tagging methods in vibrios, Dunn et al. (2006) noted decreased plasmid stability when using *E. coli*-based p15A donors compared to *A. fischeri*-based pES213 donors. This finding suggests that pES213-derived donor plasmids may improve the retention of GFP tags in vibrios. Several subsequent studies have successfully employed pES213-derived donor plasmids for the creation of stable GFP tags in *A. fischeri* (Wang et al., 2010), *V. harveyi* (Travers et al., 2008; Delavat et al., 2018), *V. parahaemolyticus* (Frischkorn et al., 2013; Getz & Thomas, 2018), *V. coralliilyticus* (Gavish et al., 2021), *V. aestuarianus* (Aboubaker et al., 2013), and *V. tapetis* (Rahmani et al., 2021). However, a formal side-by-side comparison of conjugation methods and the acquired plasmid retention is needed to standardize these methods across different vibrios.

Through this research, we present a simple protocol for GFP tagging of vibrios using a pES213-derived donor plasmid system and evaluate the plasmid retention of transconjugant strains. Through the combined use of the helper plasmid pEVS104 (*tra trb* Kn^r) (Stabb & Ruby, 2002) and the pES213-derived donor plasmid pVSV102 (*gfp* Kn^r) (Dunn et al., 2006) we successfully tagged species across a range of known the Vibrionaceae clades (Tables 1 and 2). The efficacy of the GFP tags were evaluated with subsequent culture-based methods and fluorescent microscopy to determine the experimental limitations of the species-specific GFP retention.

Results

GFP Expression. This method successfully transferred GFP tags to 12 out of 14 tested vibrios (Table 1). All successfully tagged species showed strong conjugation efficiency (Table S1) when mated triparentally on kanamycin amended media equivalent to the stress concentration designated in Table 1. Tagged species consisted of important human and animal pathogens and represented eight of the 23 proposed clades of the Vibrionaceae family (Sawabe et al., 2013). Bright GFP expression was observed in all transconjugants allowing them to be readily differentiated from non-tagged background vibrios within complex mixtures (Figures 1, S14, and S15). No evidence of interspecies self-mobilization of pVSV102 was observed in the absence of antibiotic stress (Table S2). GFP expression was retained in all tagged strains following revival from -80^{o}C frozen stocks.

Persistence of GFP Retention. Plasmid retention of all transconjugant strains was assessed over time in media and artificial seawater to estimate the level of plasmid loss that occurred under growth and stagnation conditions, respectively. In antibiotic-free media, mean GFP retention for all transconjugants was ≥80 % (ranging from 100-80%) after 48 h, excluding *V. cholerae* in

which showed a mean retention of only 36.8%. After 5 days, retention varied by species with *P. damselae*, *V. alginolyticus*, *V. anguillarum*, *V. campbellii*, *V. parahaemolyticus,* and *V. vulnificus* showing minor plasmid loss with a mean GFP retention of 90-99%. Moderate loss was observed in cultures of *V. splendidus*, *V. mediterranei,* and *V. pelagius* with a mean retention of 80-90%. Substantial loss was observed in cultures of *V. cholerae*, *V. coralliilyticus*, and *V. harveyi* at <70% retention (Figure 2). In the presence of antibiotics (300 μg mL^{-1} kanamycin), which maintained selective pressure, 100% GFP retention was observed after 5 days of growth for all tested species, excluding *V. mediterranei* in which retention declined to 90.7% by day three (Table S3).

In artificial sea water (ASW), all tagged vibrios showed a mean retention of ≥80% after 48 h. Moderate GFP loss (80-90% retention) was observed in *V. cholerae* and *V. vulnificus*, minor loss (90-99% retention) was observed in *P. damselae*, *V. coralliilyticus*, *V. harveyi*, and *V. mediterranei*, and no loss (100% retention) was observed for *V. anguillarum*, *V. alginolyticus*, *V. campbellii*, and *V. parahaemolyticus* (Figure 3). *V. pelagius* and *V. splendidus* were not recoverable in ASW beyond 24 and 48 h, respectively.

GFP Retention during Subculture. Subculture experiments assessed the retention of GFP plasmids following multiple passages in antibiotic-free media to determine the effect(s) of culture regrowth on plasmid loss. GFP was retained at ≥80% in transconjugant strains for the duration of the experiment (up to four passages). After four passages, *V. alginolyticus* and *P. damselae* showed moderate plasmid loss (80-90% retention). Minor loss (90-99% retention) was observed in cultures of *V. anguillarum*, *V. campbellii*, *V. cholerae*, *V. harveyi*, *V. mediterranei*, *V. pelagius*, and *V. vulnificus.* No loss (100% retention) was observed in *V. parahaemolyticus*, *V.*

coralliilyticus, and *V. splendidus* (Figure 4). After one passage all strains demonstrated 100% retention, except for *P. damselae* which began at 92% retention (Figure 4).

Discussion

Vibrios play multifaceted roles within marine and coastal ecosystems, through symbioses, interspecies competition, and pathogenicity (Thompson et al., 2004; Takemura et al., 2013). The ability to localize vibrios of interest on or within host tissues is critical for helping to understand the ecological mechanisms that can influence these relationships. Of keen interest for this work was to optimize a GFP-tagging system across a wide range of vibrios and assess its efficacy for use in experiments designed to track host colonization of vibrios from ambient sea water.

We used a pES213-derived donor plasmid system to revisit several important vibrios previously tagged by Sawabe et al. (2006) using a p15A-derived system. Prior research indicates that *A. fischeri*-based plasmids containing the pES213 origin of replication may produce more stable GFP expression in vibrios compared *E. coli*-based p15A-derived plasmids (Dunn et al., 2006). Using this system, successful transconjugant vibrios were created from 12 of the 14 tested species, covering eight clades (Sawabe et al., 2013). These species include several understudied vibrios such as the coral pathogens *V. mediterranei* and *V. coralliilyticus*, the wide host range pathogens *V. alginolyticus* and *V. harveyi*, as well as the better studied human pathogens *V. vulnificus* and *V. parahaemolyticus*, demonstrating a broad application of this system within Vibrionaceae (Chakraborty et al., 1997; Kushmaro et al, 2001; Ben-Haim et al., 2003; Travers et al., 2008). Furthermore, we expand on the Sawabe et al. (2006) list of tagged vibrios through our addition of the fish pathogen *V. anguillarum* and the well-known human pathogen *V. cholerae* (Chakraborty et al., 1997; O'Toole et al., 2004). It should be noted, that while this research

prioritizes the use of pVSV102 in contrast to p15A-derivatives, other plasmid alternatives such as pRL1383a (Ushijima et al., 2012; Ushijima et al., 2014), pUTat (Xaio et al., 2011), pET28a (Dai et al., 2020), and pRK600 (Pollock et al., 2015) have also been shown to persist stably in vibrios.

Evaluation of the transconjugant strains showed that the pES213-derived donor plasmid pVSV102 conferred bright GFP fluorescence when conjugated triparentally with the helper plasmid pEVS104. This fluorescence allowed all tagged vibrios to be readily differentiated and localized within complex bacterial mixtures. No evidence of interspecies self-mobilization was observed in mixtures of GFP *V. parahaemolyticus* and non-GFP *V. cholerae* and *V. vulnificus* suggesting that pVSV102 has a low likelihood of interspecies mobilization in the absence of antibiotic stress (Table S2). Despite this observation, it should be noted that pVSV102 has been found to mobilize in conjunction with the self-mobilizable *A. fischeri* plasmid pES100 (Dunn et al., 2005) suggesting that vibrio strains carrying this plasmid or homologous plasmids may enable non-target plasmid transfer in the absence of antibiotic stress.

Plasmid retention in pVSV102 provided equivalent or greater GFP stability in vibrios compared to p15A-derived plasmids (Sawabe et al., 2006). At least 80% GFP retention was observed in all target recipients, excluding *V. cholerae*, following 48 h of growth in antibiotic-free media. A gradual increase in plasmid loss was observed between days 3 and 5 in several species namely, *V. coralliilyticus*, *V. harveyi*, and *V. mediterranei*. This loss was consistent with previously reported observations from Sawabe et al. (2006) who noted a similar reduction by day 4 of experimentation. Despite this loss, these GFP strains remained >60% retentive throughout the entirety of the experiment compared to 30-40% retention observed by Sawabe et al. (2006), suggesting increased stability with a pES213-derived donor. Furthermore, several strains in the

present work (*P. damselae*, *V. alginolyticus*, and *V. campbellii*) demonstrated near complete retention (≥95%) after 5 days of growth suggesting that high plasmid stability may exceed this duration depending on the target species of interest. It should be noted that GFP retention reported by Sawabe et al.(2006) was determined using direct microscopy counts whereas this study utilized culture-based detection. Thus, these two values may not be directly comparable in all instances.

Under the nutrient limiting conditions of ASW, persistence of GFP retention was ≥95% after 48 h in 10 of the 12 species, excluding *V. cholerae* and *V. vulnificus*, which retained 90% and 81%, respectively. Increased plasmid stability in ASW compared to media is likely related to decreased cellular growth under these conditions, which has also been shown for lower incubation temperatures (Liao, 1991). Based on these patterns, we hypothesize that ASW-maintained cultures would show a minor but progressive decrease in plasmid stability if allowed to persist beyond 48 h but would remain more retentive than media-maintained cultures. Interestingly, *V. vulnificus* demonstrated similar patterns of GFP loss under ASW persistence as observed in antibiotic-free media growth suggesting this species may be less amenable to ASW experimentation. This discrepancy may be due to stress induced by the lower salinity tolerance of *V. vulnificus* compared to other vibrios (Randa et al., 2004).

The results of subculture experimentation were consistent with those observed in persistence trials with ≥80% retention of the GFP plasmid observed in all transconjugants following four subculture passages (the maximum tested). These results suggest that pES213-derived plasmids are amenable to experimental methods requiring subculturing to prepare samples. Though it should be noted that while pVSV102 was resistant to loss during subculturing, some strains showed a small decline in plasmid retention especially between

passages 3 and 4 (Figure 4), suggesting that experimental use of such strains should limit the number of subcultures to reduce the risk of retention bias.

Under the scope of the present research, the mechanism(s) contributing to *V. cholerae* plasmid loss in persistence experiments are unclear. As the only non-halophilic bacterium tested, we hypothesize that this loss may be related to metabolic stress from the media, which is known to reduce plasmid stability (Summers, 1991; Lau et al., 2013). Furthermore, it has been shown that some strains of *V. cholerae* possess plasmid defense mechanisms which may further contribute to the loss of GFP tags in the absence of antibiotic stress (Jaskólska et al., 2022). Optimal stability may be achievable in *V. cholerae* through modification of the methods by reducing the salt content of the mating, persistence, and purification media used to facilitate transfer; however, further experimentation is required. Of the tested strains, *V. furnissii* and *V. tubiashii*, were the only species that were unsuccessful in acquiring the GFP plasmid. These two species along with *P. damselae* were noted to have the lowest kanamycin tolerance threshold of all tested vibrios. During experimentation, 'non-tolerant' species (minimum inhibitory concentration [MIC] of kanamycin of ≤ 50 μg mL^{-1}) showed increased sensitivity to the stress concentration used to transfer the GFP. While tagging was achievable in non-tolerant species (as evidenced by *P. damselae*), a more highly resolved determination of kanamycin MIC for the stress concentration may be required for these or similar tolerance-level vibrios.

Based on the observed patterns of plasmid stability, experimentation using these strains should be limited to exposure durations where the species-specific retention is ≥80%. Keeping within this range would ensure that major stability biases are avoided. To apply this work to experiments where quantification is required, assays to specifically determine the expected plasmid loss for the target species under the defined culture/experimental conditions (e.g., media,

incubation temperature, oxygenation level, and number of anticipated subculture passages) are needed to account for plasmid drift over the course of the experiment. For presence-absence experimentation, microscopic visualization of the tagged strains is possible even at low levels of GFP retention (*V. cholerae* remained detectable microscopically at ~10% retention) allowing for potentially longer duration experiments. However, differentiation of GFP-tagged bacteria may be difficult to discern at these levels if the matrix of interest is highly complex such as within host tissues or attached to a substrate.

While the use of GFP for bacterial localization can provide important insights into the ecology of a species, GFP-tagged bacteria are not true wild-type strains. The creation of a transconjugant bacterium intrinsically changes the biology of the individual. This alteration can give rise to physiological, behavioral, and/or morphological differences in phenotype that may not be representative of wild-type strains. Such differences have been observed previously (Rang et al., 2003) and were noted in our media retention experiments where the colony size of *V. cholerae* increased when the GFP plasmid was lost compared to colonies that were retentive, suggesting increased fitness for non-retentive cells (Figure S16). While some differences are not unexpected, care is needed when designing experiments using GFP-tagged strains to ensure any conjugation-induced experimental biases are accounted for prior to the start of the research.

Conclusion.

The results of this research demonstrate the utility and stability of pVSV102 as a conjugative tool for the GFP tagging of vibrios. The methods present a standardized protocol for conjugation-based transfer of pVSV102 using a tri-parental mating assay with the helper plasmid pEVS104 and kanamycin-amended media. Using these GFP strains, researchers can better design experiments to identify and/or describe potential vector species, reservoirs, bacterial

aggregation patterns, and chemotaxis, which can be used to better understand the ecology and/or manage the pathogenic burden vibrios.

Methods

Strain Selection. Experimental vibrio strains were obtained from American Type Culture Collection (ATCC) (Table 1). *E. coli* strains carrying the helper and donor plasmids were created and graciously provided by the Stabb Lab (Eric Stabb, University of Illinois Chicago, Chicago, IL) (Table 2). Experimental vibrios were selected to represent a range of phylogenetic clades with particular emphasis given to type strains, where possible. All storage cultures were maintained at -80^{o}C in 20% glycerol (v/v, final concentration) prior to the start of the experiments.

Kanamycin Tolerance Assessment. The helper and donor plasmids selected in this study carry kanamycin (Kn^{r}) resistance (Stabb & Ruby, 2002; Dunn et al., 2006). Thus, the strain-specific tolerance of all experimental vibrios was assessed to determine a minimum inhibitory concentration (MIC) of this antibiotic. Assessment of the MIC was used to establish a stress concentration, or the concentration at which the antibiotic becomes detrimental but does not completely inhibit growth (Table 1). Overnight cultures of the frozen vibrio stocks were grown in antibiotic-free lysogeny broth (LB, Sigma Aldrich, Miller formulation) amended with 3% w/v NaCl (termed LBS 3% henceforth) at 30^{o}C with 100 rpm shaking agitation (New Brunswick Scientific, C24 Incubator Shaker). Cultures were then streaked for isolation onto thiosulfate citrate bile salts sucrose agar (TCBS) or LBS 3% agar, each amended with 50 μg mL^{-1} kanamycin. The use of TCBS or LBS 3% agar was determined by species-specific preference to each media as noted in Table 1. Any strains that successfully grew at 50 μg mL^{-1} were deemed 'Kan-tolerant' and subsequently cultured at 75, 100, 125, 150, and 200 μg mL^{-1} concentrations

of kanamycin to establish a lethal limit. Any strains that did not successfully grow at 50 µg mL^{-1} were considered 'non-tolerant' and were subsequently cultured at 2, 5, 10, 25, and 35 µg mL^{-1} to determine a lower tolerance threshold. The stress concentration for each species was calculated as a midpoint of the highest antibiotic concentration at which strains would grow in culture and the lowest lethal concentration (Table 1). The stress concentration was later utilized in the mating assay as the baseline antibiotic concentration for the transfer of the GFP plasmid.

GFP Conjugation Culture Preparation. To begin the mating assay, all bacterial stocks were cultured overnight (18 h) in broth to ensure adequate growth of the strain and/or retention of the plasmid. Vibrio stocks were cultured in 3 mL of antibiotic-free LBS 3% at 30ºC with 100 rpm shaking agitation. *E. coli* stocks were cultured in 3 mL LB broth (Sigma Aldrich, Miller formulation) amended with 40 µg mL^{-1} kanamycin at 35 ºC with 100 rpm of shaking agitation. Following incubation, 1 mL of vibrio and *E. coli* cultures were pelleted by centrifugation at ~4,000 x *g* for 2 min then resuspended in 1 mL of sterile 1X phosphate-buffered saline (PBS). This procedure was repeated twice to wash cells and remove residual media. 100 µL (colony forming units [CFU] reported in Table 1 and 2) of the washed helper, donor, and target recipient was removed and combined in a 1.5 mL microcentrifuge tube. The combined aliquots were centrifuged at ~4,000 x *g* for 2 min to pellet the cells and the supernatant was discarded. Pelleted cells were resuspended in 10 µL of fresh antibiotic-free LB broth amended with 2% w/v NaCl (LBS 2%). This salt concentration allowed growth of both vibrio and *E. coli*. The reduced volume of this final suspension was selected to increase the concentration of cells.

Tri-parental Mating Assay. Following culture preparation, the resuspended mixed bacteria pellet was spot-plated onto a thick (~10 mm) LBS 2% plate amended with kanamycin, equivalent to the stress concentration determined in kanamycin tolerance evaluation for each

vibrio strain (Table 1). The mating mixtures were incubated at 28 ^{o}C for 24-72 h and checked daily with a 495 nm blacklight for fluorescence. Extended duration incubation was utilized to account for the reduced rate of growth of the target vibrio under the given level of kanamycin stress. Mating mixtures that successfully produced green fluorescent patches within the cell masses were indicative of successful transfer of the GFP plasmid (Figure S1). Mixtures were then streaked onto TCBS plates amended with 300 µg mL^{-1} kanamycin to remove the helper and donor *E. coli* strains, which do not grow well on this media, and ensure the plasmid was retained within the vibrio culture. Vibrio species deemed 'non-tolerant' during the kanamycin tolerance experiment were sequentially streaked first onto 100, then 200, and finally 300 µg mL^{-1} kanamycin TCBS plates to ensure the antibiotic stress did not overwhelm the target *Vibrio.* Successful removal of *E. coli* strains was confirmed using tandem growth on modified mTEC agar (Difco, Fischer Scientific), an *E. coli* specific medium. GFP transfer was confirmed for all purified vibrio strains using fluorescent microscopy (Olympus BX41 Fluorescence Microscope) (Figures S2-S13). Conjugation efficacy was assessed for 24 mixtures of each species of target vibrio (Table S1). Successfully tagged strains were cultured in LBS 3% broth amended with 300 µg mL^{-1} kanamycin overnight at 30 ^{o}C. Broth cultures were stored long-term at -80 ^{o}C in a 1:1 mixture of 40% glycerol (20% final concentration) and the kanamycin amended LBS 3% broth. It should be noted that while TCBS agar is valid for the removal of *E. coli*, this media does not always produce optimal growth for some vibrio species, thus working stocks of these cultures should be maintained on LBS amended with 300 µg mL^{-1} kanamycin once isolated. For vibrios that are not amenable to growth on TCBS, prior research has successfully utilized auxotrophic *E. coli* strains to enable selective removal following conjugation (Le Roux et al., 2007).

GFP Persistence. To determine persistence of GFP plasmids in non-subcultured samples, all transconjugant strains were grown in the absence of antibiotic stress and the level of plasmid loss was measured over time. Plasmid loss was evaluated as the percent loss of fluorescent colony forming units (CFU) following growth in a long-term media culture and persistence in sterile ASW. Long-term media cultures were maintained in 4 mL of antibiotic-free LBS 3% for a duration of 5 days (120 h). ASW cultures were maintained in 10 mL of 0.2 µm filter sterilized Instant Ocean® (35 practical salinity units [PSU]) for a duration of 2 days (48 h). The larger volume was selected for ASW trials to stabilize the cultures under low-nutrient conditions which were observed to have low survivability at the 4 mL volume (used in media experiments). All cultures were revived from -80 ^{o}C storage and incubated overnight in LBS 3% amended with 300 µg mL^{-1} kanamycin at 30 ^{o}C with 100 rpm of shaking agitation. Fluorescence was confirmed for all parent cultures using fluorescent microscopy. Parent cultures were pelleted by centrifugation at ~4,000 x *g* for 2 min then resuspended in sterile 1X PBS, in duplicate, to remove any excess kanamycin before the start of the experiment. 100 µL of washed cells were inoculated in 4 mL (~2.5 x 10^6 CFU/mL) of antibiotic-free LBS 3% and 10 mL (~10 x 10^6 CFU/mL) of sterile ASW. Cultures were maintained at 28 ^{o}C under 100 rpm of shaking agitation for up to 5 d. Daily, a 100 µL aliquot of each culture was removed from the incubator, serially diluted (10-fold), spread plated with glass rattler beads (Zymo Rattler^{TM} Plating Beads, 4.5 mm) onto agar plates (species-specific media preference, see Table 1), and incubated at 30 ^{o}C overnight, in duplicate. Plates were examined the following day (~18 h) and the number of fluorescent and non-fluorescent CFU were counted with the aid of a 495 nm blacklight. (Figure 5). GFP loss was calculated as the percent reduction of fluorescent CFU over time.

GFP Retention during Subculture. To determine plasmid retention following subculturing, all transconjugant strains were subcultured sequentially in the absence of antibiotic stress to measure generational loss of the GFP plasmid. Parent cultures were revived, confirmed, and washed as described above and 100 µL of washed cells were inoculated into 4 mL of antibiotic-free LBS 3% to create a new subculture. This process was repeated daily to produce four sequential subcultures. Subcultures were incubated at 28 ^{o}C under 100 rpm of shaking agitation overnight (~18 h) to reach stationary phase equating to an average of 5.42 generations elapsed per subculture (see Table S4 for species-specific generation time data). From each subculture (up to passage number 4), 100 µL of washed cells were serial diluted (10-fold) and spread plated with glass rattler beads (Zymo Rattler^{TM} Plating Beads, 4.5 mm) onto antibiotic-free agar plates (species-specific media preference, see Table 1), and incubated overnight (~18 h) at 30 ^{o}C, in duplicate. Isolated colonies were picked randomly from the spread plates (N = 50) and patch plated onto agar plates amended with 300 µg mL^{-1} kanamycin. This method was employed to diversify subculture passages on both liquid and solid media. Patches that did not grow on the antibiotic amended media were deemed non-retentive. Plasmid retention was calculated as the percentage of successful patches following each subculture series.

Evaluation of Complex Mixtures. To determine the success of GFP-based differentiation of tagged vibrios from non-tagged vibrios using microscopy, mixed communities were created by combining cultures of *V. alginolyticus*, *V. campbellii*, *V. harveyi*, *V. parahaemolyticus*, and *V. vulnificus*. Communities were prepared by combining equal parts of the above species to differentiate one GFP-tagged strain from the other four non-tagged species in the mixture. Mixture 1 contained GFP-tagged, *V. alginolyticus*, mixture 2 contained GFP-tagged *V. parahaemolyticus*, and mixture 3 contained GFP-tagged *V. harveyi*. To prepare communities,

non-GFP cultures were revived from -80 ºC storage in 3 mL of antibiotic-free 3% LBS and GFP-tagged strains were revived in 3 mL of LBS 3% amended with 300 µg mL^{-1} kanamycin. Cultures were grown overnight (~18 h) at 30 ºC with 100 rpm of shaking agitation. Following growth, 1 mL of each culture was pelleted by centrifugation at ~4,000 x *g*, supernatant fluid was discarded, and pellets were resuspended in 1 mL of sterile 1X PBS, in duplicate, to wash cells. 100 µL of each culture was combined in a 1.5 mL centrifuge tube and vortexed for 1 min to homogenize the mixture. 5 µL aliquots of the mixed community were observed using light and fluorescence microscopy to confirm the localization of the GFP strain among the complex mixture (Figures 1, S14, and S15).

To evaluate the potential of interspecies plasmid mobilization, a mixture of non-tagged *V. vulnificus, V. cholerae,* and GFP-tagged *V. parahaemolyticus* was combined in co-culture to determine if pVSV102 could self-mobilize into non-tagged strains. Non-GFP cultures were revived from frozen stocks in 3 mL of antibiotic free LBS 3% and GFP-tagged cultures were revived in 3 mL of LBS 3% amended with 300 µg mL^{-1} kanamycin incubated at 30 ºC overnight (~18 hr). Following incubation, 1 mL of each culture was removed, pelleted by centrifugation at ~4,000 x *g*, the supernatant fluid was discarded, and resuspended in 1 mL of sterile 1X PBS, in duplicate, to wash cells. 100 µL of each culture was combined in a 1.5 mL centrifuge tube and vortexed for 30 sec to homogenize the mixture. 100 µL of the mixture was inoculated into 4 mL of antibiotic free LBS 3% broth and incubated at 30 ºC for 5 days. Daily, a 100 µL aliquot of the mixture was removed, serial diluted (10-fold), and spread plated with glass rattler beads (Zymo Rattler™ Plating Beads, 4.5 mm) onto CHROMagar™ *Vibrio* plates incubated overnight (~18 h) at 35 ºC. Following incubation, CFU were counted, speciated colorimetrically, and checked for GFP using a 495 nm black light and fluorescent microscopy. Evidence of interspecies self-

mobilization was quantified as the number *V. cholerae* and *V. vulnificus* CFU that acquired GFP in the absence of antibiotic stress.

Acknowledgments

We are very grateful to Dr. Eric Stabb and the Stabb Lab at the University of Illinois Chicago for providing the helper and donor *E. coli* strains and plasmids used to facilitate GFP tagging in this study. We would also thank Samantha Weatherly, Carolina Melendez Declet, and Charlyn Shue for their contributions in the laboratory.

Literature Cited

Aboubaker MH, Sabrié J, Huet M, and Koken. 2013. Establishment of stable GFP-tagged *Vibrio aestuarianus* strains for the analysis of bacterial infection-dynamics in the Pacific oyster, *Crassostrea gigas*. *Veterinary Microbiology.* 164(3-4): 392-398.

Austin B and Zhang XH. 2006. *Vibrio harveyi*: a significant pathogen of marine vertebrates and invertebrates. *Letters in Applied Microbiology.* 43(2): 119-124.

Beijerinck MW. 1990. On different forms of hereditary variation in microbes. *Proc K Ned Akad Wet.* 3:352-365.

Baumann P, Baumann L, and Mandel M. 1971. Taxonomy of marine bacteria: the genus *Beneckea*. *Journal of Bacteriology.* 107(1): 268-294.

Ben-Haim Y, Thompson FL, Thompson CC, Cnockaert MC, Hoste MC, Swing B, and Rosenberg E. 2003. *Vibrio coralliilyticus* sp. nov., a temperature-dependent pathogen of the coral *Pocillopora damicornis*. *International Journal of Systematic and Evolutionary Biology.* 53(1): 309-315.

Bergeman A M. 1909. Die rote Beulenkrankheit des Aals. *Ber. Kgl. Bayer Biol.* Verssta. Sta., Munchen, 2: 10-54.

Boettcher KJ and Ruby EG. 1995. Occurrence of plasmid DNA in the sepiolid squid symbiont *Vibrio fischeri*. Current Microbiology. 29: 279-286.

Brenner DJ, Hickman-Brenner FW, Lee JV, Steigerwalt AG, Fanning GR, Hollis DG, Farmer JJ 3rd, Weaver RE, Joseph SW, Seidler RJ. 1983. *Vibrio furnissii* (formerly aerogenic biogroup of *Vibrio fluvialis*), a new species isolated from human feces and the environment. *Journal Clinical Microbiology*. 18(4): 816-24.

Chakraborty S, Nair GB, and Shinoda S. 1997. Pathogenic vibrios in the natural aquatic environment. *Reviews on Environmental Health.* 12(2): 63-80.

Dai F, Zhuang Q, Zhao X, Shao Y, Guo M, Lv Z, Li C, Han Q, and Zhang W. 2020. Green fluorescent protein-tagged *Vibrio splendidus* for monitoring bacterial infection in the sea cucumber *Apostichopus japonicus. Aquaculture.* 523: 735169.

Delavat F, Bidault A, Pichereau V, and Paillard C. 2018. Rapid and efficient protocol to introduce exogenous DNA in *Vibrio harveyi* and *Pseudoalteromonas* sp. *Journal of Microbial Methods*. 154: 1-5.

Drake SL, Elhanfi D, Bang W, Drakw MA, Green DP, and Jaykus LA. 2020. Validation of a green fluorescent protein-labeled strain of *Vibrio vulnificus* for use in the evaluation of postharvest strategies for handling of raw oysters. *Applied and Environmental Microbiology*. 72(11): 7205-7211.

Dunn AK, Martin MO, and Stabb EV. 2005. Characterization of pES213, a small mobilizable plasmid from *Vibrio fischeri*. *Plasmid.* 54(2): 114-134.

Dunn AK, Millikan DS, Adin DM, Bose JL, and Stabb EV. 2006. New *rfp*- and pES213-Derived tools for analyzing symbiotic *Vibrio fischeri* reveal patterns of infection and *lux* expression *in situ. Applied and Environmental Microbiology.* 72(1): 802-810.

Durai S, Pandian SK, and Balamurugan. 2011. Establishment of a *Caenorhabditis elegans* infection model for *Vibrio alginolyticus*. *Journal of Basic Microbiology*. 51(3): 243-252.

Frischkorn KR, Stojanovski A, and Paranjpye R. 2013. *Vibrio parahaemolyticus* type IV pili mediate interactions with diatom-derived chitin and point to an unexplored mechanism of environmental persistence. *Environmental Microbiology.* 15(5): 1416-1427.

Fujino T, Okuno Y, Nakada D, Aoyama A, Fukai K, Mukai T, and Ueho T. 1953. On the bacteriological examination of Shirasu-food poisoning. *Medical Journal of Osaka University*. 4:299.

Gavish AR, Shapiro OH, Kramarsky-Winter E, and Vardi A. 2021. Microscale tracking of coral-vibrio interactions. *ISME Communications*. 1(18): https://doi.org/10.1038/s43705-021-00016-0.

Getz LJ and Thomas NA. 2018. The transcriptional regulator HlyU positively regulates expression of exsA, leading to type III secretion system 1 activation in *Vibrio parahaemolyticus*. *Journal of Bacteriology*. 200(15):e00653-17.

Goulden EF, Hall MR, Bourne SG, Pereg LL, and Høj. 2021. Pathogenicity and infection cycle of *Vibrio owensii* in larviculture of the ornate spiny lobster (*Panulirus ornatus*). *Applied and Environmental Microbiology.* 78(8): 2841-2849.

Hada HS, West PA, Lee JV, Stemmler J, and Colwell RR. 1984. *Vibrio tubiashii* sp. nov., a pathogen of bivalve mollusks. *International Journal of Systemic and Evolutinary Microbiology.* 34(1): 1-4.

Jaskólska M, Adams DW, and Blokesch M. 2022. Two defence systems eliminate plasmids from seventh pandemic *Vibrio cholerae*. *Nature* 604: 323–329.

Johnson FH and Shunk IV. 1936. An interesting new species of luminous bacteria. *Journal of*

Bacteriology. 31: 585-592.

Kong J, Wang Y, Qi W, Huang M, Su R, and He Z. 2020. Green fluorescent protein inspired fluorophores. *Advances in Colloid and Interface Science.* 285: 102286.

Kushmaro A, Banin E, Loya Y, Stackenbrant E, and Rosenberg E. 2001. *Vibrio shiloi* sp. Nov., the causative agent of bleaching of the coral *Oculina patagonica. International Journal of Systematic and Evolutionary Microbiology.* 51(4): 1383-1388.

Lau BT, Malkus P, and Paulsson, J. 2013. New quantitative methods for measuring plasmid loss rates reveal unexpected stability. *Plasmid,* 70(3), 353–361.

Le Roux F, Binesse J, Saulnier D, and Mazel D. 2007. Construction of a *Vibrio splendidus* mutant lacking the metalloprotease gene *vsm* by use of a novel counterselectable suicide vector. *Applied and Environmental Microbiology*. 73(3): 777-784.

Liao HH. 1991. Effect of temperature on the expression of wild-type and thermostable mutants of kanamycin nucleotidyltransferase in *Escherichia coli*. *Protein Expression and Purification*. 2(1): 43-50.

Ling SHM, Wang XH, Lim TM, Leung KY. 2001. Green fluorescent protein-tagged *Edwardsiella tarda* reveals portal of entry in fish. *FEMS Microbiology Letters.* 194(2): 239-243.

Love M, Teebken-Fisher D, Hose JE, Farmer JJ III, Hickman FW and Fanning GR. 1981. *Vibrio damselae*, a marine bacterium, causes skin ulcers on the damselfish *Chromis punctipinnis*. *Science* 214, 1139–1140.

Mazzarini M, Falchi M, Bani D, and Migliaccio AR. 2021. Evolution and new frontiers of histology in bio-medical research. *Microscopy Research and Technique.* 84(2): 217-237.

Millikan DS and Ruby EG. 2002. Alterations in *Vibrio fischeri* motility correlate with a delay in

symbiosis initiation and are associated with additional symbiotic colonization defects. *Applied and Environmental Microbiology.* 68(5): 2519-2528.

Miyamoto Y, Nakamuma K, and Takizawa K. 1961. Pathogenic halophiles. Proposals of a new genus "*Oceanomonas*" and the amended species names. *Japanese Journal of Microbiology*. 5(4): 477-486.

Nyholm SV, Deplancke B, Gaskins HR, Apicella MA, and McFall-Ngai MJ. 2002. Roles of *Vibrio fischeri* and nonsymbiotic bacteria in the dynamics of mucus secretion during symbiont colonization of the *Euprymna scolopes* light organ. Applied and Environmental Microbiology. 68(10): 5113-5122.

O'Toole R, von Hofsten J, Rosqvist R, Olsson PE, and Wolf-Watz H. 2004. Visualization of Zebrafish infection by GFP-labelled *Vibrio anguillarum. Microbial Pathogenesis.* 37(1): 41-46.

Pacini F. 1854. Osservazioni microscopiche e deduzioni patalogiche sul cholera asiatico. *Gazzetta Medica Italiana Federativa Toscana, Firenze.* 4 (in Italian).

Prasher DC, Eckenrode VK, Ward WW, Prendergast FG, and Cormier MJ. 1992. Primary structure of the *Aequorea victoria* green-fluorescent protein. *Gene*. 111(2): 229-233.

Prasher DC. 1995. Using GFP to see light. *Trends in Genetics.* 11(8): 320-323.

Pollock JF, Krediet CJ, Garren M, Stocker R, Winn K, Wilson B, Huete-Stauffer C, Willia BL, and Bourne DG. 2015. Visualization of coral host–pathogen interactions using a stable GFP-labeled *Vibrio coralliilyticus* strain. *Coral Reefs.* 34(2): 655-662.

Pujalte MJ and Garay E. 1986. Proposal of *Vibrio mediterranei sp. nov*.: A new marine member of the genus *Vibrio*. *International Journal of Systematic and Evolutionary Microbiology.* 36(2): 278-281

Randa MA, Polz MF, and Lim E. 2004. Effects of temperature and salinity on Vibrio vulnificus population dynamics as assessed by quantitative PCR. *Applied and Environmental Microbiology.* 70(9): 5469-5476.

Rang C, Galen JE, Kaper JB, and Chao L. 2003. Fitness cost of the green fluorescent protein in gastrointestinal bacteria. *Canadian Journal of Microbiology*. 49(9): 531-537.

Rahmani A, Delavat F, Lambert C, Le Goic N, Dabas E, Paillard C, and Pichereau V. 2021. Implication of the type IV secretion system in the pathogenicity of *Vibrio tapetis*, the etiological agent of brown ring disease affecting the Manila Clam *Ruditapes philippinarum*. *Frontiers in Cellular and Infectious Microbiology*. 11:634427.

Reichelt JL, Baumann P, Baumann L. 1976. Study of genetic relationships among marine species of the genera *Beneckea* and *Photobacterium* by means of in vitro DNA/DNA hybridization. *Archives of Microbiology.* 110(1): 101-120.

Rekecki A, Gunasekara RA, Dierckens K, Laureau S, Boon N, Favoreel H, Cornelissen M, Sorgeloos P, Ducatelle R, Bossier P, and Van den Broeck W. 2012. Bacterial host interaction of GFP-labelled *Vibrio anguillarum* HI-610 with gnotobiotic sea bass, *Dicentrarchus labrax* (L.), larvae. *Journal of Fish Diseases*. 35(4): 265-73.

Sawabe T, Fukui Y, and Stabb EV. 2006. Simple conjugation and outgrowth procedures for tagging vibrios with GFP, and factors affecting the stable expression of the *gfp* tag. *Letters in Applied Microbiology*. 43(5): 514-522.

Sawabe T, Ogura Y, Matsumura Y, Feng G, Amin AKMR, Mino S, Nakagawa S, Sawabe T, Kumar R, Fukui Y, Satomi M, Matsushima R, Thompson FL, Gomez-Gil B, Christen R, Maruyama F, Kurokawa K, and Hayashi T. 2013. Updating the Vibrio clades defined by multilocus sequence phylogeny: proposal of eight new clades, and the description of

Vibrio tritonius sp. nov. *Frontiers in Microbiology.* 4: 414 https://doi.org/10.3389/fmicb.2013.00414

Shimomura O, Johnson FH, and Saiga Y. 1962. Extraction, purification and properties of aequorin, a bioluminescent protein from the luminous hydromedusan, *Aequorea*. *Journal of Cellular and Comparative Physiology.* 59(3): 223-239.

Shimomura O. 2005. The discovery of aequorin and green fluorescent protein. *Journal of Microscopy.* 217(1): 3-15.

Stabb EV and Ruby EG. 2002. RP4-based plasmids for conjugation between *Escherichia coli* and members of the *Vibrionaceae*. *Methods in Enzymology.* 358: 413-426.

Stretton S, Techkarnjanaruk S, McLennan AM, and Goodman AE. 1998. Use of green fluorescent protein to tag and investigate gene expression in marine bacteria. *Applied and Environmental Microbiology*. 64(7): 2554-2559.

Southward CM and Surette MG. 2002. The dynamic microbe: green fluorescent protein brings bacteria to light. *Molecular Microbiology.* 45(5): 1191-1196.

Summers DK. 1991. The kinetics of plasmid loss. *Trends in Biotechnology.* 9(1): 273-278.

Takemura AF, Chien DM, and Polz MF. 2014. Associations and dynamics of Vibrionaceae in the environment, from the genus to population level. Frontiers in Microbiology. 4(38): doi.org/10.3389/fmicb.2014.00038.

Thompson FL, Iida T, and Swings J. 2004. Biodiversity of Vibrios. *Microbiology and Molecular Biology Reviews*. 68(3): 403-431.

Travers MA, Barbou A, Le Goïc N, Huchette S, Paillard C, and Koken M. 2008. Construction of a stable GFP-tagged *Vibrio harveyi* strain for bacterial dynamics analysis of abalone infection. *FEMS Microbiology Letters.* 289(1): 34-40

Ushijima B, Smith A, Aeby GS, and Callahan SM. 20012. *Vibrio owensii* induces the tissue loss disease *Montipora* White Syndrome in the Hawaiian reef coral *Montipora capitata*. *PLoS ONE*. 7:e46717.

Ushijima B, Videau P, Burger AH, Shore-Maggio A, Runyon CM, Sudek M, Aeby GS, and Callahan SM. 2014. *Vibrio coralliilyticus* strain OCN008 is an etiological agent of acute *Montipora* White Syndrome. *Applied and Environmental Microbiology.* 80(7): 2102-2109.

Valdivia RH, Hromockyj AE, Monack D, Ramakrishnan L, and Falkow S. 1996. Applications for green fluorescent protein (GFP) in the study of host-pathogen interactions. *Gene*. 173(1 Spec No): 47-52.

Valdivia RH and Falkow S. 1997. Fluorescence-based isolation of bacterial genes expressed within host cells. *Science*. 277(5334): 2007-2011.

Wang, Y, Dunn AK, Wilneff J, McFall-Ngai MJ, Spiro S, and Ruby EG. 2010, *Vibrio fischeri* favohaemoglobin protects against nitric oxide during initiation of the squid–*Vibrio* symbiosis. *Molecular Microbiology*, 78(4): 903-915.

Wang D, Loor A, Bels L, Stappen GV, Broeck WVD, and Nevejan N. 2021. Dynamic immune response to vibriosis in Pacific oyster *Crassostrea gigas* larvae during the infection process as supported by accurate positioning of GFP-tagged vibrio strains. *Microorganisms*. 9(7):1523. 10.3390/microorganisms9071523.

Xiao Y, Liu Q, Chen H, and Zhang Y. 2011. A stable plasmid system for heterologous antigen expression in attenuated *Vibrio anguillarum*. *Vaccine*. 29(40): 6986-6993.

Tables and Figures

Table 1: Kanamycin lethal limits, GFP transfer concentrations, preferred culture media type, and GFP conjugation outcomes and for all tested vibrios. Preferred culture media produces non-inhibited growth at standard culture conditions and reduces the occurrence of bacterial swarming.

Species	Strain	MIC (μg mL^{-1})[a]	Stress Concentration (μg mL^{-1})[b]	CFU Added to Mating Mix	Preferred Culture Media	Conjugation Outcome	Strain Isolation Source	Strain Citation
Photobacterium damselae	ATCC 33539	25	15	$3.8x10^7$	LBS 3%	+	Damselfish skin ulcers, USA	Love et al., 1981
Vibrio alginolyticus	ATCC 17749	100	75	$4.6x10^7$	TCBS	+	Spoiled horse mackerel, Japan	Miyamoto et al., 1961
Vibrio anguillarum	ATCC 19264	50	35	$3.0x10^7$	LBS 3%	+	Ulcerous lesion in cod	Bergeman, 1909
Vibrio campbellii	ATCC 25920	50	35	$6.3x10^7$	LBS 3%	+	Seawater	Baumann et al., 1971
Vibrio coralliilyticus	ATCC BAA-450	50	35	$3.3x10^4$	LBS 3%	+	Infected coral, Zanzibar	Ben-Haim et al., 2003
Vibrio cholerae	ATCC 14035	100	75	$2.9x10^6$	LBS 3%	+	Enteric illness in humans	Pacini, 1854

Vibrio furnissii	ATCC 35016	25	15	$4.2x10^6$	LBS 3%	-	Human feces, Japan	Brenner et al., 1983
Vibrio harveyi	ATCC 14126	35	25	$7.1x10^6$	TCBS	+	Deceased luminescent amphipod, USA	Johnson and Shunk, 1936
Vibrio mediterranei	ATCC 43341	125	100	$2.3x10^7$	LBS 3%	+	Sediment, Spain	Pujalte & Garay, 1986
Vibrio parahaemolyticus	ATCC 43996	50	35	$3.7x10^7$	LBS 3%	+	Cockles (marine bivalve), Japan	Fujino et al., 1953
Vibrio pelagius	ATCC 25916	35	25	$4.4x10^5$	TCBS	+	Seawater	Baumann et al., 1971
Vibrio splendidus	ATCC 33869	75	50	$1.16x10^7$	LBS 3%	+	Seawater, USA	Beijerinck, 1990
Vibrio tubiashii	ATCC 19109	25	15	$3.1x10^6$	LBS 3%	-	Juvenile hard clams	Hada et al., 1984
Vibrio vulnificus	ATCC 27562	50	35	$6.2x10^7$	LBS 3%	+	Human blood, USA	Reichelt et al., 1976

[a]The MIC concentration is defined as the minimum concentration of kanamycin that produced total growth inhibition of the target Vibrio.

[b]The stress concentration is defined as the concentration of kanamycin that creates a stressful but non-lethal environment for the growth of the target Vibrio. This concentration was utilized to facilitate transfer for the GFP plasmid into the target species.

Table 2: Description of the plasmids and carrier strains utilized in this study.

Plasmid Designation	Carrier Bacterium	Usage	Genes Carried	Antibiotic Resisted	CFU Added to Mating Mix	Plasmid Citation
pEVS104	*E. coli*	Helper	*tra, trb*	Kanamycin (Kn^r)	$6.0x10^6$	Stabb & Ruby, 2002
pVSV102	*E. coli*	Donor	*gfp*	Kanamycin (Kn^r)	$6.3x10^6$	Dunn et al., 2006

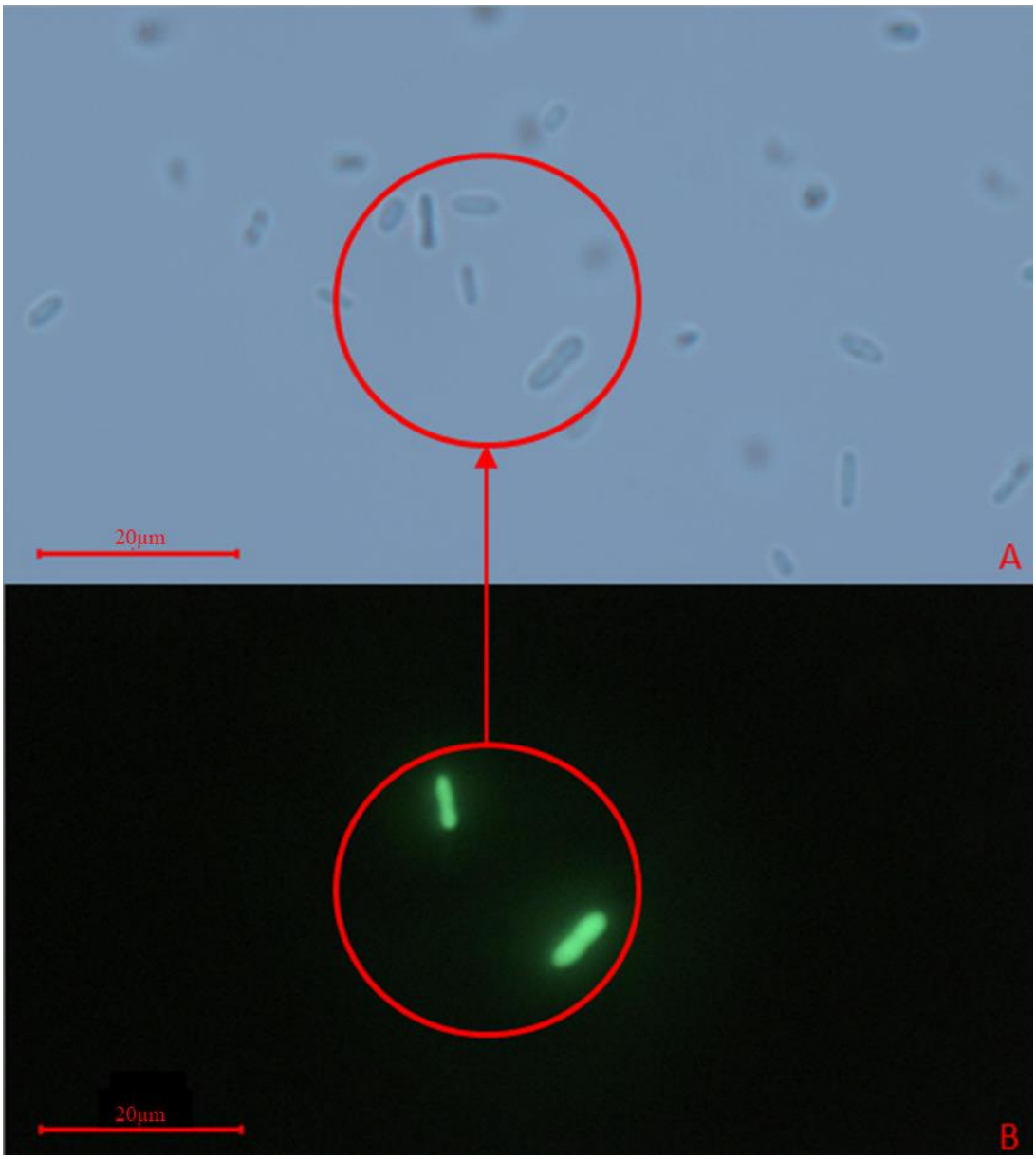

Figure 1: Differentiation of GFP-tagged *V. alginolyticus* within a complex mixture of five vibrios. Mixture contains equal parts *V. alginolyticus* (GFP), *V. campbellii*, *V. parahaemolyticus*, *V. harveyi*, and *V. vulnificus.* Images A and B compare the same micrograph under light microscopy and fluorescent microscopy (495 nm excitation wavelength) at 1000X magnification.

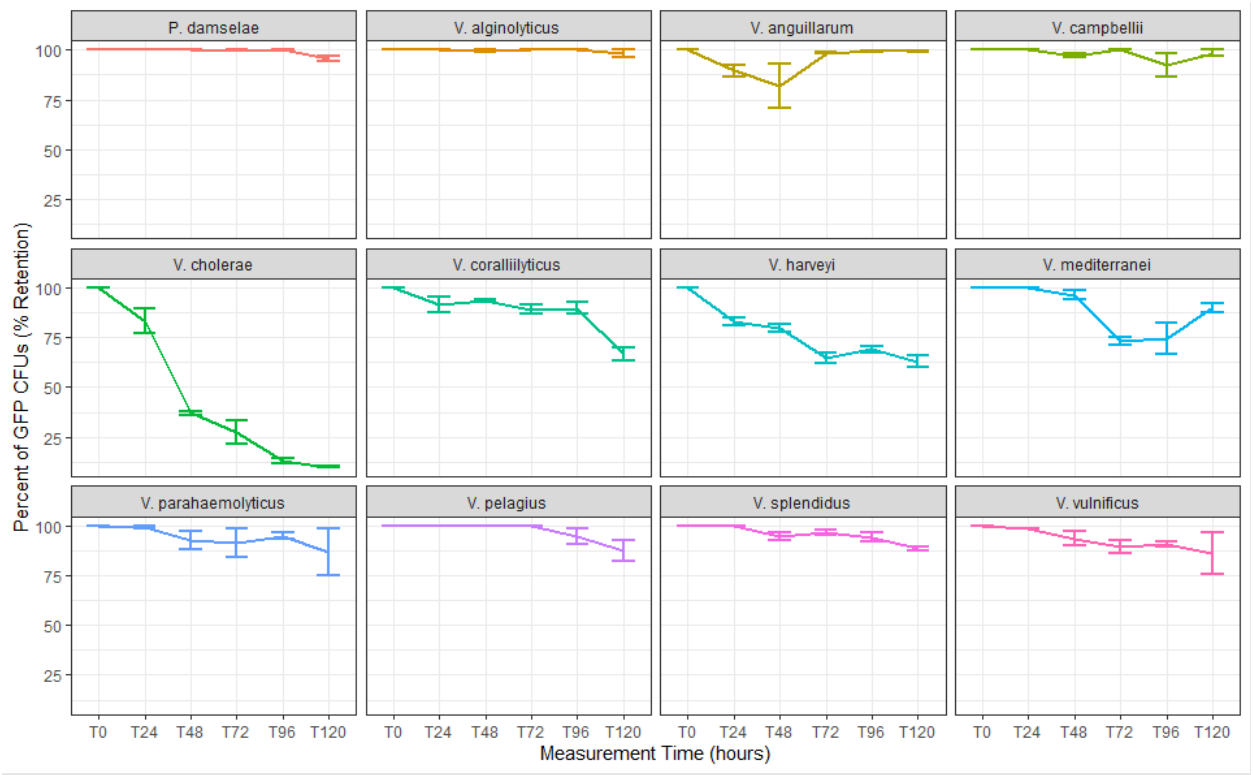

Figure 2: Persistence evaluation of GFP retention in antibiotic-free media (LBS 3%) for five days of observation at 28 ºC. Values indicate the percent of fluorescent CFU (y-axis) observed at each timepoint (x-axis). Error bars indicate the sample range (N = 2).

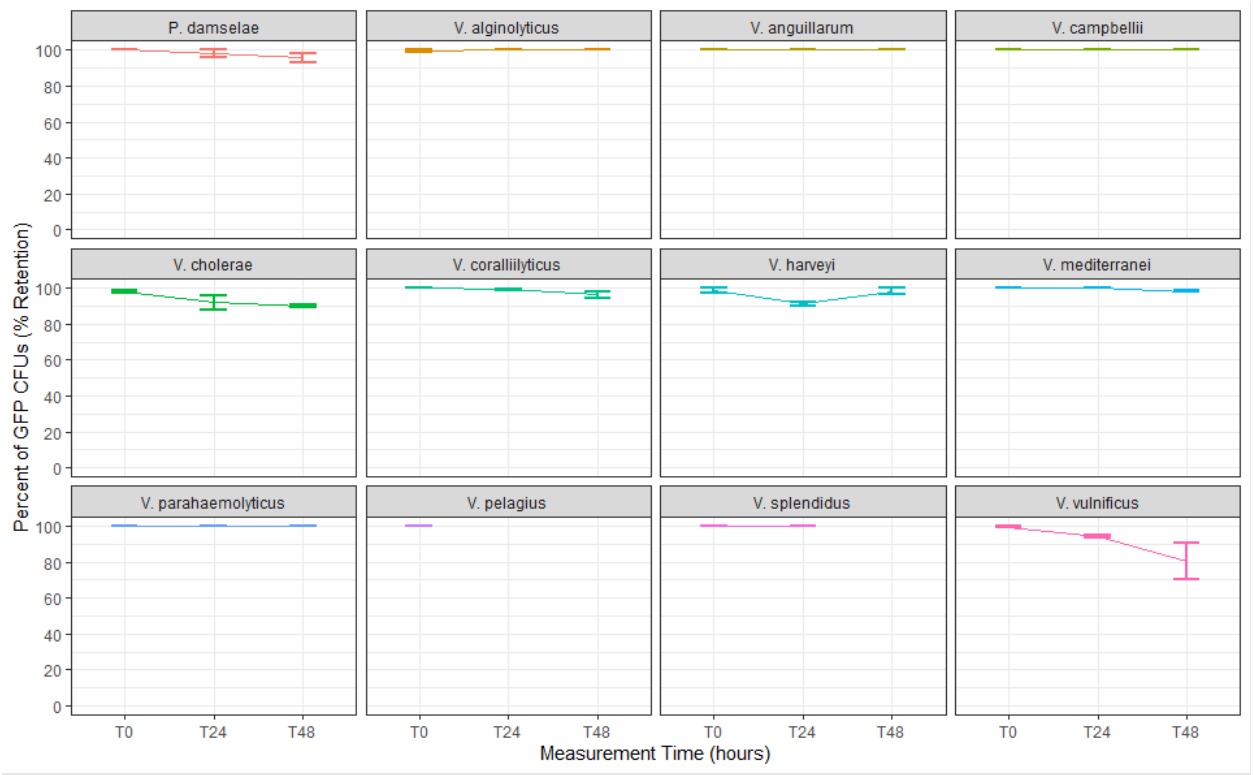

Figure 3: Persistence evaluation of GFP retention in antibiotic-free sea water (sterile ASW) for two days of observation at 28 ºC. Values indicate the percent of fluorescent CFU (y-axis) observed at each timepoint (x-axis). Error bars indicate the sample range (N = 2). Cultures of *V. pelagius* and *V. splendidus* were not recoverable in ASW beyond T_0 and T_{24}, respectively.

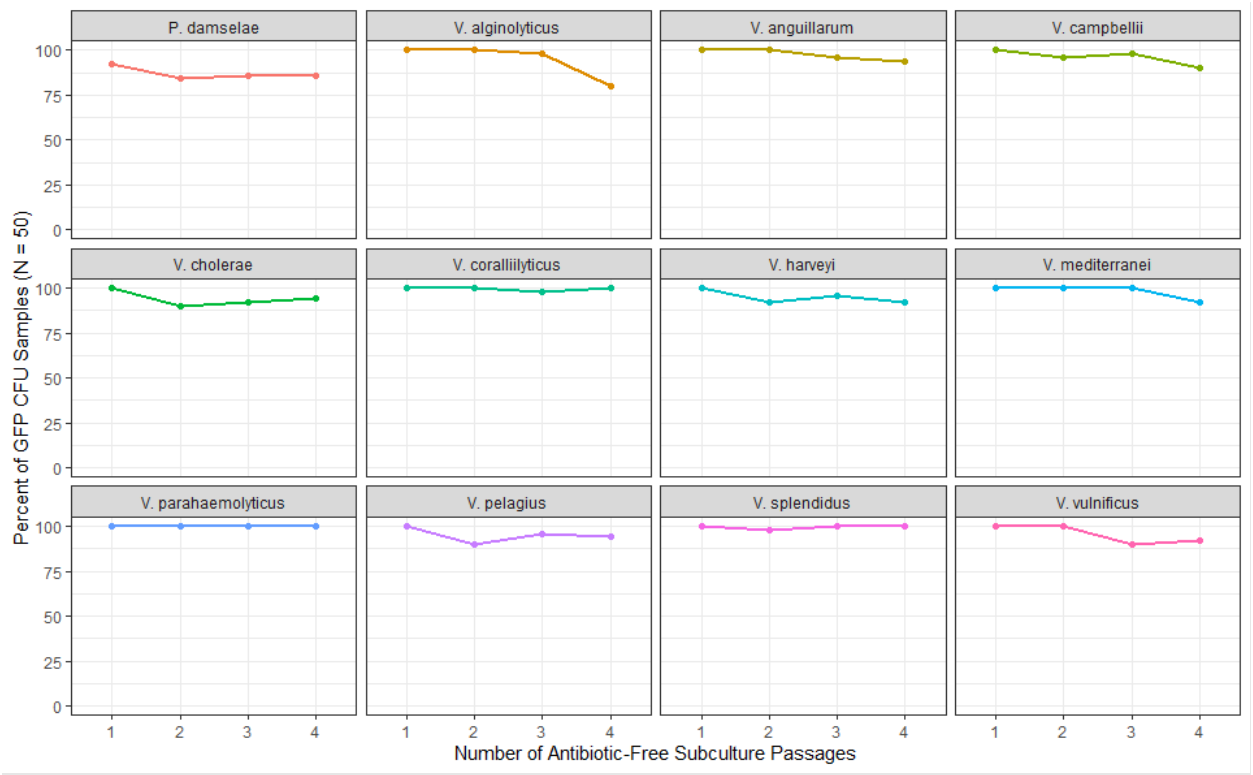

Figure 4: Subculture evaluation of GFP retention following sequential passages in antibiotic-free media. Values indicate the percent of patched CFU (N = 50) that successfully grew on 300 µg mL^{-1} kanamycin amended agar (y-axis) following each level of subculture passages (x-axis).

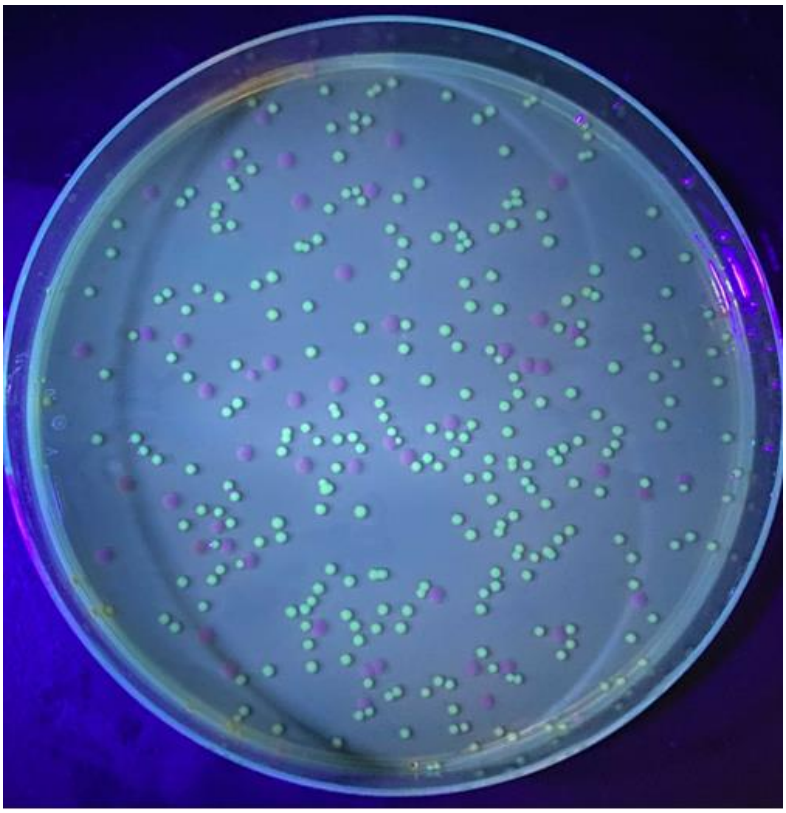

Figure 5: Assessment of *V. cholerae* GFP retention in persistence experimentation. Bright green coloration indicates retentive CFU whereas purple coloration indicates loss of GFP. Image taken at 24 hours of growth with the aid of a 495 nm blacklight.

CHAPTER 5

CORAL DISEASE AND INGESTION: INVESTIGATING THE ROLE OF HETEROTROPHY IN THE TRANSMISSION OF PATHOGENIC *VIBRIO* SPP. USING A SEA ANEMONE (*EXAIPTASIA PALLIDA*) MODEL SYSTEM

Norfolk WA , Melendez-Declet C, and Lipp EK. Submitted to *Applied and Environmental Microbiology.*

Abstract

Understanding disease transmission in corals can be complicated given the intracity of the holobiont and difficulties associated with *ex situ* coral cultivation. As a result, most of the established transmission pathways for coral disease are associated with perturbance (i.e., damage) rather than evasion of immune defenses. Here we investigate ingestion as a potential pathway for the transmission of coral pathogens that evades the mucus membrane. Using sea anemones (*Exaiptasia pallida*) and brine shrimp (*Artemia* sp.) to model coral feeding, we tracked the acquisition of the putative pathogens, *Vibrio alginolyticus*, *V. harveyi*, and *V. mediterranei* using GFP-tagged strains. *Vibrio* sp. were provided to anemones using three experimental exposures 1) direct water exposure alone, 2) water exposure in the presence of a food source (clean *Artemia*), and 3) through a "spiked" food source (*Vibrio*-colonized *Artemia*) created by exposing *Artemia* cultures to GFP-*Vibrio* via the ambient water overnight. Following a 3 h feeding/exposure duration, the level of acquired GFP-*Vibrio* was quantified from anemone tissue homogenate. Ingestion of spiked *Artemia* resulted in a significantly greater burden of GFP-*Vibrio* equating to an 829.7-fold, 3,108.2-fold, and 435.0-fold increase in CFU mL^{-1} when compared to water exposed trials and a 206.8-fold, 62.2-fold, and 27.3-fold increase in CFU mL^{-1} compared to water exposed with food trials for *V. alginolyticus*, *V. harveyi*, and *V. mediterranei*, respectively. These data suggest that ingestion can facilitate delivery of an elevated dose of pathogenic bacteria in cnidarians and may describe an important portal of entry for pathogens in the absence of perturbing conditions.

Importance

The front line of pathogen defense in corals is the mucus membrane. This membrane coats the surface body wall creating a semi-impermeable layer that inhibits pathogen entry from the

ambient water both physically and biologically through mutualistic antagonism from resident mucus microbes. To date, much of the coral disease transmission research has been focused on mechanisms associated with perturbance of this membrane such as direct contact, vector lesions (predation/biting), and waterborne exposure through preexisting lesions. The present research describes a transmission pathway that evades the defenses provided by this membrane allowing unencumbered entry of bacteria as in association with food. This pathway may explain an important portal of entry for emergence of idiopathic infections in otherwise healthy corals and can be used to improve management practices for coral conservation.

Introduction

In recent years, coral reefs have experienced unprecedented decline with regular mass mortality events occurring annually across the globe (Eddy et al., 2021). As ecosystem engineers, hermatypic corals produce the foundation of reef habitats by creating the critical three-dimensional structure that defines the reefscape (Wild et al., 2011). The loss of key coral species causes a decline in habitat complexity leading to a subsequent loss of biodiversity and reef ecosystem services (e.g., coastal protection, fisheries stability, and ecotourism) (Jones et al., 2004; Pratchett et al., 2018; Hoegh-Guldberg et al., 2019; Eddy et al., 2021). While coral decline can be attributed to many factors including global climate change, pollution, eutrophication, anthropogenic development, and overfishing, coral disease remains one of the most prominent causes of regional mortality events worldwide (Harvell et al., 1999; Green & Bruckner, 2000; Porter et al., 2001; Harvell et al., 2007; Montilla et al., 2019).

Understanding disease transmission, or how a pathogen spreads between individuals in a susceptible population, is a critical component for the management of infectious disease. A mechanistic understanding of the processes related to pathogen movement from reservoirs,

through the environment, and into a susceptible host can provide insight for the prediction of disease outbreaks. Prior investigations of coral disease transmission have demonstrated the importance of direct contact, vector transmission, and waterborne transmission via preexisting lesions (reviewed by Shore & Cadwell, 2019). However, few studies have directly investigated the mechanisms of waterborne transmission, or ambient transmission via exposure in the water column, in uninjured healthy corals. Direct acquisition of pathogenic bacteria from the water column is impeded by the mucus membrane, which creates a semi-impermeable physical and biological barrier surrounding the coral tissue and by ciliary flows that create microscale water currents reducing the efficacy of pathogen chemotaxis (Rosenberg et al., 2007; Shapiro et al., 2014; Thompson et al., 2014). Thus, in the absence of injury where these systems are degraded, pathogens must overcome these defenses or utilize alternate portals of entry to establish infection.

Two recent studies have suggested that direct bacterial ingestion or ingestion of zooplankton may play an important role in the transmission of coral disease. Certner et al. (2017) demonstrated that white-band disease (WBD) transmission can be facilitated through zooplankton ingestion following incubation in tissue homogenate from diseased corals. In a similar vein, Gavish et al. (2021) utilized a microscale visualization system to observe colonization of *Pocillopora damicornis* by *Vibrio coralliilyticus* from ambient sea water, suggesting that ingestion may be a primary route of entry for the pathogen. Corals support their carbon and nutrient needs through the mutualistic relationship with their algal symbionts and through direct feeding. Heterotrophy provides up to 35% of a healthy coral's daily metabolic needs and up to 100% in bleached corals, largely by nighttime feeding on zooplankton (Houlbrèque & Ferrier-Pagès, 2009; Ferrier-Pagès et al., 2010). While Gavish et al. (2021) demonstrates the viability of pathogen acquisition via

direct ingestion of bacteria, preferential grazing of zooplankton, which are known to be colonized by bacteria (and *Vibrio* in particular [Erken et al., 2015]), may represent an important exploitable pathway for pathogenic microbes to gain entry to a coral host. We hypothesize that pathogen-colonized zooplankton may serve as a foodborne vector for disease transmission in uninjured corals.

Vibrio spp. are ubiquitous aquatic bacteria frequently identified as the causative or putative agents of coral disease (Table 1) (Munn, 2015). As indigenous microorganisms, or bacteria that exist naturally as a part of the ambient microbial community, *Vibrio* exhibit complex interspecies interactions that allow them to inhabit a broad range of ecological niches in the environment (Takemura et al., 2014). Of particular note is the association between *Vibrio* spp. and chitinous zooplankton (Takemura et al., 2014; Erken et al., 2015). Prior studies of *Vibrio* populations frequently associate total *Vibrio* and/or specific *Vibrio* spp. with plankton presence (Kaneko & Colwell, 1977; Heidelberg et al., 2002; Thompson et al., 2004; Turner et al., 2009; Magny et al., 2011; Martinez-Urtaza et al., 2011; Main et al., 2015). This association has been suggested to facilitate bacterial dispersal (Grossart et al., 2010; Erken et al., 2015), reduce bacterivore predation (Matz et al., 2005; Liang et al., 2019), and/or enable the utilization of chitin as a substrate (Hunt et al., 2008; Pruzzo et al., 2008; Erken et al., 2015).

Research investigating cholera transmission in humans has demonstrated that *V. cholerae* cells colonize the exoskeletons of copepods where their concentration can increase to an excess of 10^4 cells copepod^{-1} (Huq et al., 1983; Tamplin et al., 1990; Colwell, 1996; Rawlings et al., 2007; Magny et al., 2011). Subsequent ingestion of colonized copepods can increase the probability of ingesting a potentially pathogenic dose of the bacterium facilitating the onset of disease (Huq et al., 1996; Nelson et al., 2009). Furthermore, pre-filtration of surface water

sources utilized for drinking with simple fabric mesh can reduce the occurrence of *V. cholerae* infections due to the reduction of colonized zooplankton (Huq et al., 1996; Colwell et al., 2003). While this *Vibrio*-zooplankton transmission pathway has been well established for *V. cholerae*, little research has been devoted to investigating the importance of these interactions for non-cholera *Vibrio* infections.

The work presented here investigates the viability of an ingestion-based transmission pathway for the acquisition of potentially pathogenic *Vibrio* spp. in corals. To alleviate difficulties of *ex situ* coral cultivation, a model system was employed utilizing sea anemones (*Exaiptasia pallida*) and brine shrimp (*Artemia* sp.) to mimic natural coral feeding. Prior research has demonstrated the utility of sea anemones in the genus *Exaiptasia* (formally *Aiptasia*, see Grajales & Rodriguez, 2014 for reclassification) as lab-friendly surrogates for coral experimentation (Belda-Baillie et al., 2001; Weis et al., 2008; Sunagawa et al., 2009; Hardefeldt & Reichelt-Brushett, 2015). Structurally, *Exaiptasia* spp. resemble large non-colonial coral polyps and feed both heterotrophically on zooplankton and autotrophically though the use of their algal symbionts (zooxanthellae) (Grajales & Rodriguez, 2014). Using this model system, we traced the acquisition of the putative coral pathogens *V. alginolyticus*, *V. mediterranei*, and *V. harveyi.*

Results

Artemia* Colonization by *Vibrio. Colonization experiments first assessed the ability of *Vibrio* spp. to attach to/associate with *Artemia*. Substantial colonization of *Artemia* gastrointestinal (GI) tracts was observed for all tested vibrios following overnight (18 h) exposure via ambient water. Total colonization for each *Vibrio* spp. exposure (~250 *Artemia*) was 4.90×10^6, 1.47×10^6, 7.59×10^6 CFU per ~250 individuals for *V. alginolyticus*, *V. harveyi*, and *V. mediterranei*,

respectively. These levels equate to a mean acquisition of 4.32%, 2.14%, and 50.21% of the initial exposure dose for *V. alginolyticus*, *V. harveyi*, and *V. mediterranei*, respectively (Figure S1). Epifluorescence microscopy showed GFP tagged cells were concentrated throughout the length of *Artemia* GI tracts in association with ingested material and feces (Figure 1). GFP cells were also observed in association with *Artemia* feces following defecation. Low exoskeletal association was observed in all experimental trials, though minor attachment and/or entanglement was noted in association with *Artemia* appendages (Figure 1). GI association was consistent across naupliiar sizes excluding the smallest, most recently hatched individuals (Figure S2), which showed little to no GFP-*Vibrio* accumulation. Visual patterns of GI association did not differ between *Vibrio* species. No distinctive behavioral changes or swimming impairment was observed in colonized *Artemia* throughout the duration of exposure (up to 24 h).

Uptake of *Vibrio* by *E. pallida*. Anemone feeding studies evaluated the efficacy of an ingestion-based transmission pathway by confirming consumption of GFP-*Vibrio*-colonized *Artemia* and quantification of the acquired GFP-*Vibrio* dose. Gross observations of feeding demonstrate that *E. pallida* readily ingested *Vibrio*-colonized *Artemia*, responding rapidly with predatory tentacle behavior when *Artemia* were introduced into the microcosm water (Figure S3). No differences in anemone feeding behavior (i.e., tentacle response) were observed for exposures using spiked and non-spiked *Artemia*.

Assessment of the acquired dose compared four major feeding/exposure treatments: 1) water exposed not fed, where GFP-*Vibrio* were inoculated into the microcosm water and no *Artemia* were added, 2) water exposed control fed, where GFP-*Vibrio* were inoculated into the microcosm water and anemones were fed with clean (non-spiked) *Artemia*, 3) spiked fed, where

no GFP-*Vibrio* were inoculated into the microcosm water and anemones were fed with *Vibrio*-colonized *Artemia,* and 4) control, where no GFP-*Vibrio* were inoculated into the microcosm water and anemones were fed clean *Artemia* (Figure 2). Significantly greater GFP-*Vibrio* levels were observed in *E. pallida* individuals exposed via spiked *Artemia* (spiked fed) compared to individuals exposed through the ambient water, regardless of the presence of *Artemia* (i.e., all other experimental conditions). Anemone homogenate from spiked fed trials showed a mean GFP-*Vibrio* concentration of 6.92×10^4, 2.59×10^5, and 1.67×10^5 CFU mL^{-1} for *V. alginolyticus, V. harveyi*, and *V. mediterranei*, respectively. Conversely, water exposed anemones showed a mean concentration of 3.33×10^2 and 8.33×10^1 CFU mL^{-1} for *V. alginolyticus*, 4.10×10^3 and 8.33×10^1 CFU ml^{-1} for *V. harveyi*, and 5.90×10^3 and 3.83×10^2 CFU mL^{-1} for *V. mediterranei* for water exposed control fed (non-spiked) and water exposed not fed (no *Artemia*) treatments, respectively. These concentrations equate to a 206.8-fold, (p-value = 0.03), 62.2-fold (p-value = 0.013), and 27.3-fold (p-value = 0.013) increase in the GFP-*Vibrio* burden of spiked fed compared to water exposed control fed anemones and a 829.7-fold (p-value = 0.028), 3,108.2-fold (p-value = 0.026), and 435.0-fold (p-value = 0.030) increase in spiked fed compared to water exposed not fed anemones for *V. alginolyticus, V. harveyi*, and *V. mediterranei*, respectively (Figure 3). Between the two water exposures, fed (non-spiked *Artemia*) anemones showed a significantly greater burden of GFP *V. harveyi* (p-value = 0.026) and *V. mediterranei* (p-value = 0.030) compared to non-fed anemones but did not differ significantly for *V. alginolyticus* (p-value = 0.51). No GFP-*Vibrio* were recovered from anemones in the control group (no exposure) or from anemone wash water (carry-over control).

Discussion

The mucus membrane serves as the front line of defense against infection for coral species. This mucus coats the epithelia creating a semi-impermeable barrier between the coral tissue and ambient water (Cooney et al., 2002; Brown & Bythell, 2005; Rosenberg et al., 2007; Thompson et al., 2014). Within this mucus layer, a variety of mutualistic and commensal microorganisms are maintained. The totality of these microbes and the coral colony are collectively known as the holobiont (Rohwer et al., 2002). Research has suggested that the coral-associated microbial community can confer improved fitness to the holobiont through community shifts in response to environmental change (Reshef et al., 2006, Thompson et al., 2014), the production of antimicrobial compounds (Shnit-Orland & Kushmaro, 2009) and/or antagonistic competition with potential pathogens (Rohwer et al., 2002; Ritchie, 2006; Teplitski & Ritchie, 2009). Together, the physical mucus barrier combined with the biological protection of the microbial community pose a substantial challenge to the direct transmission of waterborne pathogens. To date, the majority of coral disease transmission research has focused on mechanisms of pathogen spread associated with perturbance of this mucus membrane such as direct contact, vector-mediated (i.e., biting), and indirect transmission via preexisting lesions (Shore & Cadwell, 2019). While these studies provide important insight into the ecology of coral diseases, these transmission mechanisms are dependent on opportunistic occurrences related to host proximity and preexisting or active damage and there is substantial need to investigate transmission mechanisms related to disease emergence in uninjured corals.

Despite the presence of zooxanthellae, heterotrophic feeding is a critical component of coral nutrition, accounting for up to 35% of the daily metabolic needs of some coral species (Houlbrèque & Ferrier-Pagès, 2009; Ferrier-Pagès et al., 2010). Corals preferentially feed on

small zooplankton thus, we investigated the ability of pathogenic *Vibrio* spp. to be transmitted to a cnidarian host via ingestion following colonization of a zooplankton vector. Using sea anemones (*E. pallida*) and brine shrimp (*Artemia* spp.) to model coral feeding, we demonstrate that ingestion of *Vibrio*-spiked brine shrimp results in a significantly higher bacterial burden in recipient anemones compared to ambient water exposures, both with and without food sources (i.e., *Artemia*). These data suggest that ingestion could play a role in the transmission of certain coral pathogens. Furthermore, this mode of transmission bypasses the natural defense mechanisms of corals provided by their mucus membrane (Rohwer et al., 2002; Shnit-Orland & Kushmaro, 2009) which may describe an important portal of entry related to pathogenic infection of uninjured corals.

Acting as our model zooplankton, *Artemia* were readily colonized by all tested *Vibrio* spp. following direct waterborne exposure, similar to previous studies in *V. cholerae* (Huq et al., 1983). However, the preferential colonization of the GI tract noted here differed from previously described observations where colonization was predominately observed on zooplankton exoskeletons (Huq et al., 1983; Tamplin et al., 1990; Colwell, 1996). We hypothesize that this difference may be due to the fact that the present research was conducted *ex situ* where certain environmental determinants of zooplankton colonization (i.e., substrate limitation) may not be present and/or as impactful (Worden et al., 2005; Takemura et al., 2014, Liang et al., 2019). While some minor exoskeletal association was observed on *Artemia* appendages, we suspect that this may be the result of incidental entanglement rather than purposeful attachment. Due to the lack of strong external association, we postulate that the colonization of *Artemia* GI tracts is the result of active ingestion of *Vibrio* spp. by nauplii occurring over prolonged interaction (≥4 h of exposure). This hypothesis is further supported by the observation that the smallest most recently

hatched *Artemia* (Figure S2) showed minimal GI colonization. At this stage of life, nauplii are nutritionally maintained through residual yolk protein and do not actively feed until they are larger (Warner et al., 1973; Sugumar & Munuswamy, 2006). The total *Artemia*-acquired dose remained relatively consistent for all three *Vibrio* spp. at ~10^6 CFU per ~250 individuals. These data suggest that *Artemia* have a threshold for the maximum concentration of *Vibrio* spp. they can harbor via GI colonization.

Feeding experiments demonstrate that spiked fed anemones acquire a significantly greater GFP-*Vibrio* burden compared to water exposed individuals regardless of the presence of food. This pattern was observed across all three *Vibrio* spp. suggesting that ingestion of *Vibrio*-colonized zooplankton can facilitate delivery of an elevated dose of these bacteria, broadly. The higher *Vibrio* levels are likely the result of bioaccumulation of these bacteria within *Artemia* facilitating acquisition of a highly concentrated dose through targeted feeding. This is consistent with prior observations of *V. cholerae* carriage by copepods where ingestion of a small number of individuals may facilitate receipt of a potentially pathogenic dose ($\leq 10^3$ cells) (Huq et al., 1983; Colwell, 1996). While low compared to spiked fed individuals, water exposed anemones did result in some uptake of GFP-*Vibrio* with higher levels acquired in the presence of food ('clean' *Artemia*) than without. This observation is consistent with the findings of Gavish et al. (2021) and suggests that even in the absence of *Vibrio*-colonization of food sources, active feeding and ingestion may contribute to the acquisition of *Vibrio* spp. cells from the surrounding water.

At ambient levels, *Vibrio* spp. typically range from 10^1 to 10^3 CFU mL^{-1} (Urakawa and Rivera, 2006) with location-specific differences in community composition driven largely by temperature and salinity (Turner et al., 2009; Takemura et al., 2014). However, *Vibrio*

populations are known to be dynamic, fluctuating on a "boom-bust" cycle of growth and reduction in association with ephemeral pulses of limiting nutrients (Westrich et al., 2016; Westrich et al., 2018; Borchardt et al., 2020). During bloom events, total *Vibrio* can increase dramatically rising to levels 5 to 30 times greater than the typical background concentration of coastal waters (Westrich et al., 2016). Prior research has shown that seasonal increases in *Vibrio* abundance facilitate increases in both free-living and zooplankton-associated abundance (Carli et al., 1993). Thus, blooms numbers could potentially promote zooplankton colonization and enhance the likelihood of transmission via ingestion during these events. While further studies on species-specific colonization rate, transmitted dose, and uptake *in situ* are needed to assess the potential importance in coral disease, we postulate that these mechanisms provide an ecological basis for foodborne transmission of certain coral pathogens.

While the scope of this research is targeted at understanding coral disease, the results of this study have broader implications for the spread of vibriosis. *Vibrio* spp. have been implicated as the causative or putative pathogens in numerous diseases of marine organisms, most notably important aquaculture species such as Pacific White Shrimp (*Litopenaeus vannamei*), Tiger Prawn (*Penaeus monodon*), Atlantic Salmon (*Salmo salar*), and Gilt-Head Sea Bream (*Sparus aurata*) (Karunasagar et al., 1994; Press & Lillehaug, 1995; Balebona et al., 1998; Zhou et al., 2012). Zooplankton serve as the base of the marine/estuarine food web thus, there is potential for ingestion to play a role in the acquisition of these and similar pathogens. This hypothesis is supported by the work of Goulden et al. (2012) who utilized a similar GFP tracking system to demonstrate that *Panulirus ornatus* (ornate spiny lobster) mortality can be facilitated by ingestion of *V. owensii*-colonized *Artemia* in aquaculture settings. Furthermore, the non-discriminant acquisition of all three *Vibrio* spp. in the present study suggests that this pathway

may be broadly viable within the Vibrionaceae and warrants continued investigation of the role of ingestion in the spread of other pathogenic vibrios.

Conclusion.

Understanding coral disease transmission is critical to the conservation of reef habitats. The present study describes a mechanistic pathway for the acquisition of coral pathogens via zooplankton ingestion using a sea anemone (*E. pallida*) and brine shrimp (*Artemia*) model system to represent coral heterotrophy. The results of this research demonstrate that ingestion of *Vibrio*-colonized *Artemia* can facilitate receipt of a significantly elevated *Vibrio* dose when compared to exposure via the water column suggesting that heterotrophy may represent an important transmission pathway for certain coral pathogens. Characterization of this pathway illustrates a means by which pathogenic bacteria may bypass the natural immune defenses of corals conferred by their mucus membranes allowing for unencumbered acquisition of a pathogenic dose. This mechanism may help to explain a potential source of idiopathic infections that arise in otherwise healthy unperturbed corals.

Methods

Experimental Vibrio Strains. Experimental *Vibrio* strains were obtained from our culture collection (E.K. Lipp, University of Georgia) and consisted of the known coral pathogens *V. alginolyticus*, *V. mediterranei*, and the putative coral pathogen *V. harveyi* (see Table S1 for strain information). All strains were maintained at -80 ^{o} C in a 1:1 mixture of 40% glycerol (20% final concentration) and lysogeny broth (LB, Sigma Aldrich, Miller formulation) amended to 3% w/v NaCl (termed LBS 3%). To revive from storage, strains were inoculated into 4 mL LBS 3% and incubated at 30 ^{o}C with 100 rpm shaking agitation (New Brunswick Scientific, C24 Incubator Shaker) for 18-24 h.

Brine Shrimp Cultures and Maintenance. *Artemia* sp. were purchased as dehydrated cysts (Premium Grade Brine Shrimp Eggs: Brine Shrimp Direct Inc., Great Salt Lake Origin, USA). Dehydrated cysts (0.3 g) were revived in 300 mL sterile artificial sea water (35 practical salinity units [PSU] Instant Ocean®, termed ASW) incubated at room temperature under mild agitation from an aquarium bubbler (Whisper® 20, Aquarium Air Pump). Cysts hatching occurred within 1-2 days of rehydration. *Artemia* were harvested at the nauplii stage, following 1-2 additional days of incubation, using a sterile serological pipette. Free swimming nauplii were collected from below the water surface to reduce collection of any discarded or unhatched cysts. Any *Artemia* cultures that appeared discolored (cloudy water), produced poorly swimming nauplii, or hatched insufficiently (<75% hatching, estimated visually) were discarded.

Anemone Cultures and Maintenance. *E. pallida* anemones were purchased live (Carolina® Biological Supply, #162865) and maintained in laboratory holding tanks. Holding tanks were constructed using a 6 L glass aquarium equipped with a constant-flow water filter (Aqueon® QuietFlow Aquarium Power Filter 10), an in-water aquarium heater (Aqueon® Pro Heater 50W), and a 445nm aquarium light (GloFish® Blue, LED Aquarium Light). Holding aquaria were maintained under the conditions outlined in Tables S2 and S3. Prior to experimentation, all anemones were transferred to holding tanks and allowed to acclimate for a minimum of 2 weeks. Anemones were monitored daily, and any deceased individuals were removed. Long-term cultures (not used for experimentation) of *E. pallida* were kept with the experimental anemones to stabilize holding tank water chemistry. While in the holding tank, anemones were fed twice per week with 50 mL (~2,000 individuals) of decapsulated *Artemia*. Water changes (50% of tank volume) were preformed every two weeks and replaced volumetrically with fresh ASW.

Intermittent tank cleaning was performed as needed using a scrub brush and/or a serological pipette to remove anemone debris and algal build-up following feeding.

GFP Tagging. All *Vibrio* spp. used in this experiment were tagged with GFP to enable localization and quantification of the bacterium. Tagging was accomplished using the methods outlined in Norfolk & Lipp, (2022). In short, a tri-parental mating assay was used to transfer a *gfp*-containing plasmid to the target *Vibrio* sp. using bacterial conjugation. In this assay, two strains of *Escherichia coli*, the helper strain carrying the conjugative plasmid pEVS104 (*tra trb* Kn^r) and the donor strain carrying the *gfp* plasmid pVSV102 (*gfp* Kn^r), were combined in culture with the target *Vibrio* under mild kanamycin stress to promote transfer of the *gfp* plasmid. Fluorescence of all transconjugant (GFP-tagged) *Vibrio* spp. was confirmed using fluorescent microscopy (Olympus BX41 Fluorescence Microscope). Working stocks of transconjugant strains were maintained at room temperature in deep agar stabs containing LBS 3% amended with 300 µg mL^{-1} kanamycin to ensure retention of the plasmid. GFP strains were maintained at -80 ^oC in a 1:1 mixture of 40% glycerol and LBS 3% broth amended with 300 µg mL^{-1} kanamycin for long-term storage.

***Artemia* Colonization**. GFP-*Vibrio* spp. were revived from -80 ^oC storage in 4 mL of LBS 3% broth amended with 300 µg mL^{-1} kanamycin and incubated at 30 ^oC with 100 rpm of shaking agitation for 18-24 h. Following incubation, 1mL of the overnight culture was pelleted by centrifugation at ~4,000 x g, the supernatant was discarded, and replaced with 1 mL of sterile 1X phosphate buffered saline (PBS). This process was repeated three times to ensure adequate removal of residual kanamycin from the culture. Concurrently, *Artemia* cultures were grown as described above. Six mL of decapsulated nauplii (~250 individuals) were transferred to each well of a sterile six-well tissue culture plate (Cellstar® 6-Well Suspension Culture Plate). Each well of

the culture plate was inoculated with 50 µL of washed GFP *V. alginolyticus* (~1.13 x 10^8 CFU), *V. harveyi* (~6.87 x 10^7 CFU), or *V. mediterranei* (~1.51 x 10^7 CFU). The *Artemia*-*Vibrio* mixture was covered and incubated at 28 ºC under 50 rpm of shaking agitation for 18 h. Following incubation, the contents of each well was collected and filtered onto a 3.0 µm polycarbonate (PCTE) membrane (Sterlitech© 47mm, 3.0µm PCTE membranes) using vacuum filtration to capture the suspended *Artemia* while allowing any non-associated *Vibrio* cells to be discarded as flow through. The *Vibrio*-colonized *Artemia* were resuspended from the membrane by vortexing for 30 s in 6 mL of sterile ASW. Colonization or apparent attachment of GFP-labeled cells to *Artemia* nauplii was confirmed using epifluorescent microscopy. Spiked *Artemia* were then homogenized (PRO Scientific®, Series 250 Homogenizer) at max speed for 120 s, and homogenate was serial diluted (10-fold) in 1X PBS and spread plated using glass rattler beads (Zymo Rattler™ Plating Beads, 4.5 mm) onto thiosulfate citrate bile salts sucrose (TCBS) agar amended with 300 µg mL^{-1} kanamycin in duplicate. The addition of kanamycin to the TCBS plates selected against any non-GFP tagged *Vibrio* cells that may have been present. TCBS plates were incubated overnight at 30 ºC. The resulting plate counts were used to calculate the approximate level of acquired dose.

Uptake by *E. pallida*. To establish a connection between ingestion and *Vibrio* uptake, a controlled feeding study was conducted to measure the level of acquired GFP-tagged *Vibrio* spp. following exposure in a microcosm. Cultures of GFP-tagged *Vibrio* spp. and *Artemia* were prepared and combined as described above in "*Artemia* Colonization" to produce spiked *Artemia*. To increase the feeding opportunity, four *Artemia* spike exposures (~250 individuals each) were combined for a total exposure of ~1,000 individuals resulting in a maximum feeding dose (assuming ingestion of all *Artemia*) of ~1.96 x10^7 CFU, ~5.89 x 10^6 CFU, and 3.04 x 10^7

CFU for *V. alginolyticus*, *V. harveyi*, and *V. mediterranei* trials, respectively (Table 2). Colonization of the spiked *Artemia* was confirmed prior to anemone feeding using fluorescent microscopy. Control *Artemia* (non-spiked) were prepared in tandem using the protocol but were inoculated with 50 µL of sterile 1X PBS instead of GFP-*Vibrio* spp.

Experimental microcosms were constructed to house the anemones during exposure trials. Microcosms were created using 18 X 12.5 X 5 cm Pyrex® dishes filled with 750 mL of sterile ASW. Each microcosm contained a submerged six well tissue culture plate to provide substrate for *E. pallida* (N = 6 per treatment). Prior to exposure, experimental *E. pallida* were transferred to the microcosm chambers and allowed to acclimate for 18 h. Anemones used in experiments were selected based on size and consisted of individuals ranging from 1.5 cm to 3 cm (at full extension) to reduce the influence of feeding bias by large or small individuals. No discolored or wilting anemones were selected (see Figure S4 for an example of healthy *E. pallida* appearance). Care was taken during anemone detachment to ensure no damage to the tentacles or oral disc occurred. All anemones were checked visually for viability following acclimatization and replaced as needed. Experimental exposures were administered as detailed in Table 2 for a duration of 3 h. For trials were *Artemia* were fed to *E. pallida*, anemones were observed for the first 20 min following exposure to visually confirm ingestion. Anemones were checked every 30 min to ensure feeding behavior was continued and to stir microcosm water (to prevent *Artemia* from congregating out of anemone reach). Following exposure, anemones were collected from the chambers, transferred into individual 50 mL conical tubes containing 40 mL of sterile ASW, and vortexed for 30 s. This process was repeated twice to remove any non-ingested GFP-*Vibrio* cells. Washed anemones were then transferred into 10 mL of sterile ASW for homogenization. 100 µL of ASW was removed prior to homogenization and spread plated with glass rattler beads

(Zymo Rattler™ Plating Beads, 4.5 mm) onto TCBS agar amended with 300 µg mL^{-1} kanamycin to ensure no ambient GFP-*Vibrio* (non-ingested) remained in the wash water (carry-over control). All anemones were then homogenized (PRO Scientific®, Series 250 Homogenizer) at max speed for 120 s. *E. pallida* homogenate was serial diluted (10-fold) in 1X PBS and spread plated with glass rattler beads onto TCBS agar amended with 300 µg mL^{-1} kanamycin, in duplicate. Plates were incubated at 30 ^{o}C for 18 h. The resulting plate counts (CFU/mL) were used to calculate the uptake of GFP-*Vibrio* cells by the anemones under each experimental condition. Culture results were summarized and visualized in Rstudio using the packages 'tidyverse' and 'readxl.' Feeding exposures were compared using a pairwise Wilcoxon rank-sum test with a Bonferroni correction for significance.

Acknowledgements.

We kindly thank Dr. Eric Stabb, for donating the helper and donor strains used to facilitate GFP tagging of the target *Vibrio* spp. We also acknowledge the work of Charlyn Shue, Rachel Phan, and Samantha Weatherly for their assistance with laboratory processing.

Literature Cited

Arboleda MDM and Reichardt WT. 2010. *Vibrio* sp. Causing *Porites* ulcerative white spot disease. *Diseases of Aquatic Organisms.* 90: 93-104.

Arotsker L, Siboni N, Ben-Dov E, Kramarsky-Winter E, Loya Y, and Kushmaro A. 2009. *Vibrio* sp. as a potentially important member of the Black Band Disease (BBD) consortium in *Favia* sp. Corals. *FEMS Microbiology Ecology.* 70(3): 515-524.

Balebona MC, Andreu MJ, Bordas MA, Zorrilla I, Moriñigo MA, and Borrego JJ. 1995. Pathogenicity of *Vibrio alginolyticus* for cultured Gilt-Head Sea Bream (*Sparus aurata*L.). *Applied and Environmental Microbiology.* 64(11): 4269-4275.

Belda-Baillie CA, Baillie BK, and Maruyama T. 2001. Specificity of a model cnidarian-dinoflagellate symbiosis. *The Biological Bulletin*. 202(1): 74-85.

Ben-Haim Y, Thompson FL, Thompson CC, Cnockaert MC, Hoste B, Swings J, and Rosenberg E. 2003. *Vibrio coralliilyticus* sp. nov., a temperature-dependent pathogen of the coral *Pocillopora damicornis. International Journal of Systematic and Evolutionary Biology.* 53(1): 309-315.

Borchardt T, Fisher KV, Ebling AM, Westrich JR, Xian P, Holmes CD, Landing WM, Lipp EK, Wetz MS, and Ottesen EA. 2020. Saharan dust deposition initiates successional patterns among marine microbes in the Western Atlantic. *Limnology and Oceanography.* 65(1): 191-203.

Brown BE and Bythell JC. 2005. Perspectives on mucus secretion in reef corals. *Marine Ecology Progress Series.* 296: 291-309.

Carli A, Pane L, Casareto L, Bertone S, and Pruzzo C. 1993. Occurrence of *Vibrio alginolyticus* in Ligurian coast rock pools (Tyrrhenian Sea, Italy) and its association with the copepod *Tigriopus fulvus* (Fisher 1860). *Applied and Environmental Microbiology.* 59(6): 1960-1962.

Certner RH, Dwyer AM, Patterson MR, and Vollmer SV. 2017. Zooplankton as a potential vector for white band disease transmission in the endangered coral, *Acropora cervicornis*. *PeerJ.* 5:e3502; DOI 10.7717/peerj.3502.

Cervino JM, Thompson FL, Gomez-Gil B, Lorence EA, Goreau TJ, Hayes RL, Winiarski-Cervino KB, Smith GW, Hughen K, and Bartels E. 2008. The *Vibrio* core group induces yellow band disease in Caribbean and Indo-Pacific reef-building corals. *Journal of Applied Microbiology.* 105(5): 1658-1671.

Colwell RR. 1996. Global climate and infectious disease: the cholera paradigm. *Science*. 274(5295): 2025-2031.

Colwell RR, Huq A, Islam MS, Aziz KMA, Yunus M, Khan NH, Mahmud A, Sack RB, Nair GB, Chakraborty J, Sack DA, and Russek-Cohen. 2003. Reduction of cholera in Bangladeshi villages by simple filtration. *PNAS*. 100(3): 1051-1055.

Cooney RP, Pantos O, Le Tissier MDA, Barer MR, O'Donnell AG, and Bythell JC. 2002. Characterization of the bacterial consortium associated with black band disease in coral using molecular microbiological techniques. *Environmental Microbiology.* 4(7): 401-413.

Eddy TD, Lam VWY, Reygondeau G, Cisneros-Montemayor AM, Greer K, Palomares MLD, Bruno JF, Ota Y, and Cheung. 2021. Global decline in capacity of coral reefs to provide ecosystem services. *One Earth*. 4(9): 1278-1285.

Erken M, Lutz C, and McDougald. 2015. Interactions of *Vibrio* spp. with zooplankton. *Microbiology Spectrum.* 3(3): https://doi.org/10.1128/microbiolspec.VE-0003-2014.

Ferrier-Pagès C, Hoogenboom M, and Houlbrèque F. 2010. The role of plankton in coral trophodynamics. In: Dubinsky Z and Stambler N (eds). *Coral Reefs: An Ecosystem in Transition*. Springer, Dordrecht. https://doi.org/10.1007/978-94-007-0114-4_15.

Gavish AR, Shapiro OH, Kramarsky-Winter E, and Vardi A. 2021. Microscale tracking of coral-vibrio interactions. *ISME Communications.* 1(18): https://doi.org/10.1038/s43705-021-00016-0.

Gil-Agudelo DL, Smith GW, Weil E. 2006. The white band disease type II pathogen in Puerto Rico. *Revista de Biología Tropical*. 54(3): 59-67.

Goulden EF, Hall MR, Bourne DG, Pereg LL, and Høj L. 2021. Pathogenicity and infection

cycle of *Vibrio owensii* in larviculture of the Ornate Spiny Lobster (*Panulirus ornatus*). *Applied and Environmental Microbiology*. 78(8): 2841-2849.

Grajales A and Rodriguez E. 2014. Morphological revision of the genus *Aiptasia* and the family *Aiptasiidae* (Cnidaria, Actiniaria, Metridioidea). *Zootaxa*. 3826(1): 55-100.

Green EP and Bruckner AW. The significance of coral disease epizootiology for coral reef conservation. *Biological Conservation*. 96(3): 347-361.

Grossart HP, Dziallas C, Leunert F, and Tang KW. 2010. Bacteria dispersal by hitchhiking on zooplankton. *PNAS*. 107(26): 11959-11964.

Hardefeldt JM and Reichelt-Brushett AJ. 2015. Unravelling the role of zooxanthellae in the uptake and depuration of an essential metal in *Exaiptasia pallida*; an experiment using a model cnidarian. *Marine Pollution Bulletin*. 96(1-2): 294-303.

Harvell CD, Kim K, Burkholder JM, Colwell RR, Epstein PR, Grimes DJ, Hofmann EE, Lipp EK, Osterhaus ADME, Overstreet RM, Porter JW, Smith GW, and Vasta GR. 1999. Emerging marine diseases—Climate links and anthropogenic factors. *Science*. 285(5433): 1505-1510.

Harvell CD, Jordán-Dahlgren E, Merkel S, Rosenberg E, Raymundo L, Smith G, Weil E, and Willis B. 2007. Coral disease, environmental drivers, and the balance between coral and microbial associates. *Oceanography*, 20 (1): 172-195.

Heidelberg JF, Heidelberg KB, and Colwell RR. 2002. Bacteria of the γ-subclass *Proteobacteria* associated with zooplankton in Chesapeake Bay. *Applied and Environmental Microbiology*. 68(11): 5498-5507.

Hoegh-Guldberg O, Pendleton L, and Kaup A. People and the changing nature of coral reefs.

Regional Studies in Marine Science. 30: 100699. https://doi.org/10.1016/j.rsma.2019.100699.

Houlbrèque F and Ferrier-Pagès C. 2009. Heterotrophy in tropical scleractinian corals. *Biological Reviews.* 84(1): 1-17.

Hunt DE, Gevers D, Vahora NM, and Polz MF. 2008. Conservation of the chitin utilization pathway in the *Vibrionaceae*. *Applied and Environmental Microbiology.* 74(1): 44-51.

Huq A, Small EB, West PA, Huq MI, Rahman R, and Colwell RR. 1983. Ecological relationships between *Vibrio cholerae* and planktonic crustacean copepods. *Applied and Environmental Microbiology*. 45(1): 275-283.

Huq A, Xu B, Chowdhury MAR, Islam MS, Montilla R, and Colwell RR. 1996. A simple filtration method to remove plankton-associated *Vibrio cholerae* in raw water supplies in developing countries. *Applied and Environmental Microbiology.* 62(7): 2508-2512.

Jones GP, McCormick M, Srinivasan M, and Eagle JV. 2004. Coral decline threatens fish biodiversity in marine reserves. *PNAS*. 101(21): 8251-8253.

Kaneko T and Colwell RR. 1997. The annual cycle of *Vibrio Parahaemolyticus* in Chesapeake bay. *Microbial Ecology*. 4: 135-155.

Karunasagar I, Pai R, Malathi GR, and Karunasagar I. 1994. Mass mortality of *Penaeus monod*on larvae due to antibiotic-resistant *Vibrio harveyi* infection. *Aquaculture.* 128(3-4): 203-209.

Kemp KM, Westrich JR, Alabady MS, Edwards ML, and Lipp EK. 2018. Abundance and multilocus sequence analysis of *Vibrio* bacteria associated with diseased elkhorn coral (*Acropora palmata*) of the Florida Keys. *Applied and Environmental Microbiology.* 84(2): e01035-17. 10.1128/AEM.01035-17.

Kushmaro A, Banin E, Loya Y, Stackebrandt E, and Rosenberg E. 2001. *Vibrio shiloi* sp. nov., the causative agent of bleaching of the coral *Oculina patagonica*. *International Journal of Systematic and Evolutionary Microbiology.* 51: 1383-1388.

Liang J, Liu J, Wang X, Lin H, Liu J, Zhou S, Sun H, and Zhang XH. 2019. Spatiotemporal dynamics of free-living and particle-associated *Vibrio* communities in the Northern Chinese marginal seas. *Applied and Environmental Microbiology.* 85(9): e00217-19. https://doi.org/10.1128/AEM.00217-19.

Nelson EJ, Harris JB, Morris JG Jr, Calderwood SB, Camilli A. 2009. Cholera transmission: the host, pathogen and bacteriophage dynamic. *Nature Reviews Microbiology*. 7:693-702.

Norfolk WA and Lipp EK. 2022. Use an evaluation of a pES213-derived plasmid for the constitutive expression of *gfp* protein in pathogenic vibrios: a tagging tool for *in vitro* studies. *Microbiology Spectrum.* e02490-22.

Macro Luna G, Bongiorni L, Gili C, Biavasco F, and Danovaro. 2010. *Vibrio harveyi* as a causative agent of the White Syndrome in tropical stony corals. *Environmental Microbiology Reports.* 2(1): 120-127.

Main CR, Salvitti LR, Whereat EB, and Coyne KJ. 2015. Community-level and species-specific associations between phytoplankton and particle-associated *Vibrio* species in Delaware's inland bays. *Applied and Environmental Microbiology.* 81(17): 5703-5713.

Magny GC, Mozumder PK, Grim CJ, Hasan NA, Naser MN, Alam M, Sack RB, Huq A, and Colwell RR. 2011. Role of zooplankton diversity in *Vibrio cholerae* population dynamics and in the incidence of cholera in the Bangladesh Sundarbans. *Applied and Environmental Microbiology.* 77(17): 6125-6132.

Martinez-Urtaza J, Blanco-Abad V, Rodriguez-Castro A, Ansede-Bermejo J, Miranda A, and

Rodriguez-Alvarez. 2011. Ecological determinants of the occurrence and dynamics of *Vibrio parahaemolyticus* in offshore areas. *The ISME Journal*. 6: 994-1006. https://doi.org/10.1038/ismej.2011.156.

Matz C, McDougald D, Moreno AM, and Kjelleberg S. 2005. Biofilm formation and phenotypic variation enhance predation-driven persistence of *Vibrio cholerae*. *PNAS*. 102(46): 16819-16824.

Meyer JL, Castellanos-Gell J, Aeby GS, Häse CC, Ushijima B, and Paul VJ. 2019. Microbial community shifts associated with the ongoing stony coral tissue loss disease outbreak on the Florida reef tract. *Frontiers in Microbiology.* 10: 10.3389/fmicb.2019.02244.

Montilla LM, Ascanio A, Verde A, and Croquer A. 2019. Systematic review and meta-analysis of 50 years of coral disease research visualized through the scope of network theory. *PeerJ.* 7:e7041 http://doi.org/10.7717/peerj.7041.

Munn CB. 2015. The role of vibrios in diseases of corals. *Microbiology Spectrum.* 3(4): https://doi.org/10.1128/microbiolspec.VE-0006-2014.

Porter JW, Dustan P, Jaap WC, Patterson KL, Kosmynin V, Meier OW, Patterson ME, and Parsons M. 2001. Patterns of spread of coral disease in the Florida Keys. In: Porter, J.W. (eds) *The Ecology and Etiology of Newly Emerging Marine Diseases. Developments in Hydrobiology*, vol 159. Springer, Dordrecht. https://doi.org/10.1007/978-94-017-3284-0_1.

Pratchett MS, Thompson CA, Hoey AS, Cowman PF, and Wilson SK. 2018. Effects of coral bleaching and coral loss on the structure and function of reef fish assemblages. In: van Oppen, M., Lough, J. (eds) *Coral Bleaching. Ecological Studies*, vol 233. Springer, Cham. https://doi.org/10.1007/978-3-319-75393-5_11.

Press CMcL and Lillehaug A. 1995. Vaccination in European salmonid aquaculture: A review of practices and prospects. *British Veterinary Journal*. 151(1): 45-69.

Pruzzo C, Vezzulli L, and Colwell RR. 2008. Global impact of *Vibrio cholerae* interactions with chitin. *Environmental Microbiology*. 10(6): 1400-1410.

Rawlings TK, Ruiz GM, and Colwell RR. 2007. Association of *Vibrio cholerae* O1 El Tor and O139 Bengal with the copepods *Acartia tonsa* and *Eurytemora affinis*. *Applied and Environmental Microbiology*. 73(24): 7926-7933.

Reshef L, Koren O, Loya Y, Zilber-Rosenberg I, and Rosenberg E. 2006. The coral probiotic hypothesis. *Environmental Microbiology.* 8(12): 2068-2073.

Ritchie KB and Smith GW. 1998. Type II White-Band Disease. *Revista de Biologica Tropical*. 46(5):199–203.

Ritchie KB. 2006. Regulation of microbial populations by coral surface mucus and mucus-associated bacteria. *Marine Ecology Progress Series.* 322: 1-14.

Rohwer F, Seguritan V, Azam F, and Knowlton N. 2002. Diversity and distribution of coral-associated bacteria. *Marine Ecology Progress Series.* 243: 1-10

Rosenberg E, Koren O, Reshef L, Efrony R, and Zilber-Rosenberg I. 2007. The role of microorganisms in coral health, disease and evolution. *Nature Reviews Microbiology.* 5: 355-362. https://doi.org/10.1038/nrmicro1635.

Rubio-Portillo E, Yarza P, Peñalver C, Ramos-Esplá AA, and Antón J. 2014. New insights into *Oculina patagonica* coral diseases and their associated *Vibrio* spp. communities. *The ISME Journal.* 8: 1794-1807. https://doi.org/10.1038/ismej.2014.33.

Shapiro OH, Fernandez VI, Garren M, Guasto JS, Debaillon-Vesque FP, Kranarsky-Winter E,

Vardi A, Stocker R. 2014. Vortical ciliary flows actively enhance mass transport in reef corals. *PNAS.* 111(37): 13391-13396.

Shnit-Orland M and Kushmaro A. 2009. Coral mucus-associated bacteria: a possible first line of defense. *FEMS Microbiology Ecology*. 67(3): 371-380.

Shore-Maggio A, Aeby GS, and Callahan SM. 2018. Influence of salinity and sedimentation on *Vibrio* infection of the Hawaiian coral *Montipora capitata*. *Diseases of Aquatic Organisms.* 128: 63-71.

Shore A and Cadwell JM. 2019. Modes of coral disease transmission: how do diseases spread between individuals and among populations? *Marine Biology.* 166(45): https://doi.org/10.1007/s00227-019-3490-8.

Sugumar V and Munuswamy N. 2006. Ultrastructure of cyst shell and underlying membranes of three strains of the brine shrimp Artemia (Branchiopoda: Anostraca) from South India. *Microscopy Research and Technique.* 69(12): 957-963.

Sunagawa S, Wilson EC, Thaler M, Smith ML, Caruso C, Pringle JR, Weis VM, Medina M, and Schwarz. 2009. Generation and analysis of transcriptomic resources for a model system on the rise: the sea anemone *Aiptasia pallida* and its dinoflagellate endosymbiont. *BMC Genomics*. 10(258): https://doi.org/10.1186/1471-2164-10-258.

Sussman M, Willis BL, Victor S, Bourne DG. 2008. Coral pathogens identified for White Syndrome (WS) epizootics in the Indo-Pacific. PLOS ONE 3(6): e2393. https://doi.org/10.1371/journal.pone.0002393.

Sweet M and Bythell. 2015. White Syndrome in *Acropora* muricata: Nonspecific bacterial infection and ciliate histophagy. *Molecular Ecology.* 24(5): 1150-1159. https://doi.org/10.1111/mec.13097.

Takemura AF, Chien DM, and Polz MF. 2014. Associations and dynamics of Vibrionaceae in the environment, from the genus to the population level. *Frontiers in Microbiology*. 5(38): https://doi.org/10.3389/fmicb.2014.00038.

Tamplin ML, Gauzens AL, Huq A, Sack DA, and Colwell RR. 1990. Attachment of *Vibrio cholerae* serogroup O1 to zooplankton and phytoplankton of Bangladesh waters. *Applied and Environmental Microbiology*. 56(6): 1977-1980.

Teplitski M and Ritchie KB. 2009. How feasible is the biological control of coral diseases? *Trends in Ecology and Evolution*. 24(7): 378-385.

Thompson FL, Hoste B, Thompson CC, Huys G, and Swings J. 2001. The coral bleaching *Vibrio shiloi* Kushmaro et al. 2001 is a later synonym of *Vibrio mediterranei* Pujalte and Garay 1986. *Systematic and Applied Microbiology.* 24(4): 516-519.

Thompson FL, Iida T, and Swings J. 2004. Biodiversity of vibrios. *Microbiology and Molecular Biology Reviews*. 68(1): 403-431.

Thompson JR, Rivera HE, Closek CJ, and Medina M. 2014. Microbes in the coral holobiont: partners through evolution, development, and ecological interactions. *Frontiers in Cellular and Infection Microbiology.* 4(176): doi: 10.3389/fcimb.2014.00176.

Turner JW, Good B, Cole D, and Lipp EK. 2009. Plankton composition and environmental factors contribute to *Vibrio* seasonality. *The ISME Journal*. 3: 1082-1092. https://doi.org/10.1038/ismej.2009.50.

Ushijima B, Smith A, Aeby GS, and Callahan SM. 2012. *Vibrio owensii* induces the tissue loss disease *Montipora* White Syndrome in the Hawaiian reef coral *Montipora capitata*. *PLOS ONE*. 7(10): e46717. https://doi.org/10.1371/journal.pone.0046717.

Ushijima B, Videau P, Burder AH, Shore-Maggio A, Runyon CM, Sudek M, Aeby GS, and

Callahan SM. 2014. *Vibrio coralliilyticus* strain OCN008 is an etiological agent of acute *Montipora* white syndrome. *Applied and Environmental Microbiology.* 80(7): 2102-2109. https://doi.org/10.1128/AEM.03463-13.

Urakawa H and Rivera ING. 2006. Aquatic Environment. In Thompson FL, Austin B, and Swings J (eds). *The Biology of Vibrios*. 175-189. Washington D.C., ASM Press.

Warner AH, Beers PC, and Huang FL. 1973. Biosynthesis of the diguanosine nucleotides. I. purification and properties of an enzyme from yolk platelets of brine shrimp embryos. *Canadian Journal of Biochemistry.* 52(3): 231-24.

Weis VM, Davy SK, Hoegh-Guldberg O, Rodriguez-Lanetty M, and Pringle JR. Cell biology in model systems as the key to understanding corals. *Trends in Ecology and Evolution*. 23(7): 369-376.

Westrich JR, Ebling AM, Landing WM, and Lipp EK. 2016. Saharan dust nutrients promote *Vibrio* bloom formation in marine surface waters. *PNAS*. 113(21): 5964-5969.

Westrich JR, Griffin DW, Westphal DL, and Lipp EK. 2018. *Vibrio* population dynamics in mid-Atlantic surface waters during Saharan dust events. *Frontiers in Marine Science.* 5(12): https://doi.org/10.3389/fmars.2018.00012.

Wild C, Hoegh-Guldberg O, Naumann MS, Colombo-Pallotta MF, Ateweberhan M, Fitt WK, Iglesias-Prieto R, Palmer C, Bythell JC, Ortiz JC, Loya Y, and van Woesik. 2011. Climate change impedes scleractinian corals as primary reef ecosystem engineers. *Marine and Freshwater Research*. 62(2): 205-215.

Worden AZ, Seidel M, Smriga S, Wick A, Malfatti F, Bartlett D, and Azam F. 2006. Trophic regulation of *Vibrio cholerae* in coastal marine waters. *Environmental Microbiology.* 8(1): 21-29.

Zhenyu X, Shaowen K, Chaoqun H, Zhixiong Z, Shifeng W, and Youngcan Z. 2013. First characterization of bacterial pathogen, *Vibrio alginolyticus*, for *Porites andrewsi* white syndrome in the South China Sea. PLOS ONE 8(9): e75425. https://doi.org/10.1371/journal.pone.0075425.

Zhou J, Fang W, Yang X, Zhou S, Hu L, Li X, Qi X, Su H, and Xie L. 2012. A nonluminescent and highly virulent *Vibrio harveyi* strain is associated with "Bacterial White Tail Disease" of *Litopenaeus vannamei* shrimp. *PLOS ONE.* 7(2): e29961. https://doi.org/10.1371/journal.pone.0029961

Tables and Figures

Table 1: Published occurrences of *Vibrio* spp. as causative or putative agents of coral disease. Data organized by species. Recognized synonyms listed below. Updated from Kemp et al. (2018).

***Vibrio* spp.**	**Disease Type**	**Disease Name or Description**	**Affected Host**	**Citation(s)**
Vibrio coralliilyticus	White disease[a]	Bacterial bleaching disease	*Pocillopora damicornis* and *Oculina patagonica*	(Ben-Haim et al., 2003) (Rubio-Portillo et al., 2014)
		Montipora white syndrome[b]	*Montipora capitata*	(Ushijima et al., 2014) (Shore-Maggio et al., 2018)
		Indo-Pacific white syndrome[b]	*Acropora cytherea, Montipora aequituberculata,* and *Pachyseris speciosa.*	(Sussman et al., 2008)
Vibrio mediterranei (*Vibrio shiloi*)	White disease[a]	Bacterial bleaching disease	*Oculina patagonica*	(Kushmaro et al., 2001) (Thompson et al., 2001)
Vibrio harveyi (*Vibrio charchariae*)	White disease[a]	White band disease	*Acropora cervicornis*	(Ritchie & Smith, 1998) (Gil-Agudelo et al., 2006)
		White syndrome[b]	*Pocillopora damicornis* and *Acropora* spp.	(Marco Luna et al., 2010)
	Yellow disease	Yellow band disease[c]	*Orbicella faveolata*	(Cervino et al., 2008)

Vibrio alginolyticus	White disease[a]	*Porites andrews*i white syndrome	*Porites andrewsi*	(Zhenyu et al., 2013)
	Yellow disease	Yellow band disease[c]	*Orbicella faveolata*	(Cervino et al., 2008)
Vibrio natriegens	White disease[a]	*Porites* ulcerative white spot disease	*Porites cylindrica*	(Arboleda & Reichardt, 2010)
Vibrio owensii	White disease[a]	*Montipora* White Syndrome[b]	*Montipora capitata*	(Ushijima et al., 2012) (Shore-Maggio et al., 2018)
Vibrio parahaemolyticus	White disease[a]	*Porites* ulcerative white spot disease	*Porites cylindrica*	(Arboleda & Reichardt, 2010)
Vibrio rotiferianus	Yellow disease	Yellow band disease[c]	*Orbicella faveolata*	(Cervino et al., 2008)
Vibrio tubiashii	White disease[a]	White syndrome[b]	*Acropora muricata*	(Sweet & Bythell, 2015)
Vibrio proteolyticus	Yellow disease	Yellow band disease[c]	*Orbicella faveolata*	(Cervino et al., 2008)
Unspecified *Vibrio* spp.	Black disease	Black band disease[b]	*Favia* spp.	(Arotsker et al., 2009)
	White disease[a]	Stony coral tissue loss disease[b]	*Montastraea cavernosa*, *Orbicella faveolata*, *Diploria labyrinthiformis*, and *Dichocoenia stokesii*	(Meyer et al., 2019)

[a]Described by different authors under the names white, syndrome, pox, and/or band disease.

Disease signs are manifestations of coral tissue loss and/or zooxanthellae loss or bleaching.

[b]Associated as a part of a bacterial consortium suspected to contain non-*Vibrio* species.

[c]Associated as a part of a bacterial consortium suspected to contain multiple *Vibrio* spp.

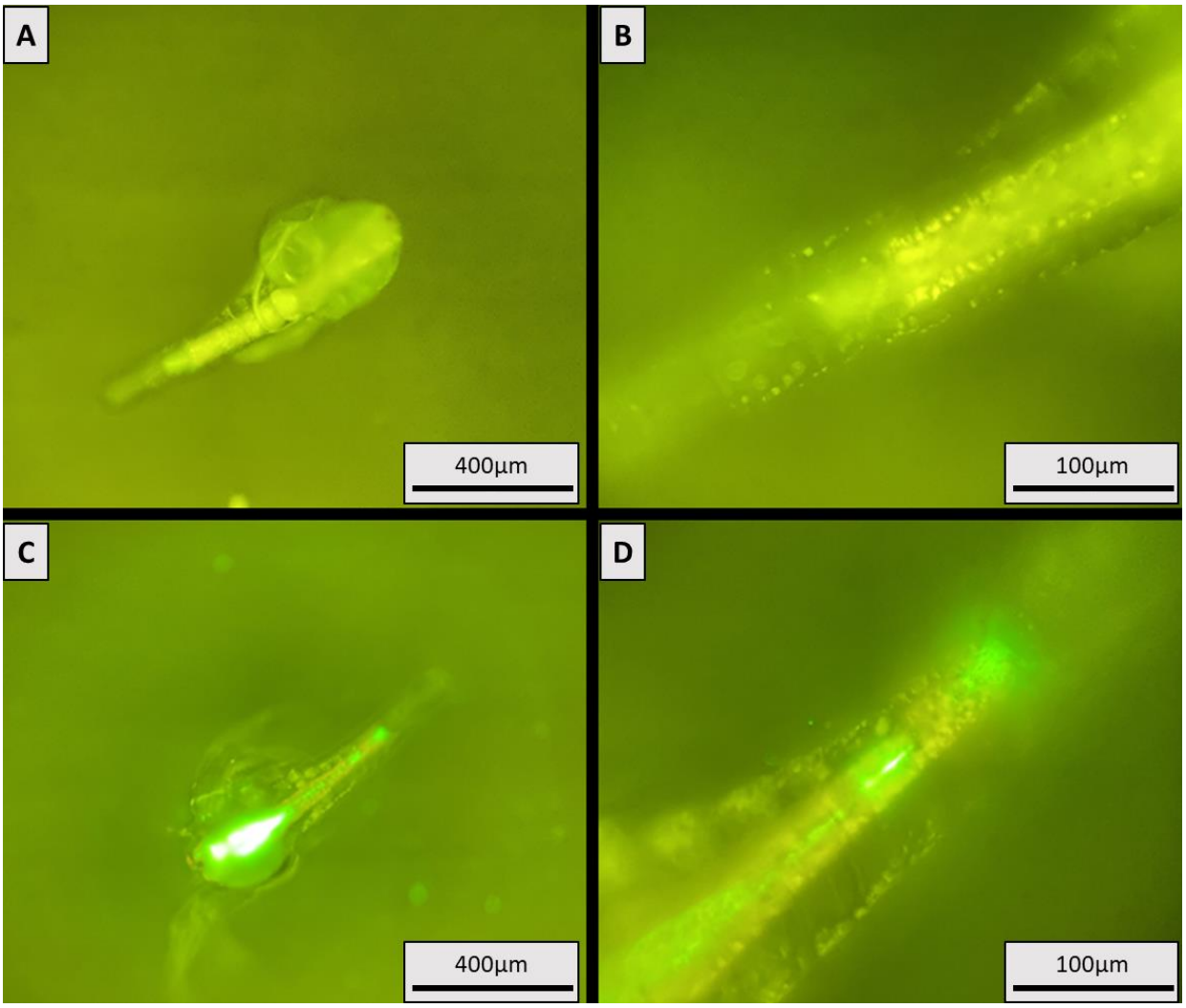

Figure 1: GFP *V. alginolyticus* colonization of *Artemia*. Cultures inoculated with ~1.13 x 10^8 CFU. Photos taken after 18 h of exposure. (A) Unexposed *Artemia* at 100X magnification. (B) Unexposed *Artemia* posterior at 400X magnification. (C) Exposed *Artemia* at 100X magnification. (D) Exposed *Artemia* posterior at 400X magnification. Bright green fluorescence indicates GFP *V. alginolyticus* presence. *Artemia* tissue appears yellow green.

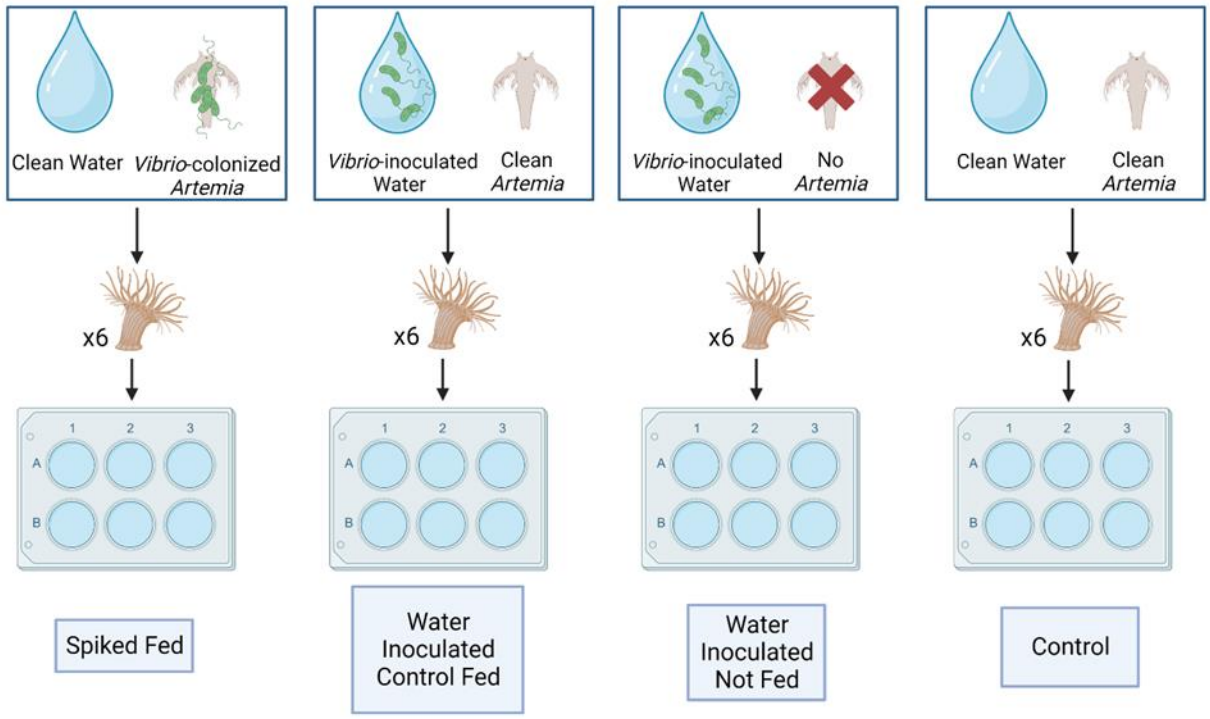

Figure 2: Feeding trial treatments used to expose *E. pallida* to GFP-*Vibrio*. *Artemia* administered at a concentration of ~1,000 individuals (when added). GFP-*Vibrio* administered at concentrations designated in Table 2.

Table 2: GFP-*Vibrio* spp. dosing patterns, *Artemia* acquisition efficacy, *Vibrio* exposure concentration, and recovered CFU from anemone homogenate. For each experimental trial ~1000 *Artemia* (individuals) and 6 anemones (individuals) were exposed.

***Vibrio* spp.**	**Treatment Name**	**Total GFP-*Vibrio* spp. Exposed to *Artemia* (CFU)[a]**	**Mean GFP-*Vibrio* spp. Carried by *Artemia* (CFU/~1000 *Artemia*)[b]**	**Total GFP-*Vibrio* spp. Inoculated into Microcosm Water (CFU)[a]**	**Mean GFP-*Vibrio* spp. Recovered from *E. pallida* Homogenate (CFU mL^{-1})**
V. alginolyticus	Spiked fed	4.53×10^8	$1.96 \times 10^7 \pm 5.60 \times 10^5$	*NA*	$6.92 \times 10^4 \pm 7.48 \times 10^3$
V. alginolyticus	Water exposed control fed	*NA*	*NA*	4.53×10^8	$3.33 \times 10^2 \pm 1.02 \times 10^2$
V. alginolyticus	Water exposed not fed	*NA*	*NA*	4.53×10^8	$8.33 \times 10^1 \pm 4.00 \times 10^1$
V. alginolyticus	Control	*NA*	*NA*	*NA*	0.00 ± 0.00
V. harveyi	Spiked fed	2.75×10^8	$5.89 \times 10^6 \pm 2.56 \times 10^5$	*NA*	$2.59 \times 10^5 \pm 1.12 \times 10^5$
V. harveyi	Water exposed control fed	*NA*	*NA*	2.75×10^8	$4.10 \times 10^3 \pm 1.61 \times 10^3$
V. harveyi	Water exposed not fed	*NA*	*NA*	2.75×10^8	$8.33 \times 10^1 \pm 5.43 \times 10^1$
V. harveyi	Control	*NA*	*NA*	*NA*	0.00 ± 0.00
V. mediterranei	Spiked fed	6.05×10^7	$3.04 \times 10^7 \pm 7.06 \times 10^5$	*NA*	$1.67 \times 10^5 \pm 5.88 \times 10^4$
V. mediterranei	Water exposed control fed	*NA*	*NA*	6.05×10^7	$5.90 \times 10^3 \pm 1.38 \times 10^3$
V. mediterranei	Water exposed not fed	*NA*	*NA*	6.05×10^7	$3.83 \times 10^2 \pm 1.51 \times 10^2$
V. mediterranei	Control	*NA*	*NA*	*NA*	0.00 ± 0.00

[a]Total GFP-*Vibrio* exposure represents the CFU concentration introduced to *Artemia* to promote colonization this was calculated during *Artemia* dose assessment as the sum of four exposure trials (~250 *Artemia* each). Initial exposures were administered at 1.13×10^8, 6.87×10^7, and 1.51×10^7 CFU/~250 *Artemia* for *V. alginolyticus*, *V. harveyi*, and *V. mediterranei*, respectively. Water exposure trials were inoculated directly into the microcosm using the same concentration.

[b]Total GFP-*Vibrio* carried by *Artemia* represents the CFU concentration acquired by *Artemia* following exposure. This was calculated during *Artemia* dose assessment as the sum of four exposure trials (~250 *Artemia* each). Exposures resulted in an *Artemia*-acquired dose of 4.90×10^6, 1.47×10^6, and 7.59×10^6 CFU/~250 *Artemia* for *V. alginolyticus*, *V. harveyi*, and *V. mediterranei*, respectively.

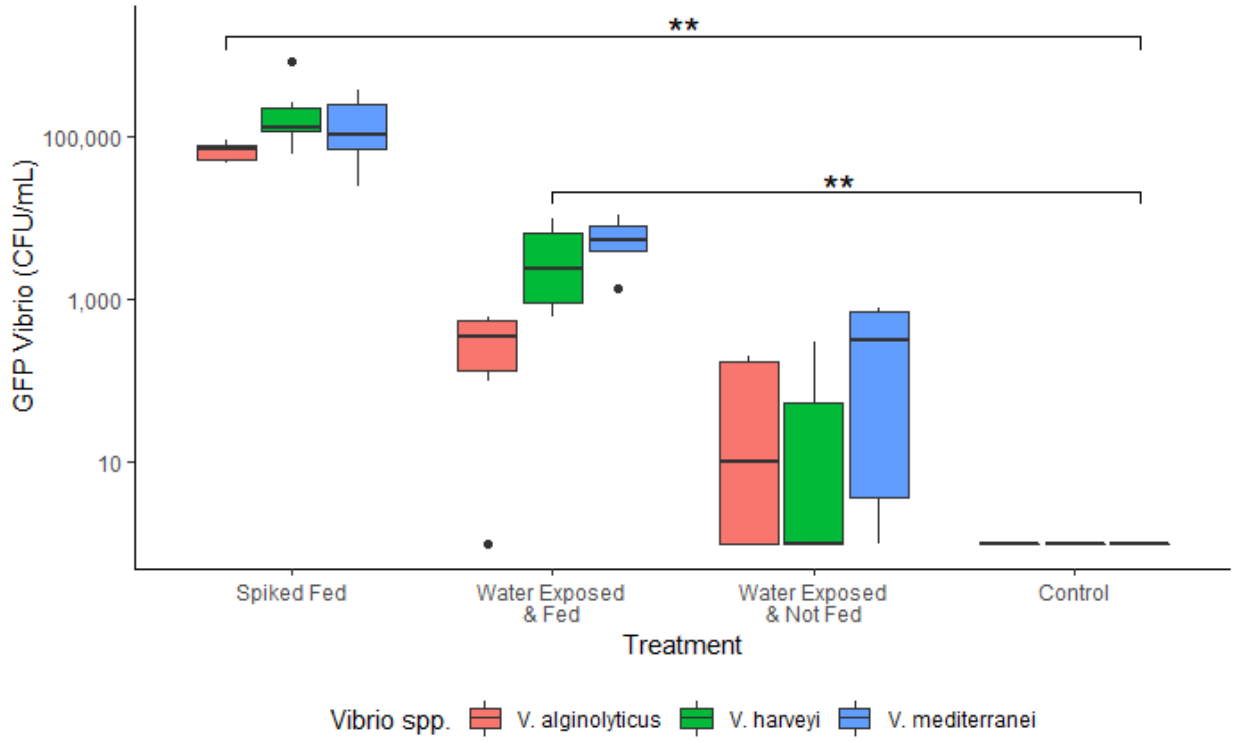

Figure 3: Recovered GFP-*Vibrio* spp. concentrations from anemone homogenate following completion of the controlled feeding study. Spiked fed anemones demonstrated a significantly greater GFP-*Vibrio* spp. burden compared to water exposed individuals. Spiked fed versus water exposed and fed resulted in p-values of 0.03, 0.013, and 0.013 and spiked fed versus water exposed not fed resulted in p-values of 0.0047, 0.0043, and 0.0049 for *V. alginolyticus*, *V. harveyi*, and *V. mediterranei*, respectively. N = 6 anemones for each exposure type and *Vibrio* spp.

CHAPTER 6

VIBRIO ALGINOLYTICUS PHYSIOLOGY AND THE ROLE OF IRON

Norfolk WA, Shue C, Henderson WM, Glinski DA, and Lipp EK. To be submitted to *Microbiology Spectrum*.

Abstract

Vibrio alginolyticus is a naturally occurring marine bacterium recognized as an emerging pathogen of both humans and animals. As an opportunistic pathogen, *V. alginolyticus* infection risk is often a function of its abundance in the environment, which is inherently limited by the abiotic conditions of the ecosystem. Here we evaluate the effects of temperature, salinity, and iron conditions on the specific growth response of three *V. alginolyticus* strains. A combination of growth kinetics and gas chromatography mass spectrometry-based metabolomics were used to evaluate the optimal and tolerable ranges of growth and to characterize the metabolic effects of iron deprivation and supplementation, respectively. All *V. alginolyticus* strains tested demonstrated broad temperature and salinity tolerance, resulting in growth at all measured temperatures (24-40 ^{o}C) and salinities between 1-6% (w/v) NaCl with optimal growth (fastest doubling time) between 30-36 ^{o}C and 2-4% NaCl. Environmental strains showed no growth limitation at iron concentrations ranging from 0.5-20 µM but produced suboptimal growth at 0.2 µM. Metabolomic assessment was consistent with growth kinetics, showing an increased number of significantly upregulated metabolites in *V. alginolyticus* cultures grown in iron replete (4 µM) media versus iron deficient (~0 µM). Detected metabolites were associated with key metabolic pathways namely, amino acid, carbohydrate, lipid and nucleotide metabolism suggesting that iron availability facilitates broad activation of *V. alginolyticus* metabolism. Combined, these data demonstrate the importance of increased temperature, stable salinity, and abundant iron as key determinants of *V. alginolyticus* abundance and risk.

Importance

Vibrio spp. are considered conditionally rare taxa in marine surface waters, comprising ~1% of the total pelagic bacterioplankton population in most systems. However, under favorable

environmental conditions these populations can increase by orders of magnitude which can consequently increase the risk of exposure/infection for opportunistic pathogens such as *V. alginolyticus*. Prior research has established the critical importance of temperature and salinity for the determination of *V. alginolyticus* abundance. However, in tropical/subtropical waters where these parameters are widely tolerable, additional environmental determinants can be critical in controlling the abundance of this species. Here we confirm the tolerance of temperature and salinity and demonstrate the importance of iron availability as a key factor for *V. alginolyticus* growth in the absence of thermal or osmotic stress. The results of this research highlight the importance of episodic iron input as a crucial metric to consider for the assessment of *V. alginolyticus* risk.

Introduction

Vibrio alginolyticus is a ubiquitous marine bacterium native to coastal and estuarine waters worldwide. An opportunistic pathogen, this bacterium is an important agent of both human and animal disease affecting a broad range of host species including marine fishes (Colorni et al., 1981; Zorrilla et al., 2003), crustaceans (Lightner & Lewis, 1975; Selvin & Lipton, 2003), mollusks (Gómez-León et al., 2005), echinoderms (Fahmy & Hamed, 2022), corals (Cervino et al., 2008; Zhenyu et al., 2013), marine mammals (Schroeder et al., 1985), sea turtles (Glazebrook & Campbell, 1990), and humans (Silfka et al., 2011; Weis et al., 2011). Animal infections have been widely described in association with the aquaculture industry and range in severity with disease signs manifesting as mild epidermal lesions (Schroeder et al., 1985) to systemic organ dysfunction and hemorrhage often leading to mass mortality (Selvin & Lipton, 2003; Zorrilla et al., 2003). Human infections are strongly associated with recreational and/or occupational exposure to seawater and manifest primarily as opportunistic infections of

the ears and preexisting or sustained wounds (Silfka et al., 2011; Weis et al., 2011). While often severe in aquaculture settings, human infections are typically non-life threatening, presenting as self-limiting or readily curable through the administration of antibiotics such as ciprofloxacin and tetracycline (Dechet et al., 2008; Zhou et al., 2021). However, infections in immunocompromised patients have been shown to progress to invasive conditions such as bacteremia and sepsis, greatly increasing the chance of mortality (English & Lindberg, 1977; Silfka et al., 2011). Collectively, the burden of *V. alginolyticus* infections imposes a substantial economic and regulatory encumbrance to aquaculture and public health with annual cost estimates in excess of 1 million dollars (USD) for the treatment of human infections in the United States (Ralston et al., 2011) and a global estimated cost of 3 billion dollars (USD) for the treatment/culling of *Vibrio* spp. aquaculture outbreaks (of which *V. alginolyticus* is a major contributor) (Sanches-Fernandes, et al., 2022).

As natural component of the marine microbial community, environmental factors that enhance or inhibit the growth of *V. alginolyticus* populations are critical to the estimation of exposure risk for this species. Prior studies have shown that temperature and salinity are the two leading environmental determinants of most *Vibrio* populations (Takemura et al., 2014; Main et al., 2015) and that increased temperature positively correlates with increased *Vibrio* abundance (Maeda et al., 2003; Oberbeckmann et al., 2011a; Böer et al., 2013; Froelich et al., 2013; Takemura et al., 2014). This correlation has been corroborated for *V. alginolyticus* specifically (Oberbeckmann et al., 2011b; Huehn et al., 2014), and provides justification for the strong seasonality of infections associated with warmer months (Hlady & Klontz, 1996; Weis et al., 2011). *V. alginolyticus* can tolerate temperatures ranging from 5-42 ^{o}C with faster growth typically occurring between 22-37 ^{o}C and optimal growth (fastest growth rate) at 35 ±2 ^{o}C

(Horie et al., 1966; Farid & Larson, 1981; Benediktsdóttir et al., 1998; Gu et al., 2016; Sheikh et al., 2022). This expansive growth range suggests that *V. alginolyticus* is amenable to the temperatures of most coastal waters with populations predominately limited by seasonal cooling, particularly in temperate regions. Second to temperature, salinity is a critical factor for the establishment of *Vibrio* spp. range. Unlike temperature, *Vibrio* salinity tolerance is more variable by species where optimal salinities range from 0-5 for low salinity adapted species such as *V. cholerae* and *V. mimicus* (Singleton et al., 1982; Chowdhury et al., 1989), 5-10 for moderate tolerance species such as *V. vulnificus* (Randa et al., 2004), and 30-35 for high salinity species such as *V. parahaemolyticus* (Liu et al., 2016). Assessment of *V. alginolyticus* has shown a wide range of salinity tolerance from 0.5-6 with optimal growth occurring at 30-35 (Sheikh et al., 2022). This range suggests that *V. alginolyticus* is broadly tolerable of coastal/estuarine water salinity and may only be limited by the presence of freshwater or atypical hypersaline environments.

While the importance of temperature and salinity has been established, the natural conditions of subtropical/tropical coastal waters rest well within the tolerable limits for this species and thus are unlikely to be major limiting factors in these regions. Consequently, additional environmental parameters may play a stronger role in the determination of *V. alginolyticus* populations in these systems. Prior studies have shown that iron availability, chlorophyll *a*, nitrogen, phosphorus, plankton abundance, pH, dissolved organic carbon, and dissolved oxygen play smaller, but important, roles influencing the structure of local *Vibrio* communities (Thompson et al., 2004; Eiler et al., 2006; Hsieh et al., 2007; Turner et al., 2009; Asplund et al., 2011). Of note from this group is the role of iron. Iron is an essential cofactor for bacterial metabolism that is often limiting in marine waters (Westrich et al., 2018; Westrich et

al., 2016). Prior research has established the importance of episodic iron input for the enrichment of *Vibrio* spp. populations during Saharan dust deposition events (Westrich et al., 2016). During these events, aerosolized ferric (Fe^{3+}) and ferrous (Fe^{2+}) iron is transported from Northern Africa via the Atlantic trade winds and deposited into the oligotrophic waters of the Southeastern United States and the Gulf of Mexico (Duce & Tindale, 1991; Westrich et al., 2016; Borchardt et al., 2020). Microbial community surveys have shown that these events trigger a substantial increase in the relative and absolute abundance of *Vibrio* in the microbial population which can swell to 5-30x the background concentration for 24-72 h following the onset of deposition (Westrich et al., 2016, Westrich et al., 2018; Borchardt et al., 2020). Termed "*Vibrio* blooms," these events have the potential to increase the risk of exposure to opportunistic *Vibrio* spp. pathogens, including *V. alginolyticus,* and are important understudied factors to consider for risk characterization.

In addition to facilitating population growth, iron acquisition is an important characteristic of virulence for *V. alginolyticus* (Wang et al., 2008). Due to the scarcity of biologically available iron in coastal waters, *V. alginolyticus* has developed a sophisticated iron acquisition system designed to compete for and scavenge iron from the ambient environment. The two major factors that comprise this system are siderophores and the TonB energy transduction system (Wang et al., 2008; Kuehl & Crosa, 2010; Kustusch et al., 2011). Siderophores are small molecular weight compounds that have a high affinity to chelate ferric iron. These compounds are secreted extracellularly where they bind ambient iron and are recognized by outer membrane proteins (Escolar et al., 1999; Kuehl & Crosa, 2010; Lv et al., 2020). Ferrisiderophore complexes are internalized via TonB, a transmembrane protein system that facilitates transfer of energy from the inner cell membrane to the outer cell membrane

enabling active transport (Wang et al., 2008; Kuehl & Crosa, 2010). While these systems enhance the competitiveness of *V. alginolyticus* in environmental settings, they also contribute to its proliferation during infection by outcompeting host iron sequestration mechanisms or directly scavenging iron from heme in blood cells (Wang et al., 2008; Kustusch et al., 2011). Scavenging of host-derived iron leads to increased bacterial replication resulting in *V. alginolyticus* persistence and increased severity of infection (Kustusch et al., 2011). Despite this importance, the relationship between iron content and *V. alginolyticus* growth and metabolism is poorly understood and there is substantial need for baseline characterization.

Here we investigate the physiology of *V. alginolyticus* across strain types in response to temperature, salinity, and iron concentrations to better understand how these factors can influence the abundance of this bacterium. The effect(s) of each of these abiotic determinants on population growth was evaluated using growth kinetics to establish an optimal and tolerable range. Growth evaluations were preformed using three *V. alginolyticus* strains, two environmental strains JW16-551 and JW16-580 from marine surface water and the American Type Culture Collection (ATCC) type strain ATCC 17749. Metabolic response of iron stimulation was further evaluated for one strain (JW16-551) using gas chromatography mass spectrometry (GC-MS)-based metabolomic profiling. In these studies, metabolomics was used to compare the biochemical profiles of *V. alginolyticus* cultures grown in iron replete (4 µM) and iron deficient (~0 µM) conditions for starved (deprived of iron for 5 d prior to the start of the experiment) and non-starved (not deprived of iron) cultures to determine the effects of iron stimulation on metabolic pathways.

Results

The results of growth kinetics experiments demonstrated the optimal and tolerable limits of temperature, salinity, and iron concentration for the growth of *V. alginolyticus*. Bacterial growth curves for all tested strains were constructed from OD_{600} measures to determine the duration of lag phase and the doubling time, which represented the time required to adapt and the productivity of the strain under the given environmental conditions, respectively. Optimal range was defined as the condition range where all three *V. alginolyticus* strains demonstrate the fastest strain-level doubling whereas the tolerable limit is defined as the condition range where no growth inhibition was observed. Tested strains were selected to highlight the differences between the environmental strains JW16-551 and JW16-580 originally isolated in 2016 from pelagic waters off the coast of Looe Key, FL during a Saharan dust deposition event and the *V. alginolyticus* type strain ATCC 17749 originally isolated in 1961 from spoiled fish in Japan.

Temperature Effects on Growth. Optimal *V. alginolyticus* growth occurred between 30 and 36 ^{o}C for all strains when grown at a 3% NaCl concentration in non-iron limiting media (Figures 1 and S1). The fastest doubling time was observed at 32 ^{o}C (81.57 min), 36 ^{o}C (71.26 min), and 30 ^{o}C (96.44 min) for strain JW16-551, JW16-580, and ATCC 17749, respectively. The shortest lag phase duration was observed at 40 ^{o}C (2.04 h), 40 ^{o}C (2.21 h), and 36 ^{o}C (2.73 h) for strain JW16-551, JW16-580, and ATCC 17749, respectively. Within the tested temperature range, all three *V. alginolyticus* strains showed similar patterns of doubling time and lag phase duration up 36 ^{o}C. At temperatures ≥36 ^{o}C doubling time diverged with strain JW16-580 showing a relatively unchanged rate, a progressively longer doubling time for JW16-551, and a substantial increase in doubling time for strain ATCC 17749. A similar divergence was noted for lag phase duration at temperatures ≥38 ^{o}C where time in lag phase continued to shorten for strains JW16-

551 and JW16-580, but increased for strain ATCC 17749 at elevated temperatures. Growth inhibition was not observed within the selected temperature range (24-40 ^{o}C); however, longer doubling times and lag phase durations were observed at temperatures ≤26 ^{o}C and ≥38 ^{o}C for all strains.

Salinity Effects on Growth. Optimal *V. alginolyticus* growth occurred between 2% and 4% (w/v) NaCl concentrations when cultures were incubated at 30 ^{o}C in non-iron limiting media (Figures 2 and S2). Fastest doubling time was observed at NaCl concentrations of 2% (90.64 min), 3% (91.51 min), and 4% (141.61 min) for strain JW16-551, JW16-580, and ATCC 17749, respectively. The shortest lag phase duration was observed at NaCl concentrations of 2% (2.75 h), 3% (2.48 h), and 3% (3.04 h) for strain JW16-551, JW16-580, and ATCC 17749, respectively. At an NaCl concentration of 1%, doubling time slowed for all tested strains. Lag phase duration remained relatively stable at 1% for both environmental strains but was notably longer for ATCC 17749. Complete inhibition (no growth) was observed in salt-free trials (0% NaCl) for all strains. At increased salinities (5-8% NaCl) a progressive slowing in doubling time and lengthening of lag phase duration was noted for all strains. Substantial inhibition of growth occurred at NaCl concentrations ≥7%, which prevented accurate calculation of bacterial doubling time although sufficient growth was observed to allow determination of the lag phase duration at these concentrations.

Iron Effects on Growth. Iron experimentation demonstrated that environmental *V. alginolyticus* strains were amenable to growth at all measured iron concentrations (0.2-20 µM) when incubated at 30^{o} C with a 3% (w/v) NaCl concentration. However, strain ATCC 17749 was substantially inhibited by the minimal media regardless of iron concentration. This inhibition prevented accurate calculation of doubling time and lag phase duration for most experimental

trials with this strain; though minimal growth detection at iron concentrations ≥3 µM enabled determination of lag phase duration from 3-20 µM and doubling time at 20 µM (Figure 3 and S3). Of the two environmental strains, the fastest doubling time was observed at 20 µM (69.13 min) and 10 µM (51.96 min) and the shortest lag phase duration was observed at 10 µM (4.68 h) and 10 µM (5.38 h) for strain JW16-551 and JW16-580, respectively. Both environmental strains demonstrated similar patterns of doubling time response throughout the experiment with faster rates observed between 0.5-20 µM iron concentrations and markedly slowed rates at 0.2 µM. This consistency was also observed for lag phase response where increasing iron facilitated a progressively shorter lag phase duration for both environmental strains peaking at 10-20 µM. No growth inhibition was observed at an iron concentration of 20 µM, therefore no upper optimal or tolerable limit could be determined.

GC-MS Metabolomics. Endo- and exometabolite profiles for *V. alginolyticus* strain JW16-551 were compared across for different conditions related to the iron content of the initial culture used for inoculation (referred to as the starvation condition) and the experimental culture (referred to as the iron condition). These trials consisted of 1) non-starved iron replete (NSFe+), where cultures were initially grown under non-limiting iron conditions and inoculated into iron replete experimental media (4 µM $FeCl_3$), 2) non-starved iron deficient (NSFe-), where cultures were initially grown under non-limiting iron conditions and inoculated into iron deficient experimental media (0 µM $FeCl_3$), 3) starved iron replete (SFe+), where cultures were initially starved of iron for 5 d in iron deficient media then inoculated into iron replete experimental media, and 4) starved iron deficient (SFe-), where cultures were initially starved of iron for 5 d in iron deficient media then inoculated into iron deficient experimental media (Figure 4). Growth evaluation demonstrated that *V. alginolyticus* replication was substantially reduced in all trials

using iron deficient experimental media regardless of starvation condition (Figure 5). At 18 h of growth, iron replete cultures showed a mean colony forming units (CFU) mL^{-1} of 3.50×10^7 and 4.03×10^7 whereas, iron deficient cultures showed a mean CFU mL^{-1} of 2.07×10^6 and 6.53×10^5 for non-starved and starved cultures, respectively. These values equate to a 15.9-fold and 60.7-fold increase in culturable *V. alginolyticus* under iron replete conditions for non-starved and starved cultures, respectively. Furthermore, comparison of starvation condition indicated that pre-starved cultures responded more rapidly to iron supplementation compared to non-starved. When transferred to iron replete media, starved cultures showed a mean of 2.78×10^7 CFU ml^{-1} at 11 h of growth whereas non-starved cultures only reached 5.03×10^6 CFU ml^{-1} at the same time point, representing a 4.5 fold-increase based on starvation (Figure 5).

Endometabolites. Endometabolomic (metabolites extracted from cell pellets) assessment detailed the metabolic response of *V. alginolyticus* growth under iron and starvation conditions. Principle component analysis (PCA) shows distinct grouping of the cultures by exposure condition (Figure 6). Fluxes in the endogenous metabolome of iron replete cultures show similar patterns of clustering and confidence interval overlap regardless of starvation condition whereas iron deficient samples show starvation-dependent groupings with minor overlap in principle component space. Comparison of iron conditions showed upregulation of metabolites in response to iron supplementation with 49 and 47 significantly elevated metabolites identified in iron replete trials for non-starved and starved cultures, respectively; compared to 20 elevated metabolites identified from iron deficient trials (both starvation conditions) (Table 2). Pathway analysis of the metabolites from replete cultures were found to be associated with 25 and 30 unique metabolic pathways (≥2 constituents detected) for non-starved and starved cultures, respectively with alanine, aspartate, and glutamate metabolism as the most strongly represented

pathway under both starvation conditions (Figure 7). Conversely, analysis of iron deficient metabolites corresponded to 6 and 4 pathways for non-starved and starved cultures, respectively with aminoacyl-tRNA biosynthesis as the most strongly represented pathway regardless of starvation condition. No unique metabolic pathways were detected in iron deficient samples that were absent in iron replete samples (Tables 2, S1, Figures 6, S4, and S8).

Comparison of starvation conditions demonstrated that starved cultures responded more robustly to iron replete media compared to non-starved cultures. Starved iron replete cultures showed significant upregulation of 30 unique metabolites corresponding to 19 different metabolic pathways with alanine, aspartate, and glutamate metabolism and beta-alanine metabolism as the most represented pathways. Comparatively, non-starved cultures showed upregulation of 14 metabolites corresponding to one biochemical pathway, glycerophospholipid metabolism. Iron deficient starvation trials demonstrated indistinct results with 19 and 12 significantly upregulated metabolites detected corresponding to 3 and 2 metabolic pathways for starved and non-starved trials, respectively (Tables 2, S1, Figures 6, S5, and S9).

Exometabolites. Exometabolomic (spent media) assessments compared the extracellular metabolomic profiles of *V. alginolyticus* in response to iron and starvation conditions. Overall, the results of these assessments were consistent with those observed from endometabolite analyses showing similar patterns across PCA models with respect to iron and starvation comparisons. PCA of the detected metabolites showed distinct clustering by sample type where iron replete cultures showed similar patterns of grouping, and iron deficient cultures separated markedly by starvation condition (Figure 6). Comparison of iron condition demonstrated increased metabolic upregulation in conjunction with iron supplementation with replete samples showing significant upregulation of 19 and 30 metabolites for non-starved and starved cultures,

respectively (Table 2 and Figure 8). These correlate to the fluxes in 14 total metabolic pathways for both starvation conditions with alanine, aspartate, and glutamate metabolism representing the most impacted pathway. Iron deficient samples showed significant upregulation of 15 and 10 metabolites associated with 6 metabolic pathways each with glyoxylate and decarboxylate metabolism and C5-branched dibasic acid metabolism as the most represented for non-starved and starved cultures, respectively. Of the detected pathways detected, five (amino sugar and nucleotide sugar metabolism, C5-branched dibasic acid metabolism, galactose metabolism, gluconeogenesis/glycolysis, and methane metabolism) were only identified in iron deficient cultures (Tables 2, S2, Figures 7, S7, and S10).

Comparison of starvation condition was also consistent with endometabolite data showing increased metabolic activity in starved cultures under replete conditions. Starved iron replete cultures showed significantly elevated levels of 11 metabolites corresponding to 9 metabolic pathways with alanine, aspartate, and glutamate metabolism identified as the most altered pathway. Comparatively, non-starved iron replete cultures showed significant elevation of 9 metabolites corresponding to three pathways, alanine, aspartate, and glutamate metabolism, glutathione metabolism, and aminoacyl-tRNA-biosynthesis. Iron deficient cultures showed inverse results with significant upregulation of 9 and 23 metabolites corresponding to 6 and 10 metabolic pathways for starved and non-starved cultures, respectively (Tables 2, S2, Figures 7, S8, and S11).

Discussion

As a naturally occurring microorganism, risk of *V. alginolyticus* infection is strongly associated with the abundance of its population in the environment. Prior *Vibrio* community surveys have successfully demonstrated the importance of both temperature and salinity as the

two major factors influencing *Vibrio* populations (Takemura et al., 2014; Main et al., 2015). However, in tropical/subtropical regions the influence of these factors wane as ambient conditions rest well within the tolerable limits of most *Vibrio* spp. Thus, in these regions, tertiary abiotic determinants such as iron availability can function as limiting factors for the growth and proliferation of *Vibrio* populations (Westrich et al., 2016; Westrich et al., 2018). Through this research we describe the physiological response of three *V. alginolyticus* strains in relation to changing temperature, salinity, and iron availability. Furthermore, we demonstrate the importance of iron availability as a key limiting nutrient for the stimulation of *V. alginolyticus* metabolism.

Growth Kinetics. The results of temperature and salinity assessment showed that all tested *V. alginolyticus* strains were amenable to growth at all measured temperatures (24-40 ^{o}C) and NaCl concentrations from 1-6% (w/v) with optimal growth occurring at 30-36 ^{o}C and 2-4% NaCl. While these values are consistent with previously reported optimal and tolerable limits of *V. alginolyticus* (Farid & Larson, 1981; Sheikh et al., 2022), strain-specific growth variation within these limits demonstrated key differences in *V. alginolyticus* phenotype. Notably, the two environmental strains JW16-551 and JW16-580 demonstrated increased thermo- and halotolerance compared to the ATCC type strain 17749. These differences are most notable at temperatures $\geq$34 ^{o}C and NaCl concentrations $\leq$3% where the growth rate and/or lag phase duration for ATCC 17749 increased substantially. While the exact mechanism for this difference is unknown under the scope of this study, we hypothesize these tolerance differences are likely the result of horizontally acquired adaptations to the specific environment where the isolate was collected. Prior research on *V. alginolyticus* genetic diversity has shown that much of the variation between isolates is found on mobile genetic elements (MGE) suggesting that horizontal

gene transfer plays an important role in *Vibrio* niche partitioning and the establishment of regional strain characteristics (Hunt et al., 2008; Hazen et al., 2010; Lou et al., 2012; Chibani et al., 2020).

The results of iron growth kinetics experiments differed from temperature and salinity evaluations in that a distinctive tolerance range and optimal iron concentration was not observed. Instead, iron concentrations ≥0.5 µM enabled growth of environmental *V. alginolyticus* strains (JW16-551 and JW16-580) facilitating a reduction in doubling time and progressive reduction lag phase duration as iron increased. At elevated iron concentrations (10 and 20 µM) no growth inhibition or decline was observed as seen with elevated salinities and temperatures. This plateauing trend suggests that iron is a critical limiting nutrient at low concentrations (<0.5 µM) but can be overshadowed at elevated levels (≥0.5 µM) by other limiting factors such as carbon availability. This is important to note as coastal waters are highly iron limited typically ranging from 0.02-1.0 nM at ambient concentrations (Sunda, 2012). Thus, episodic iron input may facilitate rapid expansion of *V. alginolyticus* populations during these events. This hypothesis is consistent with the observations of Westrich et al. (2016) where *V. alginolyticus* levels increased substantially following the addition of simulated Saharan dust at iron levels ranging from 0.0 to 0.84 µM.

Under the scope of the present research, it is unclear why strain ATCC 17749 was not amenable to growth in the iron limiting media (VibFeL) regardless of iron concentration. We suspect that this difference may be the result of adaptations associated with geographic and/or isolation source differences between the animal-derived ATCC 17749 (Japan) and the seawater-derived JW16-551 and JW16-580 (United States, Florida). Prior research by Westrich et al. (2016) successfully utilized VibFeL as an iron-limiting minimal media for the growth of a

sweater-derived ATCC *V. alginolyticus* strain 33839; however, this research represents the first attempt to utilize this media with an animal-derived strain. Efforts to develop a differential *V. alginolyticus* media has stressed the importance of sucrose concentration for the successful growth of *V. alginolyticus* strains (Chang et al., 2011). It is possible that the relatively low sucrose concentration utilized in VibFeL (0.4% [w/v] compared to 2.0% [w/v] in thiosulfate bile salts sucrose agar [TCBS]) is limiting the growth of ATCC 17749, however further research is needed to corroborate this hypothesis.

Iron Metabolomics. Metabolomics assessment provides biochemical context for the observed changes in growth kinetics (Figure 3), and cell counts (Figure 5) between iron replete and iron deficient cultures. PCA (Figure 6) demonstrated distinct class separation by sample type with consistent overlap observed in iron replete samples. These data suggest that iron supplementation facilitates activation of similar metabolic pathways regardless of starvation condition. Conversely, iron deficient samples showed little to no overlap in component space suggesting that these treatments are metabolically distinct because of starvation. We suspect that this difference may in part be due to the utilization of stored iron (Andrews, 1998; Andrews et al., 2003) by non-starved cultures facilitating low-level metabolic activity under iron deficient conditions. This hypothesis is supported by growth observations of these cultures where non-starved cultures showed slightly elevated CFU mL^{-1} counts compared to starved cultures after 18 h of growth in iron deficient VibFeL (Figure 5).

Comparison of the detected metabolites shows that iron availability is critical for the stimulation of *V. alginolyticus* metabolism. Iron supplementation facilitated an increase in the total number of upregulated metabolites and their corresponding metabolic pathways regardless of starvation condition for both endo- and exometabolites. Enriched pathways were associated

with a range of different processes linked to metabolism and/or downstream translation. Of these pathways, those associated with amino acid metabolism were the most impacted. These perturbations resulted from the significant upregulation of metabolic intermediaries and end products linked to amino acid biosynthesis and/or degradation such as succinate, fumarate, L-aspartate, L-alanine, putrescine, γ-aminobutyric acid (GABA), glutamate, and 2-oxoglutarate (α-ketoglutarate) under replete conditions. Upregulation in these biochemical processes corroborates that the availability of iron facilitates increased protein synthesis and is consistent with the established role of iron as a critical cofactor for enzyme catalyzation (Andreini et al., 2008; Frawley & Fang, 2014).

Second to amino acid metabolism, carbohydrate metabolism was also highly upregulated in iron replete samples. Enriched pathways were associated with energy production cycles/ processes namely, the tricarboxylic acid cycle (TCA), glycolysis, butonate metabolism, and glyoxylate and decarboxylate metabolism suggesting that iron is essential for energy generation in *V. alginolyticus*. This finding is consistent with established iron requirement of *Vibrio* spp. to stimulate replication (Payne et al., 2016) and provides justification for the substantially reduced level of growth observed in iron deficient cultures (Figure 5). Furthermore, the upregulation of glyoxylate and decarboxylate metabolism is of particular interest. Prior research has suggested that the use of the glyoxylate shunt (an anabolic variation of the TCA cycle) may represent an effort to reduce internal iron quota through a reduction in the use of iron-dependent enzymes for energy production (Koedooder et al., 2018). *Vibrio* utilizing this mechanism may explain the enrichment of this pathway in both iron replete and iron deficient samples.

To a lesser extent, iron supplementation also enriched pathways associated with lipid, nucleotide, vitamin/cofactor, and secondary (terpenoids and polyketides) metabolism. Similar to

amino acid metabolism, enrichment of these pathways was associated with the upregulation of intermediary and end-point metabolites related with these processes including L-aspartate, L-valine, L-tyrosine, uracil, succinate, thymine, D-ribose 5`-phosphate, adenine, and urea further demonstrating a broad activation of metabolic processes under replete conditions. It should be noted that iron supplementation also facilitated an enrichment of the translation pathway, aminoacyl-tRNA biosynthesis. While this pathway does not exclusively represent metabolism, greater pathway representation was observed in iron replete trials suggesting increased translation activity in response to iron availability. Furthermore, enrichment of methane metabolism was detected in several metabolite comparisons. While interesting to note, enrichment of this pathway in all instances was due to the upregulation of glycine and pyruvate, two metabolites commonly associated with amino acid and carbohydrate metabolism. Thus, we suspect that detection of this pathway is likely the result of false discovery of intermediaries. No pathways unique to iron deficient cultures were detected from endometabolite data, suggesting that in the absence of iron *V. alginolyticus* metabolism is largely inhibited. However, exometabolite data demonstrated an impact in three carbohydrate-centric metabolic pathways not found in iron replete samples: galactose, C5-branched dibasic acid, and amino sugar/nucleotide sugar metabolism. Due to the absence of these pathways in the endometabolite data we hypothesize that the impact in these may be due to detection of residual media carbohydrates (i.e., sucrose) that were not utilized by *V. alginolyticus* in the absence of iron.

Starvation comparisons demonstrated that initial iron deprivation (prior to the start of the experiment) facilitates increased metabolic activity once reintroduced to an iron-rich environment. Under iron replete conditions, starved samples showed elevated levels of upregulated endo- and exometabolites corresponding to increased enrichment of amino acid,

carbohydrate, vitamin/cofactor, nucleotide, and secondary metabolism pathways. This rapid response is consistent with the observed growth patterns of replete cultures where starved samples showed increased CFU mL^{-1} levels at earlier timepoints (4 and 11 h) compared to non-starved cultures suggesting faster response from these strains (Figure 5). This is important to note as natural populations of *V. alginolyticus* are consistently iron deprived, thus this response is likely representative of how these populations react following iron influx. No unique pathways were detected in starvation experiments that were absent from iron experiments suggesting that starvation does not activate alternate metabolic mechanisms but rather stimulates a more robust or exacerbated response in the identified pathways. Analysis of iron deficient samples showed variable metabolic results based on starvation suggesting that in the absence of abundant iron, pre-starvation has little metabolic effect on *V. alginolyticus*.

Beyond pathway enrichment, analysis of upregulated metabolites provides evidence of *V. alginolyticus* iron acquisition mechanisms. Prior research has demonstrated that the *Vibrio*-derived siderophore vibrioferrin is comprised of equal parts L-alanine, citric acid, 2-oxoglutatic acid, and ethanolamine (Yamamoto et al., 1994; Funahashi et al., 2002; Tanabe et al., 2003). In the present study, all of these metabolites were found to be significantly upregulated in analysis of endometabolites, exometabolites, or both under iron replete conditions. This upregulation suggests that when supplemented with iron, *V. alginolyticus* strain JW16-551 may produce vibrioferrin or a homologous siderophore as a mechanism of iron acquisition. This finding is consistent with that of Wang et al. (2007) who found similar evidence of *V. alginolyticus* production of a vibrioferrin-like siderophore through characterization of the *fur* gene cluster (a known regulator of iron acquisition mechanisms in *Vibrio* spp. [Kuehl & Crosa, 2010]) and siderophore purification from low-iron cultures. It should be noted that while detection of these

metabolites together suggests the presence of vibrioferrin, this suite of metabolites have functions in other metabolic pathways such as amino acid and lipid metabolism thus, continued investigation of *V. alginolyticus* siderophore production is needed to corroborate these findings.

Conclusion

As an indigenous microorganism and opportunistic pathogen, the risk of *V. alginolyticus* infection is directly related to the abundance of its populations in the environment. Prior research has successfully demonstrated the importance of temperature and salinity as critical factors restricting *V. alginolyticus* range and growth. However, few studies to date have examined the importance of tertiary environmental determinants which play an important role in regions where temperature and salinity are non-limiting. Here we reconfirm the tolerance of temperature and salinity and demonstrate the critical importance of iron availability to simulate the growth and metabolism of *V. alginolyticus*. Temperature and salinity evaluation demonstrate broad tolerability of *V. alginolyticus* ranging from 24-40 ^{o}C and 1-6% (w/v) NaCl. Iron supplementation resulted in a 15.9 (non-starved) and 60.7 (starved) fold-increase in culturable *V. alginolyticus* and upregulated the abundance of metabolites associated with 25 (non-starved) and 30 (starved) unique metabolic pathways demonstrating broad activation of *V. alginolyticus* metabolism in the presence of iron. Furthermore, metabolomics assessment demonstrates that iron starvation can increase the metabolic response of *V. alginolyticus* when returned to iron replete conditions. The results of this research provide important context for the environmental response of *V. alginolyticus* populations in relation to iron availability and stresses the importance of consideration of episodic iron deposition for prediction of *V. alginolyticus* infection risk.

Methods

Strains and Storage. Experimental *V. alginolyticus* strains were obtained from our culture collection (E.K. Lipp, University of Georgia). Strains consisted of two environmental strains collected from pelagic waters off the coast of Looe Key, FL during a Saharan Dust event in 2016 as well as the American Type Culture Collection (ATCC) strain for *V. alginolyticus* originally isolated from spoiled fish in Japan in 1961 (Table 1). Physiological evaluation measured the growth response of all three strains at varying temperatures, salinities, and iron content. Metabolomic analysis specifically focused on the iron response of strain JW16-551 which was previously shown to be highly responsive to Saharan dust-derived input of biologically available iron (Borchardt et al., 2020). All parent cultures were stored at -80 ^{o}C in 20% glycerol (v/v, final concentration). Prior to the start of experimentation, strains were revived in 4 mL of lysogeny broth (LB, Sigma Aldrich, Miller formulation) amended to 3% w/v NaCl (termed LBS 3% henceforth) at 30 ^{o}C with 100 rpm shaking agitation (New Brunswick Scientific, C24 Incubator Shaker).

Physiological Evaluation. Physiological evaluation compared the growth kinetics of *V. alginolyticus* under changing conditions of temperature, salinity, and iron content. Temperature effects were evaluated from 24-40 ^{o}C at 2 ^{o}C intervals controlled by incubation. Salinity effects were measured using NaCl concentration from 0-8% (w/v) at 1% intervals. NaCl concentration was controlled using "home-brew" LBS media consisting of 10 g of peptone (Sigma Aldrich), 5 g of yeast extract (Sigma Aldrich), and salt (Sigma Aldrich) added to the concentration of the desired salinity percentage (NaCl level is designated as the percent value of LBS [i.e., 6% NaCl media is abbreviated as LBS 6% in-text]). Iron effects were measured from 0.2-20 µM at 0.2, 0.5, 1, 3, 4, 10, and 20 µM concentrations. Iron concentration was controlled using a custom

low-iron media termed VibFeL prepared using the methods of Westrich et al. (2016). During VibFeL preparation, ambient iron from the basal media components is removed by chelation through a chromatography column containing Chelex® 100 (Sigma Aldrich) ion-exchange resin. Following removal, iron was restored to the media to the designated experimental concentration through the addition of ferric chloride ($FeCl_3$, Sigma Aldrich).

To begin growth kinetics experiments, cultures were revived from -80 ^oC storage as described above and incubated overnight (~18 h) to reach stationary phase. 0.015 µL of each strain (8.1×10^4, 9.3×10^4, and 4.7×10^4 CFU for JW16-551, JW16-580, and ATCC 17749, respectively) was inoculated into 150 µL of the designated media type in a clear 96-well microplate (Nunc™ Pinch-bar MicroWell™ 96-Well Microplate, ThermoFisher). Inoculated plates were loaded into a Varioskan LUX microplate reader (ThermoFisher) and growth was evaluated using OD. OD measures were taken at 600 nm every 150 sec for a period of 15 h. All plates were incubated with 120 rpm of continuous shaking agitation in twelve replicates (N = 12) for each strain under each growth condition. Unless designated as the experimental variable, plates were incubated at 30 ^oC with 3% (w/v) salt content, and a non-limiting supply of biologically available iron (non-chelated media). Growth data was analyzed in Rstudio using the packages 'tidyverse', 'readxl', 'SciViews', and 'FSA.' The duration of lag phase was calculated as the elapsed time required to reach a detectable OD threshold (signal above background noise). This threshold was calculated as the mean of all measurements recorded between an OD_{600} of 0.05 and 0.15 to account for measurement variation. Doubling time was calculated using the standard two-step OD formula.

$$Growth\ Rate\ Constant = \frac{[\ln(LateLogOD) - \ln(EarlyLogOD)]}{Time_{late} - Time_{early}}$$

$$Doubling\ Time = \frac{\ln(2)}{Growth\ Rate\ Constant}$$

Using this equation, *LateLogOD* represents the OD of the culture towards the end of log phase (~3rd quartile), *EarlyLogOD* represents the OD at the beginning of log phase (~1st quartile), $Time_{late}$ represents the elapsed time to reach the *LateLogOD* and $Time_{early}$ represents the elapsed time to reach *EarlyLogOD.* To account for sample selection variation *LateLogOD*, *EarlyLogOD*, $Time_{late}$, and $Time_{early}$ were calculated as aggregate values within specified OD ranges. This was done to improve representation of these key metrics by including data from multiple close datapoints rather than selection of a single representative datapoint. *LateLogOD* and $Time_{late}$ were calculated as the mean values of OD and elapsed time for all measures ranging from an OD_{600} of 0.65-0.75 for temperature and salinity trials and 0.15-0.20 for iron trials. A reduced range was selected for iron trials due to the overall reduced growth capacity of *V. alginolyticus* under the limiting conditions of VibFeL media. Similarly, *EarlyLogOD* and $Time_{early}$ were calculated as the mean values of OD and elapsed time for all measures ranging from an OD_{600} of 0.10-0.20 for temperature and salinity trials and 0.05-0.10 for iron trials. Strain-level doubling times and lag phase durations were tested for significance across all abiotic metrics using a Kruskal Wallis test and Shapiro Wilk test for normality (Table S3). Pairwise strain-level comparisons were tested using a Dunn's multiple comparison test with Holm p-value adjustment to identify significant differences in the strain-level growth response across treatments (Table S4).

Iron Metabolomics Culture Conditions. Metabolomic experiments were conducted to explore the biochemical effects of iron availability on *V. alginolyticu*s. These experiments focused on the response of strain JW16-551 which was previously shown to be highly responsive to Saharan

dust-derived iron input (Borchardt et al., 2020). Cultures were prepared to measure the effects of iron condition and iron starvation. Iron condition experiments compared differences between cultures grown in iron replete (VibFeL amended with 4 µM $FeCl_3$) and iron deficient (VibFeL non-amended, ~0 µM Fe) media. Iron deficient cultures are noted as approximately 0 µM iron due to small levels of ambient iron contamination from the laboratory space. To reduce the level of contamination, all iron deficient VibFeL was prepared immediately before use in experimentation with acid-washed glassware and stored for no more than 4 h. Iron starvation experiments compared the differences between cultures that were initially "starved" of iron for 5 days in iron deficient media (~0 µM VibFeL) at 30 ºC and "non-starved" cultures grown for 18 h in non-iron limiting media (LBS 3%) at 30 ºC. Non-starved and starved parent cultures were subsequently inoculated into experimental media (either iron replete or deficient) for growth and metabolomic measurement.

To prepare experimental cultures, strain JW16-551 was revived from -80 ºC storage as described above and incubated overnight (~18 h) to reach stationary phase. 1 mL of cultured cells was removed, pelleted by centrifugation at ~4,000 x *g* for 2 min, and resuspended in 1 mL of sterile 1X phosphate buffered saline (PBS) in triplicate to wash cells of residual media. 100 µL of washed cells (5.00×10^6 and 1.02×10^4 CFU for non-starved and starved cultures, respectively) were inoculated into 10 mL of VibFeL media amended to iron deficient or iron replete conditions designated by the experimental trial. Inoculated cultures were incubated aerobically for 18 h at 30 ºC with 100 rpm of shaking agitation (New Brunswick Scientific, C24 Incubator Shaker). At 4, 8, 11, and 18 h, cellular growth was quantified using culture-based plate counts where 100 µL of culture was removed, serial diluted (10-fold), and spread plated with glass rattler beads (Zymo Rattler™ Plating Beads, 4.5 mm) onto TCBS agar. At 18 h cultures

were removed, pelleted by centrifugation at ~4,000 x *g* for 10 min, and the supernatant (henceforth termed "spent media") was removed. Cell pellets were immediately quenched in ice cold 100% methanol (Sigma Aldrich), transferred to 1.5 mL microcentrifuge tubes, and stored at -20 ^{o}C for endometabolite analysis. 1.9 mL of spent media was transferred to a 2 mL microcentrifuge and quenched through the addition of 100 µL of acetone (Sigma Aldrich) and stored for exometabolite analysis at -20 ^{o}C.

Extraction. Prior to analysis, all endometabolite samples were lysed and extracted to target polar and non-polar metabolites using liquid-liquid extraction. Samples were dried using a SpeedVac® Plus (Savant) for 18 h to remove residual methanol. Dried cell pellets were resuspended in 485 µL of 82.5% methanol:water and a 3.2 mm diameter stainless steel disruption bead (BioSpec Products Inc.) was added to each sample. Samples were lysed using a Qiagen TissueLyser II bead mill following a step-wise extraction protocol. First, samples were processed for 10 min at a frequency of 15 s^{-1}. Next, samples were centrifuged for 15 sec using a bench top microcentrifuge, 300 µL of chloroform (Sigma Aldrich) was added and they were disrupted on the bead mill for 20 min at a frequency of 15 s^{-1}. Lastly, samples were centrifuged for 15 sec using a bench top microcentrifuge, 200 µL of chloroform (Sigma Aldrich) and 200 µL of dH_2O (18.2 MΩ water) was added and returned to the bead mill once more for 10 min at a frequency of 15 s^{-1}. Following lysis, samples were centrifuged at 1,000 x *g* for 15 min at 4 ^{o}C. Centrifugation resulted in the production of two phases an upper methanol-water phase containing polar metabolites and a lower chloroform phase containing non-polar metabolites separated by a thin lay of protein debris. Each phase was removed and dispensed into a 2 mL glass vial. Care was taken not to disturb the protein debris layer when removing each phase.

Exometabolite (spent media) samples did not require extraction. All samples were retrieved from -20 ^{o}C storage and thawed at room temperature. Thawed samples were vortexed for 30 sec to homogenize the mixture and 200 µL of spent media was transferred to a 2 mL vial. Both endometabolite (polar and non-polar) and exometabolite samples were dried overnight as described above prior to derivatization.

Derivatization. Lyophilized samples were derivatized sequentially with methoxyamine hydrochloride (MeOX) (Sigma Aldrich) and N,O-bis(trimethylsilyl)trifluoroacetamide containing 10% trimethylchlorosilane (BSTFA + 10% TMCS) (Thermo Scientific). For methoxyamination, 60 mg of MeOX was dissolved into 3 mL of pyridine (Thermo Fisher) and 30 µL added to each sample vial and vortexed for 10 sec. All samples were incubated at 60 ^{o}C for 2.5 h with intermediate vortexing (i.e, every 30 mins). After 2.5 h samples were removed and allowed to cool for 10 min. 50 µL of BSTFA was added to each sample and vortexed for 10 sec. Sample vials were incubated at 60 ^{o}C for 1.5 h and removed every 30 min for vortexing. This process was repeated for both endometabolite and exometabolite samples.

GC-MS Analysis. Metabolomics samples were analyzed on an Agilent 8890 gas chromatograph coupled to a 7250 quadrupole time of flight mass spectrometer (GC/q-ToF-MS) equipped with a DB-5MS ultra inert column (30 m x 250 µm x 0.25µm; Agilent Technologies) using electron impact ionization scanning from 50-600 *m/z*. Samples (1 µL) were injected in split mode at 10:1 and helium was used as the carrier gas. Initial oven temperature was held at 60 °C for 1 min then ramped 10 °C/min to 325 °C and held for 10 min (total runtime 37.5 min). Post-acquisition, spectra were imported into MetAlign (Lommen, 2009) for pre-processing and alignment. Vendor recommended parameters for high resolution GC/qToF-MS were used. Retention time and *m/z* paired data:m/z were analyzed using MetaboAnalyst (for PCA analysis) and Rstudio for

additional statistical analyses using the R libraries ‘tidyverse’ and ‘readxl.’ Retention times were compared by iron and starvation condition resulting in eight major comparisons not-starved iron replete verses not-starved iron deficient (NSFe+/NSFe-), starved iron replete verses starved iron deficient (SFe+/SFe-), not-starved iron replete verses starved iron replete (NSFe+/SFe+), not-starved iron deficient verses starved iron deficient (NSFe-/SFe-), and the inverse of these. Relative concentrations were compared using a student’s *t*-test to identify significantly (p-value ≤ 0.05) perturbed spectral features from each comparison. Following metabolite identification using both the NIST and Agilent’s Fiehn Metabolomics libraries. Functional analysis of significant metabolites was then preformed using the MetaboAnalyst’s ‘Pathway Analysis’ feature with the *Escherichia coli* K-12 MG1655 prokaryote pathway library. To account for differences in the total number of metabolites per pathway, pathway hits were normalized using the equation:

$$z_i = \frac{(x_i - \min(x))}{(\max(x) - \min(x))}$$

where z_i is the normalized value, x_i is the total pathway hits, $min(x_i)$ is the minimum pathway hits, or 1, and $max(x)$ is the maximum pathway hits or the total metabolites in the pathway. All pathways with a hit count of 1 were removed from analysis to account for the possibility of false discovery.

Acknowledgements.

We would like to thank the U.S. Environmental Protection Agency, Office of Research and Development (ORD), Center for Environmental Measurement and Modeling (CEMM) for their assistance with metabolomics processing and instrumentation. We thank the University of Georgia, Graduate School for their financial support of this project through the 2022 Summer

Research Grant program. We also thank Ms. Rachel Phan, Ms. Carolina Melendez-Declet, and Mr. Carter Coleman for their assistance with laboratory processing. The views expressed in this manuscript are those of the author(s) and do not necessarily represent the views or policies of the US Environmental Protection Agency. Any mention of trade names or commercial products does not constitute EPA endorsement or recommendation for use.

Literature Cited

Andreini C, Bertini I, Cavallaro G, Holliday GL, and Thornton JM. 2008. Metal ions in biological catalysis: from enzyme databases to general principles. *Journal of Biological Inorganic Chemistry.* 13: 1205-1218.

Andrews SC. 1998. Iron storage in bacteria. *Advances in Microbial Physiology.* 40: 281-351.

Andrews SC, Robinson AK, and Rodríguez-Quiñones F. 2003. Bacterial iron homeostasis. *FEMS Microbiology Reviews.* 27(2-3): 215-237.

Asplund ME, Rehnstam-Holm AS, Atnur V, Raghunath P, Saravanan V, Härnström K, Collin B, Karunasagar I, and Godhe. 2011. Water column dynamics of *Vibrio* in relation to phytoplankton community composition and environmental conditions in a tropical coastal area. *Environmental Microbiology.* 13(10): 2738-2751.

Benediktsdóttir E, Helgason S, and Sigurjónsdóttir. 2008. *Vibrio* spp. isolated from salmonids with shallow skin lesions and reared at low temperature. *Journal of Fish Diseases*. 21(1): 19-28.

Böer SI, Heinemeyer EA, Luden K, Erler R, Gerdts G, Janssen F, and Brennholt N. 2013. Temporal and spatial distribution patterns of potentially pathogenic *Vibrio* spp. at recreational beaches of the German North Sea. *Environmental Microbiology.* 65: 1052-1067.

Borchardt T, Fisher KV, Ebling AM, Westrich JR, Xian P, Holmes CD, Landing WM, Lipp EK, Wetz MS, and Ottesen EA. 2020. Saharan dust deposition initiates successional patterns among marine microbes in the Western Atlantic. *Limnology and Oceanography.* 65(1): 191-203.

Cervino JM, Thompson FL, Gomez-Gil B, Lorence EA,Goreau TJ, Hayes RL, Winiarski-Cervino KB, Smith GW, Hughen K, and Bartels E. 2008. The *Vibrio* core group induces yellow band disease in Caribbean and Indo-Pacific reef-building corals. *Journal of Applied Microbiology.* 105(5): 1658-1671.

Chibani CM, Roth O, Liesegang H, and Wendling CC. 2020. Genomic variation among closely related *Vibrio alginolyticus* strains is located on mobile genetic elements. *BMC Genomics*. 21: 354.

Chowdhury MA, Yamanaka H, Miyoshi S, Aziz KM, and Shinoda S. 1989. Ecology of *Vibrio mimicus* in aquatic environments. *Applied and Environmental Microbiology.* 55(8): 2073-2078.

Colorni A, Paperna I, and Gordin H. 1981. Bacterial infections in gilt-head sea bream *Sparus aurata* cultured at Elat. *Aquaculture.* 23(1-4): 257-267.

Dechet AM, Yu PA, Koram N, and Painter J. 2008. Nonfoodborne *Vibrio* infections: An important cause of morbidity and mortality in the United States, 1997–2006. *Clinical Infectious Diseases.* 46(7): 970-976.

Duce RA and Tindale NW. 1991. Atmospheric transport of iron and its deposition in the ocean. *Limnology and Oceanography*. 36(8): 1715-1726.

Eiler A, Johansson M, and Bertilsson S. 2006. Environmental influences on *Vibrio* populations

in northern temperate and boreal coastal waters (Baltic and Skagerrak Seas). *Applied and Environmental Microbiology.* 72(9): 6004-6011.

English VL and Lindberg RB. 1997. Isolation of *Vibrio alginolyticus* from wounds and blood of a burn patient. *American Journal of Medical Technology.* 43(10): 989-993.

Escolar L, Pérez-Martín J, and De Lorenzo V. 1999. Opening the iron box: Transcriptional metalloregulation by the Fur protein. *Journal of Bacteriology.* 181(20): 6223-6229.

Fahmy NM and Hamed ESAE. 2022. Isolation and characterization of *Vibrio alginolyticus* strain HAT3 causing skin ulceration disease in cultured sea cucumber *Holothuria atra* (Jaeger, 1833). *The Egyptian Journal of Aquatic Research.* 48(1): 75-81.

Farid AF and Larsen JL. 1981. Growth of *Vibrio alginolyticus*: Interacting effects on pH, temperature, salt concentration, and incubation time. *Zentralblatt für Bakteriologie Mikrobiologie und Hygiene: I. Abt. Originale C: Allgemeine, angewandte und ökologische Mikrobiologie.* 3(4): 68-75.

Frawley ER and Fang FC. 2014. The ins *and outs* of bacterial iron metabolism. *Molecular Microbiology.* 93(4): 609-616.

Froelich B, Boewn J, Gonzalez R, Snedeker A, and Noble R. 2013. Mechanistic and statistical models of total *Vibrio* abundance in the Neuse River Estuary. *Water Research.* 47(15): 5783-5793.

Funahashi T, Moriya K, Uemura S, Miyoshi SI, Shinoda S, Narimatsu S, and Yamamoto S. 2002. Identification and characterization of *pvuA*, a gene encoding the ferric vibrioferrin receptor protein in *Vibrio parahaemolyticus. Journal of Bacteriology.* 184(4): 936-946.

Glazebrook JS and Campbell RSF. 1990. A survey of the diseases of marine turtles in northern Australia. I. Farmed turtles. *Diseases of Aquatic Organisms.* 9: 93-95.

Gómez-León J, Villamil L, Lemos ML, Novoa B, and Figueras A. 2005. Isolation of *Vibrio alginolyticus* and *Vibrio splendidus* from aquacultured Carpet Shell Clam (*Ruditapes decussatus*) larvae associated with mass mortalities. *Applied and Environmental Microbiology.* 71(1): https://doi.org/10.1128/AEM.71.1.98-104.2005.

Gu D, Guo M, Yang M, Zhang Y, Zhou X, and Wang Q. 2016b. A σ^E-mediated temperature gauge controls a switch from LuxR-mediated virulence gene expression to thermal stress adaptation in *Vibrio alginolyticus. PLoS Pathogens*. 12(6): e1005645.

Hazen TH, Pan L, Gu JD, and Sobecky PA. 2010. The contribution of mobile genetic elements to the evolution and ecology of *Vibrios*. *FEMS Microbiology Ecology.* 74(3): 485-499.

Hlady WG and Klontz KC. 1996. The epidemiology of *Vibrio* infections in Florida, 1981-1993. *The Journal of Infectious Diseases.* 173: 1176-1183.

Horie S, Okuzumi M, Kato N, and Saito K. 1966. Comparative observation on the range of growth temperature among three biotypes of *Vibrio parahaemolyticus*. *Bulletin of the Japanese Society of Scientific Fisheries.* 32(5): 424-426.

Hsieh JL, Fries S, and Noble RT. 2007. Dynamics and predictive modelling of Vibrio spp. in the Neuse River Estuary, North Carolina, USA. *Environmental Microbiology.* 10(1): 57-64. https://doi.org/10.1111/j.1462-2920.2007.01429.x.

Huehn S, Eichhorn C, Urmersbach S, Breidenbach J, Bechlars S, Bier N, Alter T, Bartelt E, Frank C, Oberheitmann B, Gunzer F, Brennholt N, Böer S, Appel B, Dieckmann R, and Strauch E. 2014. Pathogenic vibrios in environmental, seafood and clinical sources in Germany. *International Journal of Medical Microbiology.* 304(7): 843-850.

Hunt DA, David LA, Gevers D, Preheim SP, Alm EJ, and Polz MF. 2008. Resource partitioning

and sympatric differentiation among closely related bacterioplankton. *Science.* 320(5879): 1081-1085.

Koedooder C, Guéneuguès A, Geersdaële RV, Vergé V, Bouget FV, and Labreuche Y. 2018. The role of the glyoxylate shunt in the accumulation to iron limitation in marine heterotrophic bacteria. *Frontiers in Marine Science*. 5: 435.

Kuehl CJ and Crosa JH. 2010. The TonB energy transduction systems in *Vibrio* species. *Future Microbiology.* 5(9): 1403-1412.

Kustusch RJ, Kuehl CJ, and Crosa JH. 2011. Power plays: iron transport and energy transduction in pathogenic vibrios. *Biometals*. 24(3): 559-566.

Lightner DV and Lewis DH. 1975. A septicemic bacterial disease syndrome of Penaeid shrimp. *Marine Fisheries Review.* 37(5-6): 25-28.

Liu B, Liu H, Pan Y, Xie J, and Zhao Y. 2016. Comparison of the effects of environmental parameters on the growth variability of *Vibrio parahaemolyticus* coupled with strain sources and genotypes analyses. *Frontiers in Microbiology.* 7: 994.

Lommen A. 2009. MetAlign: interface-driven, versatile metabolomics tool for hyphenated full-scan mass spectrometry data preprocessing. *Analytical Chemistry.* 81(8): 3079-3086.

Luo P, Jiang H, Wang Y, Su T, Hu C, Ren C, and Jiang X. 2012. Prevalence of mobile genetic elements and transposase genes in *Vibrio alginolyticus* from the southern coastal region of China and their role in horizontal gene transfer. *International Microbiology.* 15: 199-208.

Lv T, Dai F, Zhuang Q, Zhao X, Shao Y, Guo M, Lv Z, Li C, and Zhang W. 2020. Outer membrane protein OmpU is related to iron balance in *Vibrio alginolyticus*. *Microbial Research.* 230: 126350.

Maeda T, Matsuo Y, Furushita M, and Shiba T. 2003. Seasonal dynamics in a coastal Vibrio community examined by a rapid clustering method based on 16S rDNA. *Fisheries Science.* 69: 385-394.

Main CR, Salvitti LR, Whereat EB, and Coyne KJ. 2015. Community-level and species-specific associations between phytoplankton and particle-associated *Vibrio* species in Delaware's inland bays. *Applied and Environmental Microbiology.* 81(17): 5703-5713.

Miyamoto Y, Nakamuma K, and Takizawa K. 1961. Pathogenic halophiles. Proposals of a new genus "*Oceanomonas*" and the amended species names. *Japanese Journal of Microbiology*. 5(4): 477-486.

Oberbeckmann S, Fuchs BM, Meiners M, Wichels A, Wiltshire KH, and Gerdts G. 2011a. Seasonal dynamics and modeling of a *Vibrio* community in coastal waters of the North Sea. *Environmental Microbiology.* 63: 543-551. https://doi.org/10.1007/s00248-011-9990-9.

Oberbeckmann S, Wichels A, Wiltshire KH, and Gerdts G. 2011b. Occurrence of *Vibrio parahaemolyticus* and *Vibrio alginolyticus* in the German Bight over a seasonal cycle. *Antonie van Leeuwenhoek*. 100: 291-307.

Payne SM, Mey AR, and Wyckoff EE. 2016. *Vibrio* iron transport: evolutionary adaptation to life in multiple environments. *Microbiology and Molecular Biology Reviews.* 80(1): 69-90.

Randa MA, Polz MF, and Lim E. 2004. Effects of temperature and salinity on *Vibrio vulnificus* population dynamics as assessed by quantitative PCR. *Applied and Environmental Microbiology.* 70(9): 5469-5476.

Sanches-Fernandes GMM, Sá-Correia I, and Costa R. 2022. Vibriosis outbreaks in aquaculture:

addressing environmental and public health concerns and preventive therapies using gilthead seabream farming as a model system. *Frontiers in Microbiology.* 13: 904815.

Schroeder JP, Wallace JG, Cates MB, Greco SB, and Moore WB. 1985. An infection by *Vibrio alginolyticus* in an Atlantic Bottlenose Dolphin housed in an open ocean pen. *Journal of Wildlife Diseases.*21(4): 437-438.

Selvin J and Lipton AP. 2003. *Vibrio alginolyticus* associated with white spot disease of *Penaeus monodon. Diseases of Aquatic Organism.* 57: 147-150.

Sheikh HI, Najiah M, Fadhlina A, Laith AA, Nor MM, Jalal KCA, and Kasan NA. 2022. Temperature upshift mostly but not always enhances the growth of *Vibrio* species: a systematic review. *Frontiers in Marine Science*. 9: 959830.

Singleton FL, Attwell R, Jangi S, and Colwell RR. 1982. Effects of temperature and salinity on *Vibrio cholerae* growth. *Applied and Environmental Microbiology.* 44(5): 1047-1058.

Slifka KM, Newton AE, and Mahon BE. 2017. *Vibrio alginolyticus* infections in the USA, 1988-2012. *Epidemiology & Infection.* 145:1491-1499.

Sunda WG. 2012. Feedback interactions between trace metal nutrients and phytoplankton in the ocean. *Frontiers in Microbiology.* 3: 204.

Takemura AF, Chien DM, and Polz MF. 2014. Associations and dynamics of Vibrionaceae in the environment, from the genus to the population level. *Frontiers in Microbiology*. 5(38). https://doi.org/10.3389/fmicb.2014.00038.

Tanabe T, Funahashi T, Nakao H, Miyoshi SI, Shinoda S, and Yamamoto S. 2003. Identification and characterization of genes required for biosynthesis and transport of the siderophore vibrioferrin in *Vibrio parahaemolyticus. Journal of Bacteriology.* 185(23): 6938-6949.

Thompson JR, Randa MA, Marcelino LA, Tomita-Mitchell A, Lim E, and Polz MF. 2004.

Diversity and dynamics of a North Atlantic coastal *Vibrio* community. *Applied and Environmental Microbiology.* 70(7): 4103-4110.

Turner JW, Good B, Cole D, and Lipp EK. 2009. Plankton composition and environmental factors contribute to *Vibrio* seasonality. *The ISME Journal*. 3: 1082-1092.

Wang Q, Liu Q, Ma Y, Zhou L, and Zhang Y. 2007. Isolation, sequencing and characterization of cluster genes involved in the biosynthesis and utilization of the siderophore of marine fish pathogen *Vibrio alginolyticus*. *Archives of Microbiology.* 188: 433-439.

Wang Q, Liu Q, Cao X, Yang M, and Zhang. 2008. Characterization of two TonB systems in marine fish pathogen *Vibrio alginolyticus*: their roles in iron utilization and virulence. *Archives of Microbiology.* 190: 595-603.

Weis KE, Hammond RM, Hutchinson R, and Blackmore CGM. 2011. Vibrio illness in Florida, 1998-2007. *Epidemiology and Infection.* 139: 591-598.

Westrich JR, Ebling AM, Landing WM, Joyner JL, Kemp KM, Griffin DW, and Lipp EK. 2016. Saharan dust nutrients promote *Vibrio* bloom formation in marine surface waters. *PNAS.* 113(21): 5964-5969.

Westrich JR, Griffin DW, Westphal DL, and Lipp EK. 2018. *Vibrio* population dynamics in mid-Atlantic surface waters during Saharan dust events. *Frontiers in Marine Science.* 5: 12.

Yamamoto S, Okujo N, Yoshida T, Matsuura S, and Shinoda S. 1994. Structure and iron transport activity of vibrioferrin, a new siderophore of *Vibrio parahaemolyticus. Journal of Biochemistry.* 115(5): 868-874.

Zhenyu X, Shaowen K, Chaoqun H, Zhixiong Z, Shifeng W, and Youngcan Z. 2013. First characterization of bacterial pathogen, *Vibrio alginolyticus*, for *Porites andrewsi* white syndrome in the South China Sea. *PLoS One* 8:e75425.

Zhou K, Tian KY, Liu XQ, Liu W, Zhang XY, Liu JY, and Sun F. 2021, Characteristic and otopathogenic analysis of a Vibrio alginolyticus strain responsible for chronic otitis externa in China. *Frontiers in Microbiology.* 12: 750642.

Zorrilla I, Moriñigo MA, Castro D, Balebona MC, and Borrego JJ. 2003. Intraspecific characterization of *Vibrio alginolyticus* isolates recovered from cultured fish in Spain. *Journal of Applied Microbiology*. 95(5): 1106-1116.

Tables and Figures

Table 1: *V. alginolyticus* strain details and documentation. Strains ATCC 17749, JW16-551, and JW16-580 were used for growth kinetics experiments and strain JW16-551 was used for iron metabolomics experiments.

Species	Strain Designation[a]	Strain Type	Isolation Source	Citation
V. alginolyticus	ATCC 17749	Type strain	Spoiled horse mackerel, Japan	Miyamoto et al., 1961
V. alginolyticus	JW16-551	Environmental isolate	Seawater, Looe Key, FL	Borchardt et al., 2020
V. alginolyticus	JW16-580	Environmental isolate	Seawater, Looe Key, FL	Borchardt et al., 2020

[a]ATCC strains obtained from the American Type Culture Collection.

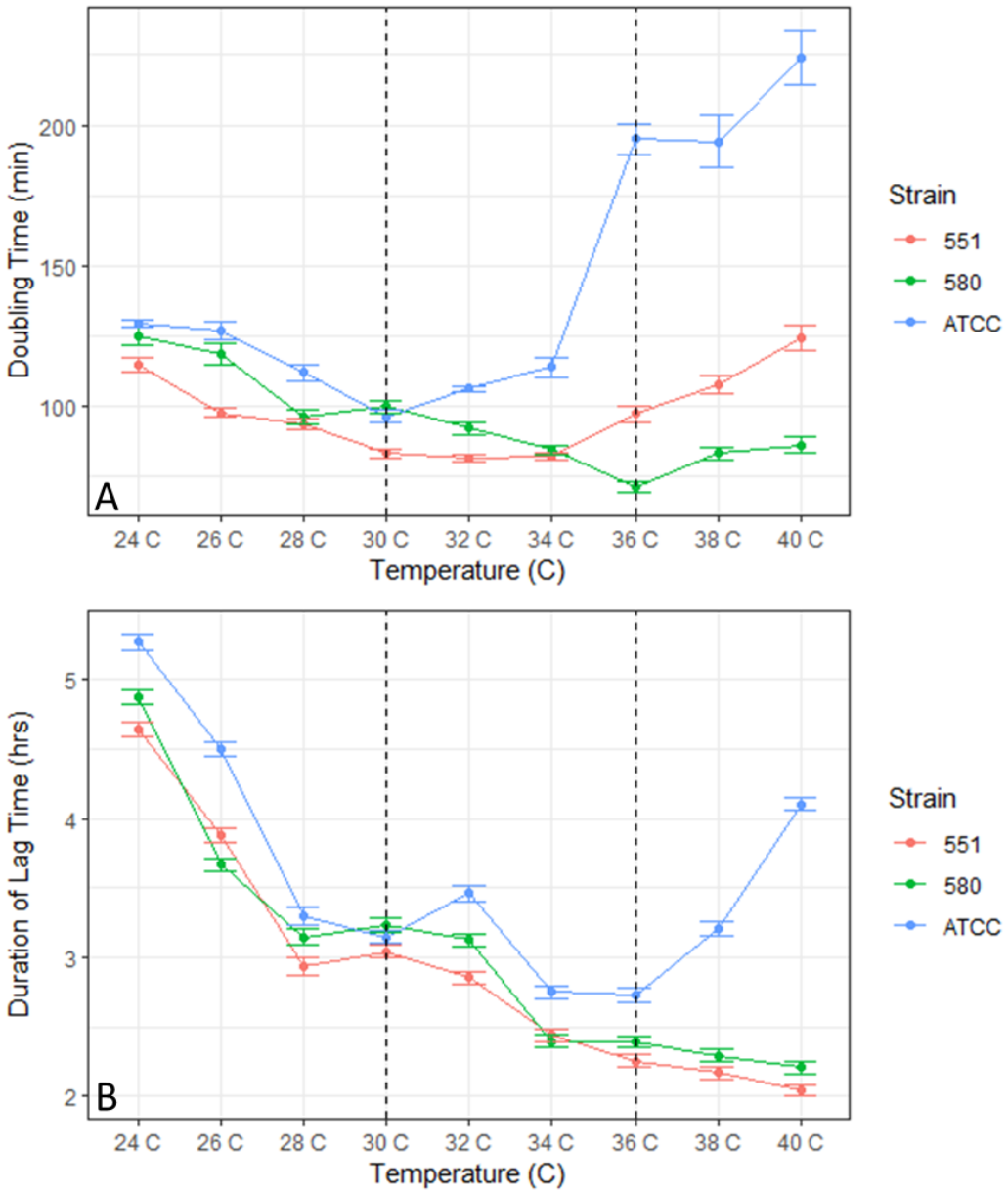

Figure 1: Growth response of *V. alginolyticus* at varying temperatures. Optimal growth range indicated by dashed vertical lines. All cultures grown in LBS 3% (w/v) NaCl broth under non-limiting iron conditions. Linerange values represent the standard error of reported metrics. (A) *V. alginolyticus* doubling time from 24 ^{o}C to 40 ^{o}C.(B) *V. alginolyticus* lag phase duration from 24 ^{o}C to 40 ^{o}C.

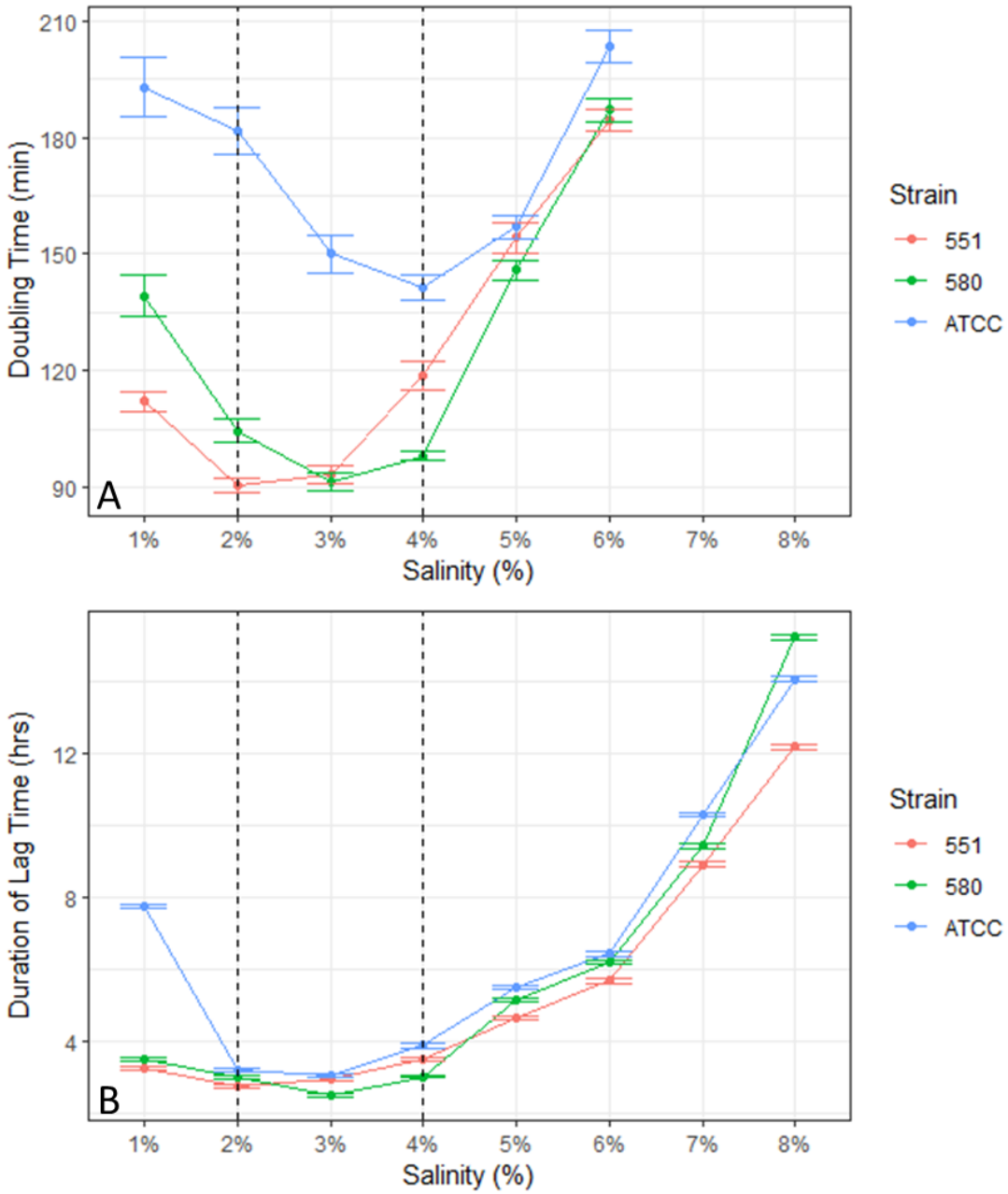

Figure 2: Growth response of *V. alginolyticus* at varying NaCl concentrations. Optimal growth range indicated by dashed vertical lines. All cultures grown in non-iron limiting LBS broth amended to the NaCl concentration designated by the experimental condition and incubated at 30 ^{o}C. Linerange values represent the standard error of reported metrics. (A) *V. alginolyticus* doubling time from 1% to 8% (w/v) NaCl. (B) V. alginolyticus lag phase duration from 1%-8%

(w/v) NaCl. Substantial inhibition of all strains was observed at salt concentrations ≥7% preventing accurate calculation of doubling time, however minor increases in optical density were detected thus, lag time duration measures were collected for these concentrations.

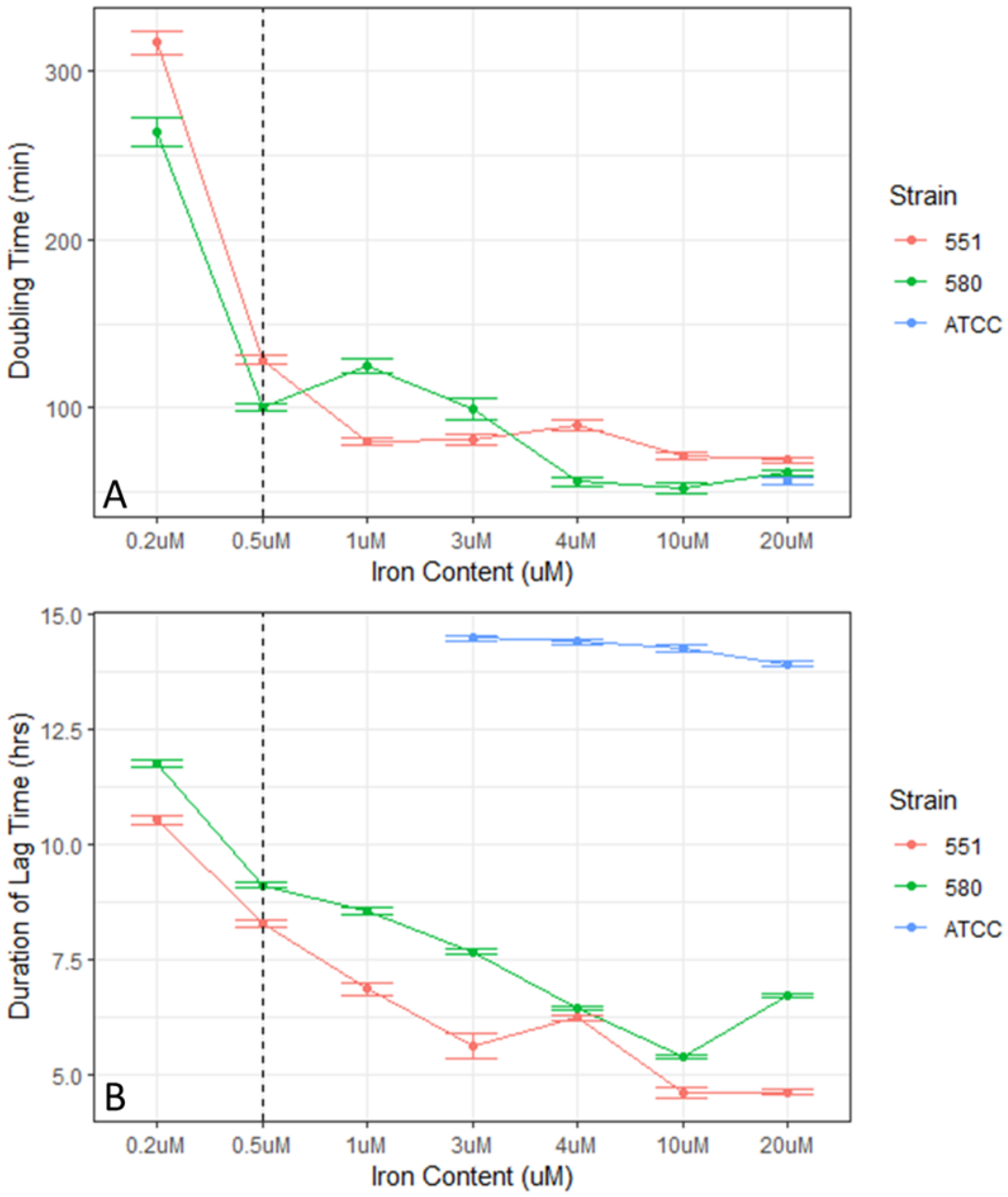

Figure 3: Growth response of *V. alginolyticus* at varying iron concentrations. Optimal growth occurred at all values ≥0.5 µM (indicated by dashed line) with no discernable upper limit. All cultures grown in VibFeL broth at 3% NaCl (w/v) and incubated at 30 ^{o}C. Linerange values represent the standard error of reported metrics. (A) *V. alginolyticus* doubling time from 0.2 to 20 µM iron. (B) *V. alginolyticus* lag phase duration from 0.2 to 20 µM iron. Growth of strain

ATCC 17749 was substantially inhibited at all tested concentrations of iron, thus accurate calculation of the growth rate was not possible for this strain except for the 20 µM concentration. Minor increases in OD were observed at iron concentrations ≥ 3µM allowing for calculation of lag phase duration from 3-30 µM.

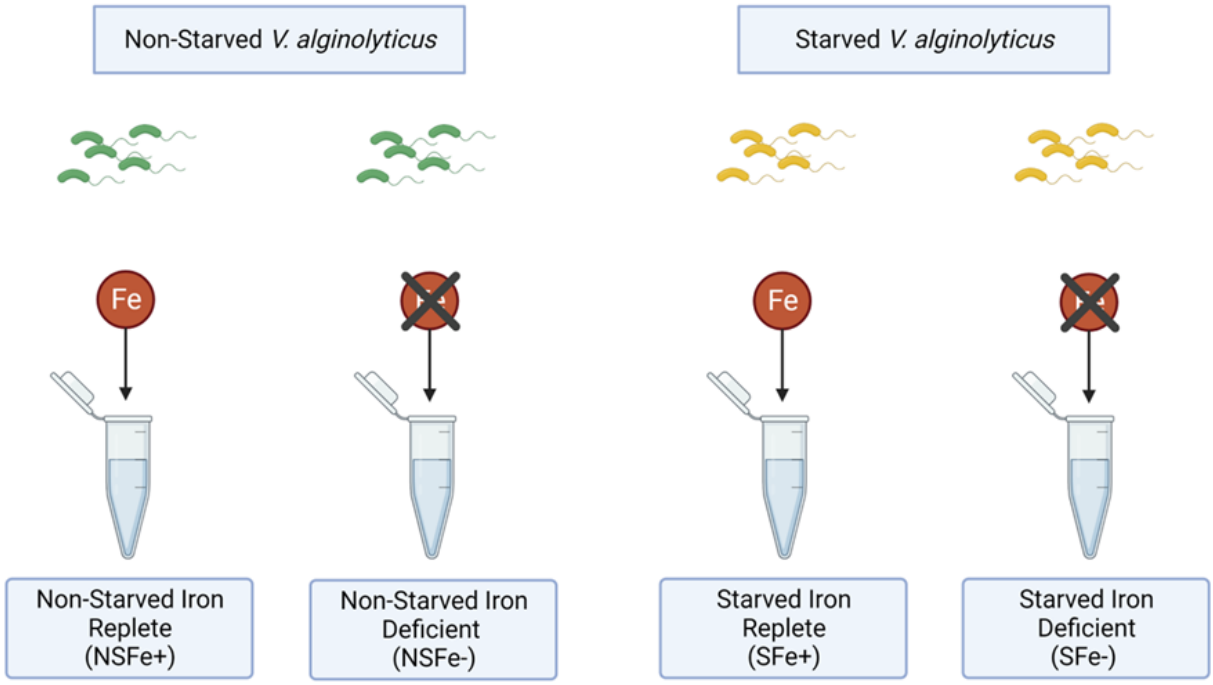

Figure 4: Sample preparation scheme for iron metabolomics experiments. Starvation condition (NS or S) represents the iron content of the initial inoculum culture where non-starved (NS) cultures were grown in non-limiting LBS 3% broth for 18 h at 30° C before inoculation and starved (S) cultures were grown in iron deficient VibFeL (0 µM $FeCl_3$) for 5 d before inoculation. Iron condition (Fe+ or Fe-) represents the iron content of the experimental culture where iron replete (Fe+) cultures were grown in VibFeL broth amended with 4 µM $FeCl_3$ and iron deficient (Fe-) were grown in non-amended VibFeL broth (0 µM $FeCl_3$). All cultures were inoculated with *V. alginolyticus* strain JW16-551. All experimental VibFeL broth cultures were amended to 3% (w/v) NaCl concentration and incubated for 18 h at 30 °C under 100 rpm of shaking agitation.

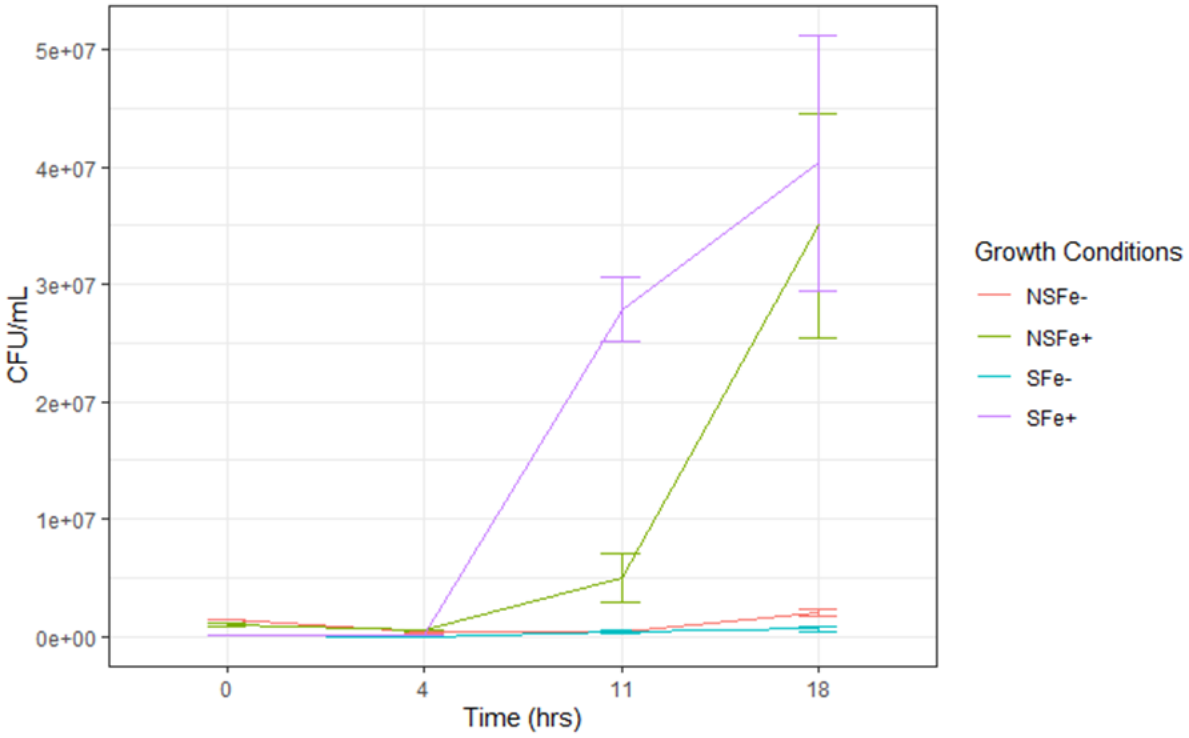

Figure 5: *V. alginolyticus* growth response (CFU mL^{-1}) of iron metabolomics samples. Starvation conditions (NS or S) represent the iron content of the initial inoculation culture and iron conditions (Fe+ or Fe-) represent the iron content of the experimental culture. NSFe+ represents non-starved iron replete cultures, NSFe- represents non-starved iron deficient cultures, SFe+ represents starved iron replete cultures, and SFe- represents starved iron deficient cultures. Cultures measured at 0, 4, 11, and 18 h prior to collection for GC-MS analysis.

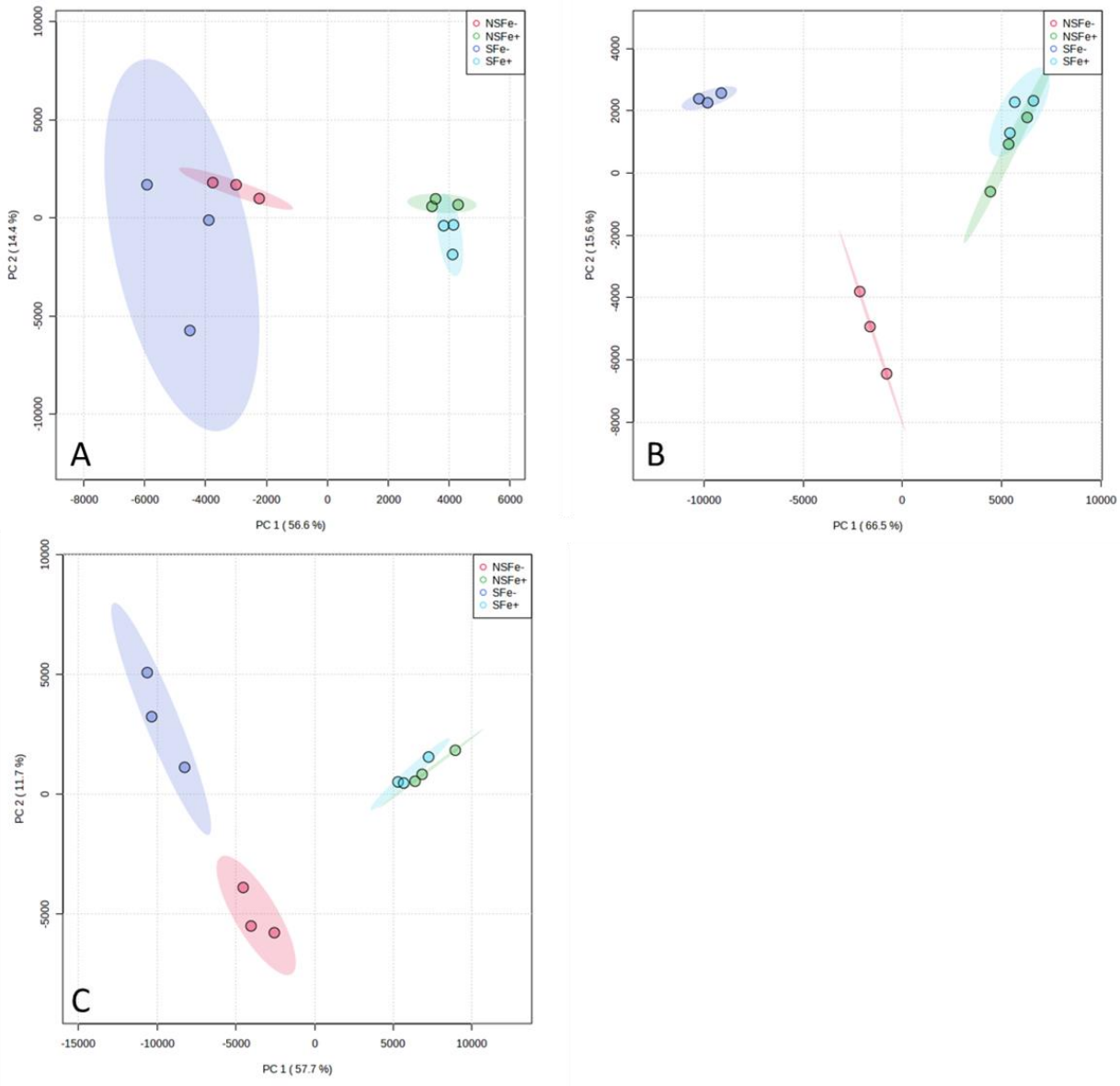

Figure 6: Principal component analysis (PCA) of spectral features identified in strain JW16-551 GC-qToF/MS-based metabolomics; (A) polar endometabolites, (B) nonpolar endometabolites, and (C) exometabolites. Shaded regions represent a 95% confidence interval of the sample group. N = 3 for each sample type.

Table 2: Summary of upregulated metabolites and associated metabolic pathways identified for iron and starvation comparisons.

Sample Comparison[a,b]	Iron Condition	Starvation Condition	Metabolite Type	Number of Upregulated Metabolites Identified	Number of Associated Metabolic Pathways
NSFe+/NSFe-	Replete	Non-starved	Endometabolites	49	25
NSFe-/NSFe+	Deficient	Non-starved	Endometabolites	20	6
SFe+/SFe-	Replete	Starved	Endometabolites	47	30
SFe-/SFe+	Deficient	Starved	Endometabolites	20	4
NSFe+/SFe+	Replete	Non-starved	Endometabolites	14	1
SFe+/NSFe+	Replete	Starved	Endometabolites	30	19
NSFe-/SFe-	Deficient	Non-starved	Endometabolites	12	2
SFe-/NSFe-	Deficient	Starved	Endometabolites	19	3
NSFe+/NSFe-	Replete	Non-starved	Exometabolites	19	14
NSFe-/NSFe+	Deficient	Non-starved	Exometabolites	15	6
SFe+/SFe-	Replete	Starved	Exometabolites	30	14
SFe-/SFe+	Deficient	Starved	Exometabolites	10	6
NSFe+/SFe+	Replete	Non-starved	Exometabolites	9	3
SFe+/NSFe+	Replete	Starved	Exometabolites	11	9
NSFe-/SFe-	Deficient	Non-starved	Exometabolites	23	10
SFe-/NSFe-	Deficient	Starved	Exometabolites	9	6

[a]Sample comparison indicates the two metabolite profiles that were compared where elevated metabolite and pathway totals correspond to the sample in the numerator. Starvation conditions (NS and S) indicate the iron conditions of the initial inoculum culture, whereas iron conditions (Fe+ or Fe-) indicate the iron conditions of the experimental culture.

[b]Non-starved iron replete (NSFe+), non-starved iron deficient (NSFe-), starved iron replete (SFe+), and starved iron deficient (SFe-)

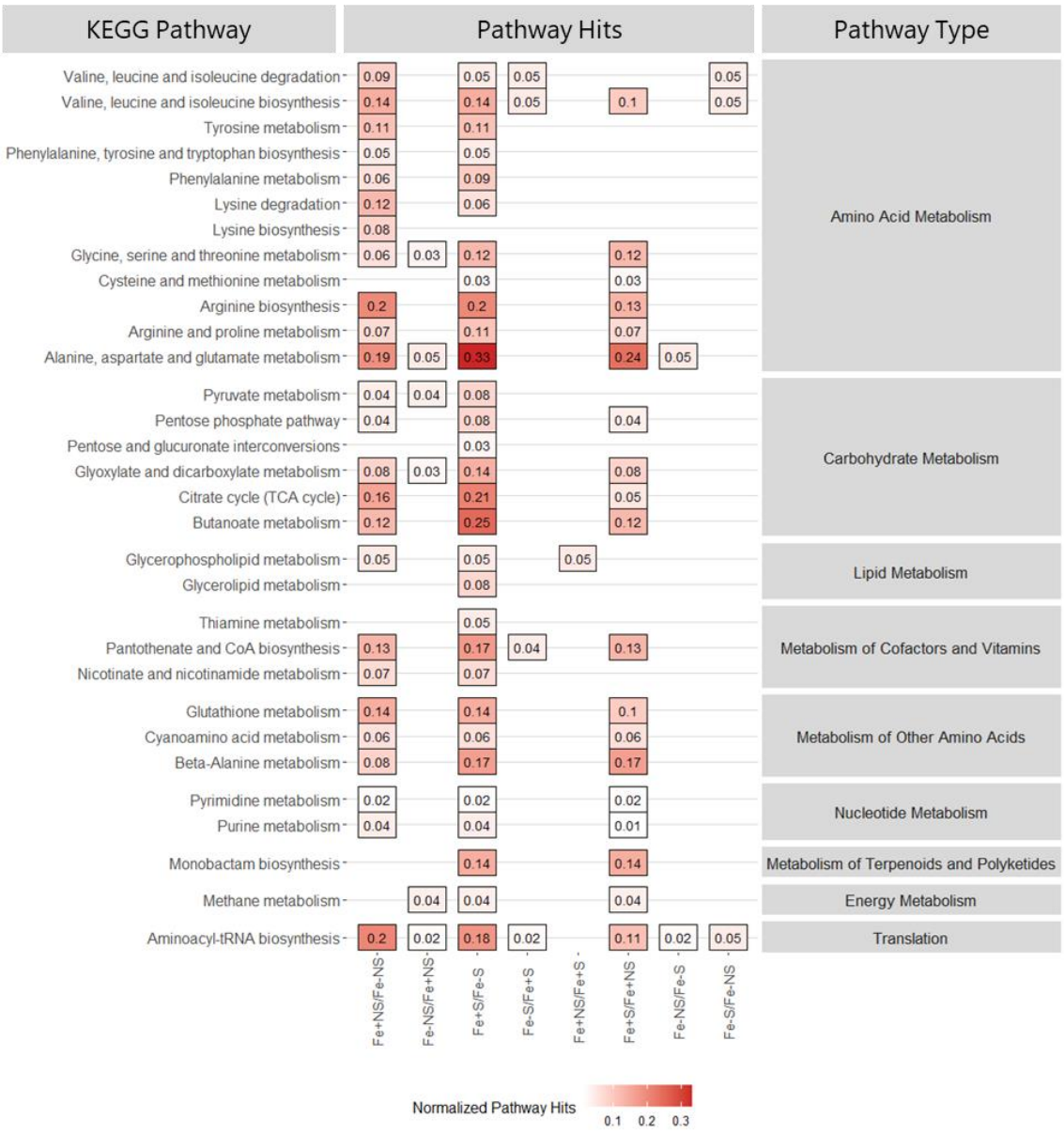

Figure 7: Metabolic pathways associated with significantly upregulated endometabolites detected in *V. alginolyticus* cultures under iron supplementation and iron starvation conditions. The left y-axis lists all associated KEGG pathways, the right y-axis illustrates the broad category of each KEGG pathway, the fill color represents the normalized number of pathway hits found for the metabolites detected, and the x-axis shows the experimental comparison. From left to right, columns 1-4 illustrate iron comparisons and columns 5-8 represent starvation comparisons.

Figure 8: Metabolic pathways associated with significantly upregulated exometabolites detected in *V. alginolyticus* cultures under iron supplementation and iron starvation conditions. The left y-axis lists all associated KEGG pathways, the right y-axis illustrates the broad category of each KEGG pathway, the fill color represents the normalized number of pathway hits found in the metabolites detected, and the x-axis shows the experimental comparison. From left to right, columns 1-4 illustrate iron comparisons and columns 5-8 represent starvation comparisons.

CHAPTER 7

CONCLUSION

Collectively, the works of this dissertation utilize an ecological and public health lens to examine critical aspects of *V. alginolyticus* biology to better understand factors that contribute to the proliferation and distribution of this bacterium in the ambient environment. Through this work we (re)evaluate three major areas of *V. alginolyticus* research need through the characterization of 1) abiotic physiological limits, 2) the metabolic effects of iron, and 3) the role of interspecies interactions in disease transmission. The findings of these works address the substantial need for foundational research on *V. alginolyticus* and can be used to improve methods of risk assessment and outbreak control in both aquaculture and public health settings. Furthermore, this dissertation stands as an appeal to recognize *V. alginolyticus* as a major non-cholera vibrio pathogen on par with highly recognized species such as *V. vulnificus* and *V. parahaemolyticus*.

Chapter 2 presents a detailed review of the published *V. alginolyticus* literature to date and summarizes the current trends of human infections in the United States. Through this work, we highlight the ecological characteristics of this bacterium with an emphasis on attributes that contribute to infection risk and demonstrate the importance of *V. alginolyticus* as an emerging marine pathogen using epidemiological data. In chapter 3 we describe the design and test the use of a prototype optical density meter built for the spectrophotometric measurement of bacterial growth. Though this validation, we demonstrate that the use of this meter is comparable to existing benchtop spectrophotometer methods and highlight the advantages of its design in terms

of cost, user interface, and portability. Chapter 4 presents a standardized protocol for the tagging of vibrios using green fluorescent protein (GFP) and evaluates the stability of transconjugants for *in situ* experiments. The transconjugant strains created through this work allow for the differentiation of target *Vibrio* spp. within complex mixtures and are critical to the experimental methods of chapter 5. Chapter 5 explores the viability of an ingestion-based transmission pathway for the acquisition of *V. alginolyticus* following colonization of a zooplankton vector. Using sea anemones as models for coral ingestion we demonstrated that ingestion of colonized zooplankton facilitates receipt of a significantly higher acquired *V. alginolyticus* dose when compared to exposure via the ambient water suggesting that ingestion may represent and important transmission pathway for this bacterium. Lastly, in chapter 6 we describe the optimal and tolerable physiological limits of *V. alginolyticus* in relation to changing temperature, salinity, and iron content. Through these experiments, we demonstrate the importance of these abiotic determinants on the regulation of *V. alginolyticus* populations and stress the critical importance of iron availability as a limiting nutrient for the stimulation of metabolism. Combined, the works of this dissertation represent a modernized fundamental characterization of *V. alginolyticus* with an emphasis on understanding this bacterium from a one health perspective. While much remains to be discovered, we hope the research presented here provides much needed groundwork for continued investigation, characterization, and surveillance of *V. alginolyticus* in the future.

APPENDIX 1: CHAPTER 3 SUPPLEMENTAL MATERIAL

Supplemental Tables and Figures

Table S1: Cost of ArdOD components. Costs values based on price as of January 2023.

Component Name	Manufacturer	Cost (USD)	Quantity (Pieces)
Arduino Uno	Arduino	$28.50	1
USB Connector	Arduino	$0.00[a]	1
Protoscrew-shield	Adafruit	$14.95	1
600nm LED	Chanzon	$7.99	10
200Ω Resistor	EDGELEC	$5.49	100
9-Volt Battery Clips	KASSupply	$5.99[b]	3
LED Adapter (AC Adapter Model 1250)	LEDMO	$12.99[c]	1
Light Sensor (BH1750)	HiLetgo	$7.99	3
Printed Circuit Board	EPLZON	$12.59	7
2.54mm Terminal Block Pins	Adafruit ASIN	$1.55	1
22-Gauge Tinned Copper Jumper Wires	Tuofend 600v	$15.99	6 (13.4 ft rolls)
Electrical Tape	Scotch	$2.99	1 (0.75 ft roll)
3-D Printed Housing	*NA*	*Variable*	*NA*

[a]USB connecter is included with most Arduino Uno purchase options.

[b]Battery clips are only required for battery supplied power.

[c]LED adapter is only required for outlet supplied power.

APPENDIX 2: CHAPTER 4 SUPPLEMENTAL MATERIAL

Supplemental Tables and Figures

Table S1: pVSV102 conjugation efficacy for all target vibrios. Mixtures mated triparentally with E. coli carrying the helper plasmid pEVS104 and the donor plasmid pVSV102 on kanamycin amended media equivalent to the designated stress concentration. Mating mixtures were performed on LBS 3% agar plates amended with 300 µg mL^{-1} kanamycin and incubated at 28 ºC for up to 72 h.

Species	**Strain**	**Kanamycin Stress Concentration (µg mL^{-1})**	**Number of Mating Mixtures Attempted**	**CFU of Target Vibrio Added[a]**	**Development of Fluorescent Patches[b] (hours)**	**Number of Successful Mating Mixtures**
Photobacterium damselae	ATCC 33539	15	24	$3.8x10^7$	NA[c]	24
Vibrio alginolyticus	ATCC 17749	75	24	$4.6x10^7$	24	21
Vibrio anguillarum	ATCC 19264	35	24	$3.0x10^7$	48	24
Vibrio campbellii	ATCC 25920	35	24	$6.3x10^7$	24	24
Vibrio coralliilyticus	ATCC BAA-450	50	24	$3.3x10^4$	72	24
Vibrio cholerae	ATCC 14035	50	24	$2.9x10^6$	48	20
Vibrio harveyi	ATCC 14126	25	24	$7.1x10^6$	72[c]	16
Vibrio mediterranei	ATCC 43341	100	24	$2.3x10^7$	24	24
Vibrio parahaemolyticus	ATCC 43996	35	24	$3.7x10^7$	24	24

Vibrio pelagius	ATCC 25916	25	24	$4.4x10^5$	48	11
Vibrio splendidus	ATCC 33869	75	24	$1.16x10^7$	48	10
Vibrio vulnificus	ATCC 27562	50	24	$6.2x10^7$	48	24

[a]All mating mixtures contained 6.0x106 CFU of E. coli carrying the helper plasmid pEVS104, 6.3x106 CFU of E. coli carrying the donor plasmid pVSV102, and the target vibrio indicated in this column.

[b]The development of fluorescent patches suggests that the mating mixture resulted in a successful conjugation trial. Observation of these patches can be used as a laboratory diagnostic tool to indicate potentially successful mixtures to progress to purification. Confirmation of the purified vibrio must be accomplished using fluorescent microscope.

[c]Fluorescence is not visible in the gross morphology of P. damselae mating mixtures and is not always visible in V. harveyi mating mixtures. Conjugation success for these species must be identified via microscopy following purification of the mixture on TCBS agar.

Table S2: Evaluation of interspecies mobilization of pVSV102 from tagged *V. parahaemolyticus* into non-tagged *V. cholerae* and *V. vulnificus* grown in co-culture in antibiotic-free media. Species identity confirmed using CHROMagar *Vibrio*. Fluorescence identified using gross observation of the CFU illuminated by a 495 nm blacklight and confirmed with fluorescent microscopy (495 excitation wavelength).

Time (hours)	**Total V. parahaemolyticus (CFU)**	**Fluorescent V. parahaemolyticus (CFU)**	**Non-Fluorescent V. parahaemolyticus (CFU)**	**Total V. cholerae or V. vulnificus (CFU)**	**Total Fluorescent V. cholerae or V. vulnificus (CFU)**	**Total Non-Fluorescent V. cholerae or V. vulnificus (CFU)**
0	28	28	0	21	0	21
24	8	8	0	45	0	45
48	8	8	0	35	0	35
72	4	4	0	40	0	40
96	5	4	1	73	0	73
120	7	5	2	90	0	90

Table S3: Maximum observed mean GFP loss for all tagged vibrio strains. Antibiotic supplemented cultures maintained at 300µg/mL kanamycin.

Species	***Strain***	***Time (hours)[a]***	***Media Type***	***Antibiotics Present (+ or -)***	***Percent of CFU that Lost Fluorescence (%)[b]***
Photobacterium damselae	ATCC 33539	120	LBS 3%	-	3.4
				+	0.0
		48	ASW	-	3.0
Vibrio alginolyticus	ATCC 17749	120	LBS 3%	-	2.0
				+	0.0
		48	ASW	-	0.0
Vibrio anguillarum	ATCC 19264	48	LBS 3%	-	18.5
		120		+	0.0
		48	ASW	-	0.0
Vibrio campbellii	ATCC 25920	96	LBS 3%	-	5.6
		120		+	0.0
		48	ASW	-	0.0
Vibrio coralliilyticus	ATCC BAA-450	120	LBS 3%	-	33.3
				+	0.0
		48	ASW	-	3.8
Vibrio cholerae	ATCC 14035	120	LBS 3%	-	90.0
				+	0.0
		48	ASW	-	9.8
Vibrio harveyi	ATCC 14126	120	LBS 3%	-	37.1
				+	0.0
		24	ASW	-	8.7
Vibrio mediterranei	ATCC 43341	72	LBS 3%	-	27.3
		96		+	10.3
		48	ASW	-	1.7
Vibrio parahaemolyticus	ATCC 43996	72	LBS 3%	-	7.9
		120		+	0.0
		48	ASW	-	0.0
Vibrio pelagius	ATCC 25916	120	LBS 3%	-	11.1
				+	0.0*
		0	ASW	-	0.0
Vibrio splendidus	ATCC 33869	120	LBS 3%	-	11.4
				+	0.0
		24	ASW	-	0.0*

Vibrio vulnificus	ATCC 27562	72	LBS 3%	-	10.9
		120		+	0.0
		48	ASW	-	18.4

[a]Indicates the timepoint at which each transconjugant vibrio demonstrated the greatest loss of GFP.

[b]A loss value of 0.0% indicates that no CFU lost fluorescence under the described culture conditions. Values denotes with a * symbol indicate cultures that were not recoverable throughout the entirety of the experiment.

Table S4: Generation estimation, CFU concentrations, and optical density for subculture experimentation. Generations calculated as the number of doubling cycles required for the inoculation CFU to surpass the stationary phase CFU rounded to the nearest whole generation.

Species	**Strain**	**CFU Inoculated Per Subculture (100 µL)**	**Total CFU at Stationary Phase (4 mL)**	**OD_{600} After Inoculation (0 h)**	**OD_{600} at Stationary Phase (~18 h)**	**Estimated Generations to Stationary Phase**
Photobacterium damselae	ATCC 33539	$4.2x10^7$	$6.8x10^8$	0.046	1.647	6
Vibrio alginolyticus	ATCC 17749	$1.4x10^7$	$8.8x10^8$	0.099	2.006	5
Vibrio anguillarum	ATCC 19264	$3.5x10^7$	$1.2x10^9$	0.054	1.835	6
Vibrio campbellii	ATCC 25920	$6.7x10^7$	$1.84x10^9$	0.065	1.434	5
Vibrio coralliilyticus	ATCC BAA-450	$4.0x10^7$	$1.64x10^8$	0.070	1.371	5
Vibrio cholerae	ATCC 14035	$1.6x10^7$	$2.08x10^8$	0.075	1.741	5
Vibrio harveyi	ATCC 14126	$2.6x10^7$	$1.12x10^8$	0.041	1.514	6
Vibrio mediterranei	ATCC 43341	$2.4x10^7$	$1.56x10^9$	0.050	1.557	5
Vibrio parahaemolyticus	ATCC 43996	$3.7x10^7$	$2.32x10^9$	0.067	1.824	5
Vibrio pelagius	ATCC 25916	$1.7x10^6$	$1.32x10^7$	0.031	1.361	6

Vibrio splendidus	ATCC 33869	$1.18x10^{7}$	$1.08x10^{8}$	0.044	1.564	6
Vibrio vulnificus	ATCC 27562	$4.6x10^{7}$	$2.44x10^{9}$	0.052	1.636	5

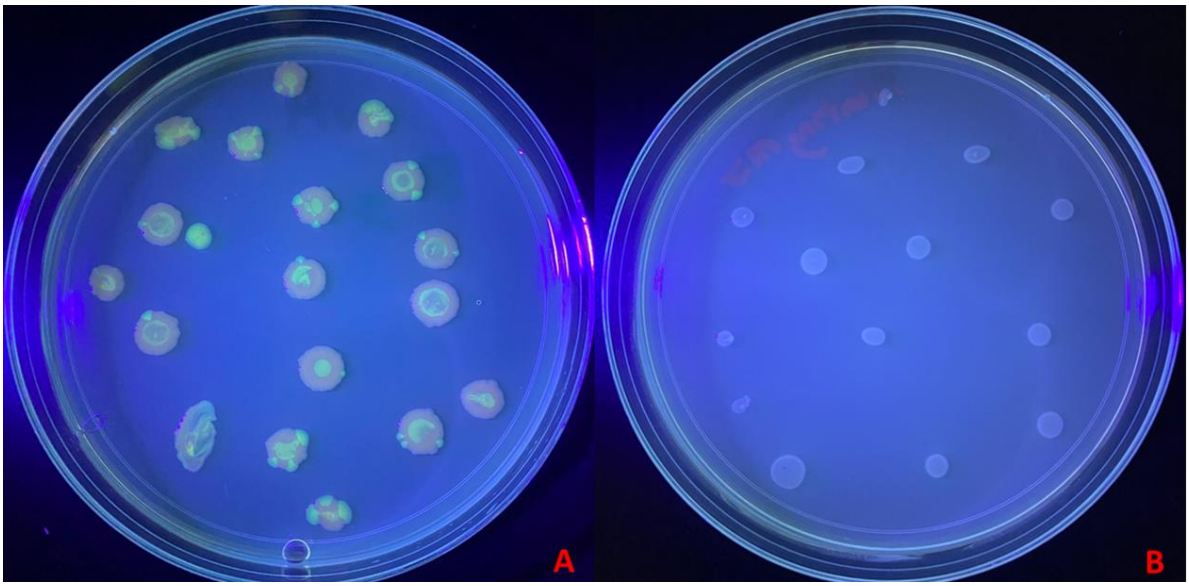

Figure S1: GFP mating mixtures of *V. mediterranei* illuminated with the aid of a 495 nm blacklight. (A) Mating mixture demonstrating potentially successful conjugation of the *gfp*. Bright green patches within the cell masses indicate successful transfer trials that can be moved to the purification (TCBS streaking) step. (B) Unsuccessful mating mixture with no visible fluorescence. The unsuccessful result of this mixture was due to the use of a kanamycin concentration (150 µg mL^{-1}) that was above the tolerance limit for *V. mediterranei* which likely resulted in death of the cells before conjugation could be accomplished. It should be noted that while this visible check was useful in the transfer of pVSV102, this method my not be amenable to other more subtle reporters.

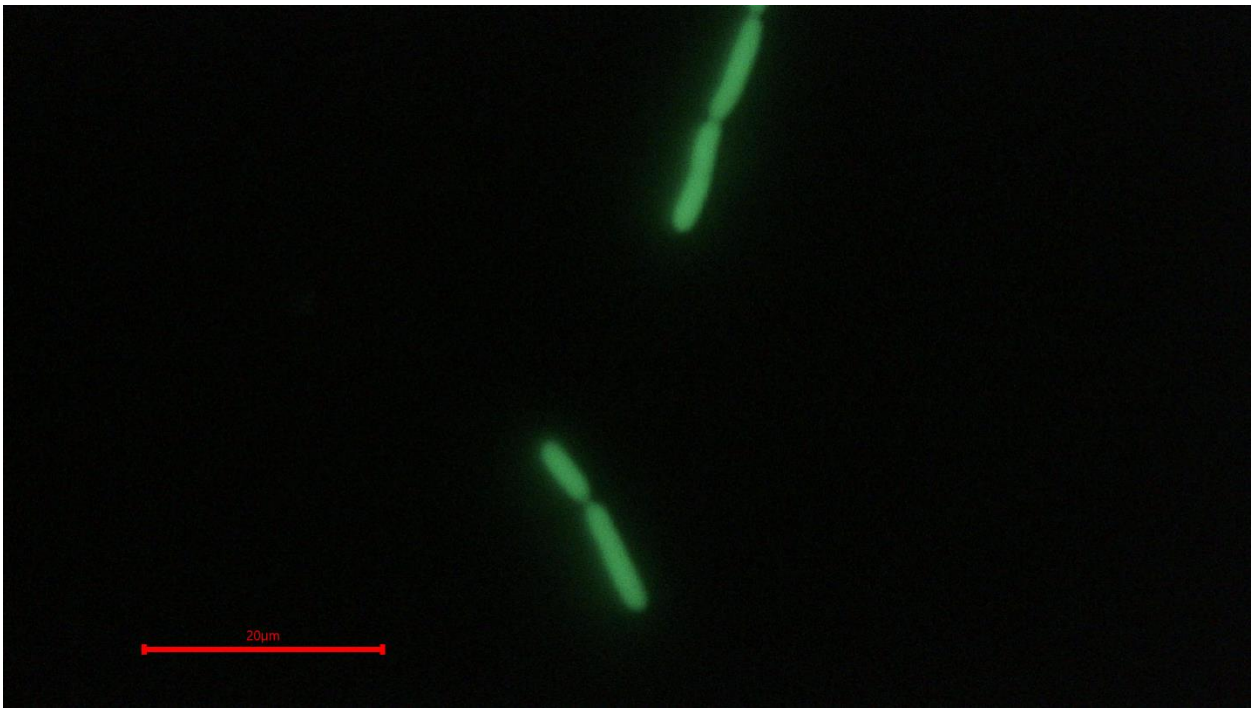

Figure S2: GFP tagged *P. damselae*. Culture grown from a -80^{o}C frozen stock of the purified GFP-tagged culture. Image taken after overnight growth in LBS 3% amended with 300µg/mL kanamycin. Source strain ATCC 33539. Magnification at 1000X.

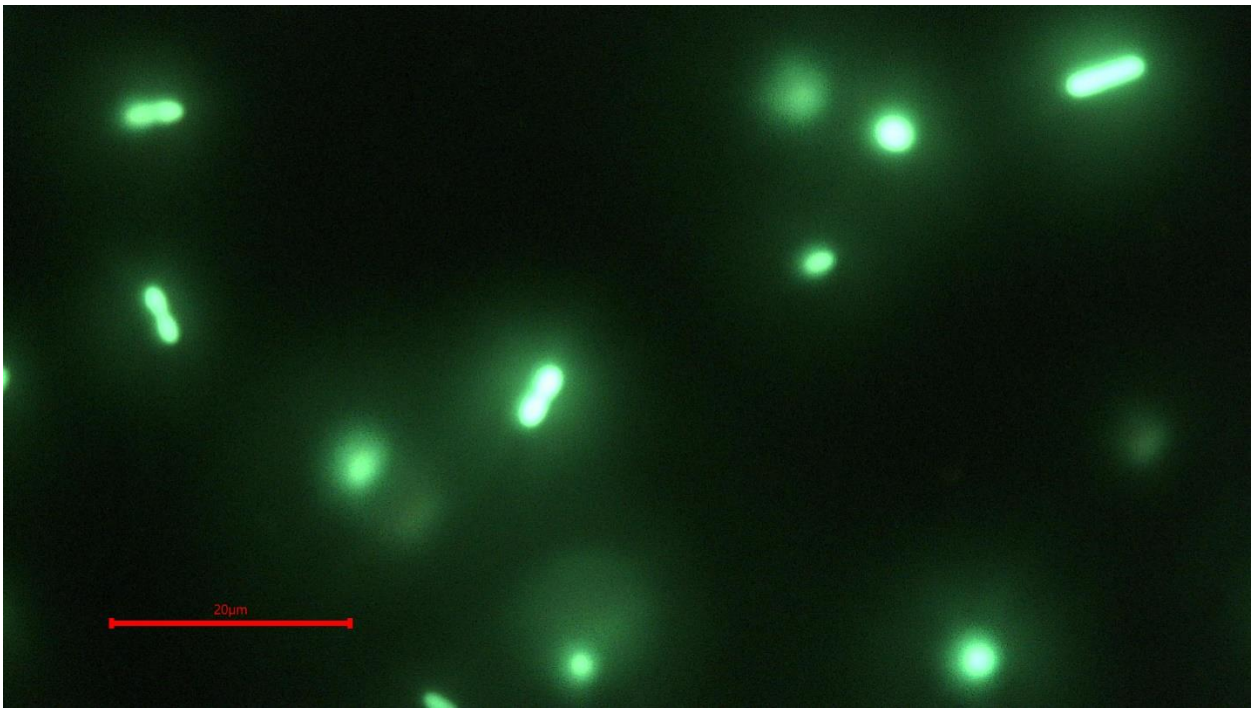

Figure S3: GFP tagged *V. alginolyticus*. Culture grown from a -80ºC frozen stock of the purified GFP-tagged culture. Image taken after overnight growth in LBS 3% amended with 300µg/mL kanamycin. Source strain ATCC 17749. Magnification at 1000X.

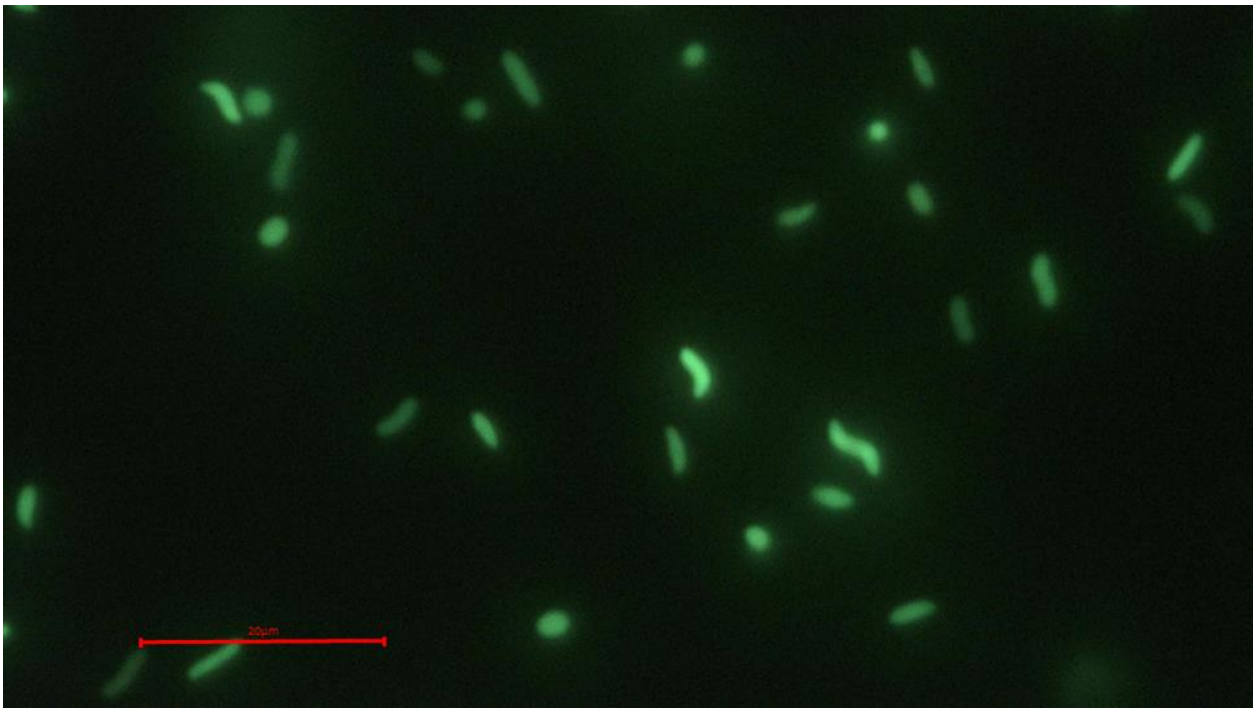

Figure S4: GFP tagged *V. anguillarum*. Culture grown from a -80ºC frozen stock of the purified GFP-tagged culture. Image taken after overnight growth in LBS 3% amended with 300µg/mL kanamycin. Source strain ATCC 19264. Magnification at 1000X.

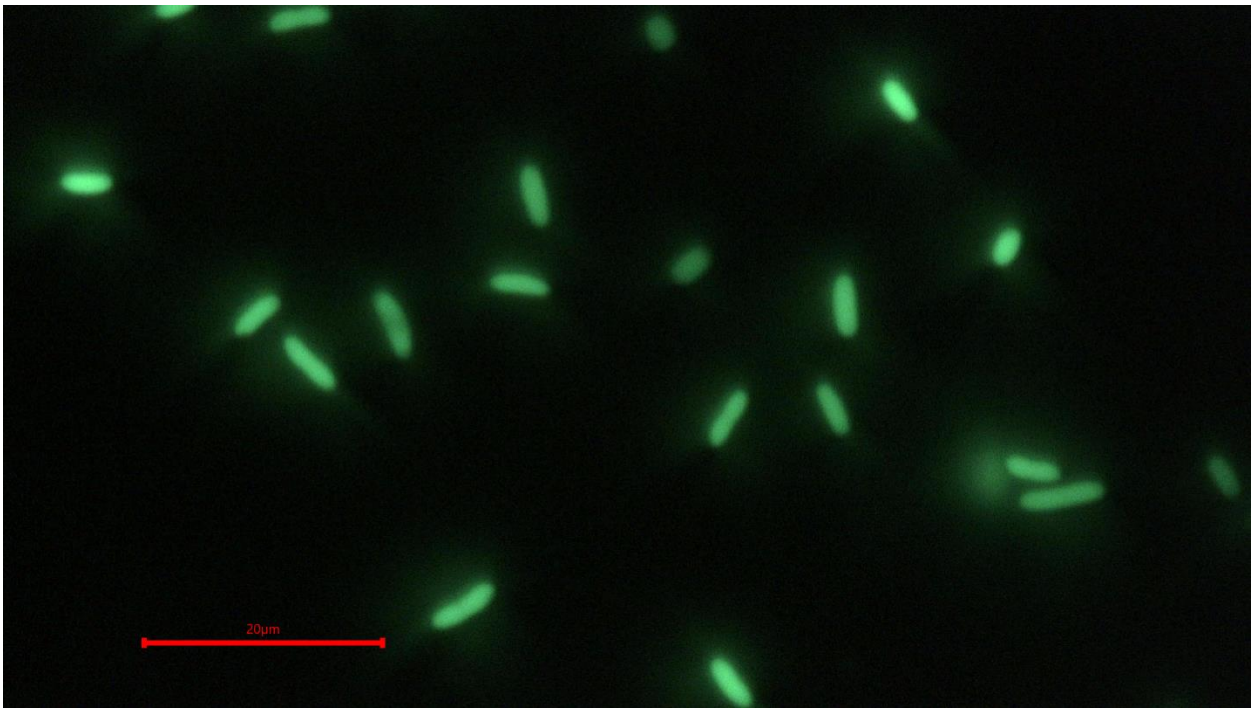

Figure S5: GFP tagged *V. campbellii*. Culture grown from a -80^{o}C frozen stock of the purified GFP-tagged culture. Image taken after overnight growth in LBS 3% amended with 300µg/mL kanamycin. Source strain ATCC 25920. Magnification at 1000X.

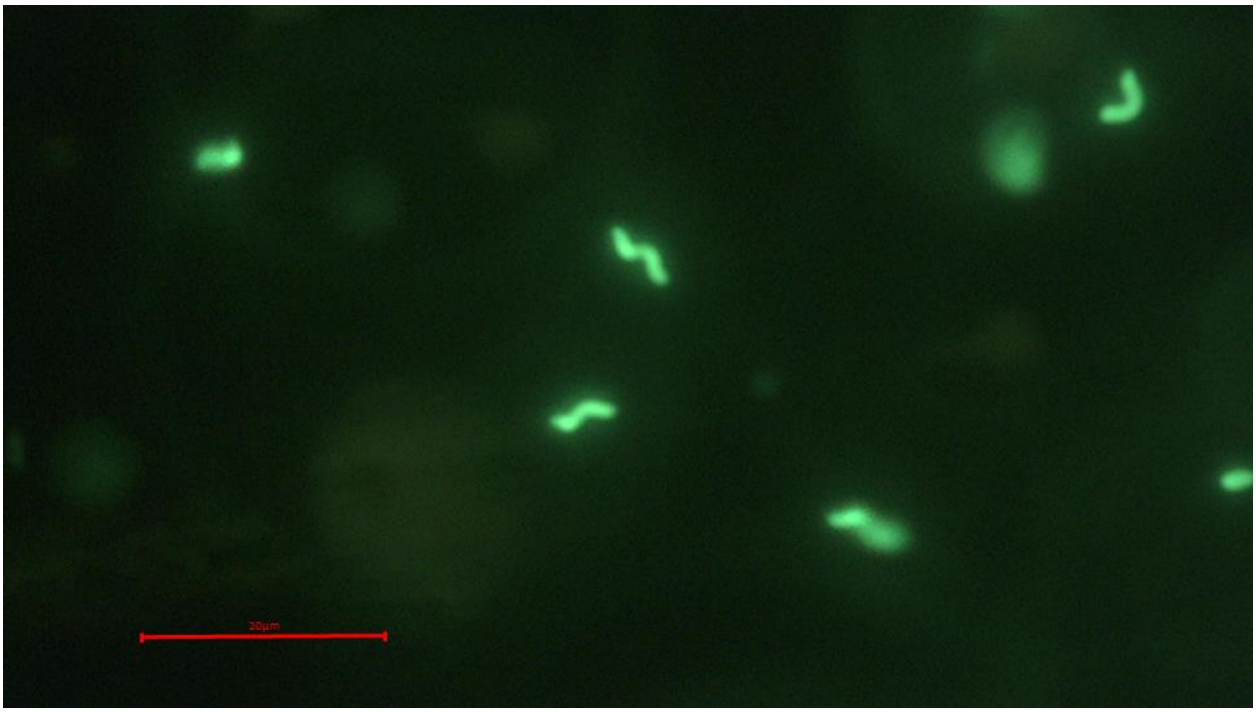

Figure S6: GFP tagged *V. coralliilyticus*. Culture grown from a -80ºC frozen stock of the purified GFP-tagged culture. Image taken after overnight growth in LBS 3% amended with 300µg/mL kanamycin. Source strain ATCC BAA-450 Magnification at 1000X.

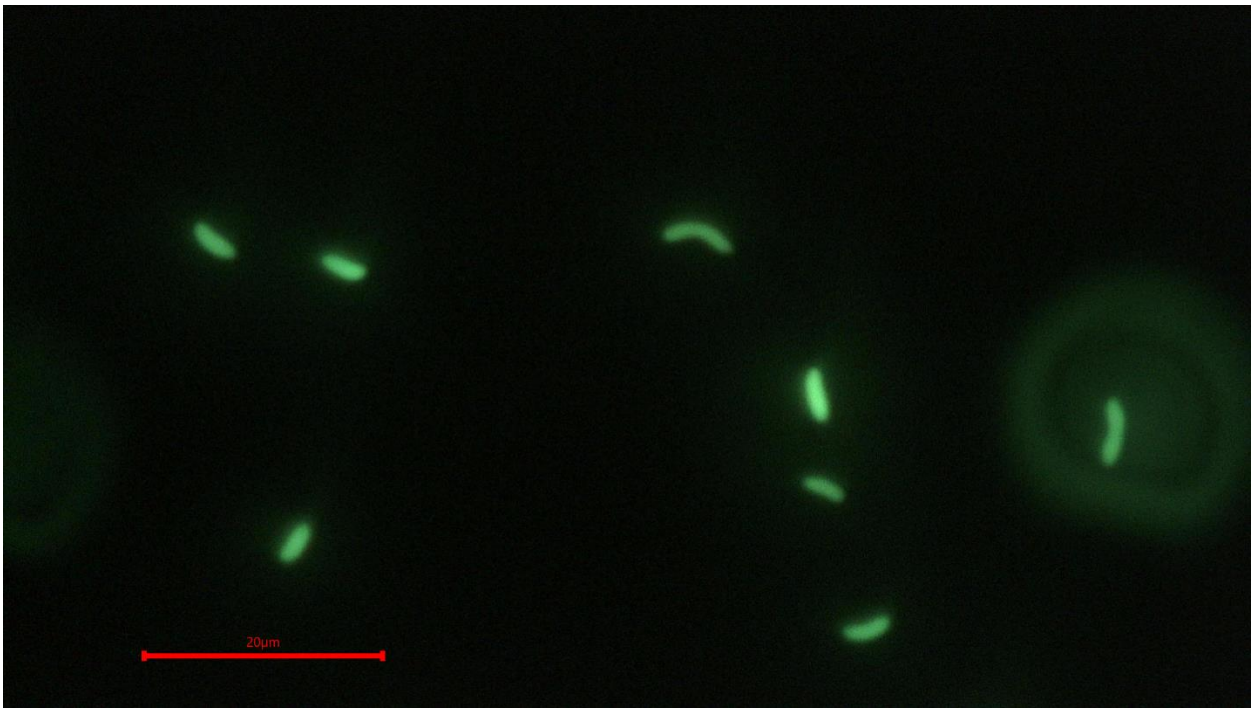

Figure S7: GFP tagged *V. cholerae*. Culture grown from a -80ºC frozen stock of the purified GFP-tagged culture. Image taken after overnight growth in LBS 3% amended with 300µg/mL kanamycin. Source strain ATCC 14035. Magnification at 1000X.

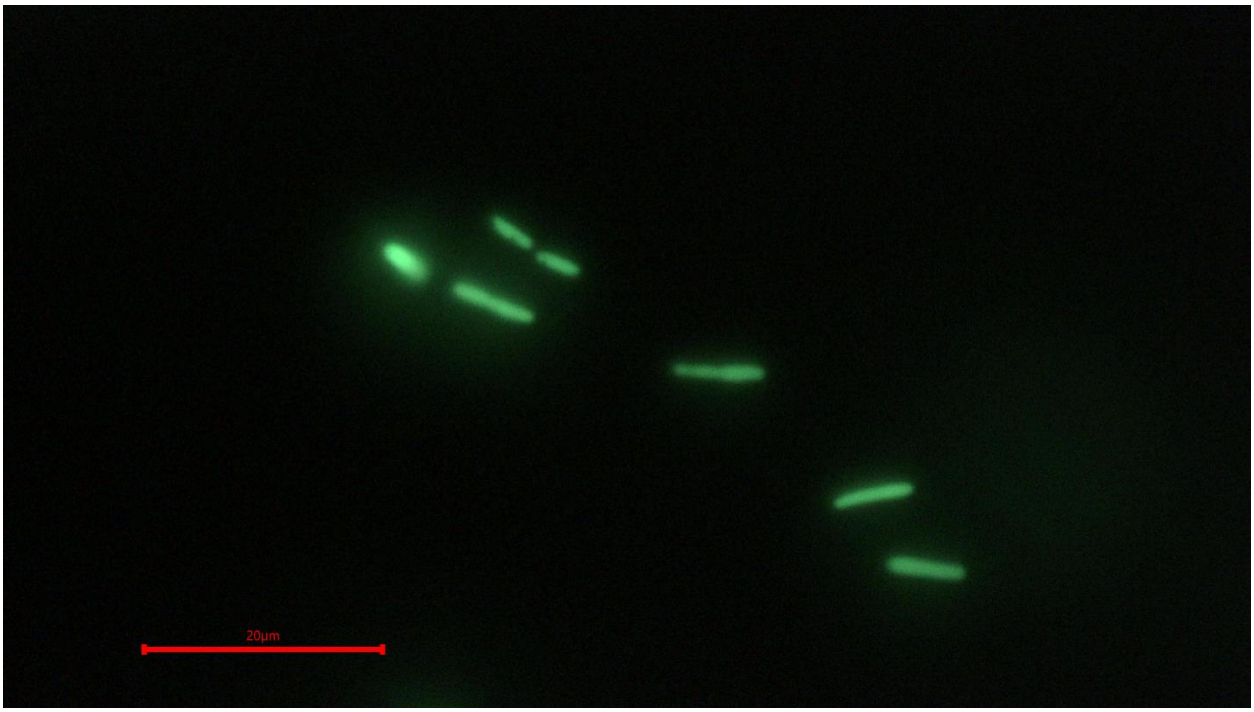

Figure S8: GFP tagged *V. harveyi*. Culture grown from a -80ºC frozen stock of the purified GFP-tagged culture. Image taken after overnight growth in LBS 3% amended with 300µg/mL kanamycin. Source strain ATCC 14126. Magnification at 1000X.

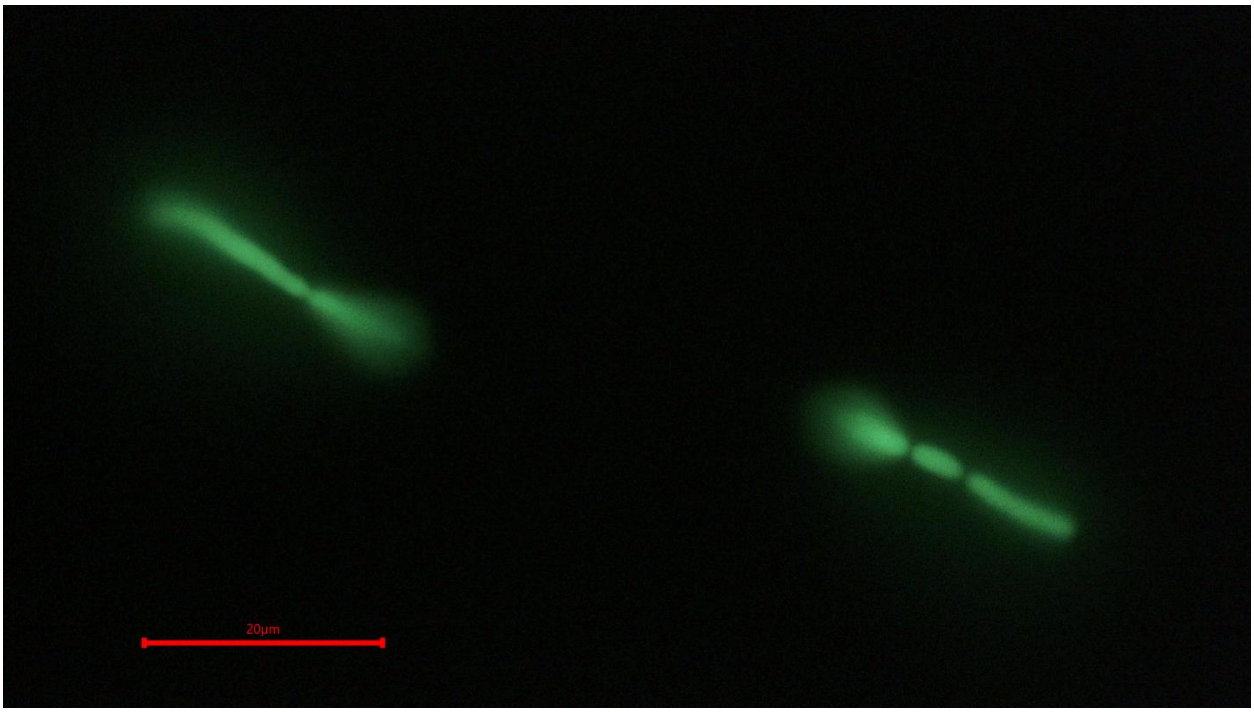

Figure S9: GFP tagged *V. mediterranei*. Culture grown from a -80ºC frozen stock of the purified GFP-tagged culture. Image taken after overnight growth in LBS 3% amended with 300µg/mL kanamycin. Source strain ATCC 43341. Magnification at 1000X.

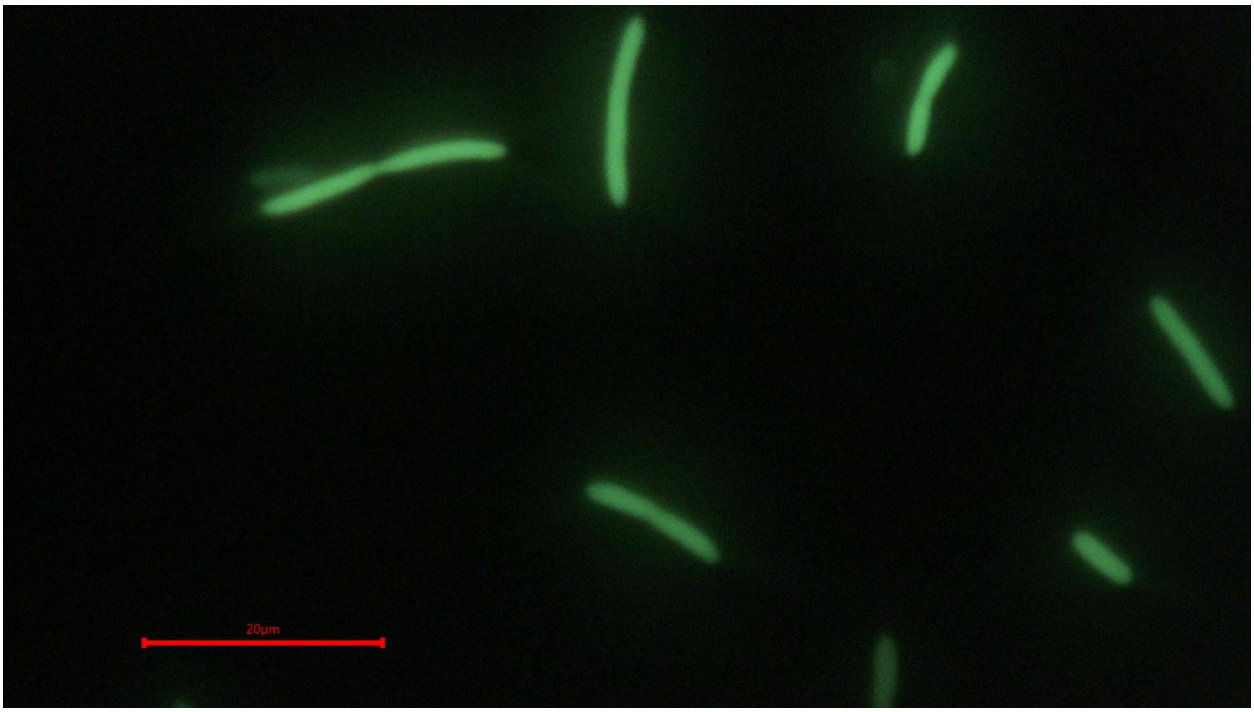

Figure S10: GFP tagged *V. parahaemolyticus*. Culture grown from a -80^{o}C frozen stock of the purified GFP-tagged culture. Image taken after overnight growth in LBS 3% amended with 300µg/mL kanamycin. Source strain ATCC 43996. Magnification at 1000X.

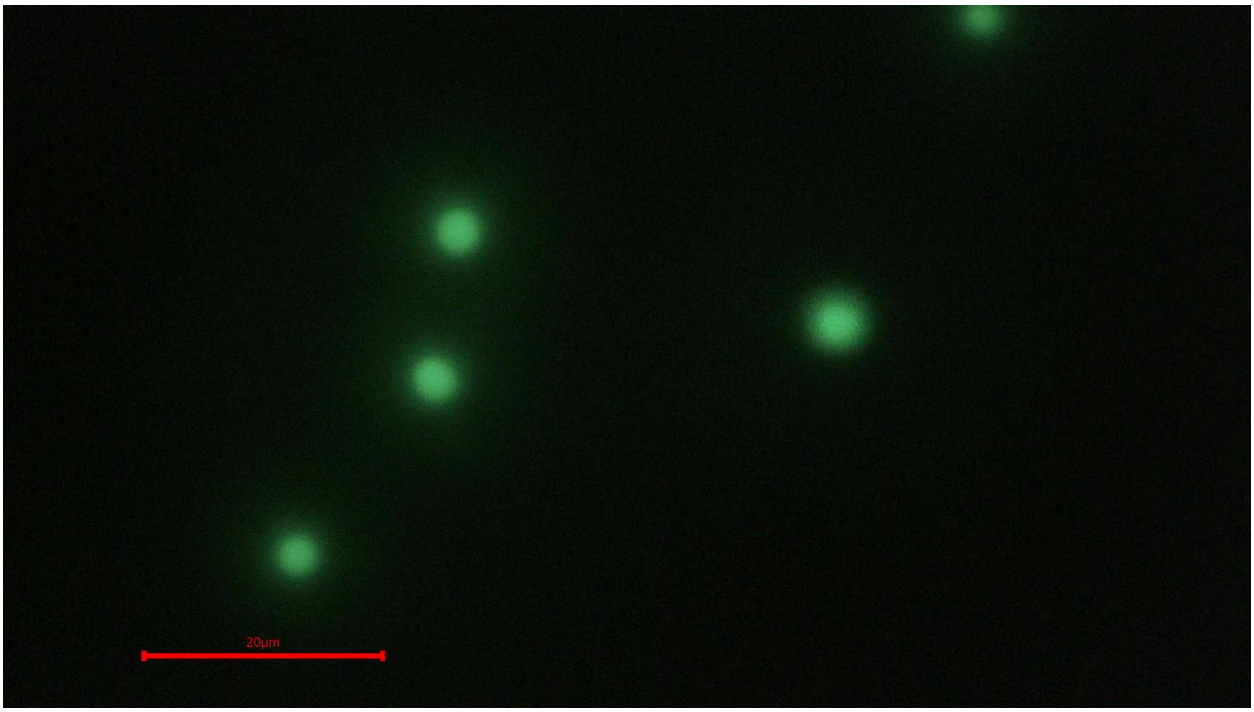

Figure S11: GFP tagged *V. pelagius*. Culture grown from a -80ºC frozen stock of the purified GFP-tagged culture. Image taken after overnight growth in LBS 3% amended with 300µg/mL kanamycin. Source strain ATCC 25916. Magnification at 1000X.

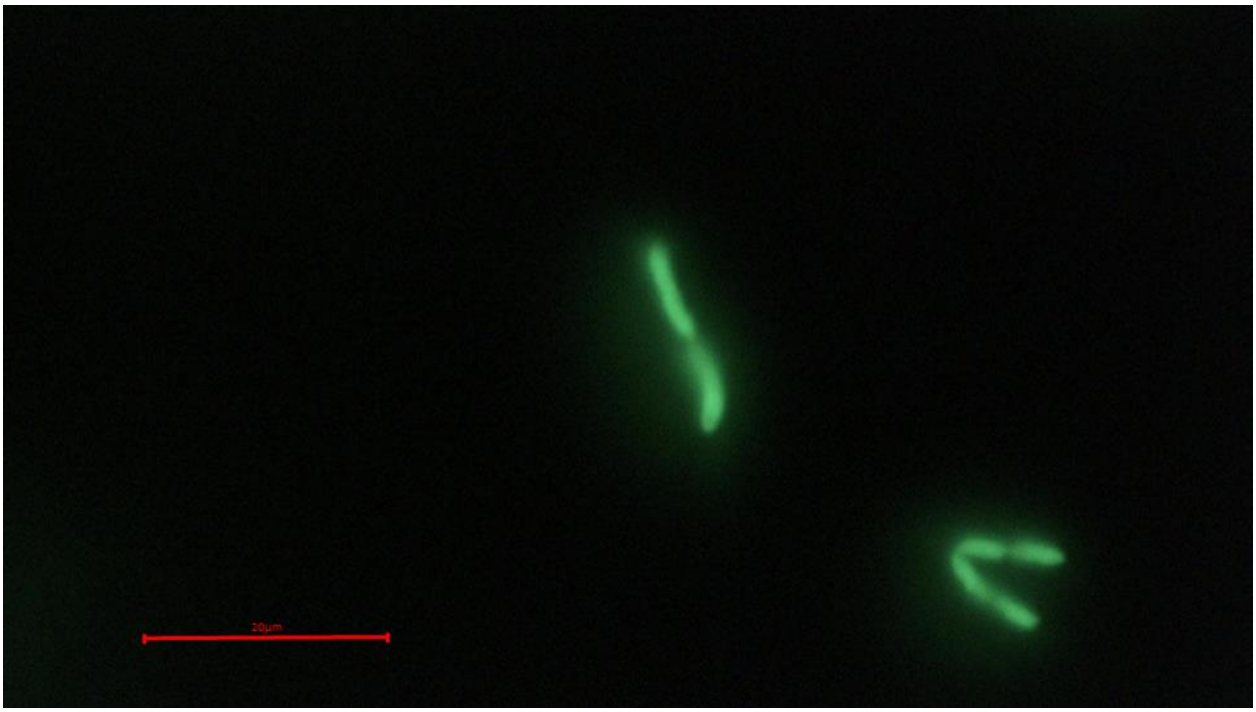

Figure S12: GFP tagged *V. splendidus*. Culture grown from a -80ºC frozen stock of the purified GFP-tagged culture. Image taken after overnight growth in LBS 3% amended with 300µg/mL kanamycin. Source strain ATCC 33869. Magnification at 1000X.

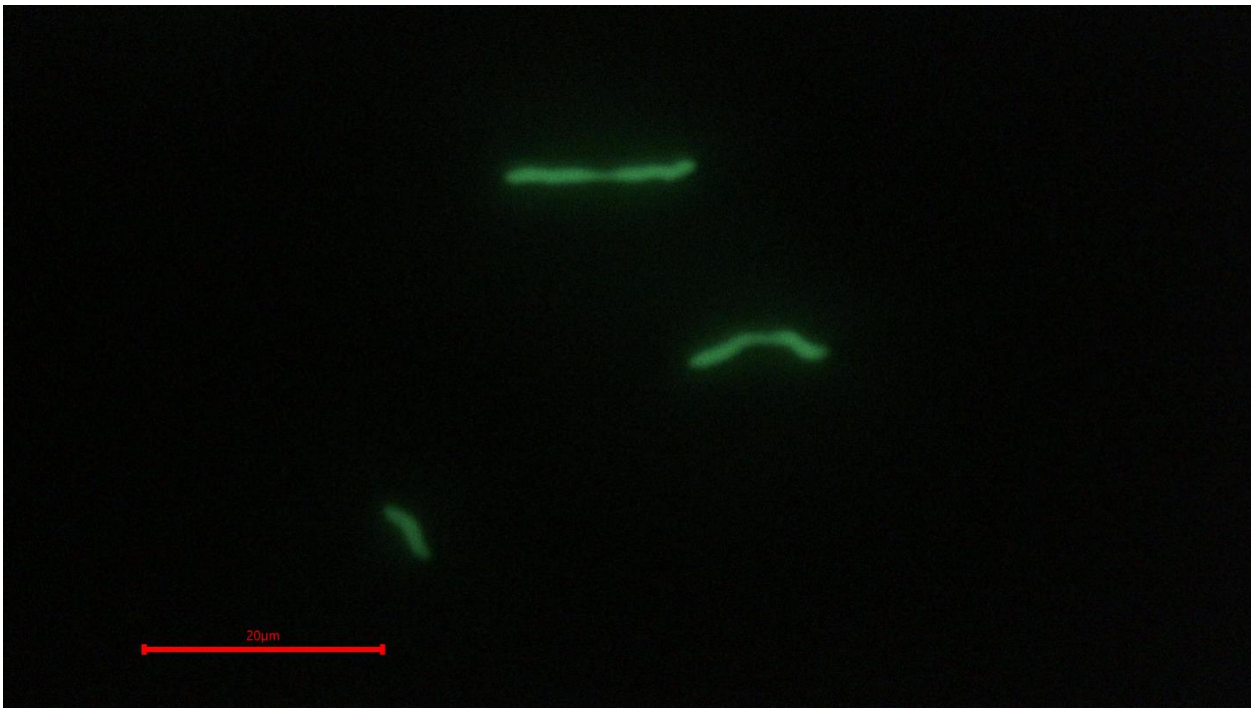

Figure S13: GFP tagged *V. vulnificus*. Culture grown from a -80ºC frozen stock of the purified GFP-tagged culture. Image taken after overnight growth in LBS 3% amended with 300µg/mL kanamycin. Source strain ATCC 27562. Magnification at 1000X,

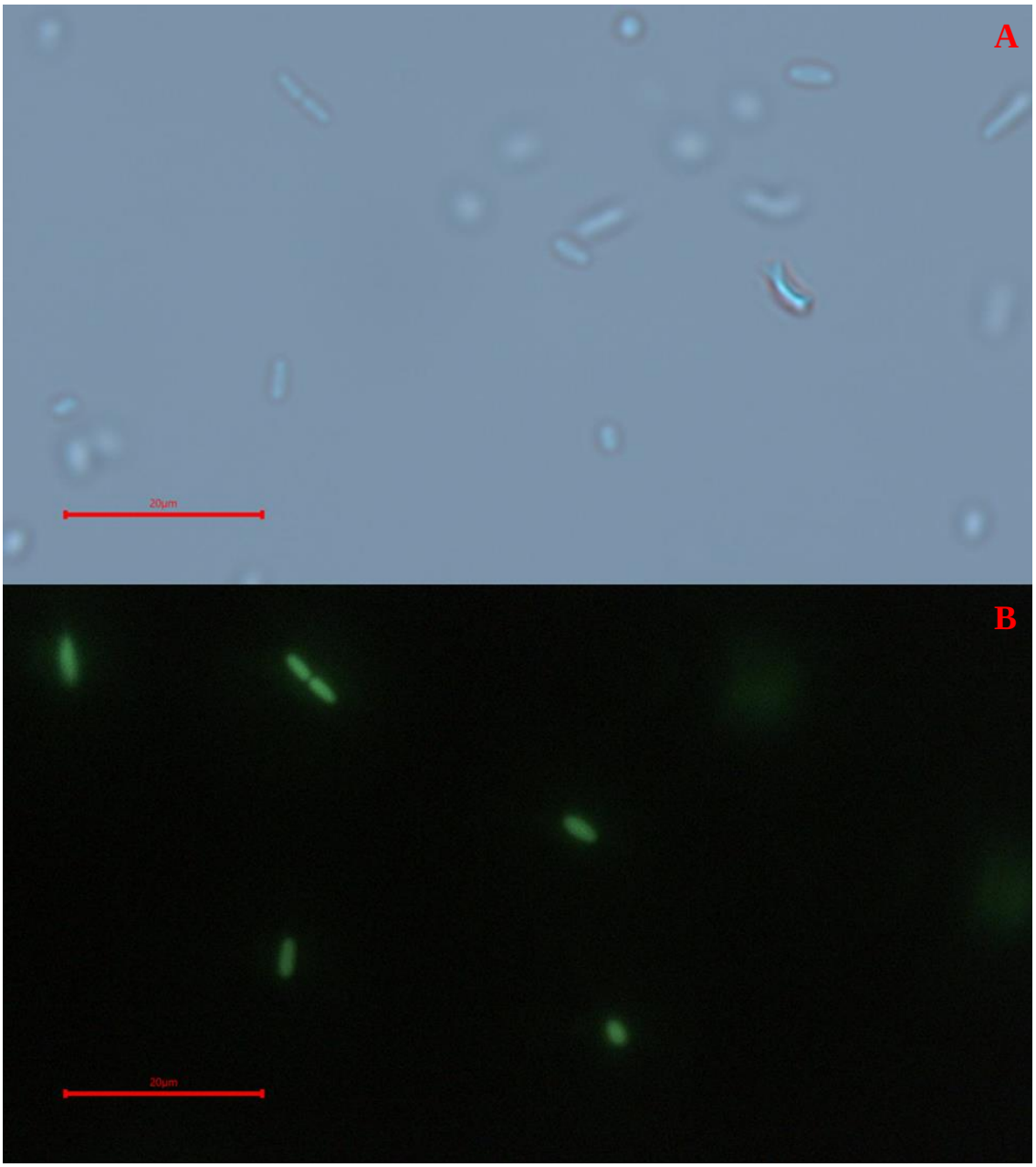

Figure S14: Differentiation of GFP-tagged *V. harveyi* within a complex mixture of vibrios. Mixture contains equal parts *V. alginolyticus* (GFP), *V. campbellii*, *V. parahaemolyticus*, *V. harveyi*, and *V. vulnificus*. Images A and B compare the same micrograph under light microscopy and fluorescent microscopy (495 nm excitation wavelength) at 1000X magnification.

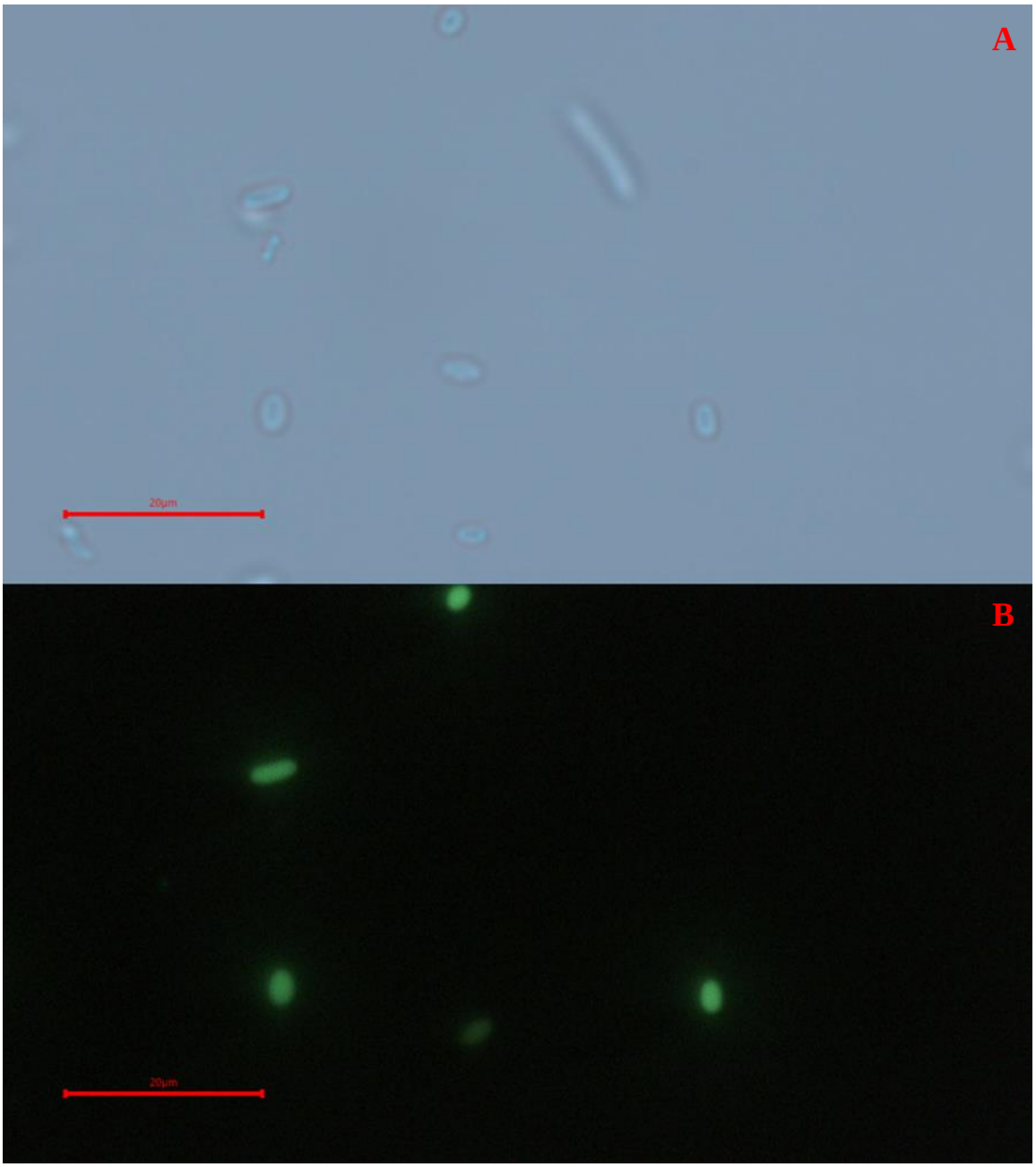

Figure S15: Differentiation of GFP-tagged *V. parahaemolyticus* within a complex mixture of vibrios. Mixture contains equal parts *V. alginolyticus* (GFP), *V. campbellii*, *V. parahaemolyticus*, *V. harveyi*, and *V. vulnificus.* Images A and B compare the same micrograph under light microscopy and fluorescent microscopy (495 nm excitation wavelength) at 1000X magnification.

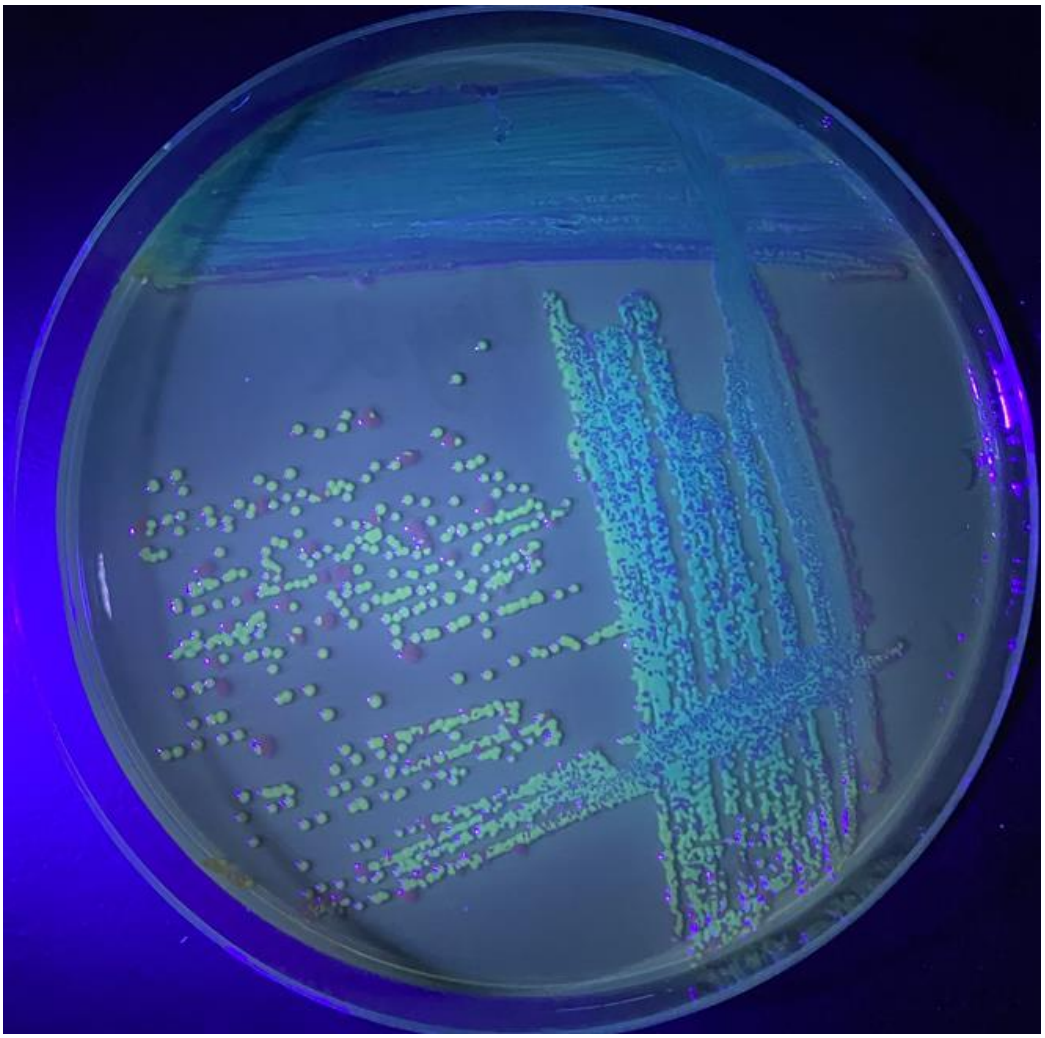

Figure S16: Subculture of *V. cholerae* retention study at T_{48}. Increased colony size was observed in non-fluorescent (purple) colonies compared to fluorescent colonies (green). Image of a100x15mm culture dish with 495 nm blacklight illumination.

APPENDIX 3: CHAPTER 5 SUPPLEMENTAL MATERIAL

Supplemental Tables and Figures

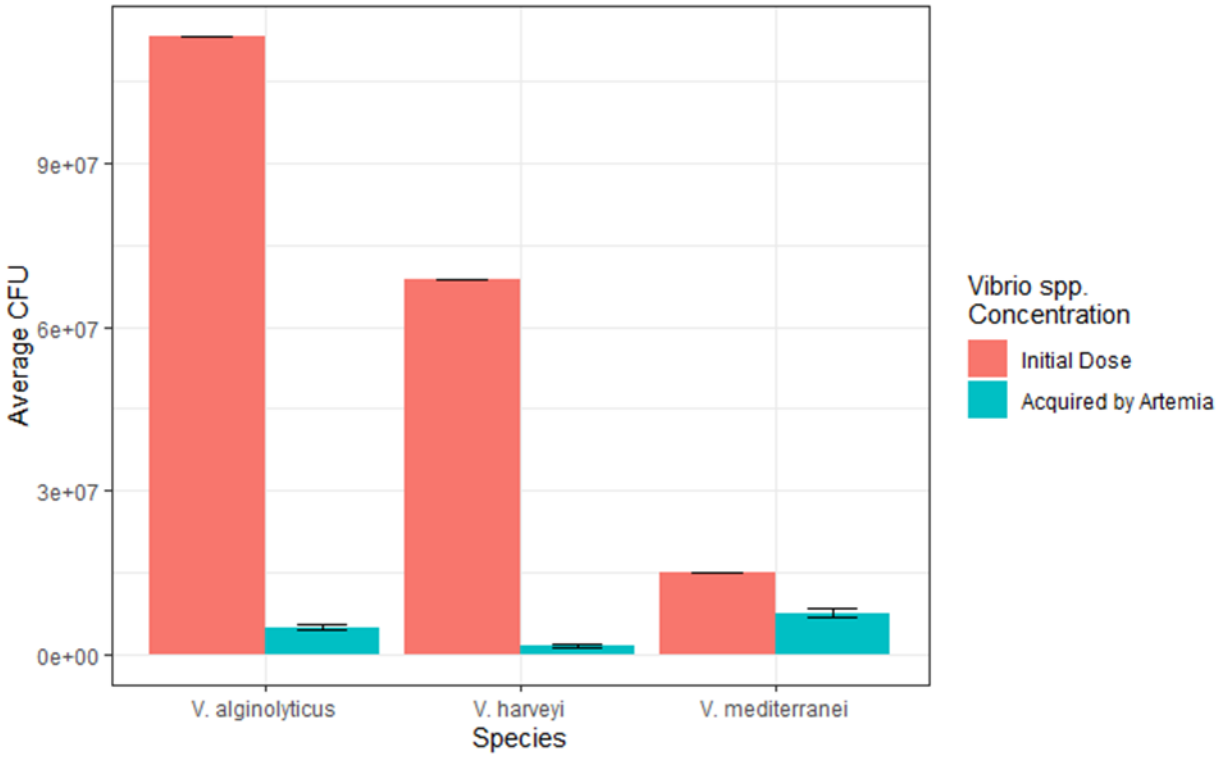

Figure S1: Average *Artemia*-acquired dose of GFP *Vibrio* spp. following an 18 h exposure via ambient water at 28°C under 50 rpm of shaking agitation. *V. alginolyticus* was initially dosed with 1.13 x 10^8 CFU resulting in an *Artemia*-acquired dose of 4.90 x 10^6 CFU. *V. harveyi* was initially dosed with 6.87 x 10^7 CFU resulting in an *Artemia*-acquired dose of 1.47 x 10^6 CFU. *V. mediterranei* was initially dosed with 1.51 x 10^7 CFU resulting in an *Artemia*-acquired dose of 7.59 x 10^6 CFU.

Figure S2: Hatchling verses 24 h matured *Artemia* sp. (A) 24 h matured *Artemia* identifiable by the longer length abdomen and more visible internal features. (B) Recently hatched (<24 h) *Artemia* demonstrating shorter posterior abdominal length. Recently hatched *Artemia* were not observed to accumulate a substantial burden GFP-*Vibrio* spp. following exposure via water inoculation.

Figure S3: Images of *E. pallida* ingesting GFP-*Vibrio* (*V. alginolyticus*) spiked brine shrimp. Anemone tissue appears red/pink with intermittent green/yellow coloration around the oral disc. *Artemia* tissue appears translucent with bright green fluorescence concentrated throughout the length of the GI tract. (A) Image *of E. pallida* oral disc with *Artemia* captured by the lower right tentacle. (B) *E. pallida* tentacles capturing *Artemia*. Images taken at 40X magnification with 495nm excitation wavelength.

Figure S4: Example of a healthy *E. pallida* suitable for ingestion experimentation. Healthy anemones appear tan-brown in color with occasional dark brown striping (particularly on the tentacles). Specific shades of anemone color may vary between individuals but, should remain largely uniform. Atypical darkening or multifocal discoloration is a sign of stress. During the daytime, healthy anemones will typically rest with their tentacles outstretched flowing with the movement of the water. Intermittent curling or retraction of the tentacles is normal however, persistence in a retracted state is a sign of stress. If disturbed, healthy anemones will react to touch or sudden movement in the water in a defensive fashion by quickly retracting away from the disturbance.

Table S1: Experimental *Vibrio* strains used for controlled feeding studies.

Species	**Strain Designation**	**Strain Isolation Source**	**Strain Citation**
V. alginolyticus	ATCC 17749	Spoiled horse mackerel, Japan	Miyamoto et al., 1961
V. harveyi	ATCC 14216	Deceased luminescent amphipod, USA	Johnson and Shunk, 1936
V. mediterranei	ATCC 43341	Sediment, Spain	Pujalte & Garay, 1986

Table S2: Water conditions for the maintenance of *E. pallida* long-term holding tanks. Water level based on acceptable fill level 6L glass aquarium.

Tank Parameter	**Acceptable Range**	**Frequency Checked**
Temperature	26-28^{o}C	Weekly
Salinity	30-35	Weekly
pH	8.0-8.5	Weekly
Light Level	15 LUX	Daily
Water Level	5 ± 0.2L	Daily

Table S3: Maintenance requirements for the management *E. pallida* holding tanks.

Maintenance Requirement	**Frequency Required**	**Maintenance Details**
Anemone Feeding	Weekly[a]	Feeding of resident anemones with non-inoculated Artemia (50mL of decapsulated Artemia per tank)
Water Change	Every 2 weeks[b]	Removal and replacement of ~50% of the total volume of artificial sea water
Glass Cleaning	Weekly[b]	Gentle scrubbing of algal buildup on tank glass
Pump Cleaning	Monthly[b]	Scrubbing and rinsing of pump internal compartments to reduce algal and salt buildup
Filter Replacement	Monthly	Replacement of charcoal pump filters
Heater Cleaning	Monthly[b]	Scrubbing and rinsing of heater components to reduce algal and salt buildup
Light Cleaning	Monthly[b]	Cleaning of tank lights to reduce salt buildup
Water Top-Off	Daily	Addition of fresh deionized water to maintain tank fill level and stabilize tank salinity due to evaporation

[a]Feeding frequency can be increased if a tank is highly populated and/or to promote asexual reproduction of the resident anemones.

[b]Denotes minimum frequency but may be required more often based on feeding.

APPENDIX 4: CHAPTER 6 SUPPLEMENTAL MATERIAL

Supplemental Tables and Figures

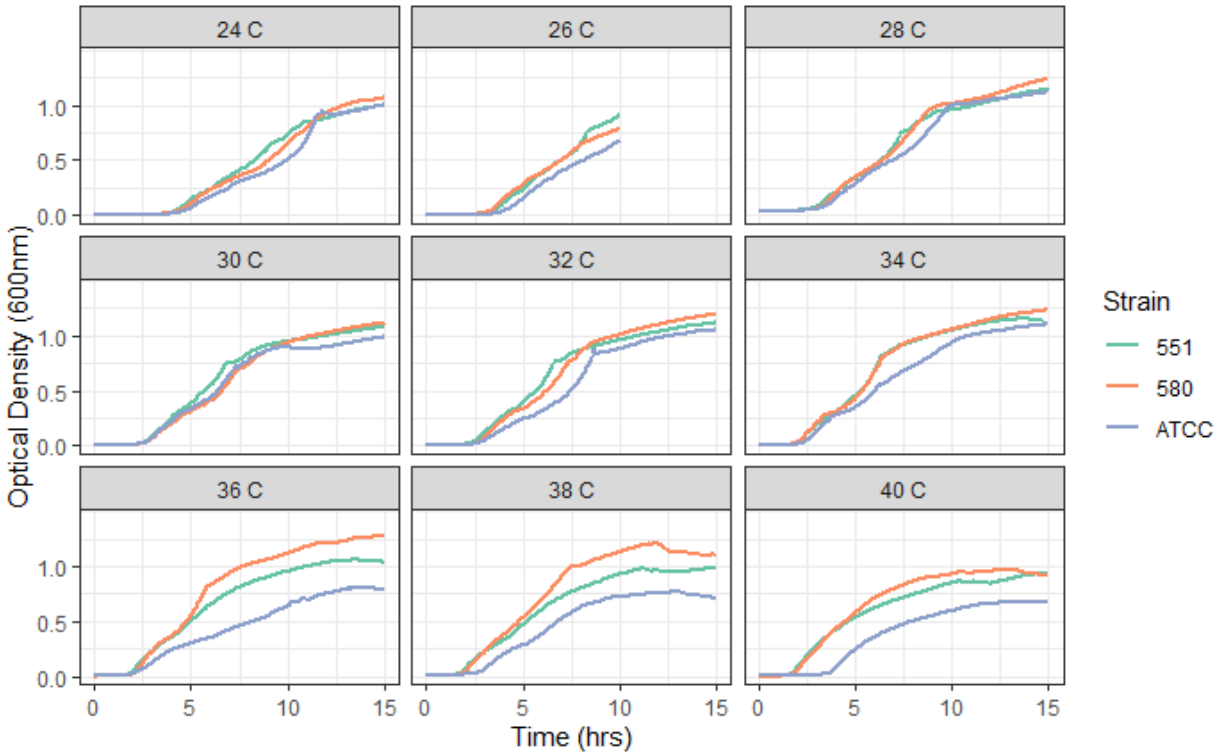

Figure S1: *V. alginolyticus* bacterial growth curves for temperature experimentation. All cultures grown in LBS 3% (w/v) NaCl broth at the indicated incubation temperature. N = 12 per strain and temperature combination.

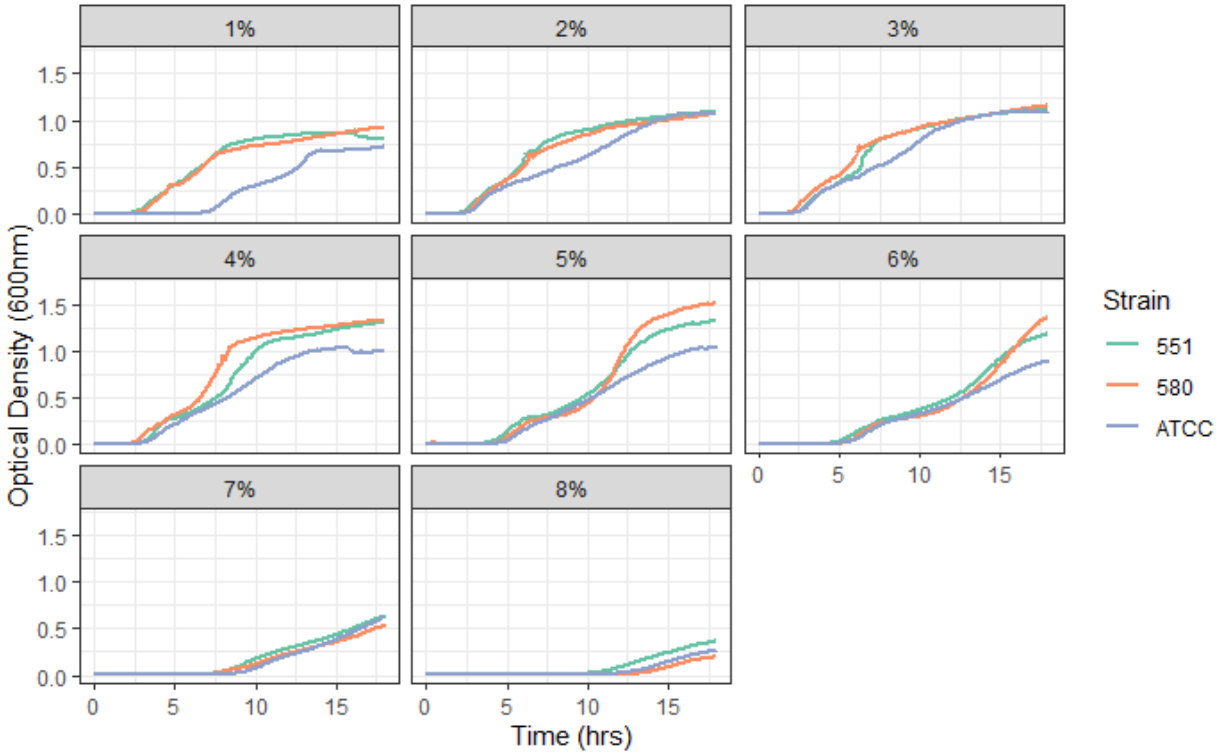

Figure S2: *V. alginolyticus* bacterial growth curves for salinity experimentation. All cultures grown in LBS broth amended to the indicated NaCl percent (w/v) at 30 ^{o}C. N = 12 per strain and salinity combination.

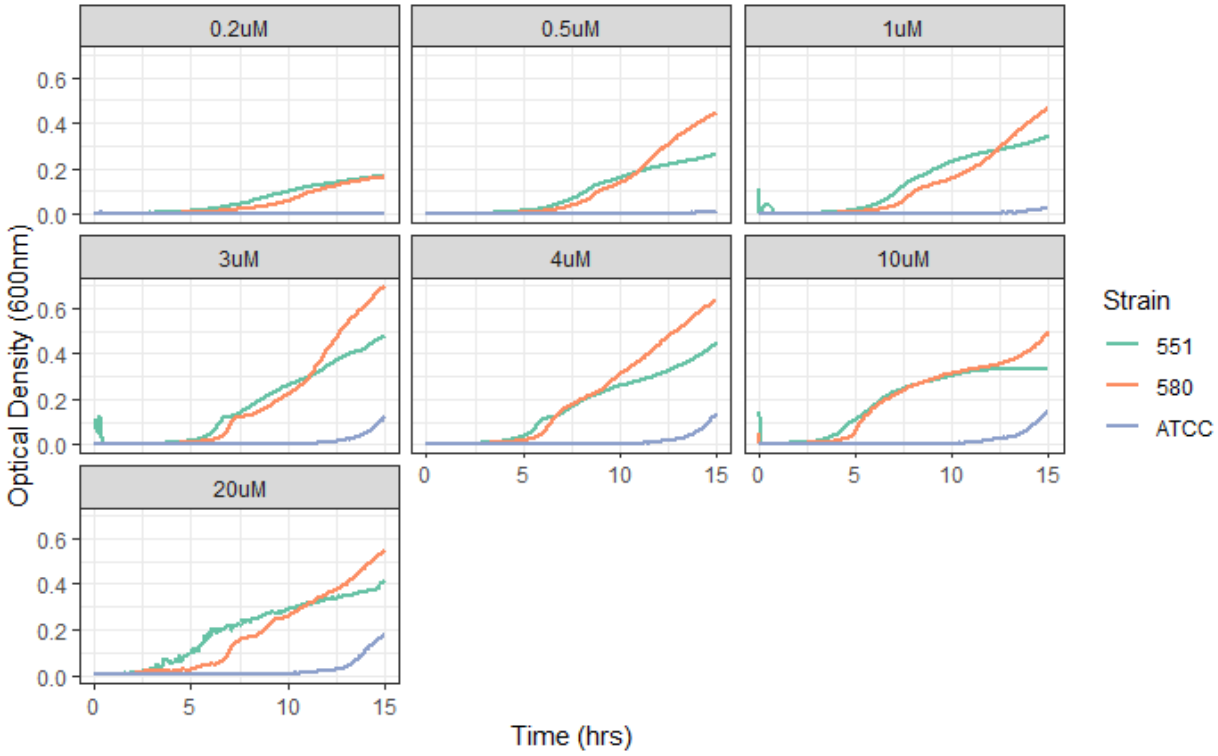

Figure S3: *V. alginolyticus* bacterial growth curves for iron experimentation. All cultures grown in VibFeL broth with an NaCl concentration of 3% (w/v) incubated at 30 ^{o}C. N = 12 per strain and iron combination.

Table S1: Significantly upregulated *V. alginolyticus* endometabolites detected during iron supplementation and iron starvation experiments. Significance designated as any metabolite with a mean relative abundance p-value of ≥ 0.05.

Metabolite Name	MetaboAnalyst Hit[a]	P-value	HMDB Number[b]	Up Regulated When[c]
Iron Comparisons				
3-methyl-2-oxobutanoic acid	Alpha-ketoisovaleric acid	0.0052	HMDB0000019	Iron Replete (non-starved)
3-aminobutanoic acid	3-Aminobutanoic acid	0.0023	HMDB0031654	Iron Replete (non-starved)
3-phosphoglycerate	3-Phosphoglyceric acid	0.0011	HMDB0000807	Iron Replete (non-starved)
5-methyluridine	Ribothymidine	0.021	HMDB0000884	Iron Replete (non-starved)
Adenine	Adenine	0.048	HMDB0000034	Iron Replete (non-starved)
ADP	ADP	0.0013	HMDB0001341	Iron Replete (non-starved)
Aspartic acid	L-Aspartic acid	0.00016	HMDB0000191	Iron Replete (non-starved)
Benzoic acid	Benzoic acid	0.044	HMDB0001870	Iron Replete (non-starved)
Capric acid	Capric acid	0.036	HMDB0000511	Iron Replete (non-starved)
Citric acid	Citric acid	0.0044	HMDB0000094	Iron Replete (non-starved)
Dodecenoic acid	11-Dodecenoic acid	0.0053	HMDB0032248	Iron Replete (non-starved)
Elaidic acid	Elaidic acid	0.019	HMDB0000573	Iron Replete (non-starved)
Ethanolamine	Ethanolamine	0.0012	HMDB0000149	Iron Replete (non-starved)
Fumaric acid	Fumaric acid	0.0062	HMDB0000134	Iron Replete (non-starved)
Glutamic acid	L-Glutamic acid	0.013	HMDB0000148	Iron Replete (non-starved)
Glycerol-3-phosphate	Glycerol 3-phosphate	0.029	HMDB0000126	Iron Replete (non-starved)

Glycine	Glycine	0.011	HMDB0000123	Iron Replete (non-starved)
Glycolic acid	Glycolic acid	0.00048	HMDB0000115	Iron Replete (non-starved)
Heptadecanoic acid	Heptadecanoic acid	0.0060	HMDB0002259	Iron Replete (non-starved)
Lauric acid	Dodecanoic acid	0.0040	HMDB0000638	Iron Replete (non-starved)
Leucine	L-Leucine	0.036	HMDB0000687	Iron Replete (non-starved)
Lysine	L-Lysine	0.019	HMDB0000182	Iron Replete (non-starved)
Malic acid	Malic acid	0.00053	HMDB0000744	Iron Replete (non-starved)
Methyl phosphoric acid	Heptaethylene glycol	0.0020	HMDB0061835	Iron Replete (non-starved)
Methylmalonic acid	Methylmalonic acid	0.030	HMDB0000202	Iron Replete (non-starved)
Methylsuccinic acid	Methylsuccinic acid	0.0075	HMDB0001844	Iron Replete (non-starved)
Myristic acid	Myristic acid	0.019	HMDB0000806	Iron Replete (non-starved)
Octadecanoic acid	Stearic acid	0.032	HMDB0000827	Iron Replete (non-starved)
Oxalic acid	Oxalic acid	0.016	HMDB0002329	Iron Replete (non-starved)
Oxoglutaric acid	Oxoglutaric acid	0.041	HMDB0000208	Iron Replete (non-starved)
Palmitelaidic acid	Palmitelaidic acid	0.038	HMDB0012328	Iron Replete (non-starved)
Palmitic acid	Palmitic acid	0.023	HMDB0000220	Iron Replete (non-starved)
Pentadecanoic acid	Pentadecanoic acid	0.038	HMDB0000826	Iron Replete (non-starved)
Phenylalanine	L-Phenylalanine	0.014	HMDB0000159	Iron Replete (non-starved)
Proline	L-Proline	0.015	HMDB0000162	Iron Replete (non-starved)
Putrescine	Putrescine	0.029	HMDB0001414	Iron Replete (non-starved)
Pyroglutamic acid	Pyroglutamic acid	0.014	HMDB0000267	Iron Replete (non-starved)
Pyrophosphate	Pyrophosphate	0.019	HMDB0000250	Iron Replete (non-starved)

Ribose	D-Ribose	0.013	HMDB0000283	Iron Replete (non-starved)
Ribose-5-phosphate	D-Ribose 5-phosphate	0.020	HMDB0001548	Iron Replete (non-starved)
Steric acid	Octadecanoic acid	0.0024	HMDB0000827	Iron Replete (non-starved)
Succinic acid	Succinic acid	0.0055	HMDB0000254	Iron Replete (non-starved)
Threonine	L-Threonine	0.0047	HMDB0000167	Iron Replete (non-starved)
Thymine	Thymine	0.015	HMDB0000262	Iron Replete (non-starved)
Tyrosine	L-Tyrosine	0.0020	HMDB0000158	Iron Replete (non-starved)
Uracil	Uracil	0.045	HMDB0000300	Iron Replete (non-starved)
Urea	Urea	0.013	HMDB0000294	Iron Replete (non-starved)
Valine	L-Valine	0.011	HMDB0000883	Iron Replete (non-starved)
Xylose	D-Xylose	0.0012	HMDB0000098	Iron Replete (non-starved)
1-dodecanol	Dodecanol	0.00015	HMDB0011626	Iron Replete (starved)
3-aminobutanoic acid	3-Aminobutanoic acid	0.0013	HMDB0031654	Iron Replete (starved)
3-butenoic acid	4-(3-Pyridyl)-3-butenoic acid	0.0033	HMDB0001424	Iron Replete (starved)
3-methyl-2-oxobutanoic acid	Alpha-ketoisovaleric acid	0.016	HMDB0000019	Iron Replete (starved)
3-phosphoglycerate	3-Phosphoglyceric acid	0.000073	HMDB0000807	Iron Replete (starved)
5-methyluridine	Ribothymidine	0.0024	HMDB0000884	Iron Replete (starved)
Adenine	Adenine	0.0098	HMDB0000034	Iron Replete (starved)
Adenosine	Adenosine	0.012	HMDB0000050	Iron Replete (starved)
ADP	ADP	0.028	HMDB0001341	Iron Replete (starved)
Alanine	L-Alanine	0.00050	HMDB0000161	Iron Replete (starved)
Aspartic acid	L-Aspartic acid	0.0015	HMDB0000191	Iron Replete (starved)

Carbonic acid	Carbonic acid	0.00036	HMDB0003538	Iron Replete (starved)
Citric acid	Citric acid	0.0056	HMDB0000094	Iron Replete (starved)
Ethanolamine	Ethanolamine	0.020	HMDB0000149	Iron Replete (starved)
Fumaric acid	Fumaric acid	0.0067	HMDB0000134	Iron Replete (starved)
GABA	Gamma-Aminobutyric acid	0.020	HMDB0000112	Iron Replete (starved)
Glutamic acid	L-Glutamic acid	0.0025	HMDB0000148	Iron Replete (starved)
Glyceric acid	Glyceric acid	0.0051	HMDB0000139	Iron Replete (starved)
Glycerol-3-phosphate	Glycerol 3-phosphate	0.011	HMDB0000126	Iron Replete (starved)
Glycine	Glycine	0.017	HMDB0000123	Iron Replete (starved)
Heptanoic acid	Heptanoic acid	0.017	HMDB0000666	Iron Replete (starved)
Hydroxyvaleric acid	Hydroxyvaleric acid	0.010	HMDB0000531	Iron Replete (starved)
Lauric acid	Dodecanoic acid	0.0024	HMDB0000638	Iron Replete (starved)
Malic acid	Malic acid	0.0012	HMDB0000744	Iron Replete (starved)
Methyl phosphoric acid	Heptaethylene glycol	0.0020	HMDB0061835	Iron Replete (starved)
Methylmalonic acid	Methylmalonic acid	0.0057	HMDB0000202	Iron Replete (starved)
Methylsuccinic acid	Methylsuccinic acid	0.022	HMDB0001844	Iron Replete (starved)
Myristic acid	Myristic acid	0.015	HMDB0000806	Iron Replete (starved)
Octadecanoic acid	Stearic acid	0.027	HMDB0000827	Iron Replete (starved)
Oxoglutaric acid	Oxoglutaric acid	0.00034	HMDB0000208	Iron Replete (starved)
Palmitic acid	Palmitic acid	0.044	HMDB0000220	Iron Replete (starved)
Phenylalanine	L-Phenylalanine	0.0031	HMDB0000159	Iron Replete (starved)
Proline	L-Proline	0.00052	HMDB0000162	Iron Replete (starved)

Putrescine	Putrescine	0.0076	HMDB0001414	Iron Replete (starved)
Pyroglutamic acid	Pyroglutamic acid	0.0013	HMDB0000267	Iron Replete (starved)
Pyrophosphate	Pyrophosphate	0.0065	HMDB0000250	Iron Replete (starved)
Pyruvic acid	Pyruvic acid	0.019	HMDB0000243	Iron Replete (starved)
Ribose	D-Ribose	0.018	HMDB0000283	Iron Replete (starved)
Ribose-5-phosphate	D-Ribose 5-phosphate	0.032	HMDB0001548	Iron Replete (starved)
Serine	Serine	0.020	HMDB0062263	Iron Replete (starved)
Succinic acid	Succinic acid	0.0014	HMDB0000254	Iron Replete (starved)
Threonine	L-Threonine	0.0051	HMDB0000167	Iron Replete (starved)
Tyrosine	L-Tyrosine	0.029	HMDB0000158	Iron Replete (starved)
UMP	Uridine 5'-monophosphate	0.0044	HMDB0000288	Iron Replete (starved)
Uracil	Uracil	0.00059	HMDB0000300	Iron Replete (starved)
Valine	L-Valine	0.0018	HMDB0000883	Iron Replete (starved)
Xylose	D-Xylose	0.014	HMDB0000098	Iron Replete (starved)
1-dodecanol	Dodecanol	0.025	HMDB0011626	Iron Deficient (non-starved)
3-Hydroxypropionic acid	Hydroxypropionic acid	0.000015	HMDB0000700	Iron Deficient (non-starved)
Glycolic acid	Glycolic acid	0.00011	HMDB0000115	Iron Deficient (non-starved)
Lactic acid	L-Lactic acid	0.0049	HMDB0000190	Iron Deficient (non-starved)
Pyruvic acid	Pyruvic acid	0.0055	HMDB0000243	Iron Deficient (non-starved)
Urea	Urea	0.031	HMDB0000294	Iron Deficient (non-starved)
Alanine	L-Alanine	0.010	HMDB0000161	Iron Deficient (non-starved)
Carbonic acid	Carbonic acid	0.025	HMDB0003538	Iron Deficient (non-starved)

Ethanamine	Ethylamine	0.025	HMDB0013231	Iron Deficient (non-starved)
Glycerol 1-phosphate	Glycerol 3-phosphate	0.0019	HMDB0000126	Iron Deficient (non-starved)
Glycine	Glycine	0.0097	HMDB0000123	Iron Deficient (non-starved)
Hydroxyvaleric acid	Hydroxyvaleric acid	0.0032	HMDB0000531	Iron Deficient (non-starved)
Lactic acid	L-Lactic acid	0.00040	HMDB0000190	Iron Deficient (non-starved)
Monostearin	Monostearin	0.00071	HMDB0011131	Iron Deficient (non-starved)
Nonanoic acid	Pelargonic acid	0.0013	HMDB0000847	Iron Deficient (non-starved)
Oleic acid	Oleic acid	0.0046	HMDB0000207	Iron Deficient (non-starved)
Oxalic acid	Oxalic acid	0.00039	HMDB0002329	Iron Deficient (non-starved)
Palmitelaidic acid	Palmitelaidic acid	0.0037	HMDB0012328	Iron Deficient (non-starved)
Phosphoric acid	Phosphoric acid	0.030	HMDB0002142	Iron Deficient (non-starved)
Threose	Erythrose	0.0085	HMDB0002649	Iron Deficient (non-starved)
Beta Alanine	Beta-Alanine	0.0040	HMDB0000056	Iron Deficient (starved)
Beta glycerolphosphate	Beta glycerolphosphate	0.034	HMDB0002520	Iron Deficient (starved)
Dodecenoic acid	11-Dodecenoic acid	0.0027	HMDB0032248	Iron Deficient (starved)
Ethanamine	Ethylamine	0.018	HMDB0013231	Iron Deficient (starved)
Glycolic acid	Glycolic acid	0.0027	HMDB0000115	Iron Deficient (starved)
Heptadecanoic acid	Heptadecanoic acid	0.0085	HMDB0002259	Iron Deficient (starved)
Lactic acid	L-Lactic acid	0.021	HMDB0000190	Iron Deficient (starved)
Leucine	L-Leucine	0.00060	HMDB0000687	Iron Deficient (starved)
Nonanoic acid	Pelargonic acid	0.026	HMDB0000847	Iron Deficient (starved)
Oleic acid	Oleic acid	0.013	HMDB0000207	Iron Deficient (starved)

Oxalic acid	Oxalic acid	0.027	HMDB0002329	Iron Deficient (starved)
Palmitelaidic acid	Palmitelaidic acid	0.039	HMDB0012328	Iron Deficient (starved)
Pentadecanoic acid	Pentadecanoic acid	0.026	HMDB0000826	Iron Deficient (starved)
Phenethylamine	Phenylethylamine	0.0064	HMDB0012275	Iron Deficient (starved)
Phosphoric acid	Phosphoric acid	0.042	HMDB0002142	Iron Deficient (starved)
Steric acid	Steric acid	0.00051	HMDB0000827	Iron Deficient (starved)
Sucrose	Sucrose	0.026	HMDB0000258	Iron Deficient (starved)
Threose	Erythrose	0.0066	HMDB0002649	Iron Deficient (starved)
Urea	Urea	0.0094	HMDB0000294	Iron Deficient (starved)
Valine	L-Valine	0.0026	HMDB0000883	Iron Deficient (starved)
Starvation Comparisons				
3-Hydroxypropionic acid	Hydroxypropionic acid	0.017	HMDB0000700	Not Starved (iron replete)
3-methyl-2-oxobutanoic acid	Alpha-ketoisovaleric acid	0.035	HMDB0000019	Not Starved (iron replete)
Benzoic acid	Benzoic acid	0.031	HMDB0001870	Not Starved (iron replete)
Citric acid	Citric acid	0.024	HMDB0000094	Not Starved (iron replete)
Ethanolamine	Ethanolamine	0.0029	HMDB0000149	Not Starved (iron replete)
Glycerol-3-phosphate	Glycerol 3-phosphate	0.045	HMDB0000126	Not Starved (iron replete)
Hexadecanoic acid	Palmitic acid	0.046	HMDB0000220	Not Starved (iron replete)
Malic acid	Malic acid	0.011	HMDB0000744	Not Starved (iron replete)
Methyl phosphoric acid	Heptaethylene glycol	0.00073	HMDB0061835	Not Starved (iron replete)
Oxalic acid	Oxalic acid	0.020	HMDB0002329	Not Starved (iron replete)
Palmitic acid	Palmitic acid	0.021	HMDB0000220	Not Starved (iron replete)

Putrescine	Putrescine	0.0028	HMDB0001414	Not Starved (iron replete)
Ribose	D-Ribose	0.040	HMDB0000283	Not Starved (iron replete)
Xylose	D-Xylose	0.032	HMDB0000098	Not Starved (iron replete)
3-aminobutanoic acid	3-Aminobutanoic acid	0.039	HMDB0031654	Not Starved (iron deficient)
3-butenoic acid	4-(3-Pyridyl)-3-butenoic acid	0.016	HMDB0001425	Not Starved (iron deficient)
3-Hydroxypropionic acid	Hydroxypropionic acid	0.0076	HMDB0000700	Not Starved (iron deficient)
Alanine	L-Alanine	0.012	HMDB0000161	Not Starved (iron deficient)
Ethanolamine	Ethanolamine	0.041	HMDB0000149	Not Starved (iron deficient)
Fumaric acid	Fumaric acid	0.0083	HMDB0000134	Not Starved (iron deficient)
Glycine	Glycine	0.050	HMDB0000123	Not Starved (iron deficient)
Methyl phosphoric acid	Heptaethylene glycol	0.0096	HMDB0061835	Not Starved (iron deficient)
Myristic acid	Myristic acid	0.047	HMDB0000806	Not Starved (iron deficient)
Palmitelaidic acid	Palmitelaidic acid	0.0040	HMDB0012328	Not Starved (iron deficient)
Palmitic acid	Palmitic acid	0.037	HMDB0000220	Not Starved (iron deficient)
Ribose	D-Ribose	0.0039	HMDB0000283	Not Starved (iron deficient)
1-dodecanol	Dodecanol	0.011	HMDB0011626	Starved (iron replete)
3-butenoic acid	4-(3-Pyridyl)-3-butenoic acid	0.00046	HMDB0001424	Starved (iron replete)
3-phosphoglycerate	3-Phosphoglyceric acid	0.00065	HMDB0000807	Starved (iron replete)
Adenosine	Adenosine	0.0018	HMDB0000050	Starved (iron replete)
Alanine	L-Alanine	0.037	HMDB0000161	Starved (iron replete)
Aspartic acid	L-Aspartic acid	0.0021	HMDB0000191	Starved (iron replete)
Beta glycerolphosphate	Beta glycerolphosphate	0.017	HMDB0002520	Starved (iron replete)

Dodecenoic acid	11-Dodecenoic acid	0.000063	HMDB0032248	Starved (iron replete)
Ethanamine	Ethylamine	0.0019	HMDB0013231	Starved (iron replete)
GABA	Gamma-Aminobutyric acid	0.027	HMDB0000112	Starved (iron replete)
Glutamic acid	L-Glutamic acid	0.014	HMDB0000148	Starved (iron replete)
Glyceric acid	Glyceric acid	0.0042	HMDB0000139	Starved (iron replete)
Glycine	Glycine	0.016	HMDB0000123	Starved (iron replete)
Hydroxyvaleric acid	Hydroxyvaleric acid	0.011	HMDB0000531	Starved (iron replete)
Lauric acid	Dodecanoic acid	0.031	HMDB0000638	Starved (iron replete)
Myristic acid	Myristic acid	0.015	HMDB0000806	Starved (iron replete)
Nonanoic acid	Pelargonic acid	0.019	HMDB0000847	Starved (iron replete)
O-phosphocolamine	O-Phosphoethanolamine	0.0013	HMDB0000224	Starved (iron replete)
Oxalic acid	Oxalic acid	0.017	HMDB0002329	Starved (iron replete)
Oxoglutaric acid	Oxoglutaric acid	0.017	HMDB0000208	Starved (iron replete)
Phosphoric acid	Phosphoric acid	0.0020	HMDB0002142	Starved (iron replete)
Putrescine	Putrescine	0.0024	HMDB0001414	Starved (iron replete)
Pyrophosphate	Pyrophosphate	0.027	HMDB0000250	Starved (iron replete)
Pyruvic acid	Pyruvic acid	0.036	HMDB0000243	Starved (iron replete)
Ribose	D-Ribose	0.047	HMDB0000283	Starved (iron replete)
Threonine	L-Threonine	0.035	HMDB0000167	Starved (iron replete)
Thymine	Thymine	0.041	HMDB0000262	Starved (iron replete)
Uracil	Uracil	0.0045	HMDB0000300	Starved (iron replete)
Urea	Urea	0.00078	HMDB0000294	Starved (iron replete)

Valine	L-Valine	0.016	HMDB0000883	Starved (iron replete)
Benzoic acid	Benzoic acid	0.015	HMDB0001870	Starved (iron deficient)
Beta glycerolphosphate	Beta glycerolphosphate	0.024	HMDB0002520	Starved (iron deficient)
Capric acid	Capric acid	0.029	HMDB0000511	Starved (iron deficient)
Dodecenoic acid	11-Dodecenoic acid	0.0024	HMDB0032248	Starved (iron deficient)
Glutamic acid	L-Glutamic acid	0.00012	HMDB0000148	Starved (iron deficient)
Glycolic acid	Glycolic acid	0.0058	HMDB0000115	Starved (iron deficient)
Heptadecanoic acid	Heptadecanoic acid	0.0021	HMDB0002259	Starved (iron deficient)
Lactic acid	L-Lactic acid	0.0036	HMDB0000190	Starved (iron deficient)
Lauric acid	Dodecanoic acid	0.012	HMDB0000638	Starved (iron deficient)
Leucine	L-Leucine	0.00073	HMDB0000687	Starved (iron deficient)
Oleic acid	Oleic acid	0.013	HMDB0000207	Starved (iron deficient)
Pentadecanoic acid	Pentadecanoic acid	0.016	HMDB0000826	Starved (iron deficient)
Phenethylamine	Phenylethylamine	0.030	HMDB0012275	Starved (iron deficient)
Phosphoric acid	Phosphoric acid	0.036	HMDB0002142	Starved (iron deficient)
Steric acid	Steric acid	0.00059	HMDB0000827	Starved (iron deficient)
Sucrose	Sucrose	0.030	HMDB0000258	Starved (iron deficient)
Threose	Erythrose	0.0021	HMDB0002649	Starved (iron deficient)
Urea	Urea	0.0036	HMDB0000294	Starved (iron deficient)
Valine	L-Valine	0.049	HMDB0000883	Starved (iron deficient)

[a]MetaboAnalyst hit represents the name of the metabolite as determined by the provided HMBD number.

[b]HMBD number represents the standardized Human Metabolome Database ID for the specific metabolite.

[c]Up regulated when indicates the culture condition where the specific metabolite was upregulated compared to the inverse condition (i.e., Non-Starved [iron replete] indicates metabolites that were upregulated when compared to Starved [iron replete] cultures).

Table S2: Significantly upregulated *V. alginolyticus* exometabolites detected during iron supplementation and iron starvation experiments. Significance designated as any metabolite with a mean relative abundance p-value of ≥ 0.05.

Metabolite Name	**MetaboAnalyst Hit[a]**	**P-value**	**HMDB Number[b]**	**Up Regulated When[c]**
Iron Comparisons				
2-Methyl-3-hydroxybutyric acid	2-Methyl-3-hydroxybutyric acid	0.0038	HMDB0000354	Iron Replete (non-starved)
α-Hydroxyglutaric acid	2-Hydroxyglutarate	0.0023	HMDB0059655	Iron Replete (non-starved)
Alanine	L-Alanine	0.0040	HMDB0000161	Iron Replete (non-starved)
Aspartic acid	L-Aspartic acid	0.047	HMDB0000191	Iron Replete (non-starved)
Benzoic acid	Benzoic acid	0.012	HMDB0001870	Iron Replete (non-starved)
Ethanolamine	Ethanolamine	0.000050	HMDB0000149	Iron Replete (non-starved)
Fumaric acid	Fumaric acid	0.0027	HMDB0000134	Iron Replete (non-starved)
Glutamic acid	L-Glutamic acid	0.0021	HMDB0000148	Iron Replete (non-starved)
Glycine	Glycine	0.0023	HMDB0000123	Iron Replete (non-starved)
Lactic acid	L-Lactic acid	0.0010	HMDB0000190	Iron Replete (non-starved)
Methylmalonic acid	Methylmalonic acid	0.00018	HMDB0000202	Iron Replete (non-starved)
Nonanoic acid	Pelargonic acid	0.0075	HMDB0000847	Iron Replete (non-starved)
Oxalic acid	Oxalic acid	0.042	HMDB0002329	Iron Replete (non-starved)
Putrescine	Putrescine	0.0041	HMDB0001414	Iron Replete (non-starved)
Pyroglutamic acid	Pyroglutamic acid	0.00050	HMDB0000267	Iron Replete (non-starved)
Succinic acid	Succinic acid	0.0039	HMDB0000254	Iron Replete (non-starved)

Tartronic acid	Hydroxypropanedioic acid	0.000043	HMDB0035227	Iron Replete (non-starved)
Urea	Urea	0.0050	HMDB0000294	Iron Replete (non-starved)
Valine	L-Valine	0.000041	HMDB0000883	Iron Replete (non-starved)
2-Methyl-3-hydroxybutyric acid	2-Methyl-3-hydroxybutyric acid	0.0075	HMDB0000354	Iron Replete (starved)
3-hydroxybutyric acid	3-Hydroxybutyric acid	0.00024	HMDB0000357	Iron Replete (starved)
3-hydroxyhippuric acid	3-Hydroxyhippuric acid	0.0059	HMDB0006116	Iron Replete (starved)
α-Hydroxyglutaric acid	2-Hydroxyglutarate	0.00045	HMDB0059655	Iron Replete (starved)
Alanine	L-Alanine	0.00011	HMDB0000161	Iron Replete (starved)
Aspartic acid	L-Aspartic acid	0.00076	HMDB0000191	Iron Replete (starved)
Benzoic acid	Benzoic acid	0.0075	HMDB0001870	Iron Replete (starved)
Citramalic acid	Citramalic acid	0.000030	HMDB0000426	Iron Replete (starved)
Citric acid	Citric acid	0.0057	HMDB0000094	Iron Replete (starved)
Ethanolamine	Ethanolamine	0.0054	HMDB0000149	Iron Replete (starved)
Fumaric acid	Fumaric acid	0.00017	HMDB0000134	Iron Replete (starved)
GABA	Gamma-Aminobutyric acid	0.019	HMDB0000112	Iron Replete (starved)
Glutamic acid	L-Glutamic acid	0.000053	HMDB0000148	Iron Replete (starved)
Glyceric acid	Glyceric acid	0.00027	HMDB0000139	Iron Replete (starved)
Hydroxybenzoic acid	4-Hydroxybenzoic acid	0.0011	HMDB0000500	Iron Replete (starved)
Lactic acid	L-Lactic acid	0.0000035	HMDB0000190	Iron Replete (starved)
Malic acid	Malic acid	0.000012	HMDB0000744	Iron Replete (starved)
Methylmalonic acid	Methylmalonic acid	0.0024	HMDB0000202	Iron Replete (starved)
Myristic acid	Myristic acid	0.0067	HMDB0000806	Iron Replete (starved)

Nonanoic acid	Pelargonic acid	0.0096	HMDB0000847	Iron Replete (starved)
Oxalic acid	Oxalic acid	0.014	HMDB0002329	Iron Replete (starved)
Palmitic acid	Palmitic acid	0.011	HMDB0000220	Iron Replete (starved)
Phosphoric acid	Phosphoric acid	0.00085	HMDB0002142	Iron Replete (starved)
Putrescine	Putrescine	0.0020	HMDB0001414	Iron Replete (starved)
Pyroglutamic acid	Pyroglutamic acid	0.011	HMDB0000267	Iron Replete (starved)
Sarcosine	Sarcosine	0.022	HMDB0000271	Iron Replete (starved)
Succinic acid	Succinic acid	0.000089	HMDB0000254	Iron Replete (starved)
Sucrose	Sucrose	0.00013	HMDB0000258	Iron Replete (starved)
Tartronic acid	Hydroxypropanedioic acid	0.0046	HMDB0035227	Iron Replete (starved)
Valine	L-Valine	0.0078	HMDB0000883	Iron Replete (starved)
3-hydroxybutyric acid	3-Hydroxybutyric acid	0.000014	HMDB0000357	Iron Deficient (non-starved)
3-hydroxyhippuric acid	3-Hydroxyhippuric acid	0.043	HMDB0006116	Iron Deficient (non-starved)
Citric acid	Citric acid	0.015	HMDB0000094	Iron Deficient (non-starved)
Dehydroascorbic acid	Dehydroascorbic acid	0.030	HMDB0001264	Iron Deficient (non-starved)
Fructose	D-Fructose	0.018	HMDB0000660	Iron Deficient (non-starved)
Galactose	D-Galactose	0.0031	HMDB0000143	Iron Deficient (non-starved)
Glucose	D-Glucose	0.0010	HMDB0000122	Iron Deficient (non-starved)
Glyceric acid	Glyceric acid	0.015	HMDB0000139	Iron Deficient (non-starved)
Glycolic acid	Glycolic acid	0.0028	HMDB0000115	Iron Deficient (non-starved)
Mannose	D-Mannose	0.00061	HMDB0000169	Iron Deficient (non-starved)
Mimosine	Mimosine	0.0024	HMDB0015188	Iron Deficient (non-starved)

Myristic acid	Myristic acid	0.0029	HMDB0000806	Iron Deficient (non-starved)
Phosphoric acid	Phosphoric acid	0.0027	HMDB0002142	Iron Deficient (non-starved)
Pyruvic acid	Pyruvic acid	0.0031	HMDB0000243	Iron Deficient (non-starved)
Sucrose	Sucrose	0.00087	HMDB0000258	Iron Deficient (non-starved)
Dehydroascorbic acid	Dehydroascorbic acid	0.016	HMDB0001264	Iron Deficient (starved)
Fructose	D-Fructose	0.021	HMDB0000660	Iron Deficient (starved)
Galactose	D-Galactose	0.00090	HMDB0000143	Iron Deficient (starved)
Glucose	D-Glucose	0.000019	HMDB0000122	Iron Deficient (starved)
Glycine	Glycine	0.00021	HMDB0000123	Iron Deficient (starved)
Glycolic acid	Glycolic acid	0.047	HMDB0000115	Iron Deficient (starved)
Itaconic acid	Itaconic acid	0.045	HMDB0002092	Iron Deficient (starved)
Mannose	D-Mannose	0.0051	HMDB0000169	Iron Deficient (starved)
Pyruvic acid	Pyruvic acid	0.0014	HMDB0000243	Iron Deficient (starved)
Urea	Urea	0.011	HMDB0000294	Iron Deficient (starved)
Starvation Comparisons				
2-Methyl-3-hydroxybutyric acid	2-Methyl-3-hydroxybutyric acid	0.0098	HMDB0000354	Not Starved (iron replete)
3-hydroxybutyric acid	3-Hydroxybutyric acid	0.033	HMDB0000357	Not Starved (iron replete)
Alanine	L-Alanine	0.027	HMDB0000161	Not Starved (iron replete)
Glucose	D-Glucose	0.031	HMDB0000122	Not Starved (iron replete)
Glutamic acid	L-Glutamic acid	0.0033	HMDB0000148	Not Starved (iron replete)
Oxalic acid	Oxalic acid	0.028	HMDB0002329	Not Starved (iron replete)
Pyroglutamic acid	Pyroglutamic acid	0.017	HMDB0000267	Not Starved (iron replete)

Urea	Urea	0.000041	HMDB0000294	Not Starved (iron replete)
Valine	L-Valine	0.021	HMDB0000883	Not Starved (iron replete)
2-Methyl-3-hydroxybutyric acid	2-Methyl-3-hydroxybutyric acid	0.013	HMDB0000354	Not Starved (iron deficient)
3-hydroxybutyric acid	3-Hydroxybutyric acid	0.0018	HMDB0000357	Not Starved (iron deficient)
3-hydroxyhippuric acid	3-Hydroxyhippuric acid	0.0067	HMDB0006116	Not Starved (iron deficient)
α-Hydroxyglutaric acid	2-Hydroxyglutarate	0.025	HMDB0059655	Not Starved (iron deficient)
Alanine	L-Alanine	0.0045	HMDB0000161	Not Starved (iron deficient)
Citramalic acid	Citramalic acid	0.042	HMDB0000426	Not Starved (iron deficient)
Ethanolamine	Ethanolamine	0.010	HMDB0000149	Not Starved (iron deficient)
Fumaric acid	Fumaric acid	0.022	HMDB0000134	Not Starved (iron deficient)
Glutamic acid	L-Glutamic acid	0.00029	HMDB0000148	Not Starved (iron deficient)
Glyceric acid	Glyceric acid	0.0032	HMDB0000139	Not Starved (iron deficient)
Hydroxybenzoic acid	4-Hydroxybenzoic acid	0.015	HMDB0000500	Not Starved (iron deficient)
Lactic acid	L-Lactic acid	0.00023	HMDB0000190	Not Starved (iron deficient)
Malic acid	Malic acid	0.0082	HMDB0000744	Not Starved (iron deficient)
Mimosine	Mimosine	0.012	HMDB0015188	Not Starved (iron deficient)
Nonanoic acid	Pelargonic acid	0.0068	HMDB0000847	Not Starved (iron deficient)
Oxalic acid	Oxalic acid	0.0078	HMDB0002329	Not Starved (iron deficient)
Putrescine	Putrescine	0.0094	HMDB0001414	Not Starved (iron deficient)
Pyroglutamic acid	Pyroglutamic acid	0.00057	HMDB0000267	Not Starved (iron deficient)
Succinic acid	Succinic acid	0.0084	HMDB0000254	Not Starved (iron deficient)
Tartronic acid	Hydroxypropanedioic acid	0.037	HMDB0035227	Not Starved (iron deficient)

Threose	Erythrose	0.0073	HMDB0002649	Not Starved (iron deficient)
Urea	Urea	0.000097	HMDB0000294	Not Starved (iron deficient)
Valine	L-Valine	0.00089	HMDB0000883	Not Starved (iron deficient)
α-Hydroxyglutaric acid	2-Hydroxyglutarate	0.0035	HMDB0059655	Starved (iron replete)
Aspartic acid	L-Aspartic acid	0.021	HMDB0000191	Starved (iron replete)
Fumaric acid	Fumaric acid	0.020	HMDB0000134	Starved (iron replete)
GABA	Gamma-Aminobutyric acid	0.022	HMDB0000112	Starved (iron replete)
Itaconic acid	Itaconic acid	0.039	HMDB0002092	Starved (iron replete)
Nonanoic acid	Pelargonic acid	0.013	HMDB0000847	Starved (iron replete)
Palmitic acid	Palmitic acid	0.018	HMDB0000220	Starved (iron replete)
Phosphoric acid	Phosphoric acid	0.014	HMDB0002142	Starved (iron replete)
Putrescine	Putrescine	0.038	HMDB0001414	Starved (iron replete)
Succinic acid	Succinic acid	0.015	HMDB0000254	Starved (iron replete)
Sucrose	Sucrose	0.017	HMDB0000258	Starved (iron replete)
Dehydroascorbic acid	Dehydroascorbic acid	0.014	HMDB0001264	Starved (iron deficient)
Fructose	D-Fructose	0.039	HMDB0000660	Starved (iron deficient)
Galactose	D-Galactose	0.0016	HMDB0000143	Starved (iron deficient)
Glucose	D-Glucose	0.00070	HMDB0000122	Starved (iron deficient)
Glycine	Glycine	0.0020	HMDB0000123	Starved (iron deficient)
Mannose	D-Mannose	0.010	HMDB0000169	Starved (iron deficient)
Phosphoric acid	Phosphoric acid	0.0058	HMDB0002142	Starved (iron deficient)
Pyruvic acid	Pyruvic acid	0.0014	HMDB0000243	Starved (iron deficient)

Sucrose	Sucrose	0.0091	HMDB0000258	Starved (iron deficient)

[a]MetaboAnalyst hit represents the name of the metabolite as determined by the provided HMBD number.

[b]HMBD number represents the standardized Human Metabolome Database ID for the specific metabolite.

[c]Up regulated when indicates the culture condition where the specific metabolite was upregulated compared to the inverse condition (i.e., Non-Starved [iron replete] indicates metabolites that were upregulated when compared to Starved [iron replete] cultures).

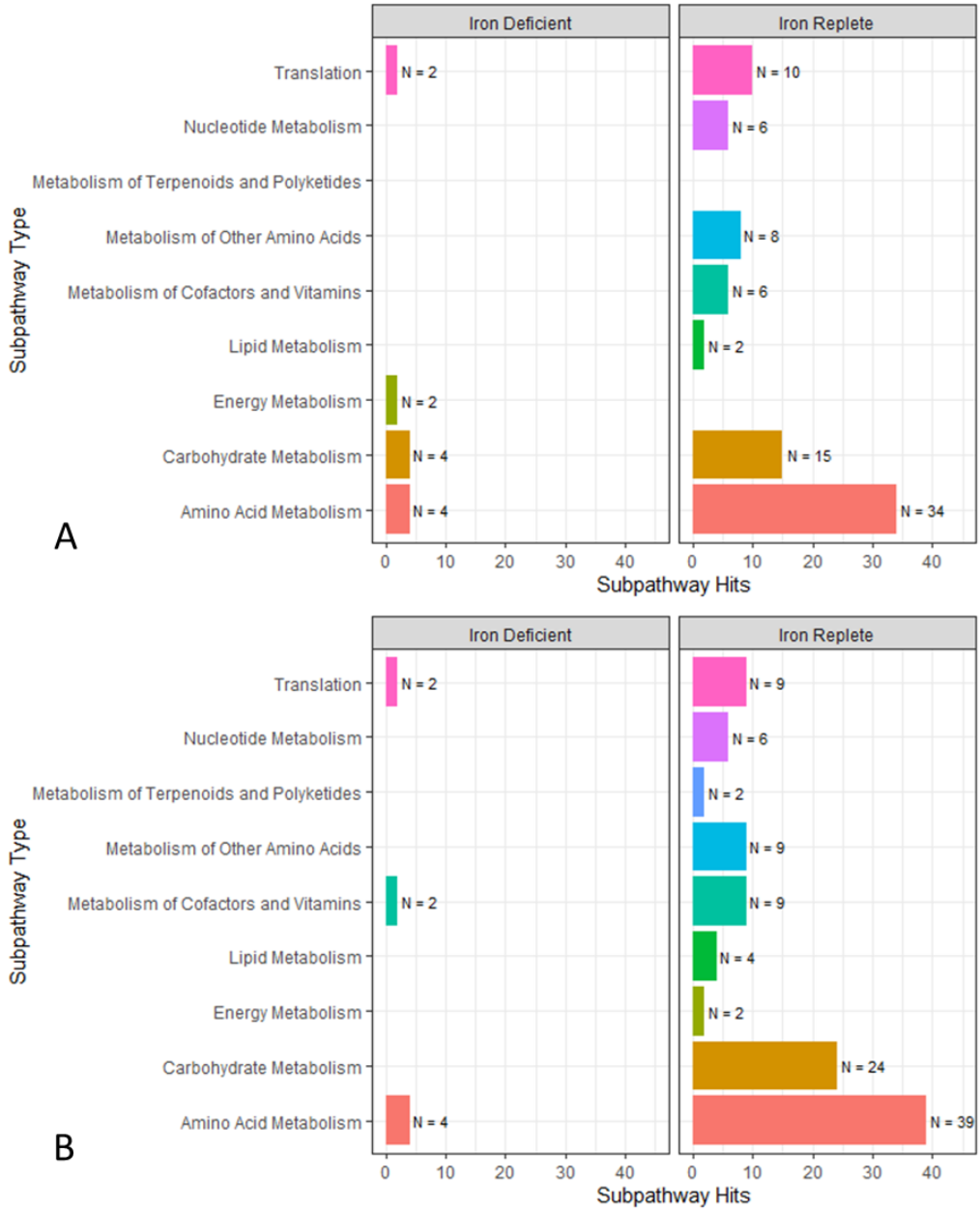

Figure S1: Upregulated metabolic pathways associated with iron replete and iron deficient *V. alginolyticus* endometabolite samples. The y-axis lists the detected KEGG subpathways and the x-axis shows the number of metabolite hits associated with each subpathway group. (A) Pathways comparisons for non-starved samples. (B) Pathway comparisons for starved samples.

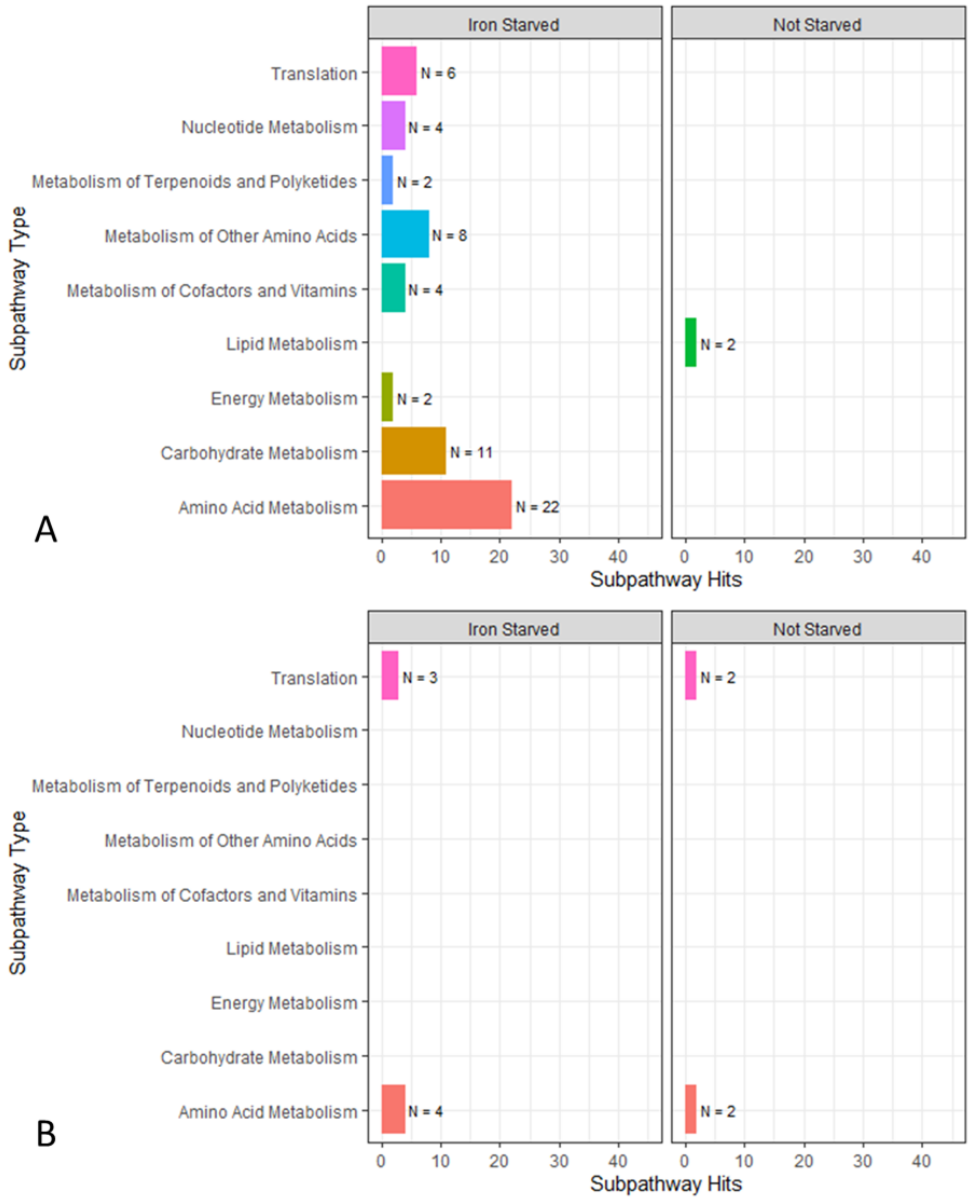

Figure S2: Upregulated metabolic pathways associated with iron starved and not starved *V. alginolyticus* endometabolite samples. The y-axis lists the detected KEGG subpathways and the x-axis shows the number of metabolite hits associated with each subpathway group. (A) Pathways comparisons for iron replete samples. (B) Pathway comparisons for iron deficient samples.

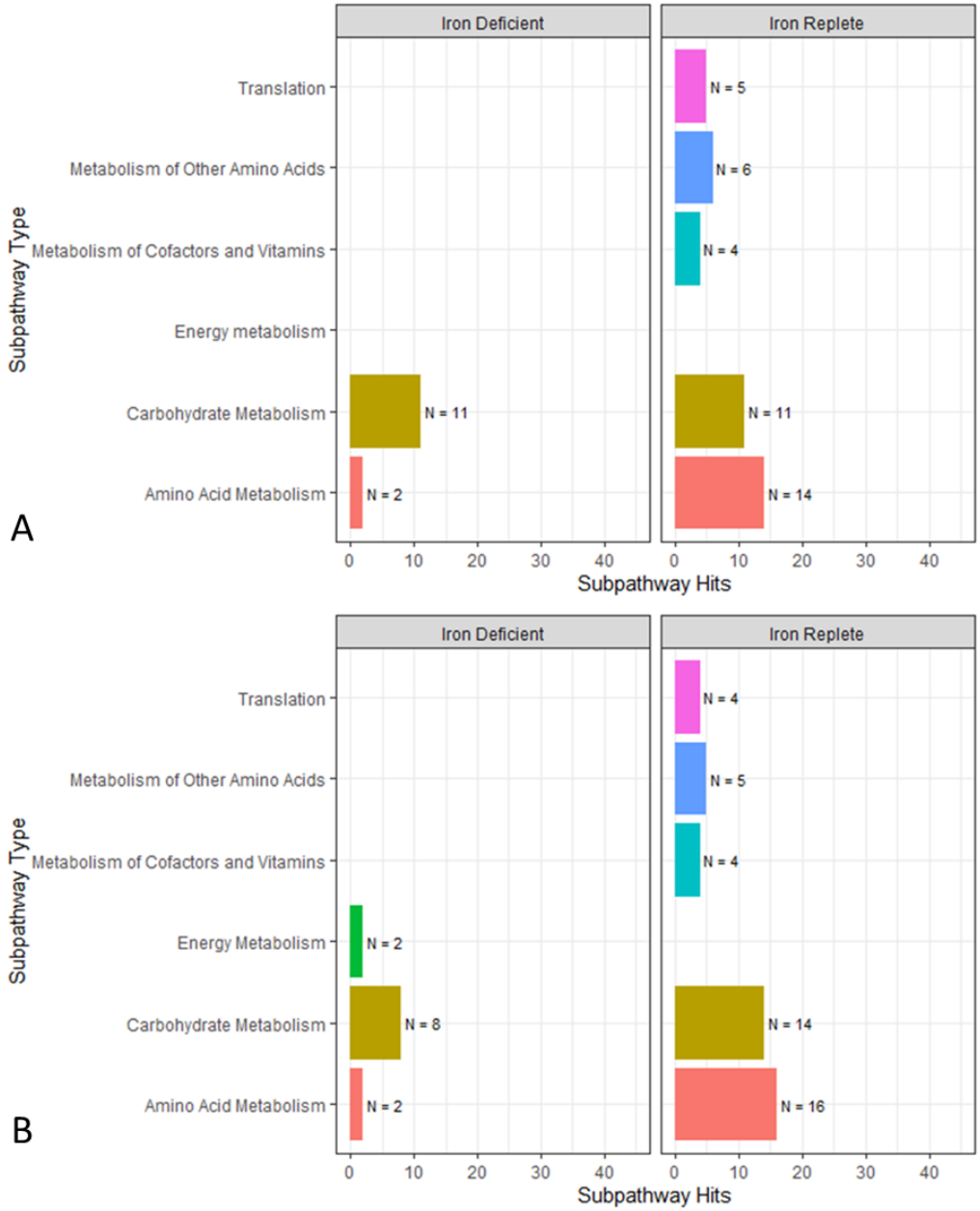

Figure S3: Upregulated metabolic pathways associated with iron replete and iron deficient *V. alginolyticus* exometabolite samples. The y-axis lists the detected KEGG subpathways and the x-axis shows the number of metabolite hits associated with each subpathway group. (A) Pathways comparisons for non-starved samples. (B) Pathway comparisons for starved samples.

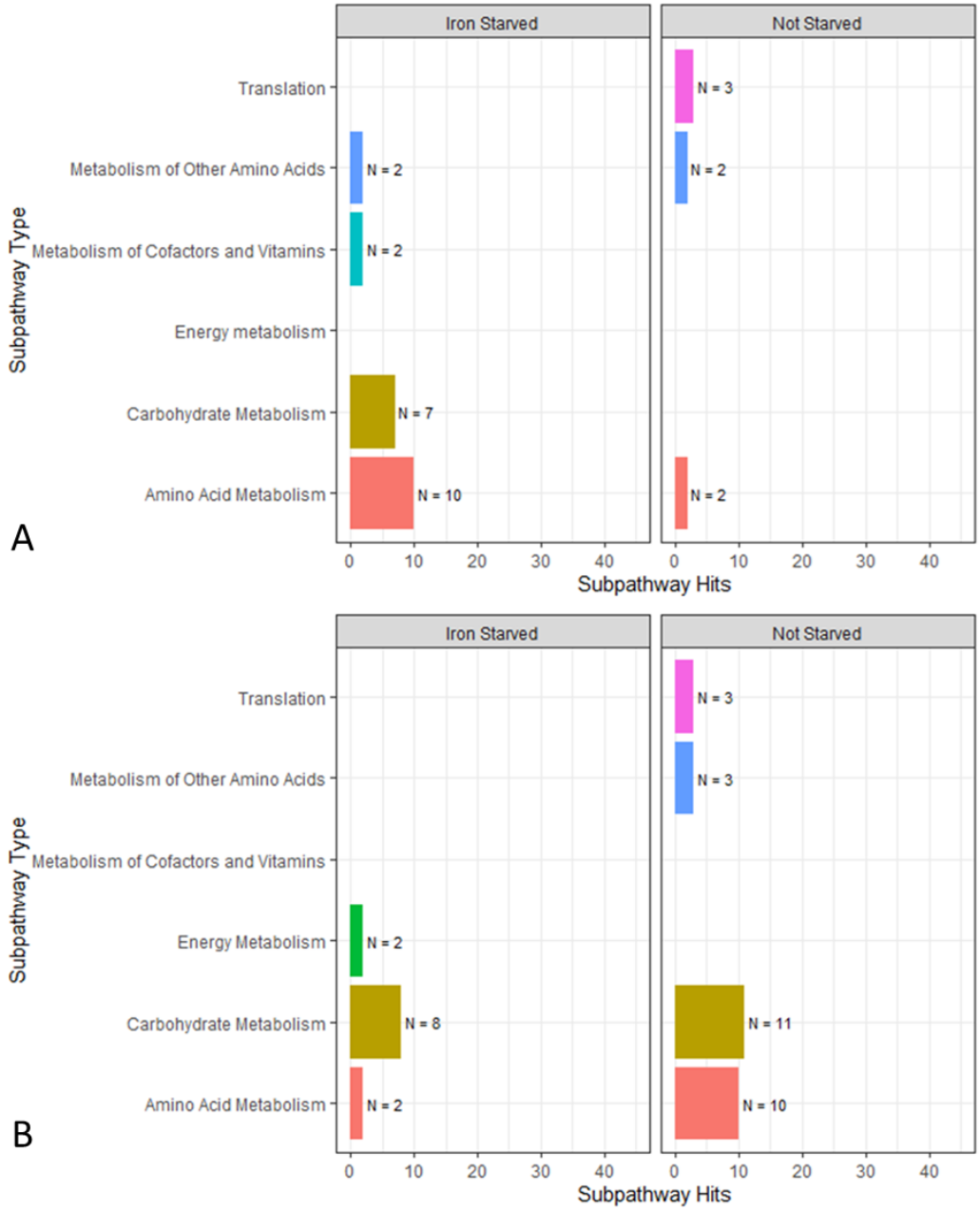

Figure S4: Upregulated metabolic pathways associated with iron starved and not starved *V. alginolyticus* exometabolite samples. The y-axis lists the detected KEGG subpathways and the x-axis shows the number of metabolite hits associated with each subpathway group. (A) Pathways comparisons for iron replete samples. (B) Pathway comparisons for iron deficient samples.

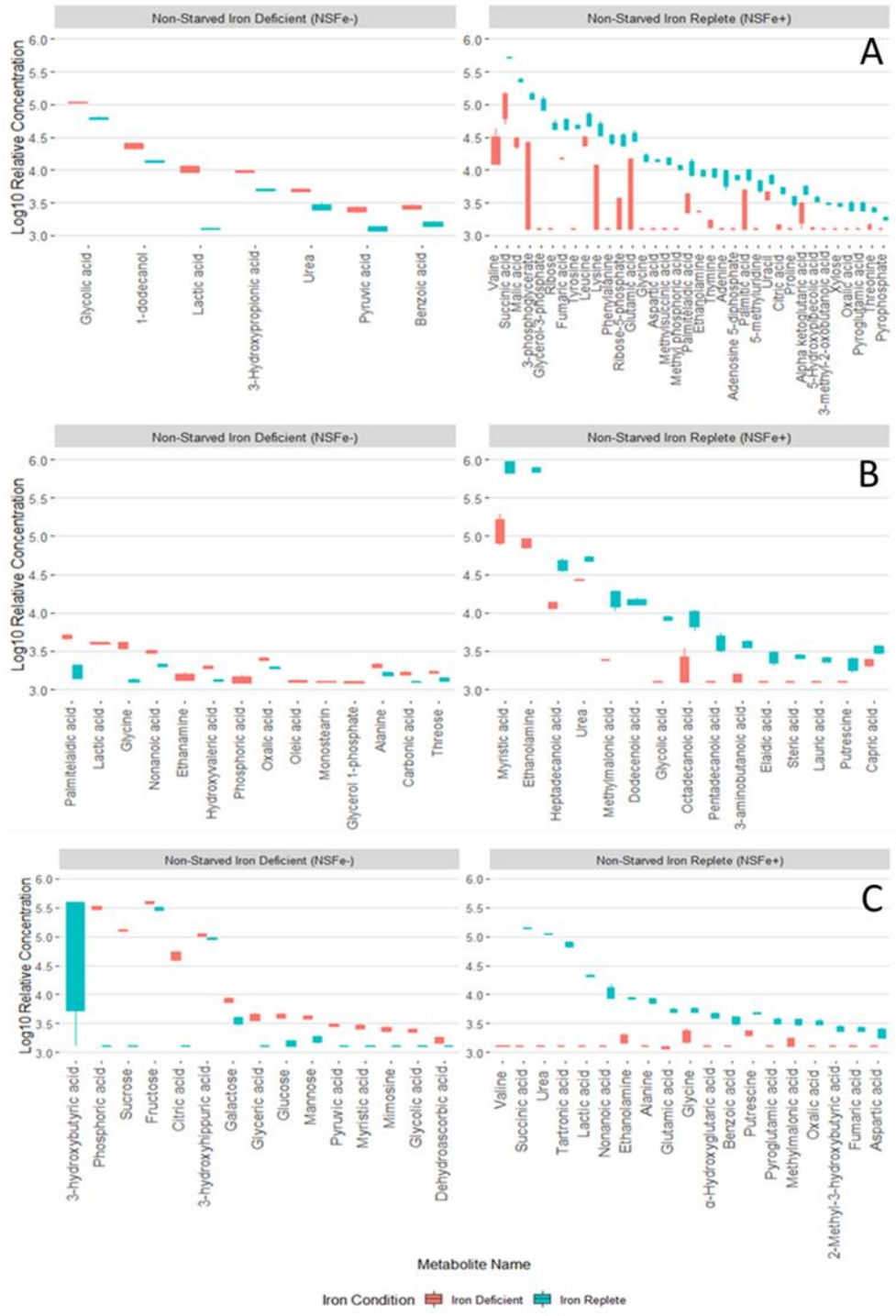

Figure S5: Up regulated metabolites identified from iron comparisons of non-starved cultures. (A) shows polar endometabolites, (B) shows non-polar endometabolites, and (C) shows exometabolites.

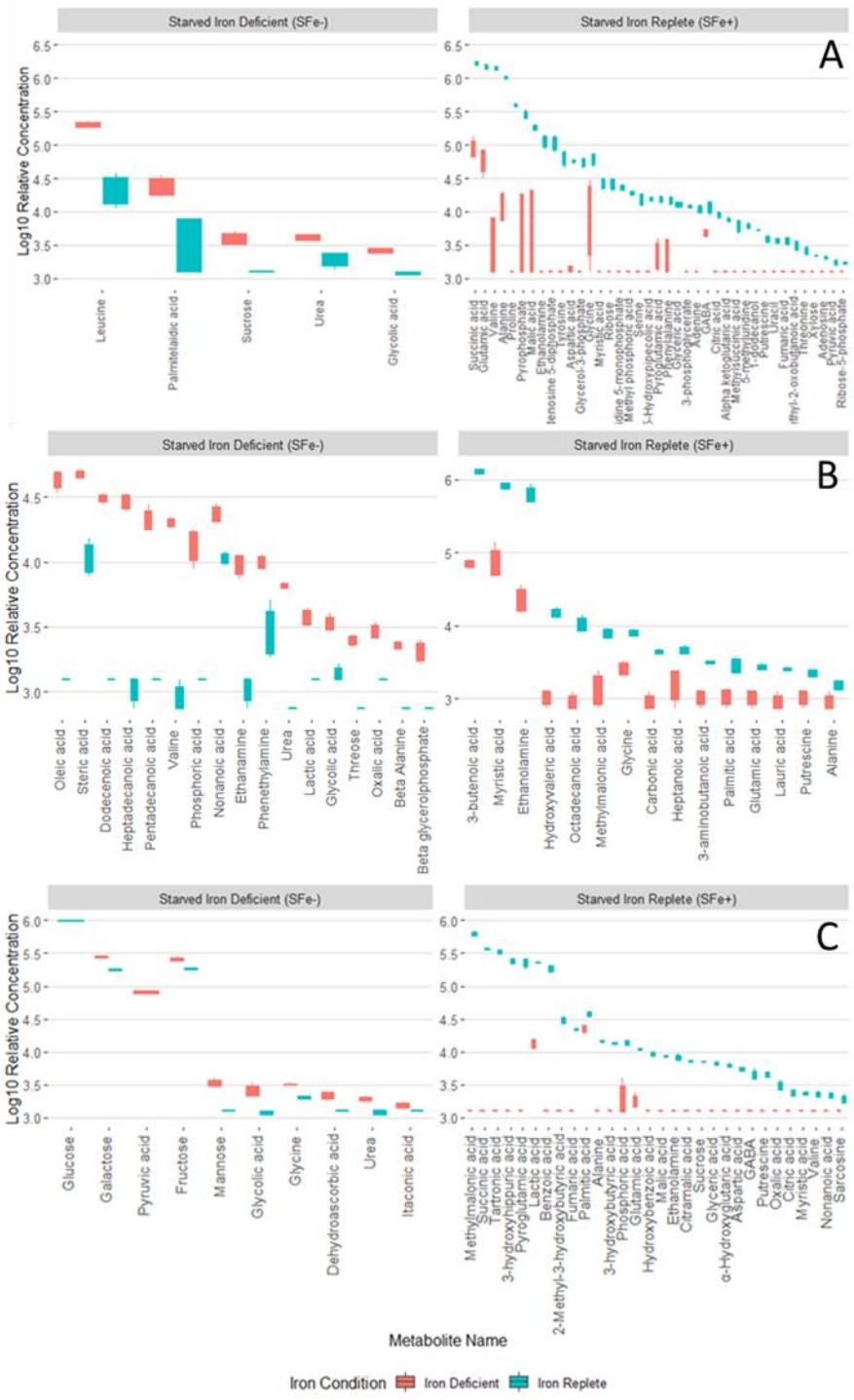

Figure S6: Up regulated metabolites identified from iron comparisons of starved cultures. (A) shows polar endometabolites, (B) shows non-polar endometabolites, and (C) shows exometabolites.

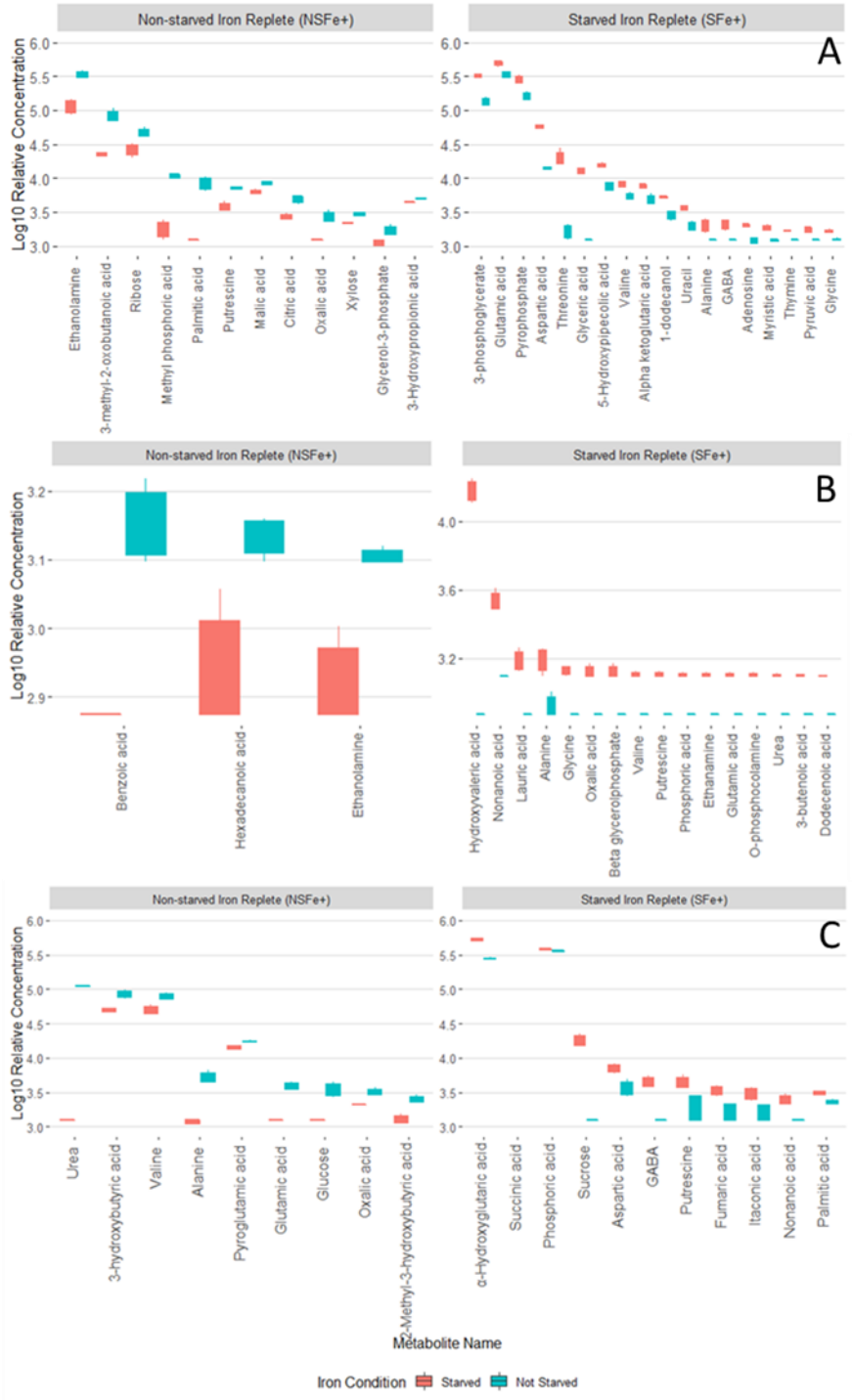

Figure S7: Up regulated metabolites identified from starvation comparisons of iron replete cultures. (A) shows polar endometabolites, (B) shows non-polar endometabolites, and (C) shows exometabolites.

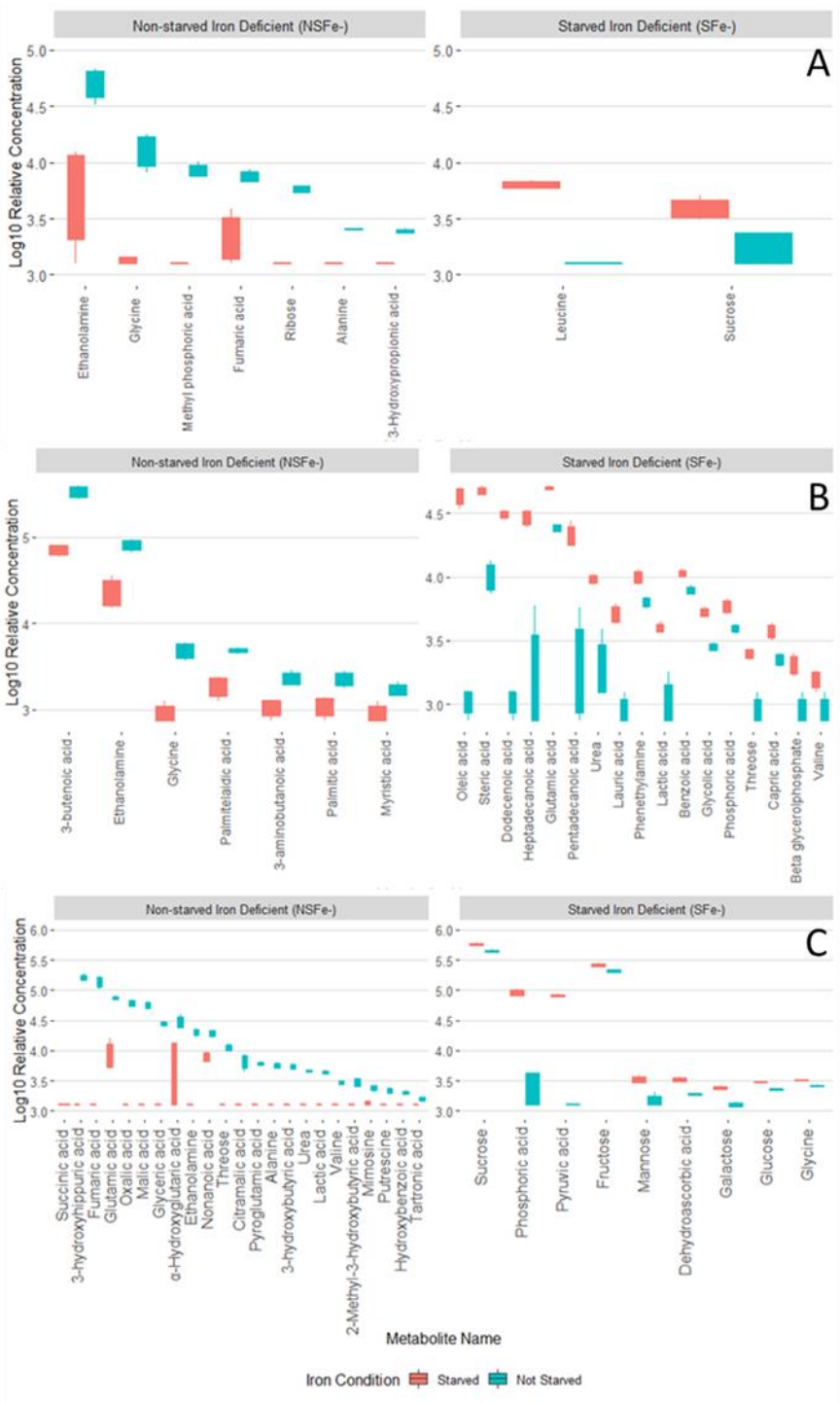

Figure S8: Up regulated metabolites identified from starvation comparisons of iron deficient cultures. (A) shows polar endometabolites, (B) shows non-polar endometabolites, and (C) shows exometabolites.

Table S3: Abiotic condition normality and significance test results. Normality tested using a Shapiro Wilk test. Significance tested using a Kruskal Wallis test.

Strain	Abiotic Metric	Growth Metric	Shapiro Wilk Normality Test P-Value	Kruskal Wallis Test P-Value
JW16-551	Temperature	Lag Phase	3.253e-07	<2.2e-16
JW16-551	Salinity	Lag Phase	2e-11	<2e-16
JW16-551	Iron Concentration	Lag Phase	9e-11	<2e-16
JW16-551	Temperature	Doubling Time	7e-14	<2e-16
JW16-551	Salinity	Doubling Time	<2e-16	<2e-16
JW16-551	Iron Concentration	Doubling Time	NA	<2e-16
JW16-580	Temperature	Lag Phase	9e-08	<2e-16
JW16-580	Salinity	Lag Phase	4e-11	<2e-16
JW16-580	Iron Concentration	Lag Phase	9e-11	<2e-16
JW16-580	Temperature	Doubling Time	<2e-16	<2e-16
JW16-580	Salinity	Doubling Time	<2e-16	<2e-16
JW16-580	Iron Concentration	Doubling Time	NA	<2e-16
ATCC 17749	Temperature	Lag Phase	4e-08	<2e-16
ATCC 17749	Salinity	Lag Phase	1e-09	<2e-16
ATCC 17749	Iron Concentration	Lag Phase	0.03	7e-06
ATCC 17749	Temperature	Doubling Time	NA	NA
ATCC 17749	Salinity	Doubling Time	<2e-16	<2e-16
ATCC 17749	Iron Concentration	Doubling Time	NA	NA

Table S4: Pairwise significance of abiotic conditions as reported using a Dunn post hoc test. P-values reported using a Holm-adjustment.

Growth Metric	Abiotic Metric	Value Comparison[a]	Dunn P-Value Strain JW16-551	Dunn P-Value Strain JW16-580	Dunn P-Value Strain ATCC 17749
Lag Phase	Temperature	24-26	1.000e+00	1.000e+00	1.000e+00
Lag Phase	Temperature	24-28	2.925e-04	9.556e-04	4.910e-09
Lag Phase	Temperature	24-30	1.685e-02	8.828e-03	1.529e-08
Lag Phase	Temperature	24-32	8.624e-04	4.368e-03	1.483e-05
Lag Phase	Temperature	24-34	1.467e-08	1.319e-10	9.798e-16
Lag Phase	Temperature	24-36	1.119e-10	3.339e-08	4.954e-18
Lag Phase	Temperature	24-38	2.230e-12	6.137e-12	9.076e-08
Lag Phase	Temperature	24-40	4.570e-13	2.005e-13	3.353e-01
Lag Phase	Temperature	26-28	5.515e-02	2.655e-01	1.722e-04
Lag Phase	Temperature	26-30	4.602e-01	6.574e-01	9.835e-05
Lag Phase	Temperature	26-32	6.108e-02	3.121e-01	1.857e-02
Lag Phase	Temperature	26-34	2.024e-05	8.349e-06	3.833e-10
Lag Phase	Temperature	26-36	3.245e-07	1.451e-04	2.274e-11
Lag Phase	Temperature	26-38	1.344e-08	7.832e-07	3.828e-04
Lag Phase	Temperature	26-40	2.367e-09	7.072e-08	1.000e+00
Lag Phase	Temperature	28-30	1.000e+00	1.000e+00	1.000e+00
Lag Phase	Temperature	28-32	7.041e-01	1.000e+00	1.000e+00
Lag Phase	Temperature	28-34	1.102e-01	8.962e-03	2.237e-02
Lag Phase	Temperature	28-36	9.358e-03	4.615e-02	1.597e-02
Lag Phase	Temperature	28-38	1.070e-03	1.354e-03	1.000e+00
Lag Phase	Temperature	28-40	2.228e-04	1.883e-04	2.214e-02
Lag Phase	Temperature	30-32	1.000e+00	1.000e+00	8.388e-01
Lag Phase	Temperature	30-34	6.670e-02	5.947e-03	3.419e-01
Lag Phase	Temperature	30-36	6.118e-03	2.965e-02	3.453e-01
Lag Phase	Temperature	30-38	8.786e-04	9.790e-04	1.000e+00
Lag Phase	Temperature	30-40	1.863e-04	1.409e-04	8.618e-03
Lag Phase	Temperature	32-34	5.301e-01	6.145e-02	1.507e-03
Lag Phase	Temperature	32-36	8.130e-02	1.795e-01	6.525e-04
Lag Phase	Temperature	32-38	1.973e-02	1.479e-02	1.000e+00
Lag Phase	Temperature	32-40	5.385e-03	3.979e-03	3.593e-01
Lag Phase	Temperature	34-36	1.000e+00	8.870e-01	9.034e-01
Lag Phase	Temperature	34-38	1.000e+00	1.000e+00	1.514e-01
Lag Phase	Temperature	34-40	6.963e-01	1.000e+00	7.351e-07
Lag Phase	Temperature	36-38	1.000e+00	1.000e+00	1.353e-01
Lag Phase	Temperature	36-40	1.000e+00	1.000e+00	1.755e-07

Lag Phase	Temperature	38-40	1.000e+00	1.000e+00	2.118e-02
Lag Phase	Salinity	1-2	1.000e+00	1.000e+00	3.277e-04
Lag Phase	Salinity	1-3	1.000e+00	5.031e-01	1.318e-04
Lag Phase	Salinity	1-4	1.000e+00	1.000e+00	6.199e-03
Lag Phase	Salinity	1-5	5.359e-01	7.254e-01	1.414e-01
Lag Phase	Salinity	1-6	1.278e-02	5.145e-01	8.402e-01
Lag Phase	Salinity	1-7	1.252e-06	1.090e-04	6.836e-01
Lag Phase	Salinity	1-8	1.858e-15	5.932e-13	1.264e-04
Lag Phase	Salinity	2-3	5.987e-01	1.000e+00	7.774e-01
Lag Phase	Salinity	2-4	4.506e-01	9.933e-01	6.153e-01
Lag Phase	Salinity	2-5	2.142e-02	5.575e-01	3.008e-01
Lag Phase	Salinity	2-6	5.410e-05	3.685e-02	1.212e-02
Lag Phase	Salinity	2-7	6.027e-10	1.526e-07	1.003e-08
Lag Phase	Salinity	2-8	9.270e-20	1.798e-17	7.073e-18
Lag Phase	Salinity	3-4	1.000e+00	1.000e+00	9.666e-01
Lag Phase	Salinity	3-5	1.598e-01	6.682e-02	1.729e-01
Lag Phase	Salinity	3-6	1.764e-03	2.425e-03	5.732e-03
Lag Phase	Salinity	3-7	2.125e-07	5.905e-09	3.474e-09
Lag Phase	Salinity	3-8	2.348e-15	2.810e-18	3.171e-18
Lag Phase	Salinity	4-5	1.000e+00	4.671e-01	7.744e-01
Lag Phase	Salinity	4-6	1.892e-01	4.874e-02	1.322e-01
Lag Phase	Salinity	4-7	4.173e-04	7.584e-07	3.246e-07
Lag Phase	Salinity	4-8	2.128e-10	7.982e-16	5.853e-17
Lag Phase	Salinity	5-6	8.661e-01	1.000e+00	1.000e+00
Lag Phase	Salinity	5-7	1.274e-02	5.441e-03	1.086e-04
Lag Phase	Salinity	5-8	1.676e-08	2.002e-10	3.749e-13
Lag Phase	Salinity	6-7	3.273e-01	1.514e-01	1.521e-02
Lag Phase	Salinity	6-8	2.608e-06	6.346e-08	3.043e-09
Lag Phase	Salinity	7-8	1.732e-02	8.044e-05	1.135e-02
Lag Phase	Iron Content	0.2-0.5	3.943e-09	6.299e-16	NA
Lag Phase	Iron Content	0.2-1	6.924e-25	4.095e-29	NA
Lag Phase	Iron Content	0.2-3	4.191e-45	4.309e-45	NA
Lag Phase	Iron Content	0.2-4	7.168e-45	1.531e-51	NA
Lag Phase	Iron Content	0.2-10	9.154e-76	1.672e-60	NA
Lag Phase	Iron Content	0.2-20	2.241e-92	1.556e-54	NA
Lag Phase	Iron Content	0.5-1	1.485e-05	4.089e-02	NA
Lag Phase	Iron Content	0.5-3	4.138e-13	1.805e-08	NA
Lag Phase	Iron Content	0.5-4	8.032e-14	6.113e-17	NA
Lag Phase	Iron Content	0.5-10	7.263e-32	5.877e-23	NA
Lag Phase	Iron Content	0.5-20	2.597e-38	4.411e-16	NA
Lag Phase	Iron Content	1-3	8.056e-02	1.598e-03	NA
Lag Phase	Iron Content	1-4	4.193e-02	1.129e-10	NA
Lag Phase	Iron Content	1-10	1.003e-09	9.269e-16	NA

Lag Phase	Iron Content	1-20	8.050e-12	1.431e-09	NA
Lag Phase	Iron Content	3-4	1.000e+00	1.854e-03	4.401e-01
Lag Phase	Iron Content	3-10	2.328e-05	1.849e-06	1.160e-01
Lag Phase	Iron Content	3-20	1.158e-06	1.484e-02	1.616e-05
Lag Phase	Iron Content	4-10	1.985e-04	2.807e-01	3.785e-01
Lag Phase	Iron Content	4-20	1.636e-05	4.348e-01	2.412e-04
Lag Phase	Iron Content	10-20	7.005e-01	6.195e-02	1.311e-02
Doubling Time	Temperature	24-26	1.239e-32	4.712e-04	NA
Doubling Time	Temperature	24-28	1.426e-39	4.021e-44	NA
Doubling Time	Temperature	24-30	5.636e-109	1.227e-53	NA
Doubling Time	Temperature	24-32	2.156e-81	2.305e-62	NA
Doubling Time	Temperature	24-34	2.309e-69	1.871e-83	NA
Doubling Time	Temperature	24-36	2.758e-51	5.614e-102	NA
Doubling Time	Temperature	24-38	1.148e-09	1.769e-129	NA
Doubling Time	Temperature	24-40	5.184e-10	8.973e-139	NA
Doubling Time	Temperature	26-28	2.429e-01	1.388e-32	NA
Doubling Time	Temperature	26-30	3.029e-12	2.570e-40	NA
Doubling Time	Temperature	26-32	1.451e-11	8.933e-50	NA
Doubling Time	Temperature	26-34	5.563e-10	1.212e-70	NA
Doubling Time	Temperature	26-36	8.343e-01	3.075e-89	NA
Doubling Time	Temperature	26-38	1.699e-11	8.697e-117	NA
Doubling Time	Temperature	26-40	5.837e-60	4.865e-128	NA
Doubling Time	Temperature	28-30	1.176e-05	1.412e-01	NA
Doubling Time	Temperature	28-32	7.974e-06	8.432e-02	NA
Doubling Time	Temperature	28-34	5.153e-05	2.052e-08	NA
Doubling Time	Temperature	28-36	2.698e-01	2.256e-19	NA
Doubling Time	Temperature	28-38	2.930e-17	1.335e-12	NA
Doubling Time	Temperature	28-40	3.350e-66	1.643e-09	NA
Doubling Time	Temperature	30-32	1.000e+00	1.033e-05	NA
Doubling Time	Temperature	30-34	1.000e+00	1.841e-17	NA
Doubling Time	Temperature	30-36	3.685e-15	2.228e-32	NA
Doubling Time	Temperature	30-38	1.643e-59	1.032e-28	NA
Doubling Time	Temperature	30-40	1.908e-158	1.359e-25	NA
Doubling Time	Temperature	32-34	1.000e+00	1.171e-03	NA
Doubling Time	Temperature	32-36	1.833e-13	5.318e-12	NA
Doubling Time	Temperature	32-38	7.574e-47	1.049e-05	NA
Doubling Time	Temperature	32-40	4.864e-117	1.785e-03	NA
Doubling Time	Temperature	34-36	2.515e-11	2.441e-03	NA
Doubling Time	Temperature	34-38	6.541e-40	6.509e-01	NA
Doubling Time	Temperature	34-40	2.313e-100	6.893e-01	NA
Doubling Time	Temperature	36-38	1.725e-17	2.349e-03	NA
Doubling Time	Temperature	36-40	3.699e-93	7.617e-06	NA
Doubling Time	Temperature	38-40	4.520e-34	2.603e-01	NA

Doubling Time	Salinity	1-2	1.427e-58	1.249e-120	2.673e-04
Doubling Time	Salinity	1-3	4.350e-27	6.278e-147	5.275e-84
Doubling Time	Salinity	1-4	1.134e-01	1.185e-68	9.575e-197
Doubling Time	Salinity	1-5	1.737e-30	1.211e-03	5.098e-118
Doubling Time	Salinity	1-6	1.446e-98	2.010e-75	4.511e-22
Doubling Time	Salinity	1-7	NA	NA	NA
Doubling Time	Salinity	1-8	NA	NA	NA
Doubling Time	Salinity	2-3	1.120e-01	4.519e-13	4.121e-40
Doubling Time	Salinity	2-4	3.879e-20	2.067e-03	6.918e-86
Doubling Time	Salinity	2-5	8.690e-130	3.959e-67	2.266e-39
Doubling Time	Salinity	2-6	5.448e-267	9.539e-238	7.584e-24
Doubling Time	Salinity	2-7	NA	NA	NA
Doubling Time	Salinity	2-8	NA	NA	NA
Doubling Time	Salinity	3-4	7.244e-14	9.601e-03	2.419e-04
Doubling Time	Salinity	3-5	3.432e-79	1.767e-99	4.100e-03
Doubling Time	Salinity	3-6	3.462e-155	9.522e-262	4.899e-123
Doubling Time	Salinity	3-7	NA	NA	NA
Doubling Time	Salinity	3-8	NA	NA	NA
Doubling Time	Salinity	4-5	4.705e-06	2.771e-59	4.148e-16
Doubling Time	Salinity	4-6	2.867e-17	1.777e-159	1.121e-237
Doubling Time	Salinity	4-7	NA	NA	NA
Doubling Time	Salinity	4-8	NA	NA	NA
Doubling Time	Salinity	5-6	2.457e-09	1.523e-21	1.084e-160
Doubling Time	Salinity	5-7	NA	NA	NA
Doubling Time	Salinity	5-8	NA	NA	NA
Doubling Time	Salinity	6-7	NA	NA	NA
Doubling Time	Salinity	6-8	NA	NA	NA
Doubling Time	Salinity	7-8	NA	NA	NA
Doubling Time	Iron Content	0.2-0.5	0.000e+00	0.000e+00	NA
Doubling Time	Iron Content	0.2-1	0.000e+00	0.000e+00	NA
Doubling Time	Iron Content	0.2-3	0.000e+00	0.000e+00	NA
Doubling Time	Iron Content	0.2-4	0.000e+00	0.000e+00	NA
Doubling Time	Iron Content	0.2-10	0.000e+00	0.000e+00	NA
Doubling Time	Iron Content	0.2-20	0.000e+00	0.000e+00	NA
Doubling Time	Iron Content	0.5-1	3.058e-126	2.876e-09	NA
Doubling Time	Iron Content	0.5-3	6.442e-57	9.192e-01	NA
Doubling Time	Iron Content	0.5-4	2.184e-35	3.183e-43	NA
Doubling Time	Iron Content	0.5-10	6.498e-86	9.327e-37	NA
Doubling Time	Iron Content	0.5-20	7.449e-130	6.332e-54	NA
Doubling Time	Iron Content	1-3	3.072e-01	1.158e-05	NA
Doubling Time	Iron Content	1-4	4.522e-05	4.305e-88	NA
Doubling Time	Iron Content	1-10	1.289e-02	1.713e-69	NA
Doubling Time	Iron Content	1-20	1.459e-05	9.203e-124	NA

Doubling Time	Iron Content	3-4	1.203e-02	2.578e-27	NA
Doubling Time	Iron Content	3-10	4.268e-03	4.651e-26	NA
Doubling Time	Iron Content	3-20	1.364e-05	3.905e-28	NA
Doubling Time	Iron Content	4-10	5.506e-09	5.954e-01	NA
Doubling Time	Iron Content	4-20	2.557e-14	3.032e-01	NA
Doubling Time	Iron Content	10-20	5.113e-01	4.630e-02	NA

[a]Value comparison represents the two abiotic conditions compared. Temperatures reported in ^{o}C, salinities reported in % (w/v) NaCl, and iron reported in µM.